

**Editorial Board:**

**A. Abe · A.-C. Albertsson · K. Dušek · W.H. de Jeu  
H.-H. Kausch · S. Kobayashi · K.-S. Lee · L. Leibler  
T.E. Long · I. Manners · M. Möller · E.M. Terentjev  
M. Vicent · B. Voit · G. Wegner · U. Wiesner**

# Advances in Polymer Science

Recently Published and Forthcoming Volumes

## **Modern Techniques for Nano- and Microreactors/-reactions**

Volume Editor: Caruso, F.  
Vol. 229, 2010

## **Complex Macromolecular Systems II**

Volume Editors: Müller, A.H.E.,  
Schmidt, H.-W.  
Vol. 228, 2010

## **Complex Macromolecular Systems I**

Volume Editors: Müller, A.H.E.,  
Schmidt, H.-W.  
Vol. 227, 2010

## **Shape-Memory Polymers**

Volume Editor: Lendlein, A.  
Vol. 226, 2010

## **Polymer Libraries**

Volume Editors: Meier, M.A.R., Webster, D.C.  
Vol. 223, 2010

## **Polymer Membranes/Biomembranes**

Volume Editors: Meier, W.P., Knoll, W.  
Vol. 224, 2010

## **Organic Electronics**

Volume Editors: Meller, G., Grasser, T.  
Vol. 223, 2010

## **Inclusion Polymers**

Volume Editor: Wenz, G.  
Vol. 222, 2009

## **Advanced Computer Simulation Approaches for Soft Matter Sciences III**

Volume Editors: Holm, C., Kremer, K.  
Vol. 221, 2009

## **Self-Assembled Nanomaterials II**

Nanotubes  
Volume Editor: Shimizu, T.  
Vol. 220, 2008

## **Self-Assembled Nanomaterials I**

Nanofibers  
Volume Editor: Shimizu, T.  
Vol. 219, 2008

## **Interfacial Processes and Molecular Aggregation of Surfactants**

Volume Editor: Narayanan, R.  
Vol. 218, 2008

## **New Frontiers in Polymer Synthesis**

Volume Editor: Kobayashi, S.  
Vol. 217, 2008

## **Polymers for Fuel Cells II**

Volume Editor: Scherer, G.G.  
Vol. 216, 2008

## **Polymers for Fuel Cells I**

Volume Editor: Scherer, G.G.  
Vol. 215, 2008

## **Photoresponsive Polymers II**

Volume Editors: Marder, S.R., Lee, K.-S.  
Vol. 214, 2008

## **Photoresponsive Polymers I**

Volume Editors: Marder, S.R., Lee, K.-S.  
Vol. 213, 2008

## **Polyfluorenes**

Volume Editors: Scherf, U., Neher, D.  
Vol. 212, 2008

## **Chromatography for Sustainable Polymeric Materials**

Renewable, Degradable and Recyclable  
Volume Editors: Albertsson, A.-C.,  
Hakkarainen, M.  
Vol. 211, 2008

## **Wax Crystal Control · Nanocomposites Stimuli-Responsive Polymers**

Vol. 210, 2008

## **Functional Materials and Biomaterials**

Vol. 209, 2007

## **Phase-Separated Interpenetrating Polymer Networks**

Authors: Lipatov, Y.S., Alekseeva, T.  
Vol. 208, 2007

## **Hydrogen Bonded Polymers**

Volume Editor: Binder, W.  
Vol. 207, 2007

# Modern Techniques for Nano- and Microreactors/-reactions

Volume Editor: Frank Caruso

With contributions by

K. Ariga · G. Battaglia · S.L. Biswal · F. Caruso · J.P. Hill  
Q. Ji · A.P.R. Johnston · G.C. Kini · K. Landfester  
H. Lomas · M. Massignani · A.D. Price · G.K. Such  
C.K. Weiss · M.S. Wong

*Editor*  
Frank Caruso  
Department of Chemical and Biomolecular Engineering  
The University of Melbourne  
Victoria 3010, Australia  
*fcaruso@unimelb.edu.au*

ISSN 0065-3195 e-ISSN 1436-5030  
ISBN 978-3-642-12872-1 e-ISBN 978-3-642-12873-8  
DOI 10.1007/978-3-642-12873-8  
Springer Heidelberg Dordrecht London New York

Library of Congress Control Number: 2010930620

© Springer-Verlag Berlin Heidelberg 2010

This work is subject to copyright. All rights are reserved, whether the whole or part of the material is concerned, specifically the rights of translation, reprinting, reuse of illustrations, recitation, broadcasting, reproduction on microfilm or in any other way, and storage in data banks. Duplication of this publication or parts thereof is permitted only under the provisions of the German Copyright Law of September 9, 1965, in its current version, and permission for use must always be obtained from Springer. Violations are liable to prosecution under the German Copyright Law.

The use of general descriptive names, registered names, trademarks, etc. in this publication does not imply, even in the absence of a specific statement, that such names are exempt from the relevant protective laws and regulations and therefore free for general use.

*Cover design:* WMXDesign GmbH, Heidelberg

Printed on acid-free paper

Springer is part of Springer Science+Business Media ([www.springer.com](http://www.springer.com))

---

## Volume Editor

Frank Caruso

Department of Chemical and Biomolecular Engineering  
The University of Melbourne  
Victoria 3010, Australia  
*fcaruso@unimelb.edu.au*

## Editorial Board

Prof. Akihiro Abe

Professor Emeritus  
Tokyo Institute of Technology  
6-27-12 Hiyoshi-Honcho, Kohoku-ku  
Yokohama 223-0062, Japan  
*aabe34@xc4.so-net.ne.jp*

Prof. A.-C. Albertsson

Department of Polymer Technology  
The Royal Institute of Technology  
10044 Stockholm, Sweden  
*aila@polymer.kth.se*

Prof. Karel Dušek

Institute of Macromolecular Chemistry  
Czech Academy of Sciences  
of the Czech Republic  
Heyrovský Sq. 2  
16206 Prague 6, Czech Republic  
*dusek@imc.cas.cz*

Prof. Dr. Wim H. de Jeu

Polymer Science and Engineering  
University of Massachusetts  
120 Governors Drive  
Amherst MA 01003, USA  
*dejeu@mail.pse.umass.edu*

Prof. Hans-Henning Kausch

Ecole Polytechnique Fédérale de Lausanne  
Science de Base  
Station 6  
1015 Lausanne, Switzerland  
*kausch.cully@bluewin.ch*

Prof. Shiro Kobayashi

R & D Center for Bio-based Materials  
Kyoto Institute of Technology  
Matsugasaki, Sakyo-ku  
Kyoto 606-8585, Japan  
*kobayash@kit.ac.jp*

Prof. Kwang-Sup Lee

Department of Advanced Materials  
Hannam University  
561-6 Jeonmin-Dong  
Yuseong-Gu 305-811  
Daejeon, South Korea  
*kslee@hnu.kr*

Prof. L. Leibler

Matière Molle et Chimie  
Ecole Supérieure de Physique  
et Chimie Industrielles (ESPCI)  
10 rue Vauquelin  
75231 Paris Cedex 05, France  
*ludwik.leibler@espci.fr*

Prof. Timothy E. Long

Department of Chemistry  
and Research Institute  
Virginia Tech  
2110 Hahn Hall (0344)  
Blacksburg, VA 24061, USA  
*telong@vt.edu*

Maria Jesus Vicent, PhD

Centro de Investigacion Principe Felipe  
Medicinal Chemistry Unit  
Polymer Therapeutics Laboratory  
Av. Autopista del Saler, 16  
46012 Valencia, Spain  
*mjvicent@cipf.es*

Prof. Ian Manners

School of Chemistry  
University of Bristol  
Cantock's Close  
BS8 1TS Bristol, UK  
*ian.manners@bristol.ac.uk*

Prof. Brigitte Voit

Institut für Polymerforschung Dresden  
Hohe Straße 6  
01069 Dresden, Germany  
*voit@ipfdd.de*

Prof. Martin Möller

Deutsches Wollforschungsinstitut  
an der RWTH Aachen e.V.  
Pauwelsstraße 8  
52056 Aachen, Germany  
*moeller@dwf.rwth-aachen.de*

Prof. Gerhard Wegner

Max-Planck-Institut  
für Polymerforschung  
Ackermannweg 10  
55128 Mainz, Germany  
*wegner@mpip-mainz.mpg.de*

Prof. E.M. Terentjev

Cavendish Laboratory  
Madingley Road  
Cambridge CB 3 0HE, UK  
*emt1000@cam.ac.uk*

Prof. Ulrich Wiesner

Materials Science & Engineering  
Cornell University  
329 Bard Hall  
Ithaca, NY 14853, USA  
*ubw1@cornell.edu*

---

## **Advances in Polymer Sciences**

### **Also Available Electronically**

*Advances in Polymer Sciences* is included in Springer's eBook package *Chemistry and Materials Science*. If a library does not opt for the whole package, the book series may be bought on a subscription basis. Also, all back volumes are available electronically.

For all customers who have a standing order to the print version of *Advances in Polymer Sciences*, we offer the electronic version via SpringerLink free of charge.

If you do not have access, you can still view the table of contents of each volume and the abstract of each article by going to the SpringerLink homepage, clicking on "Browse by Online Libraries", then "Chemical Sciences", and finally choose *Advances in Polymer Science*.

You will find information about the

- Editorial Board
- Aims and Scope
- Instructions for Authors
- Sample Contribution

at [springer.com](http://springer.com) using the search function by typing in *Advances in Polymer Sciences*.

*Color figures* are published in full color in the electronic version on SpringerLink.

## Aims and Scope

The series *Advances in Polymer Science* presents critical reviews of the present and future trends in polymer and biopolymer science including chemistry, physical chemistry, physics and material science. It is addressed to all scientists at universities and in industry who wish to keep abreast of advances in the topics covered.

Review articles for the topical volumes are invited by the volume editors. As a rule, single contributions are also specially commissioned. The editors and publishers will, however, always be pleased to receive suggestions and supplementary information. Papers are accepted for *Advances in Polymer Science* in English.

In references *Advances in Polymer Sciences* is abbreviated as *Adv Polym Sci* and is cited as a journal.

Special volumes are edited by well known guest editors who invite reputed authors for the review articles in their volumes.

Impact Factor in 2009: 4.600; Section "Polymer Science": Rank 4 of 73



# Preface

Encapsulation technologies are widely used in medicine and pharmaceuticals, agriculture and cosmetic industries for the development of a wide range of controlled-release delivery systems. Thin films, and particulates such as liposomes, emulsions and capsules, are used for the sustained release of drugs, pesticides, fragrances and other substances. Advanced variants of these systems have also been used to perform various confined nano-/microreactions to mimic cellular processes. The impetus for this stems from the fact that many biological processes are compartmentalized within cells through the localization of proteins and other molecules, and such confinement controls the complex processes. Although the synthetic counterparts are still far from the complexity of living systems, they hold promise for advancing studies into the synthesis, encapsulation (confinement), reactions and delivery of (bio)molecules.

This volume provides an overview of a number of extensively used techniques to encapsulate a host of different materials, ranging from confined polymerization to self-assembly. The encapsulation vehicles formed include thin multi-strata films, emulsions, polymersomes, nanoparticle-based hollow spheres and polymer capsules. The potential applications of these systems for encapsulation and their use as microreactors to perform a host of complex reactions are discussed, and examples showing the diversity of properties that can be controlled in these systems are given.

In Chapter 1, Landfester and Weiss outline details of miniemulsion polymerization for the encapsulation of a range of materials such as dyes, pigments, fragrances, photo-initiators, drugs, nanoparticles and biomolecules (DNA) in polymeric nanoparticles. The preparation of nanoparticles with new properties is also presented.

Chapter 2, by Ariga, Ji and Hill, presents recent developments on the application of the layer-by-layer technique for encapsulating enzymes. Encapsulation strategies are demonstrated for enzymes in both thin film and particle formats to generate complex enzyme architectures for microreactions. The integration of such systems into advanced biodevices such as microchannels, field effect transistors and flow injection amperometric sensors is also presented.

In Chapter 3, Kini, Biswal and Wong discuss recent developments in synthetic routes and properties of hollow spheres formed from nanoparticles. It is shown that arranging nanoparticles into hollow spheres through self-assembly produces particle

systems with new properties that can be exploited for encapsulation, storage and controlled release, making them potentially useful in medical therapy, catalysis and encapsulation applications.

In Chapter 4, Massignani, Lomas and Battaglia review the fabrication processes used to form polymersomes, membrane-enclosed structures that are formed through self-assembly of amphiphilic copolymers. The resulting molecular properties, methods to control their size, loading strategies and applications of polymersomes are also detailed.

Chapter 5, by Price, Johnston, Such and Caruso, focuses on recent progress in the design of layer-by-layer capsule reactors. Fundamentals that underpin the assembly of such capsules are presented, followed by the assembly parameters that affect the retention of components within the resultant capsules. Prominent examples of layer-by-layer assembled microreactors and potential applications of such systems in biomedicine and micro-encapsulated catalysis are also discussed.

The collection of chapters in this volume will be of interest to a multidisciplinary audience working at the interface of chemistry, biology, physics, materials science and engineering. This volume is also aimed at encouraging scientists and engineers who wish to diversify their research in encapsulation and nano-/microreactor systems.

Finally, I would like to thank all of the contributors for taking valuable time from their busy schedules to write stimulating and informative chapters, and to the Springer team for assistance in publishing this volume in their leading book series “Advances in Polymer Science.”

Melbourne,  
June 2010

*Frank Caruso*

# Contents

<b>Encapsulation by Miniemulsion Polymerization</b> .....	1
Katharina Landfester and Clemens K. Weiss	
<b>Enzyme-Encapsulated Layer-by-Layer Assemblies: Current Status and Challenges Toward Ultimate Nanodevices</b> .....	51
Katsuhiko Ariga, Qingmin Ji, and Jonathan P. Hill	
<b>Non-Layer-by-Layer Assembly and Encapsulation Uses of Nanoparticle-Shelled Hollow Spheres</b> .....	89
Gautam C. Kini, Sibani L. Biswal, and Michael S. Wong	
<b>Polymersomes: A Synthetic Biological Approach to Encapsulation and Delivery</b> .....	115
Marzia Massignani, Hannah Lomas, and Giuseppe Battaglia	
<b>Reaction Vessels Assembled by the Sequential Adsorption of Polymers</b> .....	155
Andrew D. Price, Angus P.R. Johnston, Georgina K. Such, and Frank Caruso	
<b>Index</b> .....	181

# Encapsulation by Miniemulsion Polymerization

Katharina Landfester and Clemens K. Weiss

**Abstract** The miniemulsion technique offers the possibility for the encapsulation of different materials, ranging from liquid to solid, from organic to inorganic, and from molecularly dissolved to aggregated species into polymeric nanoparticles or nanocapsules. Using this technique, a wide variety of novel functional nanomaterials can be generated. This review focuses on the preparation of functional nanostructures by encapsulating organic or inorganic material in polymeric nanoparticles. The examples demonstrate the possibilities to protect the encapsulated material as dyes, pigments, fragrances, photo-initiators, drugs, magnetite, or even DNA, use them as marker systems (dyes, magnetite), or create nanoparticles with completely new properties.

**Keywords** Encapsulation of components · Hybrid particles · miniemulsion · Nanocomposites · Nanoparticles

## Contents

1	Introduction .....	3
2	Encapsulation of Soluble Materials .....	5
2.1	Encapsulation of Dyes .....	6
2.2	Encapsulation of Metal Complexes .....	13
3	Encapsulation of Solid Materials .....	16
3.1	Organic Pigments and Carbon-Based Materials .....	16
3.2	Encapsulation of Inorganic Materials .....	19
4	Encapsulation of Liquids .....	28
4.1	Capsule Formation by Phase Separation .....	29
4.2	Capsule Formation by Interfacial Polymerization .....	30
4.3	Polymer Precipitation on Preformed Nanodroplets .....	37

5	Controlled Release of Components from Nanocapsules .....	37
6	Summary .....	40
	References .....	40

## Abbreviations

AA	Acrylic acid
ADMET	Acyclic diene metathesis
AEMH2	Aminoethyl methacrylate hydrochloride
AGET	Activator generated by electron transfer
AIBN	Azo-bis-(isobutyronitrile)
ATRP	Atom transfer radical polymerization
BODIPY	Boron-dipyrrromethene
CDB	Phenyl 2-propyl dithiobenzoate
CMTE	<i>cis</i> -1,2-Bis(2,4,5-trimethyl-3-trienyl)ethane
CTAB	Cetyltrimethylammonium bromide
CTMA-Cl	Cetyltrimethylammonium chloride
DMPBA	1,2-Dimethyl-1-phenyl-butylamide
FACS	Fluorescent activated cell sorter
HR-SEM	High resolution scanning electron microscopy
KPS	Peroxodisulfate
MePEG	Methoxypoly(ethylene glycol)
MPS	Methacryloxypropyltrimethoxysilane
MRI	Magnetic resonance imaging
NMP	Nitroxide mediated polymerization
NMR	Nuclear magnetic resonance
PAEMA	Poly(aminoethyl methacrylate)
PBA	Polybutylacrylate
PBCA	Polybutylcyanoacrylate
PCL	Poly( $\epsilon$ -caprolactone)
PEG	Poly(ethylene glycol)
P(E/B-EO)	Poly((ethylene- <i>co</i> -butylene)- <i>b</i> -ethylene oxide))
PEI	Poly(ethylene imine)
PI	Polyisoprene
PLLA	Polylactide
PMAA	Poly(methacrylic acid)
PMI	<i>N</i> -(2,6-Diisopropylphenyl)perylene-3,4-dicarbonacidimide
PMMA	Poly(methylmethacrylate)
PNIPAM	Poly( <i>N</i> -isopropylacrylamide)
PPDTA	Phenyl 2-propyl phenyl dithioacetate
PS	Polystyrene
PU	Polyurethane
PUR	Polyurea

QD	Quantum dot
RAFT	Reversible addition–fragmentation chain transfer
RITC	Rhodamine isothiocyanate
SDS	Sodium dodecyl sulfate
SWNT	Single wall carbon nanotube
TEM	Transmission electron microscopy
TEOS	Tetraethylorthosilicate
tmhd	Tris(2,2,6,6-tetramethyl-3,5-heptanedionato)
TOPO	Trioctylphosphine oxide
V60	2,2'-Azobis{2-[1-(2-hydroxyethyl)-2-imidazolin-2-yl]propane}dihydrochloride

## 1 Introduction

Today, polymeric nanoparticles and nanocapsules with different encapsulated species are of great interest for a number of applications such as functional coatings, inks, adhesives, nutrition, or cosmetics, but also more and more for pharmaceutical and biomedical applications. For the preparation of nanoparticles from radically polymerized monomers, the emulsion polymerization is often applied. As the process of emulsion polymerization is limited because of diffusion processes, the generation of complex structures is often difficult or even impossible. An elegant way to circumvent these problems is the miniemulsion process. Miniemulsions consist of finely dispersed, stable droplets in a second, continuous phase. Small and narrowly distributed miniemulsion droplets are usually created from a macroemulsion with a broad droplet size distribution by the application of high shear forces via ultrasound or high pressure homogenization. The size of the miniemulsion droplets mainly depends on the type and the amount of the emulsifier used in the particular system. In addition to the emulsifier, a costabilizer is required which acts as an osmotic pressure agent within the droplets counteracting the Laplace pressure and suppressing effectively diffusion processes. The costabilizer has to show good solubility in the dispersed phase, but at the same time it has to possess a lower solubility in the continuous phase than the major compound of the dispersed phase. In the case of a direct (oil-in-water) miniemulsion, this agent is an (ultra)hydrophobe, and in the case of an inverse (water-in-oil) miniemulsion it represents an (ultra)lipophobe. In Fig. 1, the general process of the miniemulsion process is schematically shown.

The droplets can be regarded as individually acting nanoreactors, suitable for a wide variety of different reactions. It has been shown that organic reactions like esterification and saponification [1, 2], crystallization processes [3–6] and sol-gel reactions [7] can efficiently be performed in miniemulsions.

However, the main focus of the miniemulsion technique lies in the formation of polymeric nanoparticles. Whereas conventional emulsion polymerization can be applied to the formulation of homopolymer latexes by radical polymerization, the generation of copolymer or functional nanoparticles is restricted with this technique,

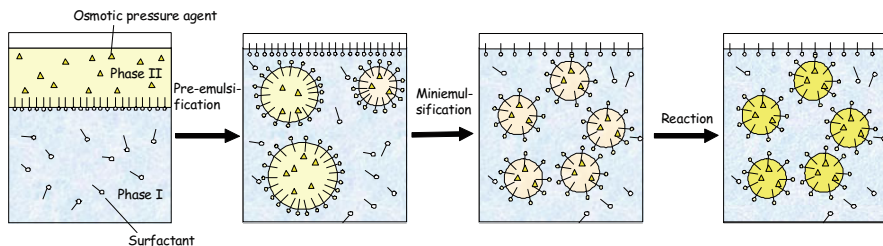


**Fig. 1** Direct miniemulsion process

as the process relies on diffusion of the monomers through the continuous phase. The realization of other polymerization types than the radical polymerization is almost impossible in conventional emulsion polymerization.

Radical polymerization can be performed with many different vinylic monomers ranging from hydrophobic ones, such as styrene, acrylates, methacrylates, fluoroacrylates, etc. to hydrophilic monomers such as acrylamides, hydroxyethyl-methacrylate, acrylic acid, etc. Whereas in the case of hydrophobic monomers, water is chosen as continuous phase, in the case of hydrophilic monomers, the continuous phase is an organic solvent. Furthermore, a radical copolymerization between two hydrophobic monomers is well suited to obtaining homogeneous copolymer materials. The copolymerization of hydrophobic and hydrophilic monomers leading to the formation of amphiphilic polymer particles is a process which can be performed in either a hydrophilic aqueous or a hydrophobic organic solvent phase. An overview of many possibilities for radical polymerizations in miniemulsion systems is given in several reviews [8–11].

Since the reaction is conducted in the small miniemulsion droplets and effective diffusion does not take place, miniemulsion polymerization is not restricted to radical polymerization. Several examples underline that other types of polymerizations can also be carried out in miniemulsion (see Fig. 2):

- Anionic polymerization: in non-aqueous miniemulsions for polyamide nanoparticles [12], and in aqueous phase for polybutylcyanoacrylate (PBCA) nanoparticles [13]
- Cationic polymerization for poly-*p*-methoxystyrene particles [14, 15]
- Catalytic polymerization for polyolefin [16, 17] or polyketone particles [18]
- Ring opening metathesis polymerization for polynorbornene nanoparticles [19, 20]
- Step-growth acyclic diene metathesis (ADMET) polymerization for oligo (phenylene vinylenes) particles [21]
- Polyaddition for polyepoxides [22] or polyurethane particles [23, 24]
- Polycondensation for polyester [25] nanoparticles
- Enzymatic polymerization for polyester particles [26]
- Oxidative polymerization for polyaniline nanoparticles [27, 28]

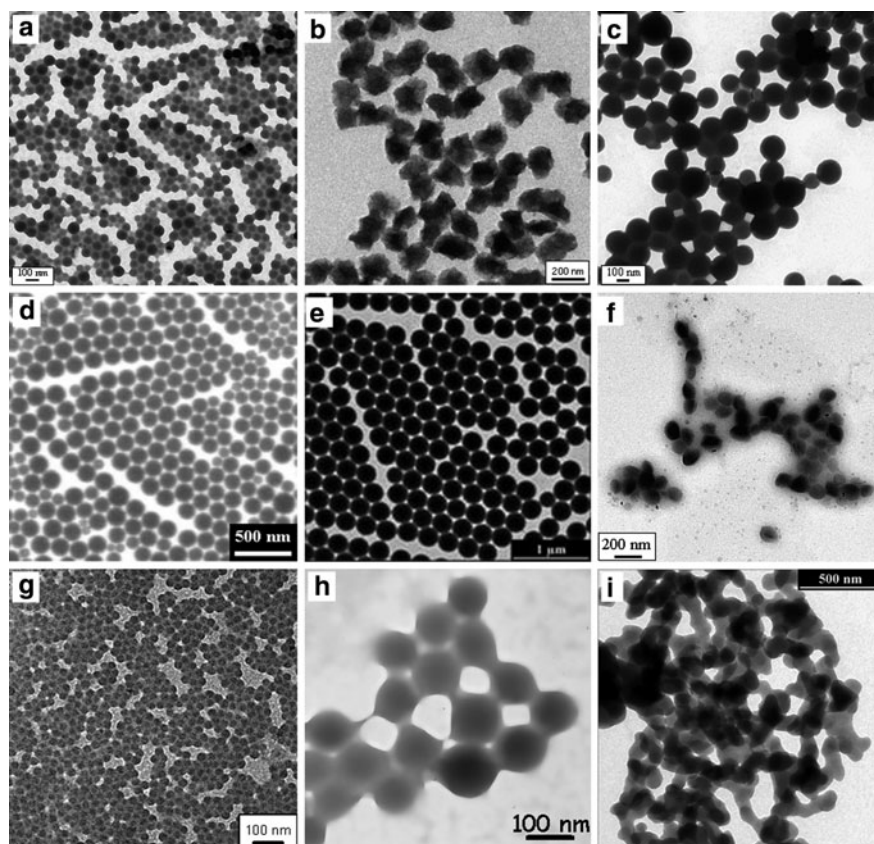


**Fig. 2** Polymeric nanoparticles as obtained by the miniemulsion process: (a) polyacrylamide; (b) polyacrylonitrile; (c) polyacrylate; (d) polyisoprene; (e) polystyrene; (f) polyester; (g) polyepoxide; (h) polybutylcyanoacrylate; and (i) polyimide nanoparticles

Additionally, the miniemulsion is excellently suited for the encapsulation of a variety of different materials, ranging from hydrophobic to hydrophilic, from solid to liquids, from inorganic to organic. The composite nanoparticles and nanocapsules can be functionalized at their surfaces and the encapsulated components can be released or not as desired. In the following review, the advantage of the miniemulsion process with many different examples will be presented.

## 2 Encapsulation of Soluble Materials

If the compounds are soluble in the dispersed monomer phase, the encapsulation in the nanoparticles is easy and straightforward. Here, the component just has to be dissolved in the monomer prior to the miniemulsification step. During the



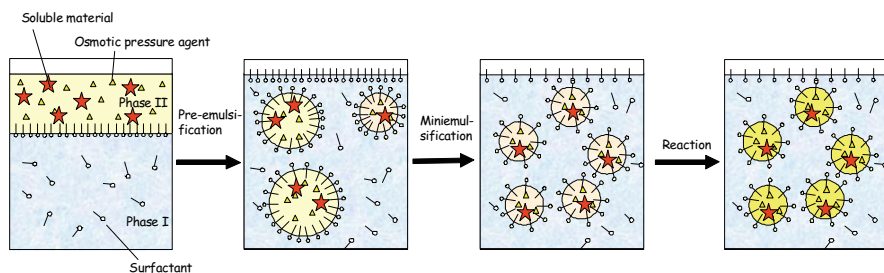


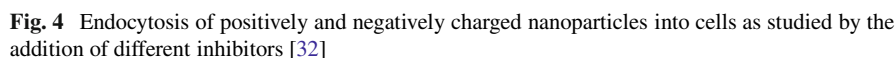
**Fig. 3** Miniemulsion polymerization process for the encapsulation of soluble materials

subsequent polymerization, the component is entrapped in the particles (Fig. 3). As effective diffusion is suppressed in miniemulsions, the concentration of the soluble compound adjusted in the monomer is retained during polymerization. In the best case, it also stays molecularly dissolved in the polymer, but also a partial or entire phase separation might occur leading to smaller or larger domains, which can be distributed as microdomains all over the matrix or assemble to form a core-shell structure. The latter case will be described in the chapter “Capsule Formation by Phase Separation.”

## 2.1 Encapsulation of Dyes

The labeling of nanoparticles with fluorescent dyes allows one to use them as markers in biomedical applications. One possibility is to immobilize the fluorescent dyes physically or chemically on the particle’s surface (e.g. FITC-dextran [29]). However, either desorption can occur, or the surface is changed that much that the biological response (cell uptake, toxicity) is significantly modified or even totally hindered. Therefore, an incorporation of hydrophobic dyes into the polymeric nanoparticles leads to marker systems where only the polymer and the highly variable surface functionality are the relevant factors for particle-cell interactions.

Carboxy- and amino-functionalized polystyrene nanoparticles have been synthesized by the miniemulsion process using styrene and the functional monomers acrylic acid (AA) or 2-aminoethyl methacrylate hydrochloride (AEMH) as functional comonomers [30, 31]. By changing the amount of the comonomer, different surface densities of the charged groups could be realized. Since a fluorescent dye was incorporated inside the nanoparticles, the uptake behavior of different cell lines could be determined as a function of the surface functionalization [30, 31]. It was found that, in general, the uptake of the nanoparticles into the cells increases with increasing functionality on the particle’s surface. For HeLa cells, for example, the internalized particle amount was up to sixfold better for carboxy-functionalized polystyrene (PS) nanoparticles than for non-functionalized PS particles. For amino functionalized PS nanoparticles, an up to 50-fold enhanced uptake could be detected. In order to investigate the actual uptake pathway into HeLa cells, positively



In addition to the above-mentioned experiments using PS-based nanoparticles, the hydrophobic fluorescent dye *N*-(2,6-diisopropylphenyl)perylene-3,4-dicarbonacidimide (PMI) could also be successfully incorporated in phosphate-functionalized poly(methylmethacrylate) (PMMA) and PS [33], polyisoprene (PI), PS-*co*-PI [34], PBCA [35, 36] and polylactide (PLLA), or poly( $\epsilon$ -caprolactone) (PCL) nanoparticles [37] in order to study the cellular response to these polymeric nanoparticles. For qualitative investigations, confocal microscopy can be used; the quantitative measurements can be realized by a fluorescent activated cell sorter (FACS).

It was shown that the uptake behavior is greatly affected by the type of the polymer (see Fig. 5). In the case of polyisoprene, the uptake of non-functionalized nanoparticles without any transfection agents into different adherent (HeLa) and also suspension (Jurkat) cell lines is extremely fast compared to other polymeric particles and, moreover, leads to high particle loading of the cells. The internalized

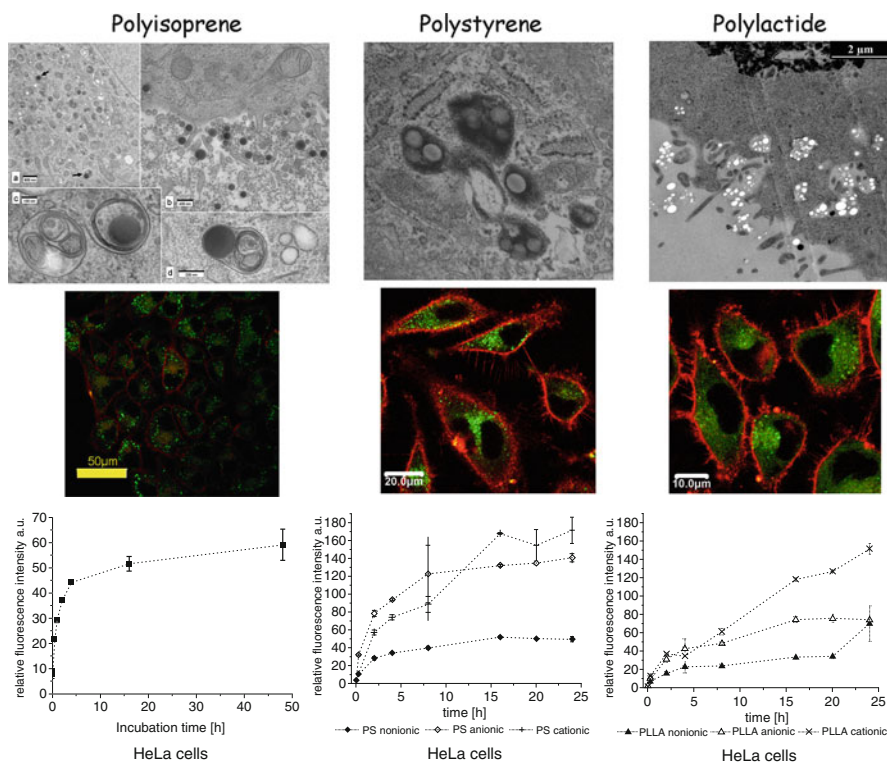


**Fig. 5** TEM and confocal microscopy after the uptake of different polymeric particles into HeLa cells; the FACS data show the differences in the uptake time (dependent on the polymer type and the type of the surfactant (non-ionic, cationic or anionic) [33,34,37]

polyisoprene particles are localized as single particles in endosomes, distributed throughout the entire cytoplasm. The uptake kinetics shows that particle uptake starts during the first minutes of incubation and finishes after 48 h of incubation. Since (non-functionalized) PS particles are internalized slower and to a far lesser extent, the uptake rates can be tuned by the amount of polystyrene in polyisoprene/polystyrene copolymer particles. As polyisoprene nanoparticles are taken up by different cell lines that are relevant for biomedical applications, they can be used to label these cells efficiently after incorporation of a marker in the nanoparticles [34].

It could be shown that PBCA particles are also internalized by HeLa, Jurkat, and mesenchymal stem cells (MSCs); however, the cellular uptake kinetics are different for HeLa and Jurkat cells (see Fig. 6) [35, 36]. While the particle size has a significant impact on particle uptake in HeLa cells, Jurkat cells are more sensitive towards surface functionalization. Especially the methoxypoly(ethylene glycol) (MePEG)-functionalized particles are internalized to a lesser extent than the rest of the investigated particles (non-functionalized, phenylalanine-functionalized).

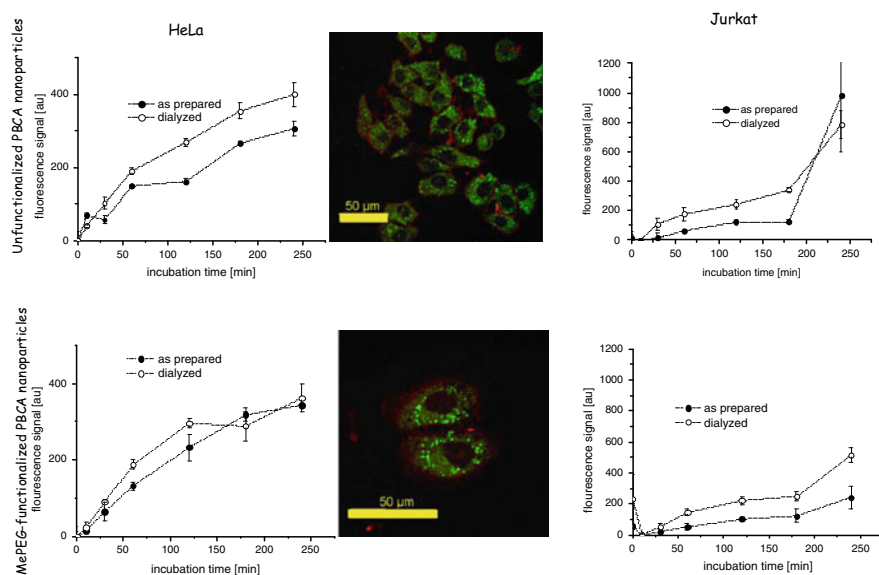


**Fig. 6** Uptake data for unfunctionalized and MePEG-functionalized PBCA nanoparticles in different cells, HeLa and Jurkat cells [35,36]

Intracellular distribution of the particles is independent of the cell line and the particles' surface characteristics. The particles are distributed evenly throughout the cells and are additionally localized within the cells by confocal microscopy and transmission electron microscopy (TEM).

For PLLA particles in the size range of 80–210 nm, it could be shown that the surfactant (cationic, anionic, or non-ionic) on the particles' surface had a greater influence on endocytosis than the particle size (Fig. 5). Uptake kinetics revealed that the PLLA and PCL particles are endocytosed much faster than polystyrene particles of the same size range [37].

Dual reporter nanoparticles could be obtained by encapsulating a fluorescent dye in combination with magnetite nanoparticles (10–12 nm) in a hydrophobic PS or poly(styrene-*co*-acrylic acid) shell. The nanocomposite nanoparticles were synthesized by a three-step miniemulsion process (see also below) [38–40]. Finally, polymerization of the monomer styrene yielded nanoparticles in the range of 45–70 nm. By copolymerization of styrene with various amounts of the hydrophilic acrylic acid, the amount of carboxyl groups on the surface was varied. For biomedical evaluation, the nanoparticles were incubated with different cell types. The introduction of carboxyl groups on the particle's surface enabled the uptake of nanoparticles as demonstrated by the detection of the fluorescent signal by FACS and laser scanning microscopy. The quantity of iron in the cells that is required for most biomedical applications (like detection by magnetic resonance imaging) has to be significantly higher than achievable with conventional carboxy-dextran coated magnetite nanoparticles (see Fig. 7). An increase of the internalized iron amount can be accomplished by transfection agents like poly-L-lysine or other

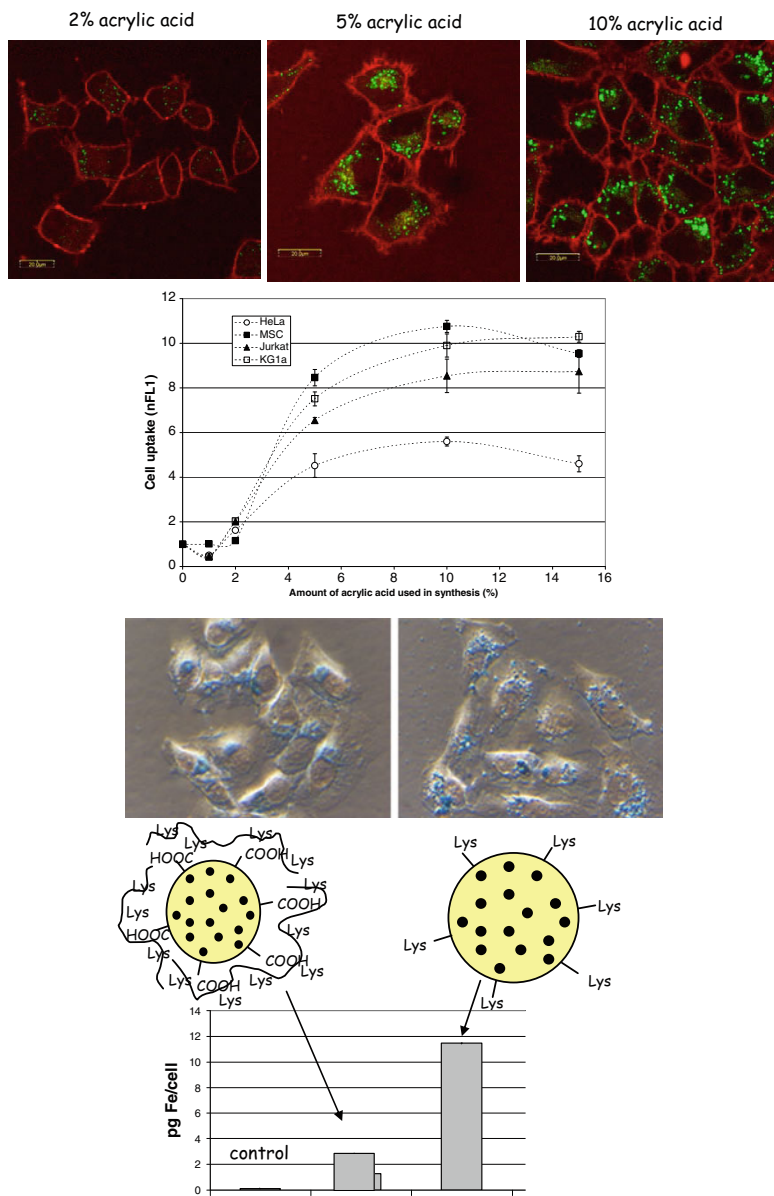


**Fig. 7** Dual reporter nanoparticles; uptake of magnetic/fluorescent nanoparticles with different acrylic acid contents (leading to different carboxylic surface densities) as detected by confocal microscopy (HeLa cells) and FACS measurements (different cell lines); the magnetite content was measured for PLL-coated nanoparticles in comparison with covalently coupled lysine (Lys) nanoparticles [38]

positively charged polymers. This functionality was also grafted onto the surface of the nanoparticles by covalently coupling lysine to the surface carboxyl groups. The amount of iron that can be transfected with these lysine modified nanoparticles was even higher than for the carboxy-functionalized nanoparticles with a physically adsorbed transfection agent. Furthermore, the subcellular localization of these nanoparticles was demonstrated to be clustered in endosomal compartments.

Also aiming at biomedical applications are nanoscaled hydrogels, prepared in inverse miniemulsion. In crosslinked poly(oligo(ethylene glycol) monomethyl ether methacrylate) (POEOMA) nanogels hydrophilic dyes as the polymeric dye (rhodamine isothiocyanate (RITC) dextran) [41], rhodamine in combination with the drug doxorubicin [42] or gold nanoparticles with bovine serum albumin [43] could be encapsulated.

Besides biomedical applications, encapsulated dyes were used for a variety of further studies and applications. Phthalocyanine dyes as well as styryl or azo dyes [44–46] were encapsulated in polymeric nanoparticles. Here, the aggregation state of the dye in the polymeric matrix and the “leaking” of the dyes, depending on their bulkiness, were examined. Diffusion from the composite particles into the aqueous phase of a so-called nanocolorant dispersion can be limited by either using a bulky dye, increasing the stiffness of the polymeric matrix (e.g. by crosslinking), or by synthesizing an impermeable shell around the particles [44].

The dye Sudan Black B, which is insoluble in the monomer and in the polymer, could be encapsulated by mixing Sudan Black B dissolved in methylisobutyl ketone with styrene and subjecting the mixture to a miniemulsion polymerization process. After polymerization and evaporation of the solvent, phase separation occurred and the solid dye was enclosed by a polymeric shell, which effectively protects the dye from photodegradation, induced by UV-activated oxygen [47]. As another dye, pyrene could be protected from oxygen quenching by encapsulating it in PMMA [48] or PS particles [49, 50]. Since no excimer emission is observed even with high concentrations in the PS nanoparticles [49, 50], it can be concluded that the molecules are molecularly dissolved in the polymer and are therefore efficiently separated from each other by the phenyl rings of the PS matrix, retaining the original luminescence properties of isolated pyrene.

The quenching of the luminescence of lanthanide complexes by the presence of water [51] can be suppressed by encapsulating lanthanide complexes such as, e.g., europium- $\beta$ -diketonato complexes (europium-(2-naphthoyl trifluoroacetone)<sub>3</sub>, (Eu(NTFA)<sub>3</sub>, and europium-(2-naphthoyl trifluoroacetone)<sub>3</sub>(trioctylphosphine oxide)<sub>2</sub>, (Eu(NTFA)<sub>3</sub>(TOPO)<sub>2</sub>), in polystyrene (PS) nanoparticles. The luminescence observed in aqueous dispersions and the increase of luminescence lifetime indicate protection from the environmental water [52].

The dyes solvent green, solvent yellow, solvent blue, and solvent red could be encapsulated in PMMA polymer particles [53, 54]. Phase separation occurred during the generation of the composite particles, to form dye crystallites encapsulated in a polymer [53]. Due to an interaction with the polymer, a small but significant bathochromic shift of the absorption maxima was observed [54].

By polymerizing poly(*N*-isopropylacrylamide) (PNIPAM) [55] or poly(2-(diethylamino)ethyl methacrylate) (PDEAEMA) [56] as a stimuli responsive polymer/hydrogel layer around a colored nanoparticle of PS-*co*-PMMA, the local refractive index and consequently the color intensity of the latex could be switched by the temperature [55] or pH [56].

Moreover, several photochromes of different structures (diarylethenes and spirobenzopyran) were successfully encapsulated in PS matrices to form composite nanoparticles [57]. Hybrid films were prepared by spin-coating and showed a reversibly switchable color change under irradiation with light.

Encapsulating two or more compounds in exact relative amounts allows the preparation of “photoswitches”. A boron-dipyrromethene (BODIPY)-based dye was co-encapsulated in with *cis*-1,2-bis(2,4,5-trimethyl-3-trienyl)ethane (CMTE), a photochromic dye [58]. Changes from the two-ring structure to the condensed three ring structure of CMTE could be switched forwards and back using UV light or visible light. The two-ring form does not interfere with the emission of the BODIPY dye, whereas the three-ring structure of CMTE efficiently quenches the fluorescence of the excited BODIPY dye. The switching efficiency is dependent on the distances between BODIPY and CMTE. Hence, at higher concentrations, the distance decreases and therefore the energy transfer is more efficient.

Photoswitchable fluorescent nanoparticles with further fluorescent dye/photochrome systems were prepared [59, 60] using a spirobenzopyran (BTF6), which was co-encapsulated with solvent green 5, disperse yellow 184 [60], and solvent yellow 44 [60]. The spectral overlap of the open-ring form of BTF6 with the emission wavelengths of the respective fluorescent dyes leads to a quenching of the encapsulated BTF6.

Dyes were also used to investigate the miniemulsion polymerization process, especially the droplet nucleation and particle formation [61–66]. Musyanovych et al. [67] investigated the particle formation process in miniemulsions containing styrene and the functional monomers aminoethylmethacrylate (AEMH) or acrylic acid (AA) in the presence of the nonionic surfactant Lutensol AT50. The fluorescent dye PMI was added to the monomer phase as probe. A bimodal particle size distribution was observed for functionalized latex particles when 1 wt% of acrylic acid or 3 wt% of AEMH as a comonomer was employed. Since the concentration of dye in the small and the large particles was the same, the bimodality was explained as a result of a budding process, which arises from the competition between amphiphilic polyacrylic acid (or polyAEMH) chains and Lutensol AT-50 on the early stage of polymerization (see Fig. 8). The UV-Vis results confirmed that the particle formation occurred inside the miniemulsion droplets, followed by a growth of the nuclei without the formation of new particles in the continuous phase via homogeneous nucleation.



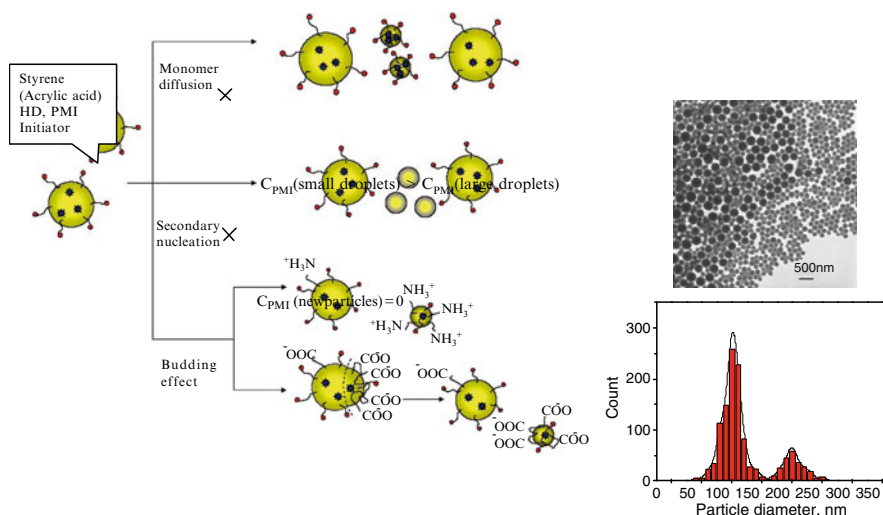


**Fig. 8** Dye distribution in nanoparticles after budding, diffusion, and homogeneous nucleation [67]

## 2.2 Encapsulation of Metal Complexes

Metal complexes which are soluble in the monomer phase can easily be encapsulated in nanoparticles with the above described procedure. In the case of hydrophobic metal complexes like platinum(II)acetylacetonate, indium(III)acetylacetonate, zinc(II)tetramethylheptadionate, zinc(II)phthalocyanine, and chromium(III)benzoylacetonate, different loading capacities and different sizes of the nanoparticles could be obtained. The preparation in miniemulsion allowed the formation of highly uniform and practically monodisperse latex particles, with the complexes homogeneously distributed in the nanoparticles. These nanoparticles were used for a novel approach of non-conventional nanolithography [68, 69]. The metal-complex loaded polymer nanoparticles of extremely narrow size distribution could be deposited in a highly ordered hexagonal array on hydrophilic Si substrates [68]. After deposition, the array was subjected to plasma and temperature treatment in order to remove the polymer and anneal the resulting metal particles. This process leads to a highly ordered array of platinum nanoparticles of about 10 nm according to the amount of metal-complex encapsulated in the polymer nanoparticles. Using the array of Pt nanoparticles as etching mask, an anisotropic reactive ion etching process was applied to transfer the particle pattern into the Si substrate, thereby obtaining ordered arrays of Si nanopillars. The hexagonal arrangement of the obtained 55 nm high, peaked Si nanopillars essentially reflects the symmetry of the Pt nanoparticles forming the initial etching mask [68]. The average diameter at half height of the pillars is about 6 nm resulting in an aspect ratio of nine. In order to “dig” nanoholes with a high aspect ratio into the Si substrate, the contrast of the etching masks has to be inverted. After obtaining Si-nanopillars by



the first reactive ion etching step, an intermediate Cr layer is evaporated with such a thickness, adjusted to avoid complete covering of the pillar sidewalls. Subsequently, the Cr-covered Si pillars are leveled off by chemomechanical polishing. Finally, the remaining Si stumps are selectively removed by a second anisotropic reactive ion etching step using the identical  $\text{CHF}_3/\text{CF}_4$  treatment as described above, resulting in the desired cylindrical nanoholes within the Si substrate. The almost cylindrical holes exhibit a depth of 180 nm and diameter of about 30 nm after an etching time of 90 min (see Fig. 9).

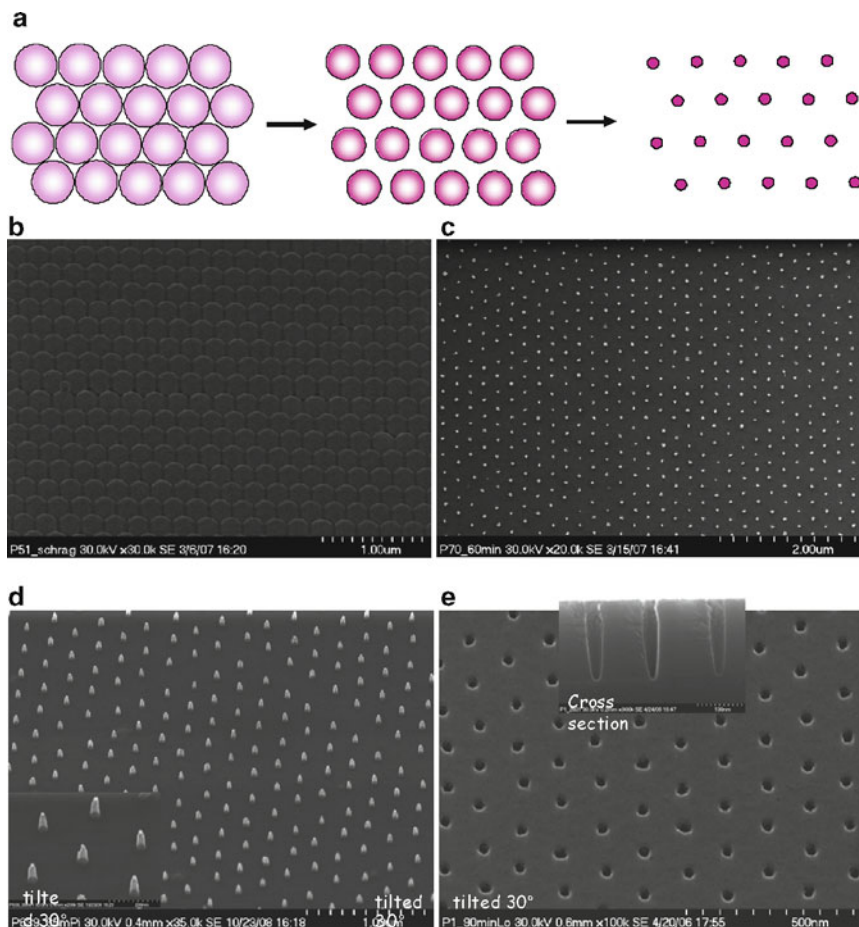


**Fig. 9** (a) Scheme of the unconventional nanolithography process with metal complex-containing nanoparticles; (b) Pt-complex containing latex after depositing a monolayer onto a silicon substrate; (c) same substrate after exposing the deposited latex to an isotropic oxygen plasma for 2 h, and subsequently annealing the sample up to 850 °C for a short period of time. The initial diameter of the latexes is 200 nm; the final diameter of the Pt-nanoparticles is around 10 nm; (d) formation of nanopyllars, and (e) nanoholes [68]

Vancaeyzeele et al. [70] encapsulated unsymmetrical lanthanide- $\beta$ -diketonato [lanthanide tris(4,4,4-trifluoro-1-(2-naphthyl)-1,3-butanedione)] complexes (Pr, Ho, La, Tb, Eu) in crosslinked polystyrene nanoparticles. They found that the entire amount of the complex is encapsulated in the nanoparticle. Both single element and multi-element particles of different sizes were obtained. The lanthanide content of the particles was determined by inductively coupled plasma mass spectrometry (ICP-MS) and optical emission spectrometry (ICP-OES). The particles were used to quantify the amount of differently sized element-encoded particles in different, clinically relevant cell lines.

Using neutral, inert inner shell lanthanide tris(2,2,6,6-tetramethyl-3,5-heptanedionato) (tmhd<sub>3</sub>) complexes such as Gd(III)tmhd<sub>3</sub>, Ho(III)tmhd<sub>3</sub>, or tris(6,6,7,7,8,8,8-heptafluoro-2,2-dimethyl-3,5-octanedionato)europium(III) (Eu(III)fod<sub>3</sub>), which are known as nuclear magnetic resonance (NMR) shift reagents and monomers such as butylacrylate in a miniemulsion polymerization process, the spontaneous formation of highly organized layered nanocomposite particles, resembling “nano-onions,” was observed [71]. The lamellar structures were thoroughly investigated by electron microscopy and small angle X-ray scattering (see Fig. 10). The nanocomposite comprises a lanthanide complex phase and a polymer phase with a lamellar repeat period of about 3.5 nm, rather independent of the system composition. Although the exact mechanism of the layer formation and the exact composition of the layers remain a piece of ongoing research, some facts became evident. The special triangular-prismatic geometry of the complex, which gives access to further coordination sites, seems to play a crucial role in structure formation, as the corresponding octahedral Al(tmhd)<sub>3</sub>-complex did not induce structure formation. It has been speculated whether either the complexes themselves assemble

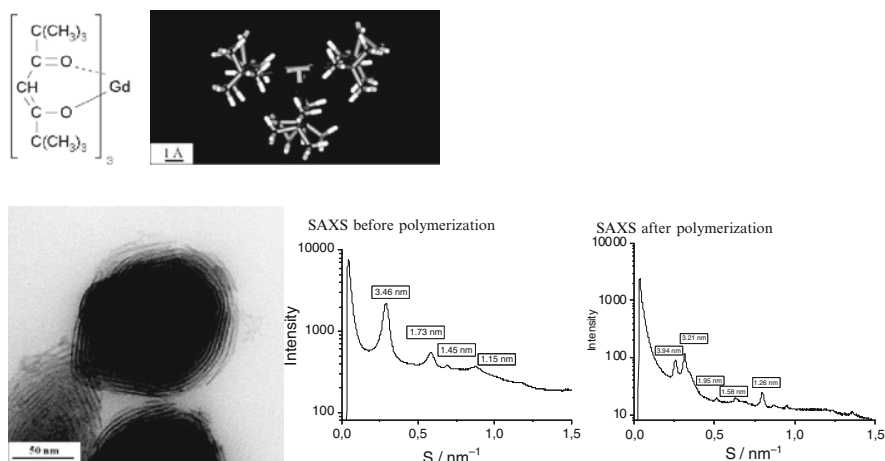


**Fig. 10** The formation of nano-onions by using inert inner shell lanthanide complexes; detection by TEM and XRD [71]

to the layer structures or coordinative interactions between the carboxy-functions of the acrylate monomers or sodium dodecyl sulfate (SDS) and the lanthanide ions generate entities assembling to lyotropic sub-phases.

### 3 Encapsulation of Solid Materials

In addition to molecularly distributed compounds, the material can also be encapsulated as aggregate, crystal, etc., as is the case for the encapsulation of pigments and, for thermally labile azo-components, photoinitiators, and highly fluorescent quantum dots in polymeric nanoparticles by using the miniemulsion process.

The encapsulation may fulfil several tasks:

- The material is protected by the polymer (quantum dots, magnetite, silica)
- The material can act as marker and the nanoparticle can be further functionalized (magnetite, quantum dots)
- The material can be released under defined conditions (e.g., photoinitiator)
- Dispersions containing the encapsulated material show improved stability against aggregation (e.g., pigments, carbon black, etc.)
- After film formation, the material is embedded in the polymer and homogeneously distributed (as aggregates) all over the film (pigments)
- Improved mechanical properties are obtained after film formation (silica)
- Gas permeation is reduced through reinforced polymer films (clay)

Since most of the inorganic materials are hydrophilic, the surfaces have to be hydrophobized prior to encapsulation. Then the material can be dispersed in the monomeric phase and a miniemulsification process can be performed in order to obtain nanodroplets containing the insoluble material (see Fig. 11a). However, with increasing amount of the dispersed material in the monomer phase, in many cases the viscosity becomes too high for an efficient dispersion in order to generate a miniemulsion. In this case, the so-called co-sonication process can be used which is suitable for, e.g., organic pigments or magnetite (see Fig. 11b). In the following section, several examples are presented to illustrate the principle, the limitations, and the possibilities for the formation of homogenous hybrid nanoparticles.

#### 3.1 Organic Pigments and Carbon-Based Materials

Organic pigments such as, e.g., carbon black, phthalocyanines, or azo-based dyes are widely used in industry. Due to their high specific surface area, they tend to aggregate. Additionally, for printing applications, a polymer is required which forms a film after the printing process. Therefore, a successful application requires separated pigment particles encapsulated in a polymeric shell. Formulating the systems in water-based miniemulsions leads to water-based dispersions.

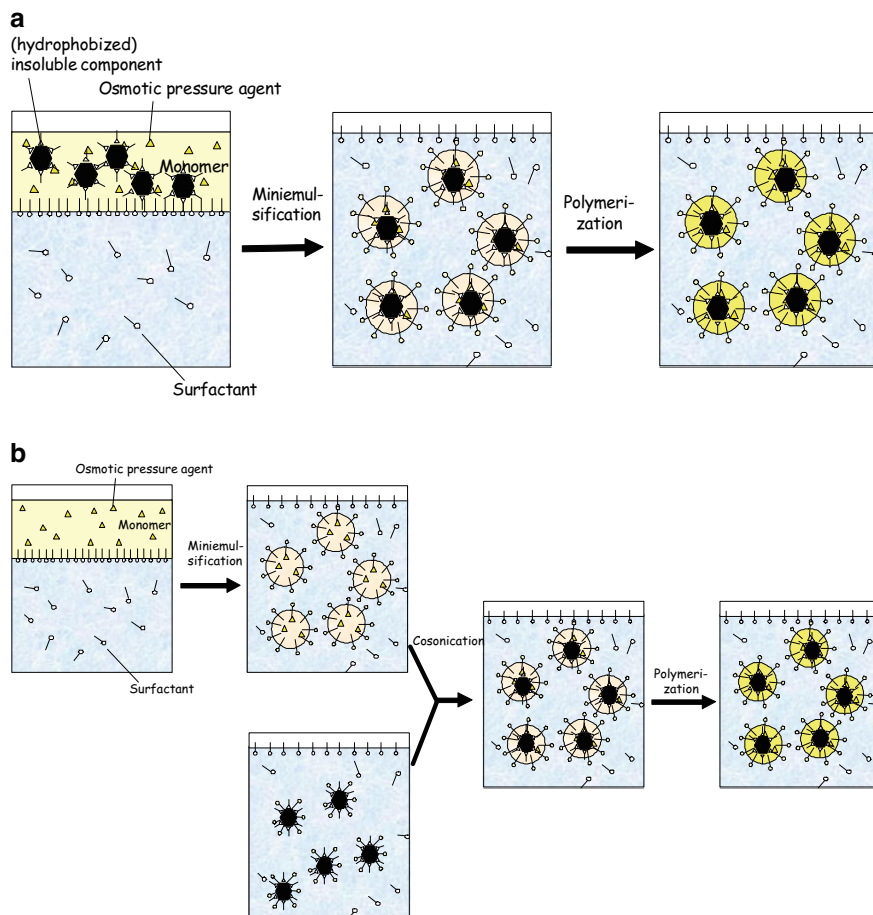


**Fig. 11** (a) Encapsulation of insoluble material (*black*) in miniemulsion. The hydrophobic or hydrophobized insoluble material is dispersed in the monomer phase. This dispersion is subsequently homogenized forming droplets in aqueous surfactant solution. (b) By polymerization, composite nanoparticles are generated in the cosonication process; the monomer miniemulsion and a dispersion of the hydrophobic or hydrophobized insoluble materials are prepared separately in an aqueous phase and mixed together followed by a sonication step leading to an encapsulation of the insoluble material in the monomer droplets. The hybrid droplets are subsequently polymerized in order to obtain the hybrid nanoparticles

Direct dispersions of carbon black or organic pigments in the monomer (e.g., styrene) are possible; however, a limited pigment content of about 10 wt% in the monomer phase can be used for further processing due to a drastic increase of the viscosity of the organic phase, making it difficult to disperse this phase in aqueous media. Thus, only less than 10 wt% [72, 73] of the pigment can be dispersed in styrene and formulated as miniemulsion. A great improvement with respect to the amount, which can be encapsulated, is offered by the so-called co-sonication process

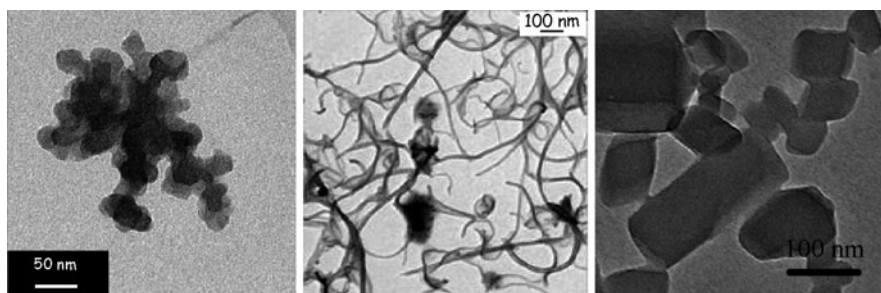


**Fig. 12** Encapsulate of materials by the cosonication process: (a) carbon black in PS [75]; (b) nanotubes in PS; (c) azo-pigment in PS [74]

(see Fig. 11b). Instead of directly dispersing the pigment in the monomer, in the first step of the process, a dispersion of the respective pigment in water is generated using a surfactant [74]. This dispersion is then mixed with a monomer miniemulsion stabilized with the appropriate surfactant. A fusion/fission process triggered by ultrasonication leads to an encapsulation of the hydrophobic or hydrophobized pigment into the monomer droplets. During the incorporation of the pigment in the monomer droplets, surfactant desorbs from the pigment as monitored by surface tension measurements [75]. Subsequent polymerization of the monomer allows the formation of hybrid nanoparticles.

Initially developed for carbon black [75], this technique was also successfully applied for other organic pigments (see Fig. 12) [74]. Surface functionalization for the adhesion process to different substrates was either obtained by physically adsorbed surfactants, as the anionic SDS, the cationic cetyltrimethylammonium chloride (CTMA-Cl), or the non-ionic Lutensol AT50, or by copolymerizing styrene or acrylates with functional comonomers.

It is interesting to mention that the presence of the pigments can significantly change the polymerization kinetics. Retardation of the reaction rate of styrene polymerized on the surface of azo-pigment particles can be attributed, e.g., to the interaction of radical species with nitrobenzene fragments. In the case of quinacridone pigments, a remarkable inhibition period was observed.

Using the cosonication process, the ratio pigment to polymer can be varied in a wide range and allowed the formation of hybrid particles with up to 80 wt% of pigment. The successful encapsulation could be shown by TEM and, in the case of using carbon black, with nitrogen sorption measurements. As the carbon black exhibits a high inner porosity, a successful encapsulation dramatically reduces the specific surface area, which is accessible for nitrogen. After encapsulation, only the surface-provided polymer can be measured [75].

The pigment itself cannot take over osmotic droplet stabilization as the number of aggregates is too low to be able to create a significant osmotic pressure. In addition to its original task of establishing an osmotic pressure to avoid diffusional degradation, the ultrahydrophobic components serve as mediator between the pigment surface and the monomer or the resulting polymer. For carbon black,

hexadecane, Jeffamine M2070, or M1000 [72], as well as a oligourethane-derived costabilizer [75] led to stable dispersions with uniform hybrid particles. In the case of phthalocyanine-based pigments, hexadecane or hexadecanol were shown to be efficient ultrahydrophobes, whereas the application of PS ( $M_n = 35,200 \text{ g} \cdot \text{mol}^{-1}$  and  $M_w = 65,600 \text{ g} \cdot \text{mol}^{-1}$ ) induced phase separation [73].

Other carbon-based, hydrophobic materials used for the encapsulation in polymeric nanoparticles are nanodiamond and single walled carbon nanotubes which could also be encapsulated in polymer shells. In particular, single wall carbon nanotubes (SWNTs) are considered to be very promising materials for novel electrode materials and highly effective reinforcements for polymeric systems. An actual application is difficult due to their tendency to aggregate, caused by the high surface area and  $\pi$ - $\pi$  interactions. The addition of surfactants allows one to obtain a slightly increased dispersions stability. However, the formation of a polymer shell is more efficient in order to prevent aggregation of the nanotubes. Since SWNTs have a length of several  $\mu\text{m}$  and miniemulsion droplets usually have diameter between 50 and 500 nm, it seems to be unrealistic to “fit” SWNTs into miniemulsion droplets. However, the monomeric material can spread on the nanotube surface as soon as a contact is ensured. Therefore, the miniemulsion polymerization can provide a platform for coating the SWNTs with polymeric material such as PS, PI, or their copolymers [76–79]. The observed structure can best be described as beaded-nano-rod [78, 80]. For the formation of the polymer-covered SWNTs, only SWNT dispersions which are stabilized with a cationic surfactant (e.g., cetyltrimethylammonium bromide CTAB) [76], or a combination of an anionic and a non-ionic surfactant (SDS and Igepal DM-970) [79], can be used. The preparation with anionic surfactants alone [SDS, 4-dodecylbenzenesulfonic acid (SDBS)] leads to unstable dispersions as the anionic surfactants tend to desorb from the carbon nanotubes in aqueous dispersions and they are therefore not suitable for the miniemulsion process [76, 77].

## 3.2 Encapsulation of Inorganic Materials

### 3.2.1 Encapsulation in Direct Miniemulsion

For many applications, the encapsulation of inorganic material is of high interest: either the inorganic components should be protected from the environment (e.g., air-sensitive components) or the environment from potentially toxic components, or polymeric films with improved color, mechanical, or gas diffusion properties, having finely distributed (and protected) inorganic material for coating applications, are desired. Furthermore, UV-blocking applications are reported [81–83].

Due to their often hydrophilic surfaces, inorganic components have to be hydrophobized in order to incorporate them in hydrophobic polymers. For the encapsulation in polystyrene shells, the surface of calcium carbonate was modified with stearic acid which allowed an encapsulation of about 5 wt% of the inorganic



material in the particles [72]. For the hydrophobization of alumina nanoparticles prior to the encapsulation process, oleic acid was used [84]. Carbon-coated silver nanoparticles (0.5 wt%) could be incorporated in PMMA nanoparticles, leading to an increase of the  $T_g$  by 14 °C [85]. Ag/polymer hybrid nanoparticles could also be obtained by using non-aqueous inverse miniemulsions with high boiling solvents which allowed the formation of silver nanoparticles in situ by the reduction of silver nitrate via the polyol route [86].

Titania nanoparticles were first surface-modified with polybutylene succinimide diethyl triamine (OLOA370) [87–91] and then 5 wt% of the hydrophobized material was dispersed in styrene prior to a miniemulsification process. About 89% of the titania could be encapsulated in 73% of the PS, but pure polystyrene particles were still detected. Another efficient compatibilizer for titania is Solsperse 32000, a polyamine/polyester. By modifying titania with this polymer, hybrid nanoparticles with PS and PS-*co*-polybutylacrylate (PS-*co*-PBA) could be generated [92–95].

For biomedical applications, fluorescing lanthanide-based nanocrystals [96] or semiconducting quantum dots can be encapsulated. Even though the quantum dots exhibit excellent fluorescent properties, the major drawback of these materials consisting of cadmium, selenium, or tellurium is their inherent toxicity, as the toxic ions can be dissolved in aqueous medium. Therefore, an efficient shielding of the toxic components from the environment is required. Thus, the encapsulation in polymeric matrices provides an excellent way to convert quantum dots (QDs) into a more biotolerable form. During the preparation of CdS or CdSe QDs, the nanocrystals are usually capped with trioctylphosphine oxide (TOPO), generating a highly hydrophobic shell which allows the direct dispersion of the QDs in the monomer and a subsequent miniemulsion polymerization procedure. Different coatings such as vinylmercaptobenzene [97] or hexadecylamine [98] neither interfere with nor improve the integration into the polymer. CdTe, stabilized by 3-mercaptopropionic acid, could be homogeneously incorporated in PS nanoparticles by using OVDAC (octadecyl-*p*-vinylbenzyltrimethylammonium chloride) or DVMAC (didecyl-*p*-vinylbenzyltrimethylammonium chloride) [97]. Another possibility to overcome the observed inhomogeneous distribution of QDs in polymeric particles is to generate a second polymeric layer on the QDs/PS hybrid nanoparticles, which can be created by seeded emulsion polymerization [98]. A polymerization from the QD surfaces was shown by Esteves et al. [99]. By coordinating a phosphine oxide-modified atom transfer radical polymerization (ATRP) starter to CdS-QDs, it was possible to generate a PBA shell around the nanocrystal. Performed in miniemulsion, the authors used the AGET (activator generated by electron transfer)-ATRP technique.

Silica nanoparticles are also hydrophilic and have therefore to be functionalized prior to encapsulation. Without functionalization, the negatively charged silica particles can be used as Pickering stabilizers, leading to hybrid nanoparticles with silica located on the surface of the nanoparticles (see Fig. 13a) [100].

Hydrophobized silica nanoparticles were obtained by adsorbing the cationic surfactant CTMA-Cl on the surface; subsequently the silica particles could be incorporated in polymer nanoparticles (Fig. 13b). Depending on the reaction conditions

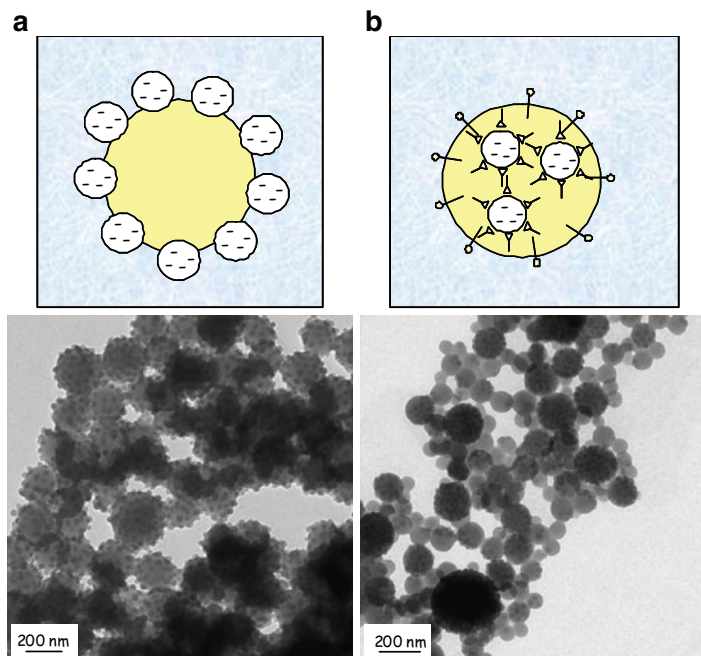


**Fig. 13** Scheme and TEM pictures of PS-*co*-P4VP/silica hybrid nanoparticles prepared with: (a) non-hydrophobized silica; (b) hydrophobized silica by CTMA-Cl [100]

(type of the surfactant or pH), several morphologies, like raspberry or hedgehog structures, can be realized. Due to their surface silanol-groups, silica nanoparticles can be very easily covalently modified with trimethoxysilanes bearing a wide variety of different functionalities. Various studies, especially investigating the influence of the size and the surface properties, have been conducted applying the miniemulsion polymerization technique.

Zhang et al. investigated the influence of the size of methacryloxypropyltrimethoxysilane (MPS)-modified silica nanoparticles on the morphology of PS/silica hybrid particles [101]. Using silica particles of 45 nm in size, 200-nm multicore hybrids were obtained. Reducing the particle size by increasing the amount of SDS led to the reduction of the number of encapsulated silica particles, eventually leading to single core-shell morphology. Single core-shell hybrids were obtained independently on the SDS concentration with 90-nm silica particles. It was found that 200-nm silica particles led to raspberry like structures with PS spheres attached to one silica bead. Comparable results were also obtained in a system with a PS/PBA copolymer matrix [102]. The successful encapsulation of at least 90% of the silica could be shown by the addition of HF which did not lead to a dissolution of the silica particles [103].

MPS-modified silica particles dispersed in styrene could be miniemulsified in water followed by a polymerization initiated by azodiisobutyramidine



dihydrochloride (AIBA). Adding titanium tetraisobutoxide to the system generated a thin titania shell around the silica/PS nanocomposites [104].

Anisotropic hybrid particles were obtained by using a miniemulsion with a dispersed phase of tetraethylorthosilicate (TEOS), styrene, and MPS, stabilized by CTAB. Styrene and MPS form a copolymer, while the addition of ammonia induces hydrolysis and condensation of TEOS to silica. During the reaction, phase separation of PS with the TEOS containing the silica is observed. The silica-containing TEOS droplets and PS particles are bridged by the PS-PMPS copolymer [105]. Asymmetric hybrids could also be generated by partial functionalization of silica beads with octadecyltrimethoxysilane (ODMS) at interfaces [106] or MPS at defined aggregates of silica beads. With this technique a great number of different morphologies could be realized by varying the ratio of monomer to silica [107].

Anisotropic PS/silica hybrids containing two different fluorescent labels were reported [108] as suitable particles for biomedical applications. While the carboxy-functionalized PS part served as anchor for green fluorescing NHS-FITC, the amino-functionalized silica part was functionalized with red fluorescing TRITC. The asymmetric distribution was confirmed by confocal laser scanning microscopy.

Attaching initiators onto the silica surfaces allows controlled radical polymerization, either nitroxide mediated polymerization (NMP) [109] or ATRP [110] resulting in core-shell particles.

Besides styrene, MMA, BA, or their copolymers, and also less commonly used polymers such as poly(styrenesulfonic acid) (PSSA), poly(hydroxyethylmethacrylate) (PHEMA), poly(aminoethylmethacrylate) PAEMA [111], polyethylene (PE) [112], or polyamides [113], were used for the encapsulation of the silica, as reported in the literature. Polyethylene [112] could also be obtained as encapsulating polymer if a nickel-based catalyst which is dispersed in the aqueous continuous phase is used. Here, lentil-shaped hybrid particles with semicrystalline polyethylene or isotropic hybrid particles with amorphous polyethylene are detected. Silica/polyamide hybrid nanoparticles were synthesized by miniemulsifying a dispersion consisting of 3-aminopropyl triethoxysilane (APS) modified silica particles and sebacylchloride [113] in an aqueous continuous phase where hexamethylene diamine is dropwise added.

More challenging for the encapsulation in polymeric shells are clays which are layered silicates with a thickness of 1 nm and several tens to hundreds of nm in lateral extension. The integration of such clay platelets into polymeric films is of high interest since the inorganic component improves mechanical properties and, due to their flat disc-like shape, greatly reduces gas permeation through polymeric films. A hydrophobization of the clay platelets can be obtained by exchanging the metal ions with hydrophobic quaternary ammonium salts as CTAB, CTMA-Cl, or functional quaternary ammonium salts as 2-methacryloyloxyethyl hexadecyldimethyl ammonium bromide (MA16) [114]), for the introduction of polymerizable groups which can act as initiator [115] for polymerization reactions. Most widely used are the naturally occurring montmorillonite [114, 116–120] or saponite [121, 122] minerals as well as commercially available Cloisite [114, 115, 123, 124] (organo-modified montmorillonite) or the synthetic Laponite RD [125].

The hydrophobized clay can be directly dispersed in monomers and subjected to miniemulsion polymerization. Due to the formation of thixotropic gels and therefore high viscosities, the concentration of clay in the monomer is limited to about 4% [121]. Tong et al. [126] could successfully disperse 30 wt% of modified saponite in styrene by modifying the clay with (ar-vinylbenzyl)trimethylammonium chloride (VBTAC) which is used as comonomer for styrene or acrylates. The dispersion in styrene was of low viscosity and therefore suitable for the miniemulsification process.

Using NMP [114, 115] or reversible addition–fragmentation chain transfer (RAFT) [119, 120, 127], agents with ammonium groups for the ion exchange allowed the attachment of initiators on the clay surface for controlled radical polymerizations (NMP, RAFT). Samakande et al. investigated the kinetics of RAFT-mediated living polymerization of styrene [120] and styrene/BA [119] mixtures in miniemulsion.

Of special interest for biomedical applications as cell separation, hyperthermia, magnetic resonance imaging (MRI) contrast enhancement, or magnetic drug targeting are superparamagnetic particles. Due to the non-toxicity, mainly magnetite ( $\text{Fe}_3\text{O}_4$ ), or maghemite ( $\gamma\text{-Fe}_2\text{O}_3$ ) are used. In order to prevent them from aggregation, a stabilizing layer is required; additionally, this layer can also shield the encapsulated material from the aqueous environment in order not to be degraded and metabolized since a fast degradation in the organism might induce toxic effects. Therefore, it is of great interest to create highly hydrophobic iron oxide containing nanoparticles. Since magnetite is hydrophilic, first a hydrophobization of the magnetite nanoparticles is required. In most of the cases, oleic acid was used, but also stearic acid has been reported. Covalent functionalization of the magnetite surface could be obtained by using silanes (aminopropyltrimethoxysilane or 3-methacryloxypropyltrimethoxysilane) [128, 129]. Coating magnetite nanoparticles with the surfactant sodium 1,2-bis(2-ethylhexoxycarbonyl)ethanesulfonate (AOT) and dispersing them directly in styrene led to an inhomogeneous distribution of magnetite in the hybrid system [130, 131] with pure PS nanoparticles as well as polymeric particles partially covered with magnetite. Moreover, in the case of using a phosphate-based dispersant (Disperbyk 106, organic amine salt composed by the phosphate partly esterified and organic amine) for stabilizing the magnetite in the monomer [128, 132], an inhomogeneous magnetite distribution in the particles was found. Additionally, the magnetite seems to be located on the polymer particle and not inside. A one-pot-reaction with maghemite nanoparticles, fluorescent pigment, polyester resin, Tween80, Span80, azo-bis-(isobutyronitrile) (AIBN), and styrene dispersed in an aqueous NaOH solution led to the formation of ferromagnetic hybrid nanoparticles [133]. The hydrophobization of magnetite with the Y-shaped surfactant 12-hexanoyloxy-9-octadecenoic acid [134] in combination with hexadecane as osmotic pressure agent allowed the encapsulation of up to 60 wt% of magnetite in polystyrene nanoparticles.

The formation of uniform nanoparticles with high amounts of magnetite can be obtained most successfully by the three-step process involving the co-sonication procedure (see Fig. 14) [135, 136]. In the first step, magnetite (10 nm) nanoparticles are formed by precipitation from a ferrous and ferric chloride solution

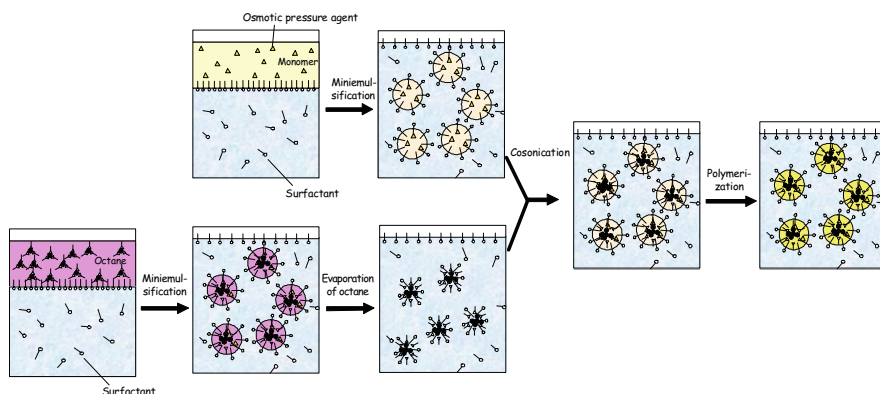


**Fig. 14** Encapsulation of magnetite nanoparticles

and hydrophobized by oleic acid. Alternatively, Wuestite particles (25 nm) can be obtained by decomposition of iron oleate. In a second step, the hydrophobized magnetic nanoparticles are dispersed in octane and this dispersion is miniemulsified in water by using sodium dodecyl sulfate as surfactant. After evaporation of octane, SDS stabilized magnetite or Wuestite aggregates in water are obtained which can then, in a third step, be added to a monomeric miniemulsion. By cosonication the aggregates and the monomer droplets are merged and the droplets containing monomer and the iron oxide aggregates can subsequently be polymerized, resulting in polymeric nanoparticles containing magnetic particles.

Using this process, more than 40 wt% of 10-nm magnetite could be successfully encapsulated in polystyrene with a highly homogeneous distribution of magnetic nanoparticles. The saturation magnetization, decreased from  $87 \text{ emu} \cdot \text{g}^{-1}$  for iron oxide to  $53 \text{ emu} \cdot \text{g}^{-1}$  as also reported by other groups [137–139], might be caused by partial oxidation or change in the crystal structure on the magnetite nanoparticle's surface. In the case of crosslinked, magnetic PMMA nanoparticles which were prepared by using a hexane-based ferrofluid [140], less than 8 wt% of magnetite were encapsulated leading to magnetic nanoparticles with a saturation magnetization of about  $4 \text{ emu} \cdot \text{g}^{-1}$ .

The homogeneity of the distribution of the magnetic nanoparticles in the polymer particles depends on different parameters. Dispersing the hydrophobized magnetite in styrene/MAA [141] or a toluene-based ferrofluid [142] in styrene leads to magnetite/polymer particles with inhomogeneous iron oxide distribution. The initiator has a further significant influence. Whereas, in the case of using the water soluble initiator potassium peroxodisulfate (KPS) with or without AIBN in combination, the magnetite is homogeneously distributed in the polymeric matrix [143] and no magnetite is located on the particle surface, the use of AIBN as sole initiator leads to a hemispherical aggregate of magnetite, which is located at the particle surface. An ultrasonic initiation of styrene polymerization [144, 145] resulted in hybrid particles, but pure polymer nanoparticles were also found. The addition of the crosslinker divinyl benzene (DVB) enhanced the homogeneity of magnetite distribution since a

diffusion in crosslinked structures is hindered, preventing a phase separation of the magnetic nanoparticles onto the nanoparticle surface [146].

To improve the encapsulation efficiency, the hydrophobicity of oleic acid-coated magnetite was increased by depositing the oleic acid in the form of a monolayer with free hydrocarbon chains [147]. Extremely high magnetite contents of 86 wt% in styrene particles could be achieved by preparing the hybrid particles with a combined miniemulsion/emulsion system [148]. Initially a miniemulsion of a ferrofluid consisting of magnetite coated with oleic acid and undecylenic acid in octane was prepared. A styrene “macroemulsion”, which was prepared by membrane emulsification using an SPG-membrane (Shirasu porous glass), was added dropwise to the previously prepared miniemulsion. The larger styrene droplets act as a reservoir, from which the monomer can diffuse to the miniemulsion droplets and polymerize there.

By adding comonomers to styrene and applying the co-sonication method, surface-functionalized magnetic PS nanoparticles were obtained [38, 39]. For this purpose, styrene was copolymerized with a defined amount of acrylic acid creating carboxy functions on the particle surface, which could subsequently be covalently functionalized by lysine or by physical adsorption of the commercial transfection agent poly(L-lysine) (PLL). It could be shown that lysine-functionalized particles are highly efficiently internalized by cells (see also above). The extent of cellular uptake even exceeds the internalization of poly(L-lysine)-functionalized particles. Such nanoparticles can be used as excellent markers in magnetic resonance imaging experiments. The additional incorporation of a fluorescent marker (e.g., PMI [38–40] or QDs [149]) into the magnetic PS-particles leads to dual marker particles with the additional possibility of optical particle tracking using fluorescence microscopy.

A carboxy-functionalization of magnetic nanoparticles for further bioconjugation could also be obtained in magnetic poly(ethylmethacrylate) (PEMA) particles by copolymerizing EMA with acrylic acid [150, 151], or by using 4,4'-azo-bis(4-cyanopentanoic acid) (ACPA) as initiator [152].

Non-spherical, surface-imprinted magnetic PMMA nanoparticles could be prepared in a miniemulsion process preparing magnetite/PMMA nanoparticles on which proteins were either immobilized by adsorption (RNase A) [153] or covalently (bovine serum albumin, BSA) [154]. After creating a shell of PMMA, the proteins were removed, leaving cavities on the particles' surface. The BSA-imprinted nanoparticles showed superparamagnetic properties and exhibited a high rebinding capacity for BSA.

Anchor groups could also be introduced by copolymerizing styrene with vinyl acetate and subsequently treating the system with ethanolic NaOH for the hydrolysis of the ethyl ester groups [155]. The conjugation of mercaptonicotinic acid with divinylsulfone introduced a highly specific ligand for the recognition of IgG antibodies. After magnetic separation of the magnetic nanoparticles from IgG containing serum, the antibody could be isolated with >99% bioactivity purity.

By hydrolyzing the methylester groups on the surface of magnetic PMMA nanoparticles, carboxylic acid groups were created which were subsequently

esterified with poly(ethylene glycol). The poly(ethylene glycol) PEG could then be further functionalized with a reactive dye (Cibacron Blue F3G-A) [140].

Emulsifier-free miniemulsion polymerization with [2, 2-azobis (2-amidinopropane) dihydrochloride (V50)] as initiator was also used for the encapsulation of oleic acid/magnetite nanocrystals in styrene [156, 157] or chloromethyl-styrene for further functionalization [158].

Shao et al. reported the preparation of all-inorganic magnetic hybrid nanoparticles by encapsulating oleic acid-coated magnetite in silica [159]. First, a ferrofluid consisting of hydrophobized magnetite in TEOS was prepared, which was subsequently miniemulsified in water. Hydrolysis and condensation of TEOS to silica was initiated by the addition of ammonia to the miniemulsion, leading to the formation of amorphous silica particles with up to 30 wt% magnetite content. The nanocomposites were successfully used for DNA separation under high ionic strength solutions. The plasmids readily adsorb to the silica surface while the magnetite enables magnetic separation.

If preformed polymers are used for the encapsulation of magnetic nanoparticles, a combination of miniemulsion and emulsion/solvent evaporation techniques

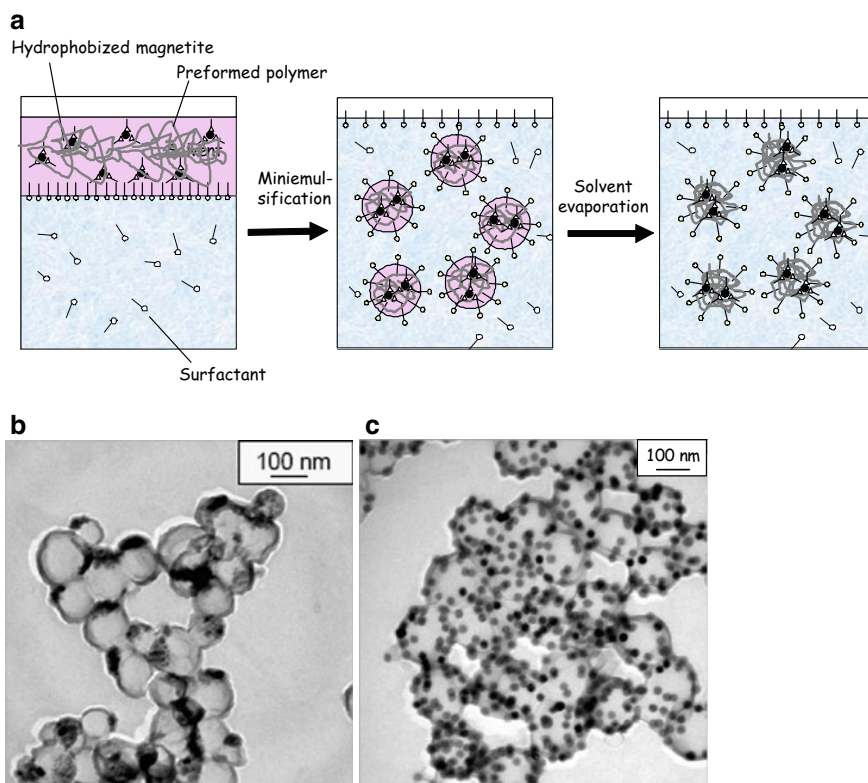


**Fig. 15** (a) Emulsion/solvent technique; TEM images of PLLA particles with (b) 10 and (c) 25 nm iron oxide (50%) particles in PLLA [49]

can be applied (see Fig. 15a). This way, hybrid PLLA nanoparticles with an average diameter between 80 and 100 nm containing encapsulated 10 nm magnetite particles were obtained. A magnetite content of up to 16.4 wt% related to the amount of solid could be achieved (see Fig. 15b). The introduction of 25-nm magnetic particles resulted in slightly bigger, approximately 120-nm, hybrid PLLA particles, which can be attributed to the higher viscosity of the organic phase caused by the usage of larger molecular weight preformed polymer. In the case of loading 10-nm magnetite (independent of the concentration), the distribution of nanoparticles within the polymeric matrix is quite heterogeneous. A homogenous distribution of 25-nm iron oxide nanoparticles was obtained when higher amounts of hydrophobic iron oxide (20 and 50 wt%) were used (see Fig. 15c). The proposed approach results in the efficient formation of narrowly sized biodegradable polylactide nanoparticles. These particles are of regular shape, show high stability in an aqueous phase, possess good magnetic properties, and have the ability to incorporate hydrophobic molecules (e.g., drug). In this regards, they are ideal candidates for magnetically targeted drug delivery.

### 3.2.2 Encapsulation in Inverse Miniemulsion

The encapsulation of superparamagnetic iron oxide nanoparticles in hydrophilic polymer shells can very easily be accomplished by using an inverse miniemulsion polymerization process. The polymer increases the stability of the magnetite and leads to the particles within the biologically interesting size range between 100 and 200 nm. Hydrophilic polymers (e.g., poly(methacrylic acid) (PMAA)) [160] or “double hydrophilic” block copolymer PEO-PMAA [161] are used for the formation of hydrophilic magnetic nanoparticles. Interestingly, the magnetite nanoparticles precipitated in the presence of PEO-PMAA are significantly smaller (5 nm) than nanoparticles prepared in the presence of either PEO or PMAA, which are each around 10 nm. The PEO-PMAA coated particles could easily be dispersed in hydroxyethylmethacrylate/acrylic acid (HEMA/AA). After miniemulsification of the ferrofluid in a poly((ethylene-*co*-butylene)-*b*-ethylene oxide) (P(E/B-EO))-decane solution, the monomer droplets were thermally polymerized to yield fairly monodispersed nanoparticles between 140 and 220 nm with an iron oxide saturation magnetization of about 60 emu per g iron oxide.

PMAA- or citrate-coated magnetite [160] or citrate-coated maghemite [162] nanoparticles could successfully be encapsulated in a crosslinked polyacrylamide matrix using an inverse miniemulsion process. Here an inert hydrocarbon (cyclohexane or dodecane) was used as continuous phase and Span80 as stabilizer.

By adding TEOS to a miniemulsion of magnetite-PMAA/water dispersed in Span80/cyclohexane, silica/magnetite hybrid nanoparticles with about 19 wt% magnetite could be generated [163]. Thermoresponsive P(NIPAM-*co*-MAA) could be obtained by using PAA-coated magnetite nanoparticles in an inverse miniemulsion polymerization process [164].



## 4 Encapsulation of Liquids

Nanocapsules can be formulated from a variety of synthetic or natural monomers or polymers by using different techniques in order to fulfil the requirements of various applications. Both, hydrophobic and hydrophilic liquids are of high interest for encapsulation. So, e.g., either sensitive or volatile substances, as drugs or fragrances have to be encapsulated and protected for applications with a sustained demand of the respective compound. DNA, proteins, peptides or other active substances can be encapsulated in order to target them to specific cells. A further benefit of the polymeric shell is the possibility to control the release from the composite particles and hence the concentration in the environment.

Besides the layer-by-layer technique, which can be applied with or without the use of sacrificial cores [165, 166] and usually requires polyelectrolytes, the miniemulsion technique is a highly suitable and versatile method for the formation of capsule formation with sizes down to 100 nm. Even the formation of inorganic capsules (e.g., [167]) by the miniemulsion polymerization is possible. For the formation of polymeric nanocapsules, three general approaches (see Figs. 16, 17, and 23) can be distinguished:

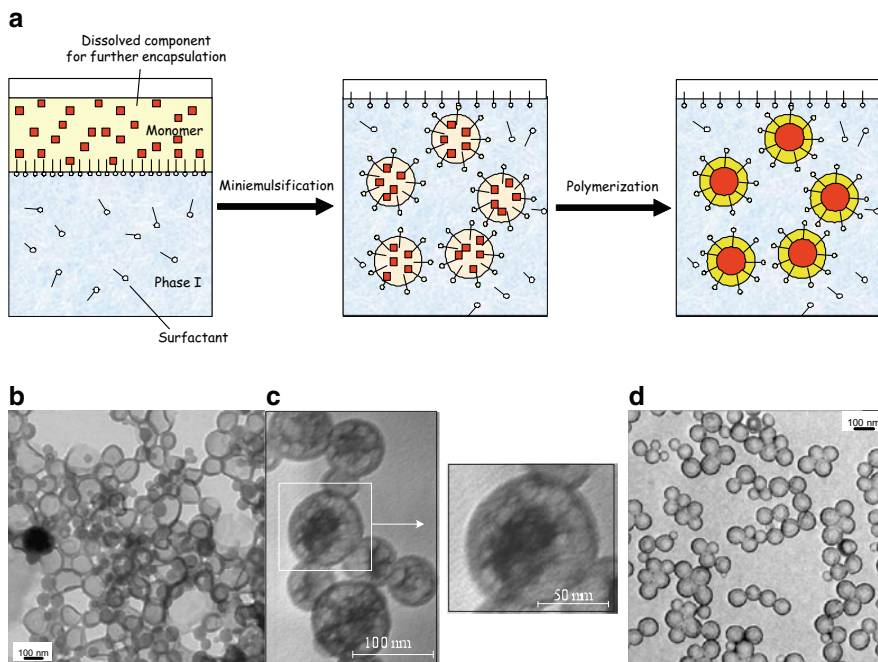


**Fig. 16** Capsule formation by phase separation. **(a)** Scheme: a solution of monomer and hydrophobic oil (*left*) is dispersed in an aqueous surfactant solution (*middle*). Phase separation between the growing polymer and the oil occurs, leading to core shell morphology with encapsulated liquid. **(b)** Nanocapsules with hexadecane by phase separation [35]. **(c)** Encapsulation of Lucirin TPO [173] and **(d)** the fragrance 1,2-dimethyl-1-phenyl-butylamide [174]

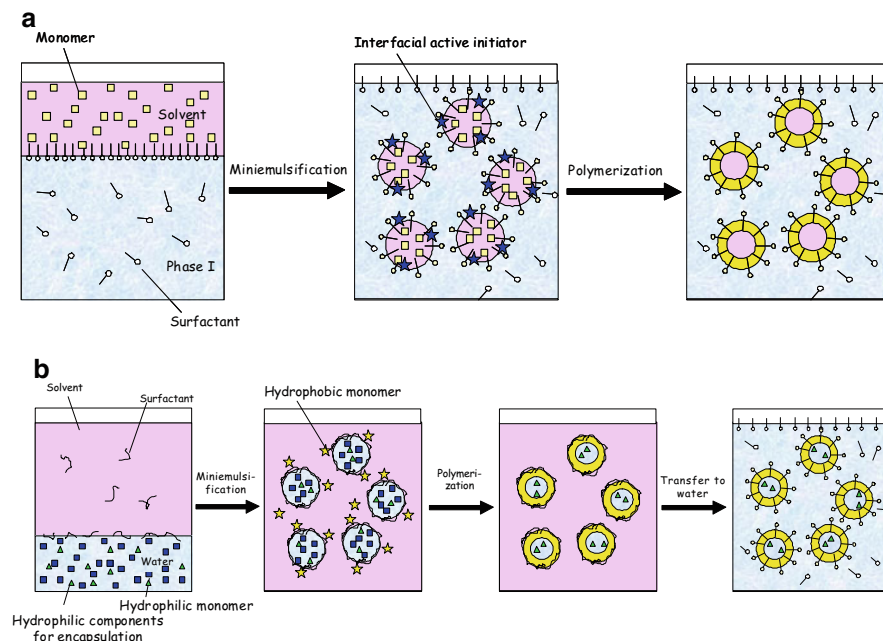


**Fig. 17** For maton of polymeric nanocapsules (a) by interfacial reaction in direct miniemulsion and (b) interfacial polyaddition in inverse miniemulsion

- Formation of polymeric nanocapsules by phase separation
- Formation of polymeric nanocapsules by an interfacial reaction
- Formation of nanocapsules by nanoprecipitation of polymer on preformed nanodroplets

### 4.1 Capsule Formation by Phase Separation

The formation of nanocapsules by a phase separation process is suitable for the encapsulation of hydrophobic liquids in a hydrophobic polymeric shell. The dispersed phase of the direct miniemulsion consists of an organic liquid which represents a solvent for the monomer(s) but a non-solvent for the polymer. By tuning the surface tensions of the participating interfaces in the system, phase separation occurs in such a way that the non-solvent is engulfed by the growing polymeric shell, leading to complete encapsulation of the organic liquid. In the case of encapsulating hexadecane with PMMA, the large differences in hydrophilicity lead to capsules independent of the use of surfactants and comonomers (see Fig. 16). In the case of the more hydrophobic styrene, the copolymerization with hydrophilic monomers such as MMA, acrylic acid (AA) [168], methacrylic acid (MAA) [169],



or *N*-isopropylacrylamide (NIPAM) [170] led to the formation of a large fraction of capsules. Their properties such as size and shell thickness could be adjusted by changing the hexadecane to monomer ratio.

Capsule morphologies could also be observed in a system applying the biodegradable surfactant lecithin and the eco-friendly hydrophobe Neobee M5 (triglyceride) [171] and, after controlled radical copolymerization of styrene and divinyl benzene (DVB), stabilized by poly(vinylalcohol) (PVA) [172].

The acid sensitive photoinitiator Lucirin TPO could effectively be shielded from an acidic environment by encapsulating it into PMMA or PBA-*co*-PMMA particles [173]. The hybrid particles show a core-shell morphology (Fig. 16c) which is generated by phase separation during the polymerization process. While the photoinitiator is readily soluble in the monomer(s), it becomes insoluble in the polymer. Therefore, Lucirin TPO precipitates during the polymerization and forms an amorphous core surrounded by a polymeric shell. The encapsulation efficiency was determined as about 90%.

The encapsulation of the volatile fragrance 1,2-dimethyl-1-phenyl-butyramide (DMPBA) in PS, PMMA, poly(butylmethacrylate) (PBMA), and copolymers was shown by Theisinger et al. [174]. The combination of TEM (see Fig. 16d) and DSC experiments suggest that, up to a DMPBA content of about 25 wt%, the particles consist of a matrix composed of the fragrance in the polymer. At larger quantities of the fragrance, small microdomains are probably formed which are homogeneously located in the particle.

## 4.2 Capsule Formation by Interfacial Polymerization

Another possibility for the formation of nanocapsules is to direct the polymerization reaction to the interface of nanodroplets. On the one hand, this can be realized either by using interfacially active initiators or water soluble initiators generating amphiphilic species, “anchoring” the growing polymeric chain to the interface. Here the monomer is only located in one, usually the dispersed phase. On the other hand, this can be realized if one hydrophilic monomer is present in the aqueous phase and the other hydrophobic monomer in the organic phase and these monomeric species only meet and react to a polymer at the interface.

Reports of interfacial radical copolymerization, anionic polymerization, and interfacial polyadditions can be found in the literature. Representatively for the formation of polymeric shells by interfacial reactions, the polyaddition in direct and inverse miniemulsions is shown in Fig. 17.

Using the interfacially active initiator PEGA200, PS capsules could be realized in direct miniemulsions [168]. Organic/inorganic PS/silica shells around an inert hydrocarbon (octane) were obtained by copolymerizing the hydrophobic styrene with the hydrophilic comonomer MPS with potassium peroxodisulfate (KPS) as initiator [175]. A subsequent condensation of about 40% of the silanol groups led to the formation of silica shells. The authors assign the capsule morphology to

the presence of the hydrophilic comonomer favoring phase separation and KPS, responsible for the above-mentioned “anchoring” effect.

A detailed study, comparing the thermodynamic prediction for the equilibrium morphology with the experimental results, was performed using a system comprising hexadecane as core material, poly(butylacrylate) (PBA) as polymeric component, and KPS as anchoring initiator [176]. Even though the thermodynamic model predicted an inverted core-shell structure with polymer engulfed by hexadecane, a core-shell structure with encapsulated hydrocarbon was found. This difference is explained by kinetic factors, as impaired diffusion, and most importantly by the initiation and propagation of the polymerization from the interface to the liquid droplet core.

Capsule formation could also be obtained in a controlled living polymerization process using styrene for the encapsulation of iso-octane and KPS as anchoring agent [177]. Two different reversible addition fragmentation chain transfer (RAFT) agents were employed in a miniemulsion polymerization process. Phenyl 2-propyl phenyl dithioacetate (PPDTA) led to very fast polymerization reactions, while phenyl 2-propyl dithiobenzoate (CDB) retards the polymerization reaction. Again, the initiator KPS was used to fix one end of the polymer to the interface. The effect of KPS could clearly be shown in comparison to the application of AIBN. Using PPDTA living polymerization with KPS and AIBN, only with KPS could capsules be generated. The initiation by using AIBN led to the formation of solid particles as no amphiphilic, anchoring species are generated, allowing the growing species to diffuse into the droplets. In the case of CDB and KPS, no capsules could be generated, since the viscosity of the growing polymeric shell was probably not high enough to reduce the chain mobility sufficiently, also allowing diffusion of the growing polymer into the droplet.

Controlled radical polymerizations can also be restricted to the interface between an organic droplet and the water phase in a direct miniemulsion by using amphiphilic oligomeric RAFT agents. The thioester group of the RAFT agent was coupled to either PAA-*b*-PSS (polyacrylic acid-*b*-polystyrenesulfonate) oligomers [178] or SMA oligomers (styrene-maleic anhydride) [179, 180]. In the first case, the carboxylic acid groups were deprotonated, in the second case ammonia is employed for ammonolysis/hydrolysis of the maleic anhydride, thus generating amphiphilic structures. Additionally, the amphiphilic oligomers are capable of stabilizing the miniemulsion droplets sufficiently.

Interfacial radical alternating copolymerization of hydrophilic vinyl ethers with hydrophobic maleates can be conducted in direct [181] and in inverse [182] miniemulsion, leading to encapsulation of organic liquids or water, respectively. Since the monomers do not homopolymerize, the alternating copolymerization can only take place at the interface where both monomers meet. The polymerization is initiated by an interfacially active azo initiator. The authors could show that the water soluble dye Rhodamine B can be encapsulated in the inverse miniemulsion process and released from the capsules [182].

The previous examples were all based on radical polymerization processes. However, in miniemulsion, other types of polymerization can also be conducted and

therefore be used for the formation of nanocapsules. The anionic polymerization of alkylcyanoacrylates (ACA) can also be performed at the interface between aqueous and organic phases. This reaction is suitable for the encapsulation of aqueous [183] as well as organic droplets [184]. In both cases, the reaction is exclusively initiated at the droplet's interface. Musyanovych et al. [183] could form a shell of poly(butylcyanoacrylate) (PBCA) around droplets of an aqueous solution of DNA with 790 base pairs. The droplets are generated by miniemulsification of the aqueous DNA solution in an inert nucleophile-free continuous phase, which is miscible with the monomer BCA, but is a non-solvent for the polymer. As soon as the BCA is added to the inverse miniemulsion, polymerization is initiated at the droplet's interface since the water inside the droplets acts as nucleophile. As the polymer is insoluble in the continuous phase and in the droplet phase, a shell around the droplets is formed. After completion of the polymerization, the capsules can be transferred to the water phase. The droplet/capsule size can be tuned between 250 and 700 nm by the type and amount of stabilizer and the continuous phase. The shell thickness could be adjusted to be in the range of 5–40 nm by the amount of monomer added (see Fig. 18). The encapsulation efficiency of the DNA was 100%, whereas 15% of the DNA was still in the free form.

For the encapsulation of organic liquids, a direct miniemulsion was formed from a BCA/Miglyol 812N solution in a methoxypolyethyleneglycol (MePEG)-containing aqueous phase [184]. MePEG, bearing a hydrophilic OH-group, is capable of initiating anionic polymerization from the water phase, eventually generating the polymeric shell around the hydrophobic droplet. In the oil core, paclitaxel, a drug for cancer therapy, could be encapsulated with 65% efficiency.

Besides the radical and anionic polymerization at the interface, polyaddition reactions can also be carried out at the droplet's interface. This technique can be realized in direct and inverse miniemulsion which enables the encapsulation of either hydrophobic or hydrophilic liquids. It is important to mention that the encapsulated liquids have to be a non-solvent for the generated polymer shell if capsules are the desired morphology.

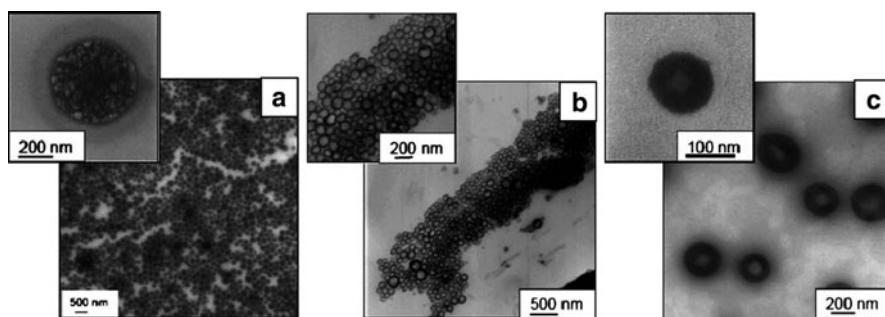


**Fig. 18** TEM images of PBCA capsules obtained in the presence of 5 wt% Span<sup>®</sup> 80 and different mounts of monomer butylcyanoacrylate: (a) 70  $\mu$ L; (b) 100  $\mu$ L; (c) 200  $\mu$ L [183]

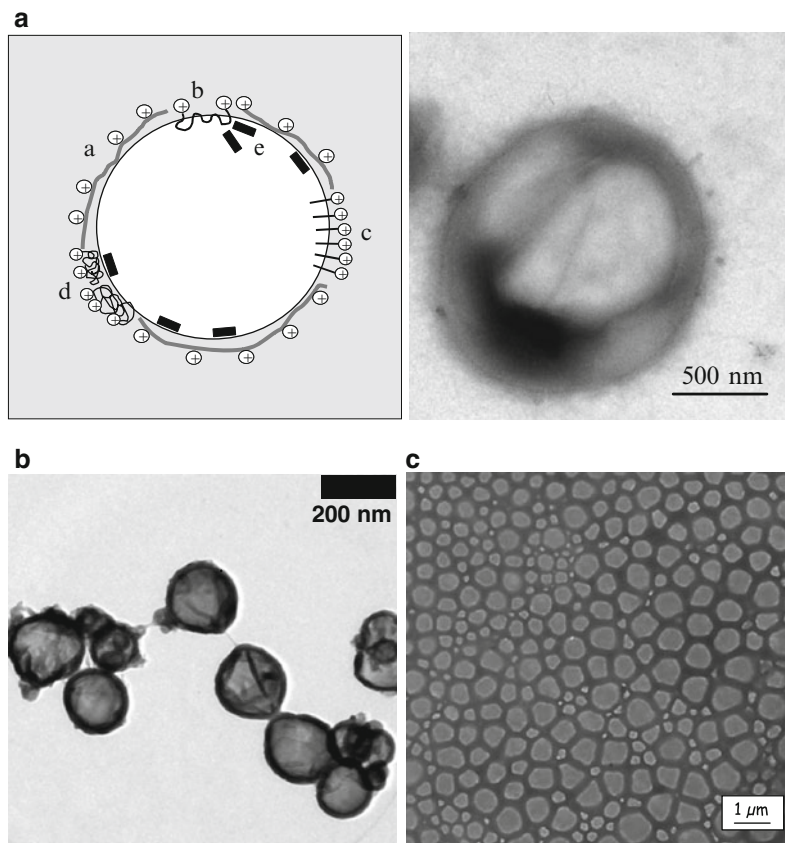


**Fig. 19** (a) *Left*: Schematic view of the formation of nanocapsules by interfacial reaction. Chitosan acts as a reactive biocompatible stabilizer from the water phase forming patches on the interface (a); costabilizer like oligomeric diamines (b) (e.g., Jeffamine D2000) or low molecular cationic surfactants (c) (e.g., CTMA molecules) can improve the surface layer structure from the inside of the droplets and the coupled stabilization efficiency. A stabilization from the water phase can also be provided by a water-soluble, but amphiphilic protein, e.g., Gluadin (d). A diepoxide (e) can additionally be used as stabilizing cross-linking agent.) and *right*: TEM picture [185]. (b) TEM images of polyurea capsules [191] and (c) polyurethane nanocapsules [188]

The interfacial polyaddition of chitosan used as stabilizer with two biocompatible costabilizers, Jeffamine D2000 and Gluadin, and a linking diepoxide in presence of an inert oil results in thin but rather stable nanocapsules (see Fig. 19a). Since both water and oil soluble aminic costabilizers can be used, these experiments show the way to a great variety of capsules with different chemical structure [185].

For the formation of polyurethane (PU) or polyurea (PUR) shells in miniemulsion systems, usually the diol- or diamine component is water soluble, while the diisocyanate is hydrophobic and thus soluble in organic media. For direct miniemulsions, mostly isophorone diisocyanate (IPDI) [186, 187] was used, as this compound

slowly reacts with the continuous phase 'water'. The reaction with water generates amine groups, which themselves can react with diisocyanates, leading to urea groups as byproduct. Despite the application of slow reacting diisocyanate, PUR is generally found in polymeric shells generated by interfacial polyaddition in miniemulsion. The reactions can be performed with or without a catalyst [e.g., dibutyltin dilaurate (DBTDL)], in the organic phase. The diol component is added to the aqueous continuous phase leading to capsules consisting of PU with urea units. In contrast to cationic or nonionic surfactants, anionic surfactants as SDS were shown to be most suitable for the stabilization of the capsules.

More interesting for biomedical applications is the encapsulation of aqueous (physiological) solutions which can be realized by using the inverse miniemulsion technique [188–191]. First, an inverse miniemulsion with stable aqueous droplets has to be created containing a hydrophilic diol or diamine, then the polymeric shell is formed in a polyaddition reaction at the interface by adding the hydrophobic diisocyanate via the organic phase. After shell formation, it is possible to transfer the capsules to water for further applications. A wide variety of hydrophilic components can be used ranging from diols, triols to polysaccharides as dextran or starch, and from diamines to amine bearing surfactants (Lubrizol U – a polyisobutylene-succinimide pentamine) acting as a crosslinking surfmer [191]. Due to the presence of amine groups in the Lubrizol molecule, it is covalently incorporated into the polymeric interfacial layer after reaction, resulting in a more compact and therefore less permeable capsule shell (see Fig. 19). The influence of the stabilizer and the monomer concentration on the shell thickness, colloidal stability, average capsule size, and capsule size polydispersity were examined in detail. The water-soluble fluorescent dye fluorescein and an aqueous dispersion of magnetite nanoparticles 10 nm in size were used as inner phase of the polyurea capsules. The encapsulation efficiency was shown to be very high. As an example for biomedical application, the fluorescein containing capsules were utilized in cell uptake experiments and visualized using fluorescence microscopy [191].

Besides the application of water as dispersed phase in an inverse miniemulsion, it is also possible to create non-aqueous miniemulsions by dispersing polar organic solvents as dimethylsulfoxide, formamide, vinylpyrrolidone, or ethylene glycol in an inert hydrocarbon (e.g., cyclohexane, dodecane, Isopar M (mixture of several hydrocarbons)) [188]. Irrespective of the dispersed phase, the size can be controlled by the amount of the stabilizer. The lowest droplet/capsule size could be obtained for ca. 9 wt% of the stabilizer P(E/B-EO), which has shown to be highly efficient in stabilizing any kind of inverse miniemulsions [9]. As the reaction of the diisocyanate with the diol or diamine is very fast, the mode of the diisocyanate addition to the reaction system is crucial. A quick addition leads to small capsules, resembling the size of the preformed droplets. Slow addition gives the components of the polar droplets (with a low but recognizable solubility in the continuous phase) time to diffuse through the continuous phase, which leads to an increase in the droplet size. The thickness of the polymeric shell can be controlled by the total amount of reactants used. It could also be shown that reactions, as the reduction of  $\text{Ag}^+$  by

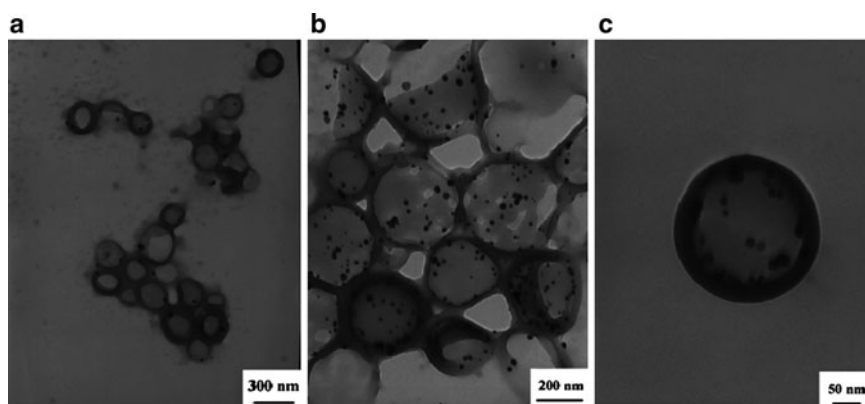


**Fig. 20** TEM micrographs of polyurea capsules loaded with different amounts of silver nanoparticles: (a) 30 mg  $\text{AgNO}_3$ ; (b,c) 120 mg  $\text{AgNO}_3$  in the aqueous phase [188]

hydrazine, can be performed within the polymer enclosed area (see Fig. 20). The number of silver particles can be varied over a wide range.

If the application requires, porous capsules can be prepared as well. The porosity of the shell material could be shown by encapsulating an aqueous solution of a gadolinium-based magnetic resonance imaging (MRI) contrast agent [Gd-diethylenetriamine pentaacetic acid (DTPA)]. First, nanodroplets of 100–550 nm are formed which are subsequently encapsulated by an interfacial polyaddition in polymeric shells of polyurethane, polyurea, and crosslinked dextran. The shell thickness was adjusted by the monomer concentration. Due to the porosity of the polymeric shell for water, exchange of water molecules through the capsule wall can be ensured and no significant compromises in the  $T_1$  relaxivity of the contrast agent is observed for MRI. The results show that the complex is restricted to the interior of the nanocapsules. This clearly indicates the potential use of the contrast agent filled nanocapsules as new MRI contrast agents. [189].

A further step towards efficient biomedical application of PU/PUR nanocapsules was shown by the work of Paiphansiri et al. [190]. Carboxy- and amino-functionalization of the nanocapsules surface can be introduced and tailored by an *in situ* carboxymethylation reaction or by physical adsorption of a cationic polyelectrolyte, i.e., poly(aminoethyl methacrylate hydrochloride) or poly(ethylene imine) (see Fig. 21). Encapsulation of an aqueous solution of suforhodamine adds a fluorescent label for fluorescence microscopic detection (see Fig. 21). Whereas the carboxy-functionalized nanocapsules do not lead to a good uptake into cells, the increased uptake of amino-functionalized fluorescent nanocapsules by HeLa cells clearly demonstrates the potential of the functionalized nanocapsules to be successfully exploited as biocarriers. These results are in good agreement with the data obtained from experiments with PS particles [192].

The PAEMA-coated nanocapsules can be further applied for physical immobilization of biologically active molecules such as, e.g., proteins. The immobilization

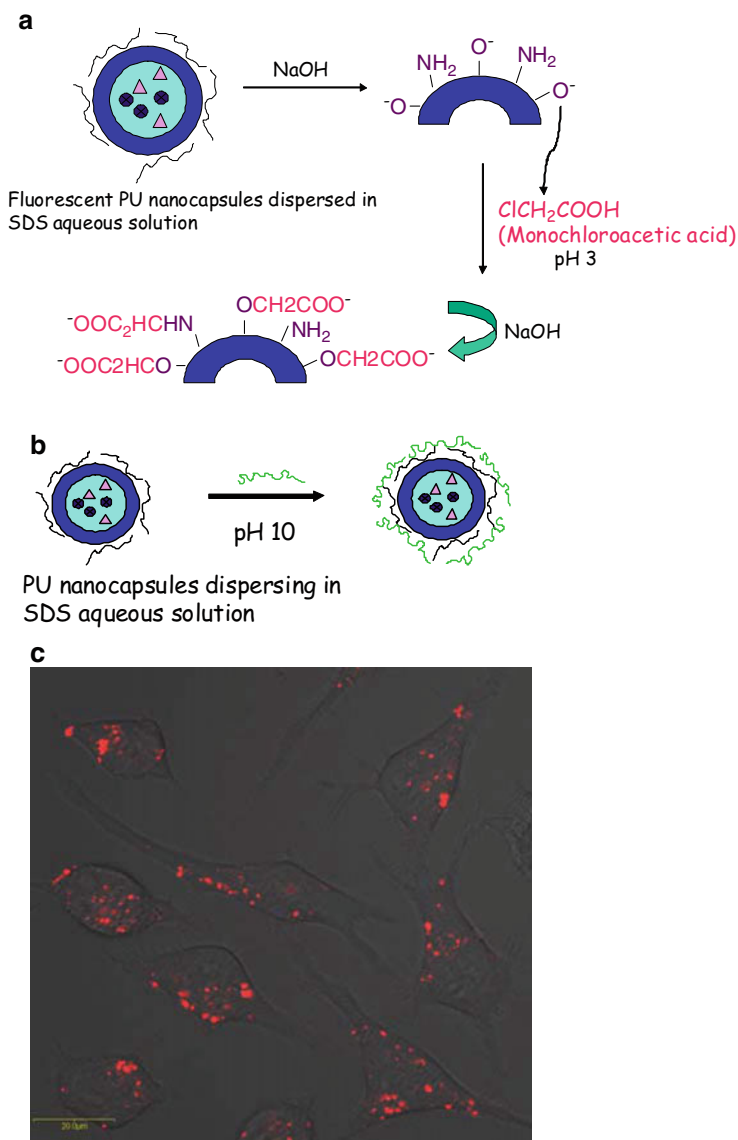


**Fig. 21** Functionalization of nanocapsules by (a) carboxymethylation reaction or (b) adsorption of poly(aminoethyl methacrylate) (PAEMA) or poly(ethylene imine) (PEI) onto PU nanocapsules (c) and uptake of amino-functionalized (PEI) nanocapsules in cells [190]

of gold-IgG antibody was carried out at pH 7 where the PAEMA-coated nanocapsules and gold-IgG having positive and negative charges, respectively. Thus the adsorption of protein onto the nanocapsules surface was governed by electrostatic interactions. After separating non-immobilized protein from nanocapsules



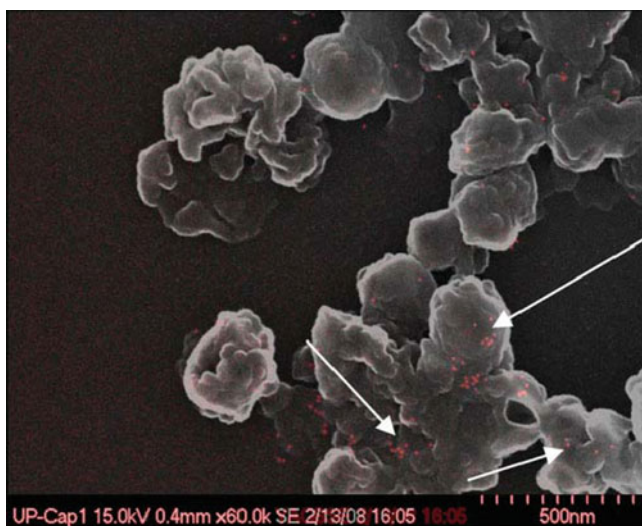


**Fig. 22** PAEMA-coated PU-capsules with physically adsorbed gold-IgG antibodies. Gold is visualized with the backscattered electron detector (*red*) in the HR-SEM [190]

dispersion using multiple centrifugation/redispersion steps, air-dried nanocapsules were then characterized by high resolution scanning electron microscopy (HR-SEM) as shown in Fig. 22.

### ***4.3 Polymer Precipitation on Preformed Nanodroplets***

Nanoprecipitation can also be a very efficient method for the encapsulation of an aqueous core with a polymeric shell. Aqueous droplets containing an active component, e.g., the antiseptic chlorohexidine digluconate [193, 194], can be obtained by miniemulsification. The continuous phase of the miniemulsion consists of a mixture of a solvent (e.g., dichloromethane, DCM) and a non-solvent (e.g., cyclohexane) for the polymer (e.g., PMMA, PCL, or polymethylacrylate PMA). After miniemulsification, the solvent is carefully evaporated in a controlled manner and the polymer precipitates onto the aqueous droplet (Fig. 23), resulting in a core-shell structure of the system.

## **5 Controlled Release of Components from Nanocapsules**

The determination of the release behavior of a copolymeric matrix consisting of P(MMA-*co*-2-EHA) with different amounts of encapsulated fragrance shows a significantly decelerated release of the encapsulated volatile substance compared to the



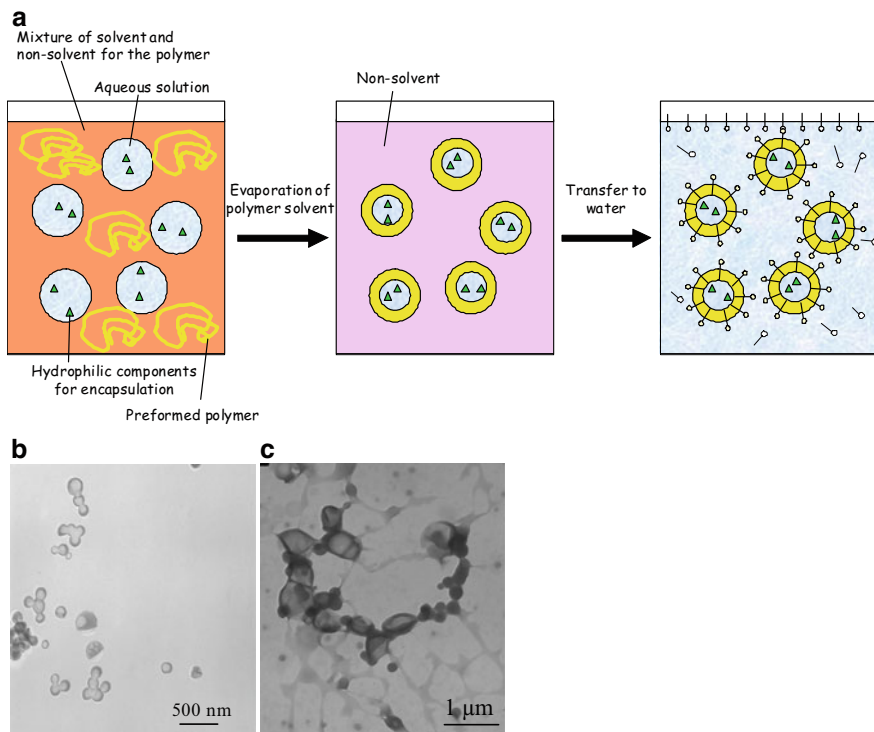


**Fig. 23** (a) Formation of polymer capsules by polymer nanoprecipitation on preformed miniemulsion droplets: Examples for capsule formation by nanoprecipitation with (b) polymethylacrylate (PMA) and (c) PMMA [193, 194]

pure DMPBA miniemulsion [174]. For lower temperatures ( $T < T_g$ ), no release can be observed. The increase of the temperature ( $T > T_g$ ) results in a significantly accelerated release of the fragrance out of the nanoparticles. The release rate can be adjusted by the temperature applied. Thereby, the release behavior of the volatile compound can easily be tuned by adjusting the release temperature in comparison to the  $T_g$  of the polymer shell.

In contrast to sustained release, some applications might require the release of the encapsulated material during a very short period of time, initiated by an external stimulus such as temperature. To achieve this goal, azoinitiators with high decomposition temperatures were encapsulated in polymeric particles (see Fig. 24) [195]. The idea is to decompose the encapsulated components very rapidly by high temperature, producing a large volume of nitrogen which literally lets the polymeric nanoparticle explode (Fig. 24a). It is important that the decomposition temperature of the azo-component is chosen below the  $T_g$  of the polymer in order to produce an overpressure in the nanoparticles.

The labile azo-component can also be part of the polymer and embedded in the shell. Here, polyurethane nanocapsules consisting of an aque-

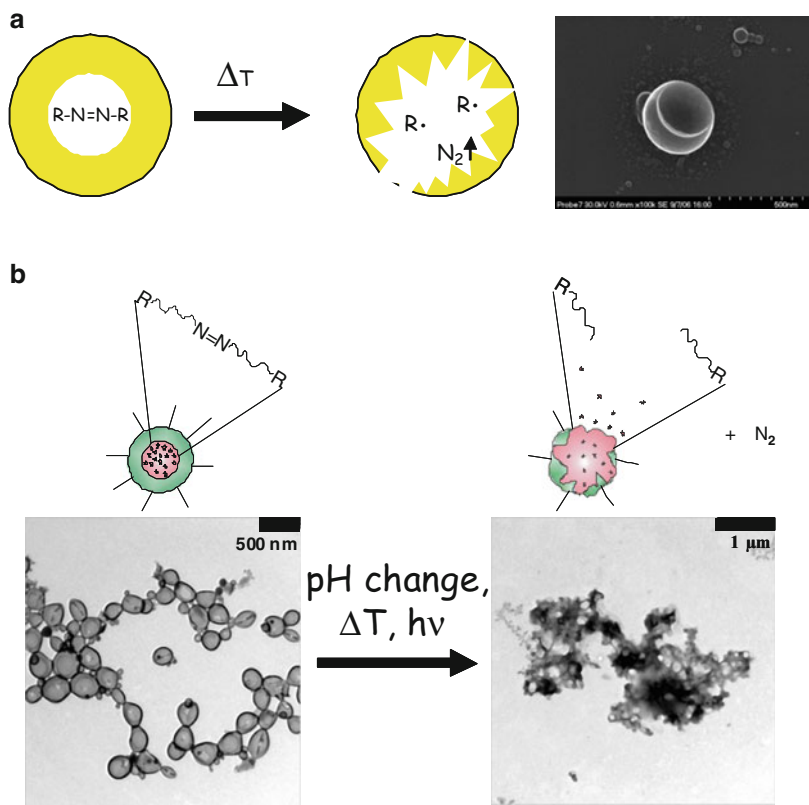


**Fig. 24** (a) Nanoparticles with encapsulated azo initiator for “nanoexplosion”: scheme and SEM picture [195]. (b) Nanocapsules with azo-containing shell which can degrade under pH or temperature change or light irradiation: scheme and TEM pictures

ous core and a polymeric shell with included azo bonds as obtained via interfacial polyaddition of the monomers toluene-2,4-diisocyanate (TDI) and an azo-containing diol [2,2'-azobis{2-[1-(2-hydroxyethyl)-2-imidazolin-2-yl]propane}dihydrochloride (V60)] in inverse miniemulsion allow the selective release of encapsulated material by stimuli such as temperature, UV light, or pH change. The capsule degradation was detected by measuring time-dependently the fluorescence intensities of the dye sulforhodamine SR101, which is dissolved as the fluorescent marker in the core, by exposing the capsules to the different stimuli. Furthermore, the capsules were characterized by transmission electron microscopy (TEM) and dynamic light scattering (DLS). The main components during the capsules' degradation were determined via NMR spectrometry directly on the azo-monomer V60. The results present proof-of-principle studies of different controlled releases with a prototype of polyurethane capsules using the fluorescence dye sulforhodamine SR101 as a model system (see Fig. 24b).

## 6 Summary

It is shown that the miniemulsion process can be used to create numerous hybrid nanoparticles by encapsulating a large number of many different materials and compounds in a wide variety of different (functional) polymeric shells. Compounds which are soluble in the monomer can very easily be integrated in the miniemulsion polymerization process. Here, the component is dissolved prior to the miniemulsification step. Then, during the polymerization process the molecules stay either molecularly dissolved or partly phase separate. The material can be incorporated to be used, e.g., as markers for biomedical applications or as active components which can be released in a controlled manner. Solid materials which are insoluble in the monomer phase can also be encapsulated in polymeric nanoparticles. Here, a compatibilization step is often required so that the material is incorporated in the monomer prior to polymerization. In the case of the encapsulation by hydrophobic monomers/polymers, the pigments, inorganic crystals, etc., have to be hydrophobized. Liquid-filled nanocapsules can be obtained by several mechanisms in miniemulsion processes. Phase separation within droplets during the polymerization step or interfacial reactions on droplets can be applied for the encapsulation of organic liquids or aqueous solutions. Nanoprecipitation of preformed polymer also allows the encapsulation of preformed aqueous droplets. A release of the encapsulated components can be obtained either by diffusion out of the nanocapsules, by (bio)degradation of the polymer or by destroying the shell by external stimuli. We are convinced that many more functional materials for a wide field of applications can still be created by the miniemulsion process, allowing the formation of complex hybrid materials.

## References

1. Aschenbrenner EM, Weiss CK, Landfester K (2009) Enzymatic esterification in aqueous miniemulsions. *Chem Eur J* 15:2434–2444
2. de Barros DPC, Fonseca LP, Cabral JMS, et al. (2009) Synthesis of alkyl esters by cutinase in miniemulsion and organic solvent media. *Biotechnol J* 4:674–683
3. Taden A, Landfester K, Antonietti M (2004) Crystallization of dyes by directed aggregation of colloidal intermediates: a model case. *Langmuir* 20:957–961
4. Taden A, Landfester K (2003) Crystallization of poly(ethylene oxide) confined in miniemulsion droplets. *Macromolecules* 36:4037–4041
5. Montenegro R, Antonietti M, Mastai Y, et al. (2003) Crystallization in miniemulsion droplets. *J Phys Chem C* 107:5088–5094
6. Montenegro R, Landfester K (2003) Metastable and stable morphologies during crystallization of alkanes in miniemulsion droplets. *Langmuir* 19:5996–6003
7. Rossmannith R, Weiss CK, Geserick J, et al. (2008) Porous anatase nanoparticles with high specific surface area prepared by miniemulsion technique. *Chem Mater* 20:5768–5780
8. Asua JM (2002) Miniemulsion polymerization. *Prog Polym Sci* 27:1283–1346
9. Landfester K (2006) Synthesis of colloidal particles in miniemulsions. *Annu Rev Mater Res* 36:231–279
10. Landfester K (2009) Miniemulsion polymerization and the structure of polymer and hybrid nanoparticles. *Angew Chem Int Ed* 48:4488–4507

11. Schork FJ, Luo Y, Smulders W, et al. (2005) Miniemulsion polymerization. *Adv Poly Sci* 175:129–255
12. Crespy D, Landfester K (2005) Anionic polymerization of  $\epsilon$ -caprolactam in miniemulsion: synthesis and characterization of polyamide-6 nanoparticles. *Macromolecules* 38:6882–6887
13. Weiss CK, Ziener U, Landfester K (2007) A route to nonfunctionalized and functionalized poly(*n*-butylcyanoacrylate) nanoparticles: preparation in miniemulsion. *Macromolecules* 40:928–938
14. Cauvin S, Ganachaud F, Moreau M, et al. (2005) High molar mass polymers by cationic polymerisation in emulsion and miniemulsion. *Chem Commun* 21:2713–2715
15. Cauvin S, Ganachaud F (2004) On the preparation and polymerization of *p*-methoxystyrene miniemulsions in the presence of excess ytterbium triflate. *Macromol Symp* 215:179–189
16. Soula R, Saillard B, Spitz R, et al. (2002) Catalytic copolymerization of ethylene and polar and nonpolar  $\dot{I} \pm$ -olefins in emulsion. *Macromolecules* 35:1513–1523
17. Wehrmann P, Zuideveld M, Thomann R, et al. (2006) Copolymerization of ethylene with 1-butene and norbornene to higher molecular weight copolymers in aqueous emulsion. *Macromolecules* 39:5995–6002
18. Held A, Kolb L, Zuideveld MA, et al. (2002) Aqueous polyketone latices prepared with water-insoluble palladium(II) catalysts. *Macromolecules* 35:3342–3347
19. Quémener D, Héroguez V, Gnanou Y (2005) Latex particles by miniemulsion ring-opening metathesis polymerization. *Macromolecules* 38:7977–7982
20. Quémener D, Héroguez V, Gnanou Y (2006) Design of PEO-based ruthenium carbene for aqueous metathesis polymerization. Synthesis by the “macromonomer method” and application in the miniemulsion metathesis polymerization of norbornene. *J Polym Sci Part A Polym Chem* 44:2784–2793
21. Pecher J, Mecking S (2007) Nanoparticles from step-growth coordination polymerization. *Macromolecules* 40:7733–7735
22. Landfester K, Tiarks F, Hentze HP, et al. (2000) Polyaddition in miniemulsions: a new route to polymer dispersions. *Macromol Chem Phys* 201:1–5
23. Tiarks F, Landfester K, Antonietti M (2001) One-step preparation of polyurethane dispersions by miniemulsion polyaddition. *J Polym Sci Part A Polym Chem* 39:2520–2524
24. Barrere M, Landfester K (2003) High molecular weight polyurethane and polymer hybrid particles in aqueous miniemulsion. *Macromolecules* 36:5119–5125
25. Barrere M, Landfester K (2003) Polyester synthesis in aqueous miniemulsion. *Polymer* 44:2833–2841
26. Taden A, Antonietti M, Landfester K (2003) Enzymatic polymerization towards biodegradable polyester nanoparticles. *Macromol Rapid Commun* 24:512–516
27. Marie E, Rothe R, Antonietti M, et al. (2003) Synthesis of polyaniline particles via inverse and direct miniemulsion. *Macromolecules* 36:3967–3973
28. Bhadra S, Singha NK, Khastgir D (2006) Polyaniline by new miniemulsion polymerization and the effect of reducing agent on conductivity. *Synth Met* 156:1148–1154
29. Alyautdin RN, Reichel A, Löbenberg R, et al. (2001) Interaction of poly(butylcyanoacrylate) nanoparticles with the blood–brain barrier in vivo and in vitro. *J Drug Target* 9:209–221
30. Holzapfel V, Musyanovych A, Landfester K, et al. (2005) Preparation of fluorescent carboxyl and amino functionalized polystyrene particles by miniemulsion polymerization as markers for cells. *Macromol Chem Phys* 206:2440–2449
31. Lorenz MR, Holzapfel V, Musyanovych A, et al. (2006) Uptake of functionalized, fluorescent-labeled polymeric particles in different cell lines and stem cells. *Biomaterials* 27:2820–2828
32. Dausend J, Musyanovych A, Dass M, et al. (2008) Uptake mechanism of oppositely charged fluorescent nanoparticles in HeLa cells. *Macromol Biosci* 8:1135–1143
33. Ziegler A, Landfester K, Musyanovych A (2009) Synthesis of phosphonate-functionalized polystyrene and poly(methyl methacrylate) particles and their kinetic behavior in miniemulsion polymerization. *Colloid Polym Sci*. <http://dx.doi.org/10.1007/s00396-009-2087-z>
34. Lorenz MR, Kohnle MV, Dass M, et al. (2008) Synthesis of fluorescent polyisoprene nanoparticles and their uptake into various cells. *Macromol Biosci* 8:711–727

35. Weiss CK, Kohnle M-V, Landfester K, et al. (2008) The first step into the brain: uptake of NIO-PBCA nanoparticles by endothelial cells in vitro and in vivo, and direct evidence for their blood-brain barrier permeation. *Chem Med Chem* 3:1395–1403
36. Weiss CK, Lorenz MR, Landfester K, et al. (2007) Cellular uptake behavior of unfunctionalized and functionalized poly(*n*-butylcyanoacrylate) particles prepared in a miniemulsion. *Macromol Biosci* 7:883–896
37. Musyanovych A, Schmitz-Wienke J, Mailaender V, et al. (2008) Preparation of biodegradable polymer nanoparticles by miniemulsion technique and their cell interactions. *Macromol Biosci* 8:127–139
38. Holzapfel V, Lorenz M, Weiss CK, et al. (2006) Synthesis and biomedical applications of functionalized fluorescent and magnetic dual reporter nanoparticles as obtained in the miniemulsion process. *J Phys Condens Matter* 18:S2581–S2594
39. Mailaender V, Lorenz Myriam R, Holzapfel V, et al. (2008) Carboxylated superparamagnetic iron oxide particles label cells intracellularly without transfection agents. *Mol Imaging Biol* 10:138–146
40. Urban M, Musyanovych A, Landfester K (2009) Fluorescent superparamagnetic polylactide nanoparticles by combination of miniemulsion and emulsion/solvent evaporation techniques. *Macromol Chem Phys* 210:961–970
41. Oh JK, Siegwart DJ, Matyjaszewski K (2007) Synthesis and biodegradation of nanogels as delivery carriers for carbohydrate drugs. *Biomacromolecules* 8:3326–3331
42. Oh JK, Siegwart DJ, Lee HI, et al. (2007) Biodegradable nanogels prepared by atom transfer radical polymerization as potential drug delivery carriers: synthesis, biodegradation, in vitro release, and bioconjugation. *J Am Chem Soc* 129:5939–5945
43. Siegwart DJ, Srinivasan A, Bencherif SA, et al. (2009) Cellular uptake of functional nanogels prepared by inverse miniemulsion ATRP with encapsulated proteins, carbohydrates, and gold nanoparticles. *Biomacromolecules* 10:2300–2309
44. Takasu M, Shiroya T, Takeshita K, et al. (2004) Improvement of the storage stability and photostability of colored latex prepared by miniemulsion polymerization. *Colloid Polym Sci* 282:740–746
45. Takasu M, Kawaguchi H (2005) Preparation of colored latex with polyurea shell by miniemulsion polymerization. *Colloid Polym Sci* 283:805–811
46. Takasu M, Shiroya T, Takeshita K, et al. (2003) Preparation of colored latex containing oil-soluble dyes with high dye content by mini-emulsion polymerization. *Colloid Polym Sci* 282:119–126
47. Zhao X, Zhou S, Chen M, et al. (2009) Effective encapsulation of Sudan black B with polystyrene using miniemulsion polymerization. *Colloid Polym Sci*
48. Bradley M, Ashokkumar M, Grieser F (2003) Sonochemical production of fluorescent and phosphorescent latex particles. *J Am Chem Soc* 125:525–529
49. Tamai T, Watanabe M, Maeda H, et al. (2008) Fluorescent polymer particles incorporating pyrene derivatives. *J Polym Sci Part A Polym Chem* 46:1470–1475
50. Taniguchi T, Takeuchi N, Kobaru S, et al. (2008) Preparation of highly monodisperse fluorescent polymer particles by miniemulsion polymerization of styrene with a polymerizable surfactant. *J Colloid Interface Sci* 327:58–62
51. Watarai H, Ogawa K, Suzuki N (1993) Formation of fluorescent complexes of Eu(III) and Sm(III) with [beta]-diketones and trioctylphosphine oxide in oil–water microemulsions. *Anal Chim Acta* 277:73–78
52. Ando K, Kawaguchi H (2005) High-performance fluorescent particles prepared via miniemulsion polymerization. *J Colloid Interface Sci* 285:619–626
53. Hu ZK, Xue MZ, Zhang Q, et al. (2007) Controlled preparation of nanocolorants via a modified miniemulsion polymerization process. *J Appl Polym Sci* 104:3036–3041
54. Hu Z, Xue M, Zhang Q, et al. (2008) Nanocolorants: a novel class of colorants, the preparation and performance characterization. *Dyes Pigments* 76:173–178
55. Yuan B, Wicks DA (2007) Thermotropic color changing nanoparticles prepared by encapsulating blue polystyrene particles with a poly-*N*-isopropylacrylamide gel. *J Appl Polym Sci* 105:446–452

56. Yuan B, States J, Sahagun C, et al. (2008) Effects of three cross-linkers on colored pH-responsive core-shell latexes. *J Appl Polym Sci* 107:4093–4099
57. Han M, Lee E, Kim E (2002) Preparation and optical properties of polystyrene nanocapsules containing photochromophores. *Opt Mater* 21:579–583
58. Furukawa H, Misu M, Ando K, et al. (2008) Light-controlled on-off switch of a fluorescent nanoparticle. *Macromol Rapid Commun* 29:547–551
59. Hu Z, Zhang Q, Xue M, et al. (2007) Fluorescent photoswitchable nanohybrids based on photochromism. *J Phys Chem Solids* 69:206–210
60. Hu Z, Zhang Q, Xue M, et al. (2008) Spirobenzopyran-based photochromic nanohybrids with photoswitchable fluorescence. *Opt Mater* 30:851–856
61. Chern CS, Chen TJ, Liou YC (1998) Miniemulsion polymerization of styrene in the presence of a water-insoluble blue dye. *Polymer* 39:3767–3777
62. Chern CS, Liou YC, Chen TJ (1998) Particle nucleation loci in styrene miniemulsion polymerization using alkyl methacrylates as the reactive cosurfactant. *Macromol Chem Phys* 199:1315–1322
63. Chern C-S, Chang H-T (2002) Particle nucleation and growth mechanisms in miniemulsion polymerization of styrene. *Polym Int* 51:1428–1438
64. Chern C-S, Liou Y-C (1998) Effects of mixed surfactants on the styrene miniemulsion polymerization in the presence of an alkyl methacrylate. *Macromol Chem Phys* 199:2051–2061
65. Chern C-S, Liou Y-C (1999) Kinetics of styrene miniemulsion polymerization stabilized by nonionic surfactant/alkyl methacrylate. *Polymer* 40:3763–3772
66. Chern C-S, Liou Y-C (1999) Styrene miniemulsion polymerization initiated by 2,2'-azobisisobutyronitrile. *J Polym Sci Part A Polym Chem* 37:2537–2550
67. Musyanovych A, Rossmanith R, Tontsch C, et al. (2007) Effect of hydrophilic comonomer and surfactant type on the colloidal stability and size distribution of carboxyl- and amino-functionalized polystyrene particles prepared by miniemulsion polymerization. *Langmuir* 23:5367–5376
68. Manzke A, Pfahler C, Dubbers O, et al. (2007) Etching masks based on miniemulsions: a novel route towards ordered arrays of surface nanostructures. *Adv Mater* 19:1337–1341
69. Schreiber E, Ziener U, Manzke A, et al. (2009) Preparation of narrowly size distributed metal-containing polymer latexes by miniemulsion and other emulsion techniques: applications for nanolithography. *Chem Mater* 21:1750–1760
70. Vancaeyzele C, Ornatsky O, Baranov V, et al. (2007) Lanthanide-containing polymer nanoparticles for biological tagging applications: nonspecific endocytosis and cell adhesion. *J Am Chem Soc* 129:13653–13660
71. Ramírez LP, Antonietti M, Landfester K (2006) Formation of novel layered nanostructures from lanthanide-complexes by secondary interactions with ligating monomers in miniemulsion droplets. *Macromol Chem Phys* 207:160–165
72. Bechthold N, Tiarks F, Willert M, et al. (2000) Miniemulsion polymerization: applications and new materials. *Macromol Symp* 151:549–555
73. Lelu S, Novat C, Graillat C, et al. (2003) Encapsulation of an organic phthalocyanine blue pigment into polystyrene latex particles using a miniemulsion polymerization. *Polym Int* 52:542–547
74. Steiert N, Landfester K (2007) Encapsulation of organic pigment particles via miniemulsion polymerization. *Macromol Mater Eng* 292:1111–1125
75. Tiarks F, Landfester K, Antonietti M (2001) Encapsulation of carbon black by miniemulsion polymerization. *Macromol Chem Phys* 202:51–60
76. Barraza HJ, Pompeo F, O'Rear EA, et al. (2002) SWNT-filled thermoplastic and elastomeric composites prepared by miniemulsion polymerization. *Nano Lett* 2:797–802
77. Ha MLP, Grady BP, Lolli G, et al. (2007) Composites of single-walled carbon nanotubes and styrene-isoprene copolymer latices. *Macromol Chem Phys* 208:446–456
78. Ham HT, Choi YS, Chee MG, et al. (2006) Singlewall carbon nanotubes covered with polystyrene nanoparticles by in-situ miniemulsion polymerization. *J Polym Sci Part A Polym Chem* 44:573–584

79. Lu HF, Xin JH, Fei B, et al. (2007) Synthesis and lubricating performance of a carbon nanotube seeded miniemulsion. *Carbon* 45:936–942
80. Ham HT, Choi YS, Jeong N, et al. (2005) Singlewall carbon nanotubes covered with polypyrrole nanoparticles by the miniemulsion polymerization. *Polymer* 46:6308–6315
81. Lu HF, Fei B, Xin JH, et al. (2006) Fabrication of UV-blocking nanohybrid coating via miniemulsion polymerization. *J Colloid Interface Sci* 300:111–116
82. Luo YD, Dai CA, Chiu WY (2008) Synthesis of P(AA-SA)/ZnO composite latex particles via inverse miniemulsion polymerization and its application in pH regulation and UV shielding. *J Polym Sci Part A Polym Chem* 46:8081–8090
83. Zhang JJ, Gao G, Zhang M, et al. (2006) ZnO/PS core-shell hybrid microspheres prepared with miniemulsion polymerization. *J Colloid Interface Sci* 301:78–84
84. Mahdavian A, Sarrafi Y, Shabankareh M (2009) Nanocomposite particles with core-shell morphology. III. Preparation and characterization of nano Al<sub>2</sub>O<sub>3</sub>-poly(styrene-methyl methacrylate) particles via miniemulsion polymerization. *Polym Bull* 63:329–340
85. Lopez-Martinez EI, Marquez-Lucero A, Hernandez-Escobar CA, et al. (2007) Incorporation of silver/carbon nanoparticles into poly(methyl methacrylate) via in situ miniemulsion polymerization and its influence on the glass-transition temperature. *J Polym Sci Part B Polym Phys* 45:511–518
86. Crespy D, Landfester K (2009) Synthesis of polyvinylpyrrolidone/silver nanoparticles hybrid latex in non-aqueous miniemulsion at high temperature. *Polymer* 50:1616–1620
87. Erdem B, Sully Y, Sudol ED, et al. (2000) Determination of miniemulsion droplet size via soap titration. *Langmuir* 16:4890–4895
88. Erdem B, Sudol ED, Dimonie VL, et al. (2000) Encapsulation of inorganic particles via miniemulsion polymerization. III. Characterization of encapsulation. *J Polym Sci Part A Polym Chem* 38:4441–4450
89. Erdem B, Sudol ED, Dimonie VL, et al. (2000) Encapsulation of inorganic particles via miniemulsion polymerization. II. Preparation and characterization of styrene miniemulsion droplets containing TiO<sub>2</sub> particles. *J Polym Sci Part A Polym Chem* 38:4431–4440
90. Erdem B, Sudol ED, Dimonie VL, et al. (2000) Encapsulation of inorganic particles via miniemulsion polymerization. I. Dispersion of titanium dioxide particles in organic media using OLOA 370 as stabilizer. *J Polym Sci Part A Polym Chem* 38:4419–4430
91. Erdem B, Sudol ED, Dimonie VL, et al. (2000) Encapsulation of inorganic particles via miniemulsion polymerization. *Macromol Symp* 155:181–198
92. Al-Ghamdi GH, Sudol ED, Dimonie VL, et al. (2006) Encapsulation of titanium dioxide in styrene/*n*-butyl acrylate copolymer by miniemulsion polymerization. *J Appl Polym Sci* 101:3479–3486
93. Al-Ghamdi GH, Sudol ED, Dimonie VL, et al. (2006) High PVC film-forming composite latex particles via miniemulsification, part 3: optical properties. *J Appl Polym Sci* 101:4526–4537
94. Al-Ghamdi GH, Sudol ED, Dimonie VL, et al. (2006) High PVC film-forming composite latex particles via miniemulsification, part 2: efficiency of encapsulation. *J Appl Polym Sci* 101:4517–4525
95. Al-Ghamdi GH, Sudol ED, Dimonie VL, et al. (2006) High PVC film-forming composite latex particles via miniemulsification, part 1: preparation. *J Appl Polym Sci* 101:4504–4516
96. Kim H, Daniels ES, Li S, et al. (2007) Polymer encapsulation of yttrium oxysulfide phosphorescent particles via miniemulsion polymerization. *J Polym Sci Part A Polym Chem* 45:1038–1054
97. Yang Y, Wen Z, Dong Y, et al. (2006) Incorporating CdTe nanocrystals into polystyrene microspheres: towards robust fluorescent beads. *Small* 2:898–901
98. Fleisshaker F, Zentel R (2005) Photonic crystals from core-shell colloids with incorporated highly fluorescent quantum dots. *Chem Mater* 17:1346–1351
99. Esteves ACC, Bombalski L, Trindade T, et al. (2007) Polymer grafting from Cds quantum dots via AGET ATRP in miniemulsion. *Small* 3:1230–1236
100. Tiarks F, Landfester K, Antonietti M (2001) Silica nanoparticles as surfactants and fillers for latexes made by miniemulsion polymerization. *Langmuir* 17:5775–5780



101. Zhang SW, Zhou SX, Weng YM, et al. (2005) Synthesis of SiO<sub>2</sub>/polystyrene nanocomposite particles via miniemulsion polymerization. *Langmuir* 21:2124–2128
102. Zhou J, Zhang SW, Qiao XG, et al. (2006) Synthesis of SiO<sub>2</sub>/poly(styrene-*co*-butyl acrylate) nanocomposite microspheres via miniemulsion polymerization. *J Polym Sci Part A Polym Chem* 44:3202–3209
103. Qi DM, Bao YZ, Weng ZX, et al. (2006) Preparation of acrylate polymer/silica nanocomposite particles with high silica encapsulation efficiency via miniemulsion polymerization. *Polymer* 47:4622–4629
104. Zhou J, Chen M, Qiao XG, et al. (2006) Facile preparation method of SiO<sub>2</sub>/PS/TiO<sub>2</sub> multi-layer core-shell hybrid microspheres. *Langmuir* 22:10175–10179
105. Lu W, Chen M, Wu L (2008) One-step synthesis of organic–inorganic hybrid asymmetric dimer particles via miniemulsion polymerization and functionalization with silver. *J Colloid Interface Sci* 328:98–102
106. Qiang W, Wang Y, He P, et al. (2008) Synthesis of asymmetric inorganic/polymer nanocomposite particles via localized substrate surface modification and miniemulsion polymerization. *Langmuir* 24:606–608
107. Ge X, Wang M, Yuan Q, et al. (2009) The morphological control of anisotropic polystyrene/silica hybrid particles prepared by radiation miniemulsion polymerization. *Chem Commun* 2765–2767
108. Wang Y, Xu H, Qiang W, et al. (2009) Asymmetric composite nanoparticles with anisotropic surface functionalities. *J Nanomater* 2009:5. Article ID 620269
109. Bailly B, Donnenwirth AC, Bartholome C, et al. (2006) Silica-polystyrene nanocomposite particles synthesized by nitroxide-mediated polymerization and their encapsulation through miniemulsion polymerization. *J Nanomater* 2006:1–10
110. Bombalski L, Min K, Dong H, et al. (2007) Preparation of well-defined hybrid materials by ATRP in miniemulsion. *Macromolecules* 40:7429–7432
111. Toepfer O, Schmidt-Naake G (2007) Surface – functionalized inorganic nanoparticles in miniemulsion polymerization. *Macromol Symp* 248:239–248
112. Monteil V, Stumbaum J, Thomann R, et al. (2006) Silica/poly ethylene nanocomposite particles from catalytic emulsion polymerization. *Macromolecules* 39:2056–2062
113. Boutti S, Bourgeat-Lami E, Zydowicz N (2005) Silica/polyamide nanocomposite synthesis via an original double emulsification process in miniemulsion. *Macromol Rapid Commun* 26:1860–1865
114. Diaconu G, Asua JM, Paulis M, et al. (2007) High-solids content waterborne polymer-clay nanocomposites. *Macromol Symp* 259:305–317
115. Diaconu G, Micusik M, Bonnefond A, et al. (2009) Macroinitiator and macromonomer modified montmorillonite for the synthesis of acrylic/MMT nanocomposite latexes. *Macromolecules* 42:3316–3325
116. Moraes RP, Santos AM, Oliveira PC, et al. (2006) Poly(styrene-*co*-butyl acrylate)-Brazilian montmorillonite nanocomposites, synthesis of hybrid latexes via miniemulsion polymerization. *Macromol Symp* 245/246:106–115
117. Bouanani F, Bendedouch D, Hemery P, et al. (2008) Encapsulation of montmorillonite in nanoparticles by miniemulsion polymerization. *Colloid Surf A Physicochem Eng Asp* 317:751–755
118. Moraes RP, Valera TS, Demarquette NR, et al. (2009) Influence of granulometry and organic treatment of a Brazilian montmorillonite on the properties of poly(styrene-*co*-*n*-butyl acrylate)/layered silicate nanocomposites prepared by miniemulsion polymerization. *J Appl Polym Sci* 112:1949–1958
119. Samakande A, Sanderson RD, Hartmann PC (2009) Rheological properties of RAFT-mediated poly(styrene-*co*-butyl acrylate)-clay nanocomposites [P(S-*co*-BA)-PCNs]: emphasis on the effect of structural parameters on thermo-mechanical and melt flow behaviors. *Polymer* 50:42–49
120. Samakande A, Sanderson RD, Hartmann PC (2008) Encapsulated clay particles in polystyrene by RAFT mediated miniemulsion polymerization. *J Polym Sci Part A Polym Chem* 46:7114–7126



121. Tong ZH, Deng YL (2006) Synthesis of water-based polystyrene-nanoclay composite suspension via miniemulsion polymerization. *Ind Eng Chem Res* 45:2641–2645
122. Tong ZH, Deng YL (2008) Kinetics of miniemulsion polymerization of styrene in the presence of organoclays. *Macromol Mater Eng* 293:529–537
123. Diaconu G, Paulis M, Leiza JR (2008) High solids content waterborne acrylic/montmorillonite nanocomposites by miniemulsion polymerization. *Macromol React Eng* 2:80–89
124. Mirzataheri M, Mahdavian A, Atai M (2009) Nanocomposite particles with core-shell morphology IV: an efficient approach to the encapsulation of Cloisite 30B by poly (styrene-*co*-butyl acrylate) and preparation of its nanocomposite latex via miniemulsion polymerization. *Colloid Polym Sci* 287:725–732
125. Sun QH, Deng YL, Wang ZL (2004) Synthesis and characterization of polystyrene-encapsulated laponite composites via miniemulsion polymerization. *Macromol Mater Eng* 289:288–295
126. Tong ZH, Deng YL (2007) Synthesis of polystyrene encapsulated nanosaponite composite latex via miniemulsion polymerization. *Polymer* 48:4337–4343
127. Samakande A, Juodaityte JJ, Sanderson RD, et al. (2008) Novel cationic RAFT-mediated polystyrene/clay nanocomposites: synthesis, characterization, and thermal stability. *Macromol Mater Eng* 293:428–437
128. Zhang QY, Zhang HP, Xie G, et al. (2007) Effect of surface treatment of magnetic particles on the preparation of magnetic polymer microspheres by miniemulsion polymerization. *J Magn Magn Mater* 311:140–144
129. Chen ZJ, Peng K, Mi YL (2007) Preparation and properties of magnetic polystyrene microspheres. *J Appl Polym Sci* 103:3660–3666
130. Betancourt-Galindo R, Saldivar R, Rodriguez-Fernandez OS, et al. (2004) Preparation and characterization of magnetic latexes using styrene monomer. *Polym Bull* 51:395–402
131. Betancourt-Galindo R, Saldivar-Guerrero R, Rodriguez-Fernandez OS, et al. (2004) Preparation of magnetic latexes using styrene monomer. *J Alloy Compd* 369:87–89
132. Zhang QY, Xie G, Zhang HP, et al. (2007) Encapsulation of magnetic particles via miniemulsion polymerization of styrene. II. Effect of some parameters on the polymerization of styrene. *J Appl Polym Sci* 105:3525–3530
133. Baharvand H (2008) Preparation and characterization of fluorescent polymer magnetic particles. *J Appl Polym Sci* 109:1823–1828
134. Quian Z, Zhicheng Z, Yun C (2008) A novel preparation of surface-modified paramagnetic magnetite/polystyrene nanocomposite microspheres by radiation-induced miniemulsion polymerization. *J Colloid Interface Sci* 327:354–361
135. Ramírez LP, Landfester K (2003) Magnetic polystyrene nanoparticles with a high magnetite content obtained by miniemulsion processes. *Macromol Chem Phys* 204:22–31
136. Landfester K, Ramírez LP (2003) Encapsulated magnetite particles for biomedical application. *J Phys Condens Matter* 15:S1345–S1361
137. Joumaa N, Toussay P, Lansalot M, et al. (2007) Surface modification of iron oxide nanoparticles by a phosphate-based macromonomer and further encapsulation into submicrometer polystyrene particles by miniemulsion polymerization. *J Polym Sci Part A Polym Chem* 46:327–340
138. Mahdavian AR, Ashjari M, Mobarakeh HS (2008) Nanocomposite particles with core-shell morphology. I. Preparation and characterization of Fe<sub>3</sub>O<sub>4</sub>-poly(butyl acrylate-styrene) particles via miniemulsion polymerization. *J Appl Polym Sci* 110:1242–1249
139. Mahdavian AR, Sehri Y, Salehi-Mobarakeh H (2008) Nanocomposite particles with core-shell morphology. II. An investigation into the affecting parameters on preparation of Fe<sub>3</sub>O<sub>4</sub>-poly (butyl acrylate-styrene) particles via miniemulsion polymerization. *Eur Polym J* 44:2482–2488
140. Liu XQ, Guan YP, Ma ZY, et al. (2004) Surface modification and characterization of magnetic polymer nanospheres prepared by miniemulsion polymerization. *Langmuir* 20:10278–10282
141. Lu SH, Forcada J (2006) Preparation and characterization of magnetic polymeric composite particles by miniemulsion polymerization. *J Polym Sci Part A Polym Chem* 44:4187–4203

142. Csetneki I, Faix MK, Szilagyi A, et al. (2004) Preparation of magnetic polystyrene latex via the miniemulsion polymerization technique. *J Polym Sci Part A Polym Chem* 42:4802–4808
143. Mori Y, Kawaguchi H (2007) Impact of initiators in preparing magnetic polymer particles by miniemulsion polymerization. *Colloid Surf B Biointerfaces* 56:246–254
144. Qiu GH, Wang Q, Wang C, et al. (2007) Polystyrene/Fe<sub>3</sub>O<sub>4</sub> magnetic emulsion and nanocomposite prepared by ultrasonically initiated miniemulsion polymerization. *Ultrason Sonochem* 14:55–61
145. Qiu GH, Wang Q, Wang C, et al. (2006) Ultrasonically initiated miniemulsion polymerization of styrene in the presence of Fe<sub>3</sub>O<sub>4</sub> nanoparticles. *Polym Int* 55:265–272
146. Gong T, Yang D, Hu J, et al. (2009) Preparation of monodispersed hybrid nanospheres with high magnetite content from uniform Fe<sub>3</sub>O<sub>4</sub> clusters. *Colloid Surf A Physicochem Eng Asp* 339:232–239
147. Yan F, Li J, Zhang J, et al. (2009) Preparation of Fe<sub>3</sub>O<sub>4</sub>/polystyrene composite particles from monolayer oleic acid modified Fe<sub>3</sub>O<sub>4</sub> nanoparticles via miniemulsion polymerization. *J Nanopart Res* 11:289–296
148. Cui L, Xu H, He P, et al. (2007) Developing a hybrid emulsion polymerization system to synthesize Fe<sub>3</sub>O<sub>4</sub>/polystyrene latexes with narrow size distribution and high magnetite content. *J Polym Sci Part A Polym Chem* 45:5285–5295
149. Tu C, Yang Y, Gao M (2008) Preparations of bifunctional polymeric beads simultaneously incorporated with fluorescent quantum dots and magnetic nanocrystals. *Nanotechnology* 19:105601
150. Nunes JS, De Vasconcelos CL, Cabral FO, et al. (2006) Synthesis and characterization of poly(ethyl methacrylate-*co*-methacrylic acid) magnetic particles via miniemulsion polymerization. *Polymer* 47:7646–7652
151. Nunes JS, de Vasconcelos CL, Dantas TNC, et al. (2008) Preparation of acrylic latexes with dispersed magnetite nanoparticles. *J Dispersion Sci Technol* 29:769–774
152. Zheng WM, Gao F, Gu HC (2005) Carboxylated magnetic polymer nanolatexes: preparation, characterization and biomedical applications. *J Magn Magn Mater* 293:199–205
153. Tan CJ, Tong YW (2007) Preparation of superparamagnetic ribonuclease a surface-imprinted submicrometer particles for protein recognition in aqueous media. *Anal Chem* 79:299–306
154. Tan CJ, Chua HG, Ker KH, et al. (2008) Preparation of bovine serum albumin surface-imprinted submicrometer particles with magnetic susceptibility through core-shell miniemulsion polymerization. *Anal Chem* 80:683–692
155. Qian H, Lin ZY, Xu HM, et al. (2009) The efficient and specific isolation of the antibodies from human serum by thiophilic paramagnetic polymer nanospheres. *Biotechnol Progr* 25:376–383
156. Faridi-Majidi R, Sharifi-Sanjani N, Agend F (2006) Encapsulation of magnetic nanoparticles with polystyrene via emulsifier-free miniemulsion polymerization. *Thin Solid Films* 515:368–374
157. Faridi-Majidi R, Sharifi-Sanjani N (2007) Emulsifier-free miniemulsion polymerization of styrene and the investigation of encapsulation of nanoparticles with polystyrene via this procedure using an anionic initiator. *J Appl Polym Sci* 105:1244–1250
158. Faridi-Majidi R, Sharifi-Sanjani N (2007) Preparation of magnetic latexes functionalized with chloromethyl groups via emulsifier-free miniemulsion polymerization. *J Magn Magn Mater* 311:55–58
159. Shao D, Xia A, Hu J, et al. (2008) Monodispersed magnetite/silica composite microspheres: preparation and application for plasmid DNA purification. *Colloid Surf A Physicochem Eng Asp* 322:61–65
160. Xu ZZ, Wang CC, Yang WL, et al. (2004) Encapsulation of nanosized magnetic iron oxide by polyacrylamide via inverse miniemulsion polymerization. *J Magn Magn Mater* 277:136–143
161. Wormuth K (2001) Superparamagnetic latex via inverse emulsion polymerization. *J Colloid Interface Sci* 241:366–377
162. Ménager C, Sandre O, Mangili J, et al. (2004) Preparation and swelling of hydrophilic magnetic microgels. *Polymer* 45:2475–2481

163. Xu ZZ, Wang CC, Yang WL, et al. (2005) Synthesis of superparamagnetic  $\text{Fe}_3\text{O}_4/\text{SiO}_2$  composite particles via sol-gel process based on inverse miniemulsion. *J Mater Sci* 40:4667–4669
164. Lin CL, Chiu WY, Don TM (2006) Superparamagnetic thermoresponsive composite latex via W/O miniemulsion polymerization. *J Appl Polym Sci* 100:3987–3996
165. Johnston APR, Cortez C, Angelatos AS, et al. (2006) Layer-by-layer engineered capsules and their applications. *Curr Opin Colloid Interface Sci* 11:203–209
166. Wang Y, Angelatos AS, Caruso F (2007) Template synthesis of nanostructured materials via layer-by-layer assembly. *Chem Mater* 20:848–858
167. zu Putlitz B, Landfester K, Fischer H, et al. (2001) The generation of “armored latexes” and hollow inorganic shells made of clay sheets by templating cationic miniemulsions and latexes. *Adv Mater* 13:500–503
168. Tiarks F, Landfester K, Antonietti M (2001) Preparation of polymeric nanocapsules by miniemulsion polymerization. *Langmuir* 17:908–918
169. Luo YW, Zhou XD (2004) Nanoencapsulation of a hydrophobic compound by a miniemulsion polymerization process. *J Polym Sci Part A Polym Chem* 42:2145–2154
170. Cao Z, Shan G (2009) Synthesis of polymeric nanocapsules with a crosslinked shell through interfacial miniemulsion polymerization. *J Polym Sci Part A Polym Chem* 47:1522–1534
171. Romio AP, Sayer C, Araújo PHH, et al. (2009) Nanocapsules by miniemulsion polymerization with biodegradable surfactant and hydrophobe. *Macromol Chem Phys* 210:747–751
172. Zetterlund PB, Saka Y, Okubo M (2009) Gelation and hollow particle formation in nitroxide-mediated radical copolymerization of styrene and divinylbenzene in miniemulsion. *Macromol Chem Phys* 210:140–149
173. Volz M, Ziener U, Salz U, et al. (2007) Preparation of protected photoinitiator nanodepots by the miniemulsion process. *Colloid Polym Sci* 285:687–692
174. Theisinger S, Schoeller K, Osborn B, et al. (2009) Encapsulation of a fragrance via miniemulsion polymerization for temperature-controlled release. *Macromol Chem Phys* 210:411–420
175. Ni KF, Shan GR, Weng ZX (2006) Synthesis of hybrid nanocapsules by miniemulsion (co)polymerization of styrene and gamma-methacryloxypropyltrimethoxysilane. *Macromolecules* 39:2529–2535
176. van Zyl AJP, Sanderson RD, de Wet-Roos D, et al. (2003) Core/shell particles containing liquid cores: morphology prediction, synthesis, and characterization. *Macromolecules* 36:8621–8629
177. van Zyl AJP, Bosch RFP, McLeary JB, et al. (2005) Synthesis of styrene based liquid-filled polymeric nanocapsules by the use of RAFT-mediated polymerization in miniemulsion. *Polymer* 46:3607–3615
178. Lu F, Luo Y, Li B (2007) A facile route to synthesize highly uniform nanocapsules: use of amphiphilic poly(acrylic acid)-*block*-polystyrene RAFT agents to interfacially confine miniemulsion polymerization. *Macromol Rapid Commun* 28:868–874
179. Luo YW, Gu HY (2006) A general strategy for nano-encapsulation via interfacially confined living/controlled radical miniemulsion polymerization. *Macromol Rapid Commun* 27:21–25
180. Luo Y, Gu H (2007) Nanoencapsulation via interfacially confined reversible addition fragmentation transfer (RAFT) miniemulsion polymerization. *Polymer* 48:3262–3272
181. Scott C, Wu D, Ho CC, et al. (2005) Liquid-core capsules via interfacial polymerization: a free-radical analogy of the nylon rope trick. *J Am Chem Soc* 127:4160–4161
182. Wu D, Scott C, Ho CC, et al. (2006) Aqueous-core capsules via interfacial free radical alternating copolymerization. *Macromolecules* 39:5848–5853
183. Musyanovych A, Landfester K (2008) Synthesis of poly(butylcyanoacrylate) nanocapsules by interfacial polymerization in miniemulsions for the delivery of DNA molecules. In Auernhammer GK, Butt H-J, Vollmer D (eds) *Surface and interfacial forces – from fundamentals to applications*. Springer, Berlin/Heidelberg
184. Zhang Y, Zhu SY, Yin LC, et al. (2008) Preparation, characterization and biocompatibility of poly(ethylene glycol)-poly(*n*-butyl cyanoacrylate) nanocapsules with oil core via miniemulsion polymerization. *Eur Polym J* 44:1654–1661

185. Marie E, Landfester K, Antonietti M (2002) Synthesis of chitosan-stabilized polymer dispersions, capsules, and chitosan grafting products via miniemulsion. *Biomacromolecules* 3:475–481
186. Torini L, Argillier JF, Zydowicz N (2005) Interfacial polycondensation encapsulation in miniemulsion. *Macromolecules* 38:3225–3236
187. Johnsen H, Schmid RB (2007) Preparation of polyurethane nanocapsules by miniemulsion polyaddition. *J Microencapsulation* 24:731–742
188. Crespy D, Stark M, Hoffmann-Richter C, et al. (2007) Polymeric nanoreactors for hydrophilic reagents synthesized by interfacial polycondensation on miniemulsion droplets. *Macromolecules* 40:3122–3135
189. Jagielski N, Sharma S, Hombach V, et al. (2007) Nanocapsules synthesized by miniemulsion technique for application as new contrast agent materials. *Macromol Chem Phys* 208: 2229–2241
190. Paiphansiri U, Dausend J, Musyanovych A, et al. (2009) Fluorescent polyurethane nanocapsules prepared via inverse miniemulsion: surface functionalization for use as biocarriers. *Macromol Biosci* 9:575–584
191. Rosenbauer E-M, Landfester K, Musyanovych A (2009) Surface-active monomer as a stabilizer for polyurea nanocapsules synthesized via interfacial polyaddition in inverse miniemulsion. *Langmuir* <http://dx.doi.org/10.1021/la9017097>
192. Mailänder V, Landfester K (2009) Interaction of nanoparticles with cells. *Biomacromolecules* 10(9):2379–2400
193. Paiphansiri U, Tangboriboonrat P, Landfester K (2006) Polymeric nanocapsules containing an antiseptic agent obtained by controlled nanoprecipitation onto water-in-oil miniemulsion droplets. *Macromol Biosci* 6:33–40
194. Paiphansiri U, Tangboriboonrat P, Landfester K (2007) Antiseptic nanocapsule formation via controlling polymer deposition onto water-in-oil miniemulsion droplets. *Macromol Symp* 251:54–62
195. Volz M, Walther P, Ziener U, et al. (2007) Nano-explosions of nanoparticles for sudden release of substances by embedded azo-components as obtained via the miniemulsion process. *Macromol Mater Eng* 292:1237–1244

# Enzyme-Encapsulated Layer-by-Layer Assemblies: Current Status and Challenges Toward Ultimate Nanodevices

Katsuhiko Ariga, Qingmin Ji, and Jonathan P. Hill

**Abstract** Alternate layer-by-layer (LbL) adsorption has received much attention as an emerging methodology. Biocompatibility is the most prominent advantage of the LbL assembly process because the technique employs mild conditions for film construction. Most enzymes, especially water-soluble ones, have charged sites at their surfaces so that electrostatic LbL adsorption is suitable for construction of various protein organizations. In this review chapter, we summarize recent developments on enzyme-encapsulated LbL devices and their related functions where “encapsulated” does not always entail entrapment within spherical structures but generally includes immobilization of enzymes within the LbL structures. Recent examples, with various functions such as reactor sensors and medical applications, are described within a classification of structural types, i.e., thin films and spherical capsules. In addition to conventional applications, advanced systems including integration of LbL structures into advanced devices such as microchannels, field effect transistors, and flow injection amperometric sensors are introduced as well as recent developments in hybridization of LbL assemblies with functional nanomaterials such as carbon nanotube, dendrimers, nanoparticles, lipid assemblies, and mesoporous materials, all of which can enhance bio-related functions of LbL assemblies.

**Keywords** Devices · Enzymes · Hollow capsules · Layer-by-layer assemblies · Thin films

---

K. Ariga (✉), Q. Ji, and J.P. Hill  
World Premier International (WPI) Research Center for Materials Nanoarchitectonics (MANA),  
National Institute for Materials Science (NIMS), 1–1 Namiki, Tsukuba, Ibaraki 305-0044, Japan  
and  
Core Research of Evolutional Science and Technology (CREST), Japan Science and Technology  
Agency (JST), Tokyo, Japan  
e-mail: [ARIGA.Katsuhiko@nims.go.jp](mailto:ARIGA.Katsuhiko@nims.go.jp)

## Contents

1	Introduction .....	53
2	LbL as Bio-Friendly Methods for Nanofabrication .....	55
3	Enzyme-Embedded LbL Devices .....	58
3.1	Thin Film Type .....	58
3.2	Particle and Capsule Type .....	65
4	Advanced Techniques .....	73
4.1	Integration into Device Structures .....	73
4.2	Advanced Medical Applications .....	75
4.3	Hybridization with Nanomaterials Toward Hierarchic Assemblies .....	76
5	Perspectives .....	80
	References .....	80

## Abbreviation

AChE	Acetylcholinesterase
ADP	Adenosine diphosphate
AFP	$\alpha$ -1-Fetoprotein antigen
ALP	Alkaline phosphatase
ATP	Adenosine triphosphate
BMS	Bimodal mesoporous silica
BSA	Bovine serum albumin
ChO	Choline oxidase
CNT	Carbon nanotube
Cyt P450 <sub>cam</sub>	Cytochrome P450 <sub>cam</sub>
DEAE	Diethylaminoethyl
DL-1	Delta-like 1
DMPC	Dimyristoyl phosphatidylcholine
DMSO	Dimethylsulfoxide
DNA	Deoxyribonucleic acid
DNase	Deoxyribonuclease
DPPC	Dipalmitoyl phosphatidylcholine
dsDNA	Double-stranded DNA
ENFET	Enzyme field-effect transistor
FAD	Flavin adenine dinucleotide
GA	Glucoamylase
GCE	Glassy carbon electrode
GDH	Glucose dehydrogenase
GOD	Glucose oxidase
HA	Hyaluronic acid
Hb	Hemoglobin
HRP	Horseradish peroxidase
HSA	Human serum albumin
IgG	Immunoglobulin G

ISFET	Ion-sensitive field-effect transistor
ITO	Indium tin oxide
LB	LangmuirBlodgett
LbL	Layer-by-layer
LDH	Lactate dehydrogenase
LOD	Lactate oxidase
Mb	Myoglobin
MWNT	Multi-wall carbon nanotube
OPH	Organophosphorus hydrolase
PAA	Poly(acrylic acid)
PAH	Poly(allylamine hydrochloride)
PAMAM	Poly(amidoamine)
PDDA	Poly(diallyldimethylammonium chloride)
PEI	Poly(ethyleneimine)
PET	Poly(ethylene terephthalate)
PGA	Poly(L-glutamic acid)
PLA2	Phospholipase A2
PLL	Poly(L-lysine)
PMA	Poly(methacrylic acid)
PMMA	Poly(methyl methacrylate)
POD	Peroxidase
PSS	Poly(styrenesulfonate)
PVP	Poly(vinylpyridine)
QCM	Quartz crystal microbalance
SAM	Self-assembled monolayer
SWNT	Single-walled carbon nanotube

## 1 Introduction

Miniaturization of functional structures into small areas or volumes as ultrasmall devices and machines has been extensively demonstrated in recent nanotechnology. However, more complex microdevices can be found in biological systems. Bio-materials such as proteins, polysaccharides, and nucleic acids have sophisticated structures which express highly specific and efficient processes of molecular recognition, materials conversion, and information transduction. In particular, enzymes that can modify chemical structure might be regarded as nanosized fabrication facilities. Higher functions of enzymes have been optimized over geological time periods during biological evolution. Following considerable efforts over the development of science and technology, we have now obtained knowledge and technology sufficient for mimicking and utilizing enzyme functions as seen in the recent progress in biotechnology, biomimicry, and supramolecular chemistry [1–20].

Research efforts have been made to synthesize artificial chemical structures that can promote enzyme-like reactions and to create various artificial enzymes

[21–24]. Molecular cavities of artificial enzymes are designed to recognize specific substrate molecules, stabilize reaction intermediates and/or their transition state, and provide reactive groups in appropriate proximity to the trapped substrate molecules. Supramolecular chemistry based on host-guest interaction is often used for molecular design of artificial enzymes. For example, imidazole-functionalized cyclodextrins [25, 26] and guanidinium-bearing molecular clefts [27–29] can promote hydrolysis of phosphate esters as a mimic of nuclease. Instead of synthesizing enzyme function purely by using organic chemistry, integration of natural enzymes into artificial structures can also be useful for exploiting enzyme function in artificial systems. Because enzymes have high affinities for biomolecules such as lipids and oligosaccharides, immobilization of enzymes at a biomolecular interface such as a lipid assembly is regarded as an effective strategy. For example, immobilization on an electrode of glucose oxidase (GOD) using the lipid-assisted Langmuir-Blodgett (LB) technique resulted in a glucose-sensitive real-time amperometric sensing device [30, 31]. Co-immobilization of enzyme (lactate dehydrogenase, LDH) and artificial receptors onto bilayer lipid membrane enabled control of the enzyme activity by chemical and photonic stimuli, resulting in a biological AND-type logic gate device [32–35]. Such interfaces can also be used as working media appropriate for recognition and accommodation of many different biological components [36–51].

Device preparation requires use of facilitative methodologies for the organization of biological components in a particular configuration. Self-assembled monolayer (SAM) [52–56] and LB methods [57–65] have been used for organization of functional elements in two-dimensional or layered structures, respectively. These methods offer opportunities for immobilization of functional components into well-organized structures. However, tight packing of the resulting formations sometimes obstructs intra-structural substrate/product transport that is often required for operation of biological devices. In addition, applicability to a wide range of materials is not always guaranteed for these methods (i.e., they are *too* specific). As a novel methodology that can compensate for deficiencies of the former techniques, alternate layer-by-layer (LbL) adsorption has been paid much attention as an emerging methodology [66–73]. As described in the following section, LbL provides a simple and inexpensive method to create layered structures of requisite thicknesses and layer sequences from a wide variety of components. Packing densities of components within LbL films is not always high, and this feature is advantageous for material transport across and along layers. Actually, these characteristics have been apparently keenly awaited in the construction of biological nanodevices. Recent research has proved the great applicability of the LbL technique not only for preparation of bio-related devices but also for producing various device structures, including sensors [74–76], photovoltaic devices [77–81], electrochromic devices [82–85], fuel cells [86–88], and rugate filters [89].

As one can easily imagine from the above-mentioned examples, it is high time to develop biological nanodevices based on LbL techniques. We here summarize recent developments on enzyme-encapsulated LbL devices and related functions where “encapsulated” does not always entail entrapment within spherical structures but generally includes immobilization of enzymes within LbL structures.



This review chapter describes both thin film and capsule type enzyme-encapsulated LbL devices. Initially, a brief explanation is given of the merits of immobilization of enzymes by using the LbL method, and this is followed by a description of recent advanced techniques and future perspectives.

## 2 LbL as Bio-Friendly Methods for Nanofabrication

The concept of LbL assembly was first proposed for charged colloidal particles in 1966 by Iler [90] who suggested that alternating adsorption of anionic and cationic species would result in the formation of regular multilayered assemblies. Decher and co-workers later realized this concept using mainly linear polyelectrolytes or bolaamphiphiles [91–94]. Concurrently, Mallouk and coworkers developed LbL-type assembly through interaction between  $\text{Zr}^{4+}$  ions and diphosphonic acids [95–97]. Subsequently, over the course of the 1990s the applicability of the LbL technique to a wide range of materials was extensively studied. Materials that can be used in LbL methods cover a wide range including conventional polyelectrolytes [98–100], conductive polymers [101–104], dendrimers [105–107], proteins [108–111], nucleic acids [112, 113], saccharides [114–116], virus particles [117], inorganic colloidal particles [118–120], quantum dots [121, 122], clay plates [123], nanosheets [124–129], nanorods [130–132], nanowires [133, 134], nanotubes [135, 136], dye aggregates [137–139], micelles [140–142], vesicles [143, 144], LB films [145], and lipid membranes [146, 147]. The LbL technique has now become one of the most powerful methods for preparation of nanostructured supermolecules.

In most cases, the LbL assembly is carried out based on electrostatic interactions. As illustrated in Fig. 1, adsorption of counterionic species at relatively high concentrations leads to excess adsorption of the substances, as a result of charge neutralization and resaturation, finally resulting in charge reversal. This process was proved by Berndt et al. through a direct surface force measurement [148]. This simple mechanism allows us to assemble required components in various sequences using a low-cost experimental set-up. In fact, well-controlled nano-sized films can be fabricated only using beakers and tweezers. Driving forces for

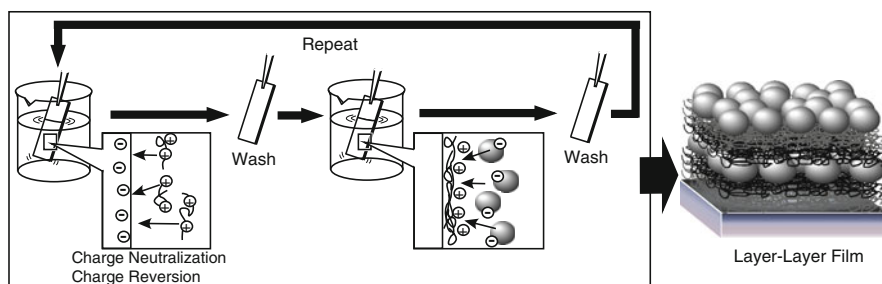


**Fig. 1** LbL assembly based on electrostatic interaction

LbL assembly are not limited to electrostatic interactions alone. Various interactions including metal-ligand interaction [149–152], hydrogen-bonding [153–155], charge transfer [156–158], supramolecular inclusion [159], bio-specific recognition [160–162], and stereo-complex formation [163, 164] can be used for LbL assembly. Wide freedom in assembling techniques is also guaranteed. For example, combination of spin-coating with LbL methods provides well-organized multilayer films within a very short time [165, 166]. LbL assembly using a spraying process can be easily controlled and is very reliable, permitting regular multilayer growth even under conditions where dipping fails to produce homogeneous films [167]. Automatic machines for film preparation have also been developed [168–171].

Biocompatibility is the most prominent advantage of the LbL assembly process because this technique requires mild conditions for film construction. Most proteins, especially those soluble in water, have charged sites on their surface, and so the electrostatic LbL adsorption is useful for the construction of various protein organizations. As has already been demonstrated, a large variety of proteins have been assembled in combination with oppositely charged polyelectrolytes [172]. Unlike other methods for protein immobilization, various types of layered structures can be prepared, where the number of layers and the layering sequence can be easily modified. Figure 2 illustrates primitive examples of LbL assemblies between enzymes and polyelectrolytes. The LbL films were prepared on the surface of a quartz crystal microbalance (QCM). Frequency shifts represent weight of adsorbed proteins and polyelectrolytes with nanogram precision [173–177]. Alternate assemblies of poly(ethyleneimine) (PEI) and GOD were assembled on the precursor film (four layers of PEI and PSS poly(sodium styrenesulfonate) (PSS) film) (Fig. 2a) [178]. Film growth was constant with an average frequency change of approximately 2,000 Hz for a single GOD-PEI layer. This assembly process was stopped at the PEI adsorption step of the 10th cycle followed by adsorption of PSS for conversion of the surface charge to negative. Then LbL assembly between peroxidase (POD) and PSS was carried out, where constant film growth was repeatedly observed with an average frequency change of approximately 180 Hz per a single POD-PSS layer. LbL assembly with a reversed protein sequence was also examined (Fig. 2b); that is, the POD-PSS film was initially assembled, and then the PEI-GOD film was assembled.

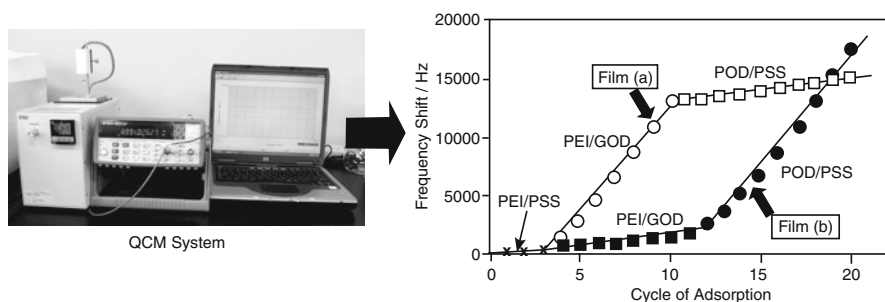


**Fig. 2** QCM evaluation of enzyme-polyelectrolyte LbL films. The QCM frequencies change in proportion to weight of adsorbed layers

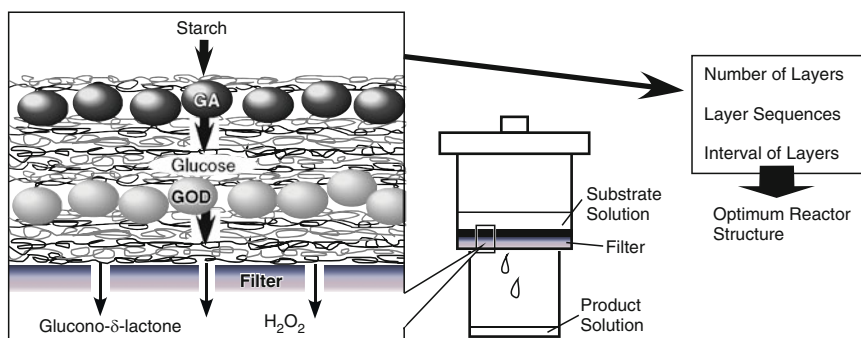


**Fig. 3** Multi-enzyme reactor of LbL films containing GA and GOD on ultrafilter

The observed frequency changes of each assembly were essentially identical to those of the former example. These two kinds of protein-polyelectrolyte assembly processes are essentially independent and inner layers do not interfere with assembly of the outer layers.

These attractive features of the LbL assembly in protein adsorption allow us to construct multi-enzyme reactors with optimized layered sequences. Figure 3 illustrates examples of multi-enzyme reactors containing GOD and glucoamylase (GA) immobilized on an ultrafilter through which a substrate solution was passed [179]. The starting material of the reaction sequence is starch, which does not rapidly diffuse through the film because of its high molecular weight. Hydrolysis of the glycoside bond in starch by GA produces glucose. Glucose is converted to glucono-lactone by GOD with H<sub>2</sub>O<sub>2</sub> as a co-product. The effect of film organization on the reaction efficiency was investigated using the multi-enzyme films with varied assembling sequences. A film with the best efficiency satisfies two essential conditions: (1) matching of enzyme sequence with reaction scheme and (2) appropriate interval between two enzyme layers. Because the sequential reaction requires that the reaction with GA proceeds before the oxidation of glucose catalyzed by GOD, the order of the enzyme layers in these films agrees with the order of the sequential enzymatic reactions. Correct intervals between GA and GOD layers are necessary for efficient reaction. This is related to possible inhibition of GA activity by glucono-lactone that is one of the products in the second reaction. These examples strikingly demonstrate the importance of well-organized layered structures in design of multi-enzyme reactors.

LbL assembly improves the stability of immobilized proteins. For example, GOD immobilized in the LbL films keeps its high activity for more than 14 weeks at 4 °C [180]. Most enzymes are denaturated and lose their activity at high temperature, but immobilization of GOD in the LbL films drastically enhances thermostability. A significant decrease in activity was not detected even after incubation at 50 °C. Immobilization of protein molecules in films through interaction with a polyelectrolyte matrix effectively prevents denaturation of protein structures. An interesting advantage of the LbL assembly over the LB technique was found in

the effect of film thickness on reaction efficiency. Reaction efficiency per enzyme in GOD-immobilized LB films decreases as the number of layers increases. Difficulties of substrate diffusion cause deterioration of enzyme activity in well-packed thick LB films. Conversely, GOD activity in LbL assembly did not decrease even when the numbers of layers increased. Loosely assembled LbL structures are advantageous in reactor applications that require easy diffusion of substrates and products.

### 3 Enzyme-Embedded LbL Devices

#### 3.1 *Thin Film Type*

As described above, the LbL technique has a wide applicability in available components and variations of layered structures, and various kinds of LbL films composed of proteins and polyelectrolytes have been explored. Typical recent examples concerned with flat films are described here.

##### 3.1.1 Progress on Fundamental Aspects

Although electrostatic interaction often stabilizes protein structures, it may actually be detrimental in cases of structurally less rigid species. Biospecific interaction such as recognition between lectin and saccharides would provide an ideal situation for protein assembly. For example, Lvov et al. demonstrated assembly of Concanavaline A with glycogen through biospecific recognition and with PEI through electrostatic interaction [181]. Biospecific interactions usually possess very high binding constants and are more effective than electrostatic interaction. Anzai et al. assembled avidin with biotin-attached poly(amine)s under conditions where electrostatic repulsions work between both positive species [182]. The deposition behavior and the structure of the avidin/poly(amine) multilayer films depend significantly on the molecular geometry of the poly(amine) components. The poly(amidoamine) (PAMAM) dendrimer with globular structure resulted in a monomolecular deposition of avidin. In contrast, multilayer deposition of avidin was observed for LbL assembly with randomly branched and linear PEI. Because biotinavidin interaction is highly specific, binding structures should be strongly influenced by the shape of poly(amine) components. This in turn means that the loading of biomaterials in the LbL thin films can be regulated by a suitable choice of polymeric materials.

Control of structures including conformation of proteins adsorbed on the surfaces of thin films is a target of some practical importance. Fibronectin is a highly flexible glycoprotein and plays essential roles in numerous biological phenomena including cell adhesion and spreading, wound healing, phagocytosis, and differentiation. These biological activities are known to be sensitive to conformation of fibronectin. Van Tassel and coworkers investigated the adsorption of fibronectin onto LbL films

of poly(allylamine hydrochloride) (PAH) and PSS [183]. Deposition density and thickness of fibronectin on a PAH-terminated positive surface were estimated as roughly double those on a negatively charged PSS-terminated film. Considerable enhancement of binding of monoclonal antibodies specific to the protein's cell binding site to fibronectin adsorbed on the PSS-layer was confirmed, which indicates that fibronectin on the PSS-layer is more accessible to incoming species. Fibronectin molecules individually adsorb onto a PSS-terminated film primarily in side-on-orientation, while those on a PAH-terminated film form clusters in end-on-oriented monolayers.

Various types of bioreactors have been fabricated based on the LbL technique. For this purpose, the surface modification of substrates for physical protein immobilization is also an important factor. Serizawa and coworkers proposed controlling the activity of  $\beta$ -galactosidase for hydrolysis of *p*-nitrophenyl- $\beta$ -D-galactopyranoside immobilized on supports coated with structurally regular poly(methyl methacrylate) (PMMA) using the stereocomplex, isotactic-PMMA and atactic-PMMA films [184]. They demonstrated that a slight difference of polymer surface structure strongly affects activities of immobilized enzymes, even though polymers have the same chemical component. Some enzymes can digest harmful chemicals and form as protective layers for inside weaker functional layers. Shutava et al. demonstrated catalase-based protective barriers to oxidative environments (Fig. 4) [185]. They examined the influence of a catalase layer located at different depths in hemoglobin/PSS LbL films on the kinetics of hemoglobin degradation under hydrogen peroxide treatment with respect to internal (film thickness and architecture) and external (hydrogen peroxide concentration) conditions. The highest activity in hydrogen peroxide decomposition was observed when the catalase layer was situated on top of the LbL multilayers. Hemoglobin (Hb) in such films was demonstrated to retain its activity for a longer period of time. Hu and coworkers also investigated the protective effect of exterior catalase layers using electroactive myoglobin (Mb) or horseradish peroxidase (HRP) in these films as a probe to monitor the extent of protein damage by  $H_2O_2$  [186]. The results similarly demonstrated that the outer catalase layers controlled the rate of  $H_2O_2$  entry into inner regions of the film.

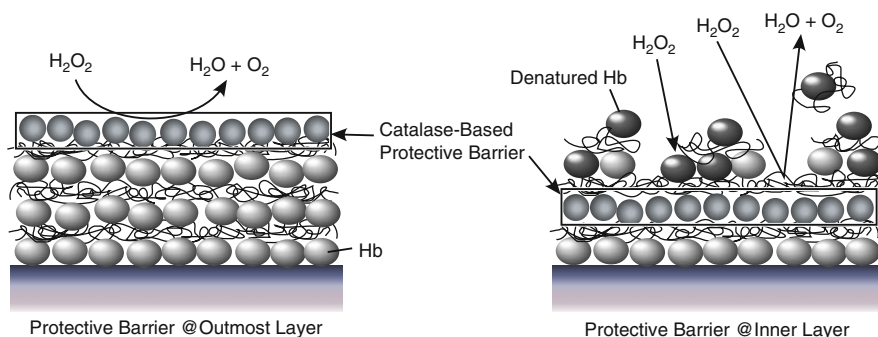


**Fig. 4** Function of catalase-based protective barrier to suppress destruction of enzyme layers

### 3.1.2 Sensor Applications

The LbL technique is undoubtedly one of the best methods to incorporate biological components into man-made devices. Therefore, sensor applications must be one of the most promising subjects for LbL assemblies of biomaterials. For example, Leblanc and coworkers used several bilayers of chitosan and poly(thiophene-3-acetic acid) as cushion layers for stable enzyme films [187]. The first five bilayers of the cushion layer allowed for better adsorption of organophosphorus hydrolase than the corresponding adsorption on a quartz slide. The immobilized enzyme becomes more stable and can be used under harsher conditions. The assembled LbL films can be used for spectroscopic detection of paraoxon, an organophosphorus compound. This cushion layer strategy provides a well-defined substrate-independent interface for enzyme immobilization, in which the bioactivity of the enzyme is not compromised. This leads to fast detection of paraoxon and quick recovery times.

Because immobilization of protein LbL films on various electrodes is a big trend of LbL-related applications, electrochemical analyses on the bio-active LbL films are important research targets. Rusling and coworkers are extensively developing LbL-based electrochemical sensors. For example, Lvov, Rusling, and coworkers assembled on gold electrodes LbL films of Mb or cytochrome P450<sub>cam</sub> (CytP450<sub>cam</sub>) with oppositely charged polyions, including DNA, acting as “electrostatic glue” [188]. Direct, reversible electron transfer between electrodes and proteins involved the heme Fe<sup>III</sup>/Fe<sup>II</sup> redox couple. The presence of oxygen induced electron transfer to the Fe<sup>II</sup>–O<sub>2</sub> complexes of these proteins resulting in production of hydrogen peroxide. Consequently, these LbL films may be used for electrode-driven enzyme-like catalysis, for example, for the epoxidation of styrene. They also pioneered DNA damage analyses using the LbL constructions. They assembled LbL films of Mb or Cyt P450<sub>cam</sub> and DNA on electrodes, which were activated by hydrogen peroxide, and the enzyme in the film generated metabolite styrene oxide from styrene metabolism. DNA damage in the human liver could then be mimicked through reaction between the resulting styrene oxide with double-stranded DNA (dsDNA) (Fig. 5) [189]. DNA damage was detected by square wave voltammetry by using catalytic oxidation with Ru(bpy)<sub>3</sub><sup>2+</sup> and by monitoring the binding of Co(bpy)<sub>3</sub><sup>3+</sup> (bpy = 2,2'-bipyridine). They proposed that their method could be suitable for in vitro screening of toxicity of organic metabolites and their parent compounds. Guo and coworkers also demonstrated that the GOD-incorporated LbL multilayer film could be used as a photoelectrochemical sensor for the detection of in situ oxidative DNA damage through the metal-induced Fenton reaction [190]. DNA damage was detected by monitoring the change of photocurrent of an indicator such as a Ru complex. Differences in affinity with the sensor films between intact and damaged DNAs induced changes in photocurrent signals.

Ram et al. reported electrochemical properties of GOD assembled with a conductive polypyrrole through LbL techniques [191]. The results obtained provided information, with respect to the electron transfer processes, on the spatial arrangement of GOD molecules on the polypyrrole surfaces, which might give crucial and important insights for construction of glucose-responsive biosensors. Wollenberger

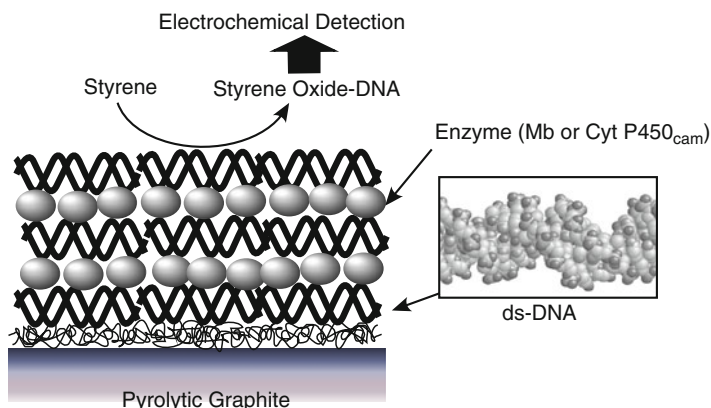


**Fig. 5** LbL sensor for DNA damage detection

and coworkers prepared LbL films of cytochrome c and sulfite oxidase with the aid of poly(aniline sulfonate) [192], which were co-immobilized on the surface of a gold electrode. Electro-catalytic properties upon sulfite addition to the electrodes were characterized and the role of the different components in the electron-transport chain was clarified. They suggested that this multilayer electrode could act as an anode in a bio-fuel cell or could be exploited as a biosensor for the detection of sulfite, which is used as a preservative in wine and other foodstuffs. Balkenhohl et al. prepared multi-enzyme LbL films of cytochrome c (inner layer) and laccase (outer layer) on a gold electrode using poly(anilinesulfonic acid) as a polyelectrolyte component [193]. The catalytic oxygen reduction current was linearly dependent on the oxygen concentration in solution indicating that cytochrome c molecules in the inner layer of the LbL multilayer film function as biological redox carriers effectively transferring electrons from the gold electrode through the multilayer film towards the immobilized laccase molecules at the outer layer. Chen and coworkers fabricated  $\text{Fe}_3\text{O}_4$  multilayer film and reported its application in promoting direct electron transfer of hemoglobin [194]. Characteristic superparamagnetic properties of  $\text{Fe}_3\text{O}_4$  nanoparticles persisted in the film and could be controlled simply by changing the assembly layers. In addition, the LbL multilayer film exhibited good compatibility with proteins, the catalytic activity of the immobilized hemoglobin was retained, and the direct electron transfer with the underlying glassy carbon electrode (GCE) could be realized.

### 3.1.3 Inclusion of Functional Nanomaterials

One of the most outstanding features of LbL assemblies lies in the great freedom in selection of assembled components, which permits us to introduce various components in the LbL structures to improve sensor performance. Incorporation of nanomaterials such as gold nanoparticles was demonstrated to enhance



sensitivity of the LbL sensors. Zhang et al. used adsorption processes of enzymes with the non-enzymatic LbL layers [195]. They first prepared LbL films using poly(diallyldimethylammonium chloride) (PDDA) and gold nanoparticles on a gold electrode, and incubation of this electrode resulted in absorption of GOD into the LbL films. Electrochemical impedance measurements revealed that these LbL films have lower electron transfer resistance, due to the presence of gold nanoparticles, than that of a conventional assembly of PDDA and GOD. Chen and coworkers fabricated LbL assembled films composed of chitosan, gold nanoparticles, and GOD onto the surface of the Pt electrode [196]. GOD immobilized in the film showed excellent catalytic properties for glucose substrate, and the gold nanoparticles not only provided a suitable environment for stable immobilization of GOD but also effectively improved the electron transfer between analyte and electrode surface. Hu and coworkers reported enhanced formation of gold nanoparticles through in situ electrodeposition in Mb-loaded LbL films of chitosan and silica nanoparticles [197]. Positively charged chitosan and negatively charged silica nanoparticles were alternately assembled on the graphite electrode which was then immersed in Mb and  $\text{HAuCl}_4$  solution. The  $\text{Au}^{\text{III}}$  loaded in the films was subsequently electrochemically reduced, giving Au nanoparticles and providing nanocomposite films. Compared with films without Au nanoparticles inside, the composite films exhibited improved electrochemical and electrocatalytic behavior of Mb, because Au nanoparticles formed inside the films were located in proximity to Mb and acted as electron bridges between Mb molecules, inducing activity in more Mb molecules in the films to become electroactive. Furthermore, the permeability or porosity of the films played an important role in realizing the direct electrochemistry of Mb. Yuan and coworkers reported an amperometric enzyme immunosensor for  $\alpha$ -1-fetoprotein antigen (AFP) using gold electrodes modified with LbL films containing HRP, anti-AFP, gold nanoparticles, and thionine on Nafion [198]. Sun and coworkers fabricated a bienzymatic sensor by covalently attachment of periodate-oxidized GOD and HRP on controlled multilayer films of sulfonate-capped gold nanoparticles/thionine as a mediator of electron transfer [199]. The resulting biosensor film exhibited good electrocatalytic response toward glucose and the electrocatalytic response increased with the number of thionine layers.

Villalonga and coworkers used specific inclusion at the cyclodextrin cavity as a supramolecular concept for preparation of an enzyme-immobilized LbL sensor [200]. This strategy was based on the supramolecular immobilization of alternating layers of HRP (either modified with 1-adamantane or  $\beta$ -cyclodextrin-branched carboxymethylcellulose residues) on Au electrodes coated with polythiolated  $\beta$ -cyclodextrin polymer. Frago et al. adopted a similar strategy by the immobilization of a first layer of thiolated cyclodextrin polymer on a gold electrode followed by the supramolecular capture of adamantane-modified HRP (Fig. 6) [201]. Successive enzyme layers were then attached using cyclodextrin-modified gold nanoparticles as linkers. This method provides a regenerable surface that can be further used for the attachment of new enzyme layers.

Dendrimers are branched polymers of controlled structures where functional groups can be immobilized in a predesignated manner [202–209]. Therefore, use



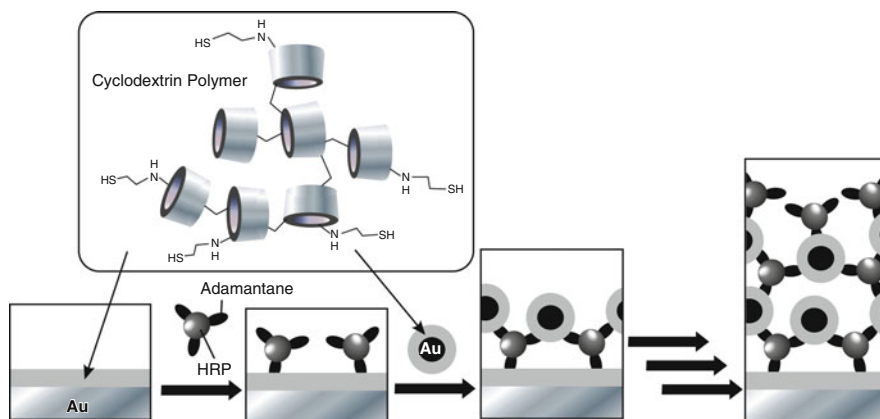


**Fig. 6** Regenerative LbL-based sensor with concept of supramolecular inclusion by cyclodextrin conjugate

of dendrimers instead of the conventional polyelectrolytes usually used for the LbL processes would be attractive for construction of functional films. For example, Kim and coworkers developed a reagentless biosensor using the surface-functionalized fourth generation PAMAM dendrimers partially modified with redox-active ferrocenyl groups [210]. The modified dendrimers were used for the construction of LbL films with periodate-oxidized GOD on a gold electrode. By taking into consideration the surface concentration of deposited ferrocenyls, active enzyme coverage, and electrode sensitivity, the degree of ferrocenyl functionalization could be optimized. Zucolotto et al. assembled LbL films of Cl-catechol 1,2-dioxygenase with PAMAM dendrimers [211]. The Cl-catechol 1,2-dioxygenase kept its activity in the LbL films, which can be used for detecting catechol in solutions at very low concentrations ( $10^{-7}$  to  $10^{-10}$  M) by employing optical and electrical measurements. The same research group recently reported an LbL method for dendrimer-assisted immobilization of alcohol dehydrogenase (ADH) onto Au-interdigitated electrodes for ethanol detection using electrical capacitance measurements [212]. By combining the electrical capacitance data from the three electrodes using principal component analyses, the system was able to detect and distinguish between ethanol solutions with concentrations as low as 1 ppmv (parts per million by volume).

### 3.1.4 With Electroactive Mediators and Wires

Incorporation of electroactive components often improves performance of electrochemical sensors. Ferreira et al. exploited the LbL technique to produce sensitive and stable glucose biosensors by the immobilization of GOD onto an indium tin oxide (ITO) substrate modified with a Prussian Blue layer [213]. The high sensitivity was attributed to the ultrathin nature of the LbL film in addition to the low operating potentials that could be used due to the efficient catalysis of  $\text{H}_2\text{O}_2$  produced in the

enzymatic reaction in the presence of Prussian Blue. These LbL biosensors showed high stability, as demonstrated in tests performed for approximately 20 days with a reliable amperometric response in almost constant sensitivity for the whole period of experiments. Tight linking of GOD to the electrode may result in such high stability. Lin and coworkers prepared LbL films of HRP with PSS in which low molecular dye methylene blue was pre-adsorbed [214]. Methylene blue can act as an electron mediator to promote the electrochemical reaction between the immobilized HRP and the electrode surface. The prepared LbL films are useful for the sensing layer of reagentless  $\text{H}_2\text{O}_2$  biosensor.

Electroactive carbon nanotubes are especially attractive components for LbL-based electrochemical sensors. Yan et al. reported fabrication of a transparent and flexible glucose biosensor where multi-wall carbon nanotubes (MWNTs) and GOD were assembled on a polymer substrate [215]. Negatively charged MWNTs and GOD were LbL assembled on the polymer substrate modified by Au. The film showed a porous structure where the assembled MWNTs were mainly in the form of individual tubes or small bundles. Electrochemical studies demonstrated that the multilayer membrane exhibits remarkable electrocatalytic activity to detect glucose molecule. Schmidtke and coworkers prepared LbL-based biosensors from enzyme-coated single-walled carbon nanotubes (SWNTs) and redox polymers [216]. Gold electrodes were first functionalized with negatively charged 11-mercaptoundecanoic acid followed by alternate assembly in solutions of a positively charged redox polymer, poly(vinylpyridine) (PVP) having Os complex and a negatively charged GOD containing SWNTs. The oxidation peak currents of this film during cyclic voltammetry increased 1.4–4.0 times as compared to films without SWNTs. Similarly the glucose electro-oxidation current also increased (6–17 times) when SWNTs were present. By varying the number of multilayers, the sensitivity of the sensors could be controlled.

If polyelectrolytes carry redox-active side chains, they can work as electroactive wires to bridge proteins and electrode. Calvo et al. demonstrated that only a small fraction of active GOD molecules electrostatically adsorbed onto PAH with Os complex on the electrode are actually wired (Fig. 7a) [217], even though there is an excess of osmium groups in the polymer with respect to the enzyme concentration. This electrochemically wired enzyme was analyzed with the catalytic current dependence on glucose concentrations for the ping-pong mechanism of glucose oxidation. The catalytic current increased with the number of LbL layers because of the increase in the enzyme loading while the efficiency of enzyme  $\text{FADH}_2$  oxidation by the Os redox polymer remained almost constant. They also made a systematic study of the structure, thickness, and electrocatalysis for the oxidation of  $\beta$ -D-glucose by GOD, mediated by an Os bipyridine complex modified PAH, in LbL multilayer structures obtained at different pH of the dipping redox polyelectrolyte solution (Fig. 7b) [218]. A systematic change in the pH of the PAH-Os dipping solution leads to a variation in the linear charge carried by the redox polyelectrolyte and strongly affects the polyelectrolyte-enzyme multilayered structure and catalytic properties. Sun and coworkers assembled LbL films through alternate deposition of negatively charged HRP and positively charged quaternized PVP with Os complex

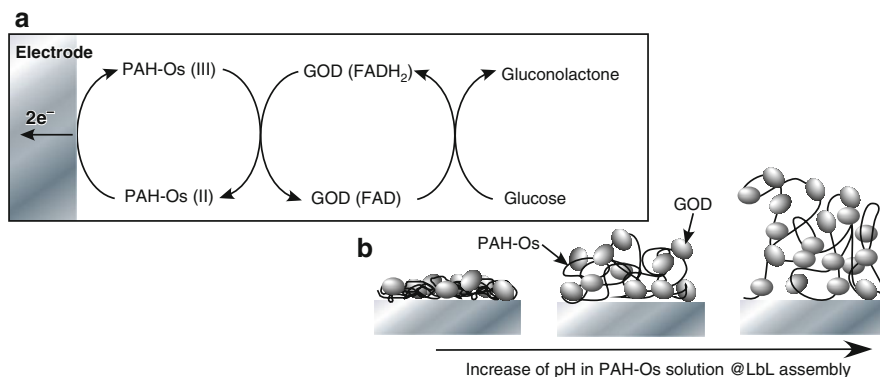


**Fig. 7** (a) Glucose sensing by electrically wired LbL assembly. (b) pH dependence of amount of immobilized GOD

on the negatively-charged alkanethiol-modified gold electrode surface [219]. This enzyme electrode of multilayer films was sensitive for the electrocatalytic reduction of hydrogen peroxide and can be used as amperometric sensors for hydrogen peroxide.

### 3.2 Particle and Capsule Type

One of the most influential innovations in the history of LbL technology so far must be LbL assembly on a colloidal particle with subsequent hollow capsule preparation [220–223]. In the first decade of LbL technology, researchers regularly assembled films on a flat solid support of visible dimensions. However, the mechanism of the LbL assembly does not exert any limitations on the size of supports or their shape. Therefore, LbL assembly on microscopic solid surfaces dispersed in solution is reasonable, opening the way to fabrication of both three-dimensional structures and nano/micro-sized objects through the LbL process. As shown in Fig. 8, the concept of the assembly is simple. LbL films are assembled sequentially on a colloidal core in a similar way to conventional LbL assembly on a flat plate. Dissolution of the central particle core upon exposure of the particles to appropriate solvents then results in hollow capsules.

The construction of LbL multilayer films of biomaterials on colloid particles is of particular interest in applications where a microscopic contact is essential, such as protein interaction and cell communication, and where high surface area is desirable, such as in catalysis. For example, enzyme LbLs on particle surfaces are useful for biorelated catalysis since microscopic objects of higher surface area can potentially yield higher enzymatic reaction efficiencies than their planar film counterparts. If the LbL assembly is conducted on microparticles with certain functions, we can

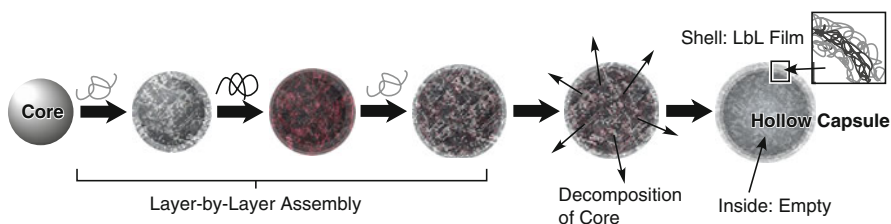


**Fig. 8** LbL assembly on colloidal particle and subsequent preparation of hollow capsule

combine properties from both LbL films and core materials. For example, the LbL assembly of enzymes on magnetic particle enables us to use biocatalytic activities and magnetic properties, leading to freely collectable biocatalytic microparticles.

### 3.2.1 Progress on Fundamental Aspects

LbL hollow capsules have excellent potential in important biological applications, such as drug delivery. Biocompatible polymers such as chitosan and chondroitin sulfate can be used as polyelectrolyte components. Storage and controlled release of small drug molecules using LbL hollow capsules are both possible and even large proteins can be entrapped in the LbL hollow capsules. For example, the capsule can be used as a nano-container for enzymes (Fig. 9) [224]. Stable hollow polyelectrolyte capsules were first produced by LbL assembly between PAH and PSS on melamine formaldehyde particles followed by particle decomposition at low pH. Capsules prepared in this way and suspended in water do not allow the enzymes to permeate to the interior. However, enzyme permeability can be induced by exposing the capsules to a water–ethanol mixture. Resuspension in water closes the capsule pores, leading to entrapment of the enzyme. The hollow capsules are permeable by small molecular species, and the entrapped enzyme then exhibits biocatalytic activity. Greater loading of enzymes into the LbL hollow capsules can be performed using enzyme crystals as core material (Fig. 10) [225]. This approach leads to extremely high enzyme loading in a nano-sized capsule. Although the enzymes are coated with very thin polyelectrolyte films, the entrapped enzymes are quite stable against protease degradation.

If template synthesis is united with LbL techniques, as depicted in Fig. 11, then formation of self-assembled microtubes can be achieved if the template contains regular pores. Sequential assembly of polymers within a controlled pore followed by template removal can result in self-standing tubular structures. Li et al. reported fabrication of microtubes based on hydrogen-bonding LbL self-assembly from poly(acrylic acid) (PAA) and PVP [226]. They also demonstrated successful removal of the PAA and the resulting porous walled tubes could also be useful as carriers in drug delivery or as catalyst supports. The same research group applied this strategy to fabrication of microtubes from biocomponents. Human serum albumin (HSA) is structurally stable under acidic or basic conditions because of strong

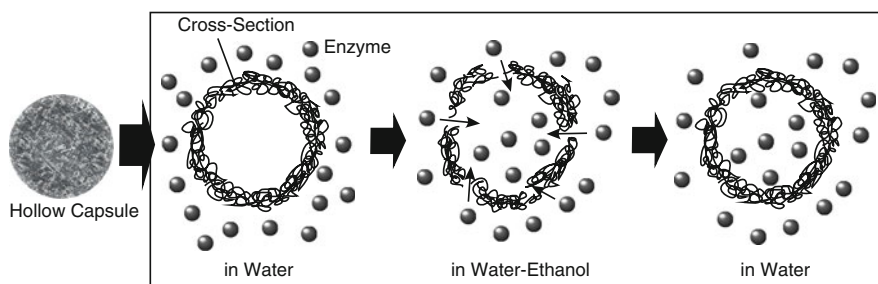


**Fig. 9** Entrapment of enzymes into hollow capsules through solvent treatment

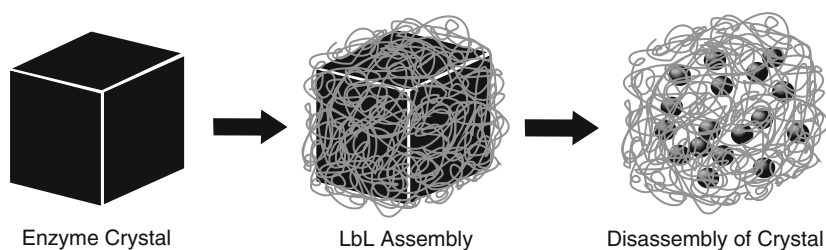


**Fig. 10** Hollow capsule formation using enzyme crystal as a core material for high loading of enzyme

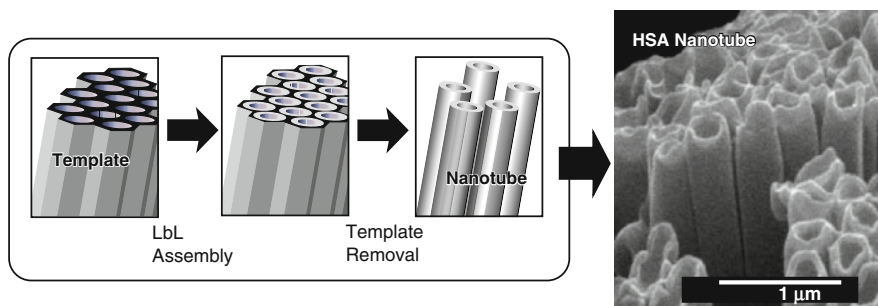


**Fig. 11** Template synthesis of protein nanotube through LbL assembly. Micrographic image of HSA nanotubes were kindly provided by Prof. Junbai Li

binding sites within its subdomains [227, 228]. The surface charge of human serum albumin can be modified to be either more positive or more negative by varying pH, making it possible to form an LbL assembly only from HSA that has smooth and clean surfaces with a wall thickness of around 30 nm and a length of 60 μm.

LbL capsules and related objects have great potential for biomaterial fabrication and applications. Research activity on LbL capsules is becoming extensive. Parts of recent examples are described below.

### 3.2.2 LbL Assembly on Colloidal Particles

In the one of the simplest yet pioneering examples, Schüler and Caruso assembled GOD on submicrometer-sized polystyrene spheres through LbL adsorption with PEI [229]. The high surface area afforded by colloids can be exploited to minimize substrate diffusion effects that limit the use of enzyme multilayer films assembled on a planar surface. Therefore, the high surface area of the bio-multilayer coated particles formed were efficiently utilized in enzymatic catalysis. The same researchers similarly investigated bicomponent colloidal reactors [230]. The coupled enzymatic reaction between GOD and POD assembled on the same poly(styrene) particle (bicomponent enzyme film) was demonstrated. Enzyme multilayers constructed by the alternating adsorption of polyelectrolyte and premixed enzyme/polyelectrolyte complexes exhibited a lower activity than the assemblies prepared from the uncomplexed species. The successful recovery and reuse of magnetic-functionalized particles coated with enzyme layers with a magnet was also demonstrated. Ball and coworkers investigated stability of immobilization of alkaline phosphatase (ALP) as a model enzyme on the surface of Affi-gel heparin beads functionalized through LbL assembly between biopolyelectrolytes, poly(L-glutamic acid) (PGA) and poly(L-lysine) (PLL) [231]. The enzyme was adsorbed either on the top of the LbL film or embedded under five polyelectrolyte layers. When ALP was adsorbed on the top of the LbL architecture, initial detachment was detected but no further desorption was observed over storage times larger than 3 months. In the case of ALP embedding under two PLL-PGA bilayers, no enzyme was released and the embedded enzyme retained about 30% of its initial activity after 3 months of storage.

On the other hand, reevaluation of the stability of enzymes entrapped in LbL layers on the colloidal core has now become an important subject. Ansorge-Schumacher and coworkers very recently pointed out the importance of the combination of capsules' polyelectrolyte, reactants, and enzyme [232]. The biocatalysts (lipase B) were adsorbed to  $\text{CaCO}_3$  or DEAE-cellulose colloidal cores on which LbL multilayers of PAH and PSS had been coated. Residual activity of the enzymes investigated gradually decreased as the number of LbL films increased. The activity decrease was attributed to mass transfer restrictions as well as direct interactions between polyelectrolytes and catalytically active molecules. It was proposed that preselection should be performed based on all available knowledge on the complex interactions between polyelectrolytes, biocatalyst, and reactants with regard to activity/productivity and stability. Zhu et al. used alginate microspheres for combined physical and chemical immobilization in order to improve stability of encapsulation and activity [233]. GOD was successfully encapsulated into calcium-cross-linked alginate hydrogel microspheres. LbL coatings were applied on alginate/GOD microspheres. The technique presented was shown to be a practical and effective way to fabricate GOD-encapsulating alginate microspheres for future use as implantable glucose biosensors.

Sensor applications are also a big target for LbL-coated colloidal systems. Rusling and coworkers used enzyme-DNA biocolloid systems for detection of DNA adducts and reactive metabolites using chromatography-mass spectrometry

analyses [234]. In their approach, silica microbead bioreactors coated with DNA and enzymes such as  $\text{cyt P450}_{\text{cam}}$  and Mb were fabricated to measure reactive metabolites and DNA-adduct formation rates relevant to genotoxicity screening using the LbL technique. The LbL-coated colloid particles formed were tested through oxidation of guaiacol, styrene, and (4-methylnitrosoamino)-1-(3-pyridyl)-1-butanone. Enzyme turnover rates for formation of reactive metabolites were monitored using gas chromatography/mass spectrometry and liquid chromatography-mass spectrometry. Dramatic improvements in surface area to volume ratio over similar films on macroscopic surfaces were confirmed. They claimed that the proposed method would be particularly useful as a chemical complement to established microbiological assays for in vitro toxicological screening, enzyme kinetic, inhibition analysis, and drug discovery. Viswanathan and Ho reported dual electrochemical determination of glucose and insulin [235]. The LbL films on the ferrocene microcrystal followed by anti-insulin antibody sensitization were employed for the biolabeled ferrocene microcapsules. The prepared microcapsules were used to perform a sandwich immunoassay for the detection of insulin. Addition of releasing-reagent such as DMSO resulted in the release of a large amount of electrochemical signal-generating ferrocene molecules into the outer medium through the permeable capsules' wall. The released ferrocene molecules were then measured amperometrically. Simultaneously, glucose was also determined amperometrically using GOD immobilized on the electrode.

Trau et al. proposed an efficient immunoassay using LbL capsules assembled on fluorescent microcrystals (Fig. 12) [236]. Their strategy starts with encapsulation of microcrystalline fluorescein diacetate with an average size of 500 nm with the LbL multilayers of PAH and PSS. Molecules for biorecognition, (immunoglobulin G, IgG) were then attached at the surface of the LbL layer for sandwich immuno-assay. Following the immuno-reaction, the fluorescein diacetate core was dissolved by exposure to organic solvent, leading to the release of the fluorescein diacetate molecules into the surrounding medium. Amplification rates between  $70\times$

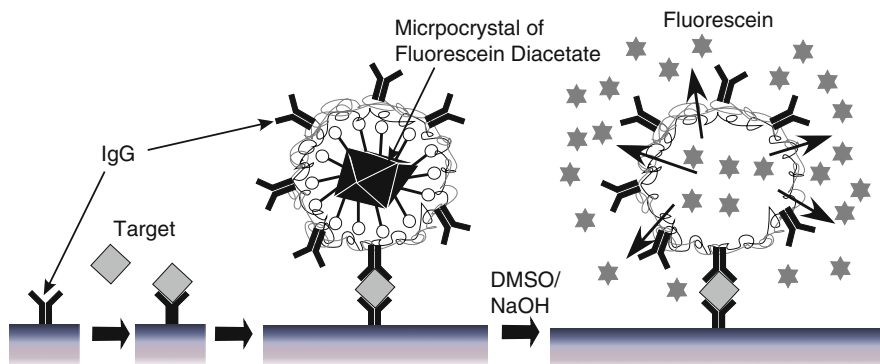


**Fig. 12** Highly sensitive immunoassay through sandwich assay using LbL capsule coated with IgG



and  $2,000\times$  of this microcrystal label-based assay compared with the corresponding immunoassay performed with direct fluorescently labeled antibodies were reported. The proposed technique has the potential to compete with enzyme-based labels since long incubation times are not required, thus speeding up bioaffinity tests. Tong and coworkers prepared LbL multilayers on drug crystals that could be used as a drug delivery system [237]. The LbL wall made of sodium alginate/chitosan multilayer film was directly deposited on indomethacin microcrystals. Erosion by pepsin induced release of indomethacin from the LbL composite. The release rate could be controlled by several factors. Increasing temperature of the LbL assembly effectively reduced the release rate of the drug because of improvements in the structure of the multilayer film. Cross-linking the neighboring layers of sodium alginate and chitosan with 1-ethyl-3-(3-dimethylamino-propyl)carbodiimide also significantly reduced the enzymatic desorption and release rate. These factors are important for protection of the multilayer film from enzymatic erosion and for prolonged release intervals of the encapsulated drug.

### 3.2.3 Hollow Capsules

Hollow capsule structures are also useful in various applications. Lvov and coworkers reported enzyme-catalyzed polymerization of phenols using LbL capsules [238]. Their approach is based on selective permeability of capsule walls to monomer molecules and their impermeability to the resulting polymeric products. Biocatalysts and polymeric products cannot leave the capsules' interior because of their high molecular weight. HRP was encapsulated within PSS/PAH LbL capsule using a pH-driven pore opening mechanism. In this case, 4-(2-aminoethyl)phenol hydrochloride (tyramine) was used as a monomer giving easily detectable fluorescent polymeric products after addition of hydrogen peroxide into the system. A wide variety of enzymes and monomers can be used to provide new types of micro- and nanocomposites with desirable properties in a biologically friendly environment. It should also be possible to synthesize functional materials in the microcapsule such as light-emitting polymers and to modify permeation properties of the microcapsule walls by depositing polymers in their walls.

McShane and coworkers demonstrated real-time evaluation of enzymatic catalysis in LbL microcapsule systems [239]. Capsules containing entrapped enzymes, GOD and HRP, were produced through polyelectrolyte LbL assembly on enzyme-doped  $\text{CaCO}_3$  microparticles. Upon template dissolution, the adsorbed GOD and HRP were released and subsequently bound to the interpenetrating polyelectrolyte matrix by electrostatic interactions, thus resulting in microcapsules containing GOD and HRP. Catalytic reactions were colorized using indicating dye, Amplex Red. Real-time observation by confocal laser scanning microscopy revealed that the encapsulated enzymes were active, and readily catalyze glucose oxidation at the capsule interior and within the capsule walls. It also indicated that the majority of glucose catalysis occurred within the capsule walls as compared with that of the capsule interior. Zhu and McShane proposed a method for enzyme-entrapment



into LbL capsules that had been prepared with photosensitive diazoresin-based polyelectrolyte on  $\text{MnCO}_3$  template [240]. The change of the multilayer wall permeability before and after UV irradiation was explored for stable enzyme (such as GOD and POD) encapsulation in diazoresin-based microcapsules. The loading procedure is simple. The permeability of the diazoresin-based multilayer wall changed substantially due to cross-linking by exposure to ultraviolet light. Akashi and coworkers reported time-modulated release of multiple proteins from the LbL capsules [241]. They prepared enzymatically degradable capsules composed of chitosan and dextran sulfate multilayers as a drug carrier. The release of encapsulated FITC-labeled albumin could be controlled by the enzymatic degradation of the chitosan membranes with chitosanase. When two kinds of guests are separately incorporated inside the capsule and into the capsule membrane, independent release of the trapped guests by exploiting the enzymatic degradation of the capsule membrane becomes possible.

LbL assemblies including lipid vesicles, which can be regarded as models of cell membrane, should provide unique opportunities for creating novel bio-assemblies. Katagiri et al. pioneered LbL assembly using a superstable organic-inorganic vesicle cerasome with a silica network at the surface [242–244]. LbL assemblies between cationic polyelectrolyte and anionic cerasome [245] as well as the LbL assemblies between the anionic cerasome and the cationic cerasome [246, 247] were demonstrated without rupture of the vesicular structures. The latter assemblies are expected to be used as multi-cellular mimics. Schaaf and coworkers demonstrated incorporation of phospholipid vesicles in the LbL films composed of PGA and PAH [248]. Composite capsules between lipid components and polyelectrolytes have also been investigated. The same research group reported liposome-embedded LbL films, where enzymes included in the vesicles showed reactor activity [249]. Shutava et al. demonstrated LbL assembly between anionic phospholipids such as phosphatidic acid and phosphatidylglycerol and polycation on poly(methacrylic acid) microspheres [250]. The composite microcapsules obtained composed of lipid and polyelectrolyte were subjected to research of intramembrane diffusion of fluorescent dye.

Katagiri and Caruso applied step-by-step LbL assembly to preparation of lipid bilayer vesicles with asymmetric structures between inner and outer shells [251]. They first assembled polyelectrolyte multilayers on melamine-formaldehyde particles and terminated the assembly with negative outermost surfaces. Monolayer of cationic lipid was then adsorbed on the anion-covered particle to give surfaces coated with hydrophobic alkyl chains. Contacting the particles formed with vesicles of an anionic lipid in aqueous solution induced monolayer coverage of the anionic lipid. The outermost layers of the composite particles formed were then coated with polycation. Removal of the core material provided asymmetric bilayer vesicles. Although asymmetry plays a very important role in naturally occurring cell membranes, conventional processes on lipid assemblies cannot give such asymmetric structures. Therefore, LbL methods should give new opportunities in model studies on biological membranes. Lipid/polyelectrolyte composite LbL capsules provide an appropriate medium for bioactive materials. Li and coworkers immobilized ATP synthase into composite capsules (Fig. 13) [252, 253]. They prepared

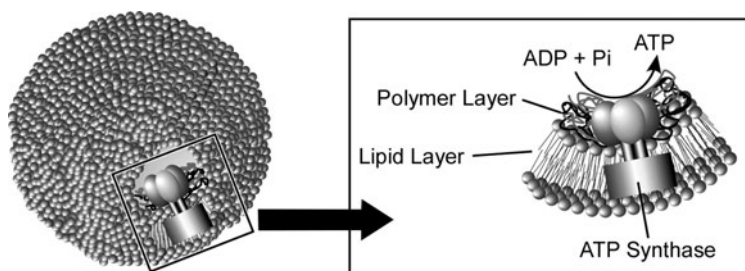


**Fig. 13** Incorporation of ATP synthase into lipid/polyelectrolyte hollow capsule and production of ATP from ADP

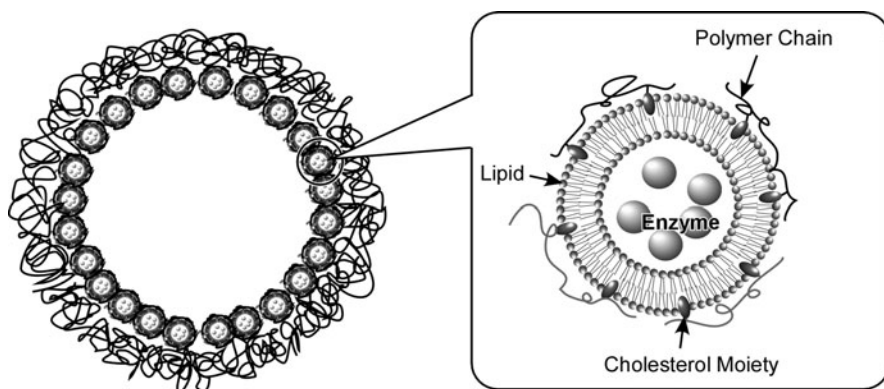


**Fig. 14** Structure of capsosome

polyelectrolyte LbL films on melamine-formaldehyde cores that were destroyed giving hollow capsules. Contact of the hollow capsules formed with vesicles incorporating ATP synthase resulted in hollow microcapsules covered with lipid bilayer and including ATP synthase. Production of ATP from ADP was realized when a proton gradient through the membrane was applied.

Caruso and coworkers invented capsosome as a microreactor with thousands of subcompartments (Fig. 14) [254]. Phospholipid liposomes (DMPC/DPPC 80:20 wt%) including model enzyme,  $\beta$ -lactamase was first stabilized on a template particle by sandwiching the liposomes between a cholesterolmodified poly(L-lysine) (PLL<sub>c</sub>) precursor layer and a poly(methacrylic acid)-*co*-(cholesteryl methacrylate) (PMA<sub>c</sub>) capping layer. The template particles were suspended in a solution of PLL<sub>c</sub>, washed three times, suspended in the phospholipid liposome solution, washed three times, and a capping layer of PMA<sub>c</sub> was adsorbed. Next, five bilayers of PVP and thiol-modified PMA (PMA<sub>SH</sub>) were sequentially adsorbed, which were then cross-linked using and the template core was removed. Destruction of liposome structures by certain surfactants such as Triton X induced release of entrapped enzyme within polyelectrolyte capsule. As the number of subcompartments and the active cargo (drugs and/or reagents) within each liposome are effectively controlled

by the assembly protocol, capsosomes are particularly attractive as novel systems for a range of biomedical applications, including drug and gene delivery, and as microreactors.

In most of the research, LbL capsules of 4–5  $\mu\text{m}$  diameters are used but they are too large for injection into the human body. For example, US FDI requirement of injections is set to the limitation that particles have to be less than 200 nm. In order to improve such practical difficulties, Lvov and coworkers developed a novel technique, sonicated LbL assembly, in which LbL polyelectrolyte shell is prepared under powerful ultrasonication [255,256]. This approach allows us to produce stable drug nanocolloids of high concentration and with good colloid stability. In contrast to common micelle delivery systems, where 3–5% of drugs are included, their LbL nanocapsules carried up to 90% of drug and its release can be adjusted within 5–50 h with appropriate designs of capsular shell architecture. Use of polycations co-polymerized with poly(ethylene glycol) at the external layer of the capsule leads to longer circulation of the capsules in blood. Introduction of antibody at the exterior layer enables us to use these LbL capsules for the targeting of cancer cells. This approach was especially successful when applied to low solubility cancer drugs. Nanoencapsulation of poorly soluble cancer drugs was achieved through powerful ultrasonication of the drug powder and simultaneous sequential polyelectrolyte deposition. Specific targeted ligands could be absorbed on the surface of nanocolloidal particles of the poorly soluble drugs by using a polymer with free reactive groups as the outer coating. In their system, drugs are not modified during the process of solubilization and are subsequently released as free drug molecules. In addition, a very small quantity of a polymer is required compared with other protocols used at present for administration of poorly soluble pharmaceuticals. Using gelatin 100-nm diameter core, LbL capsules for sustained release of polyphenols were also developed by the same research group [257].

## 4 Advanced Techniques

Because the LbL method has great flexibility in selection of support materials, various advanced uses have been considered. Recently, LbL methods have been used for various advanced purposes including integration with device structures, advanced biomedical applications, hybridization of nanomaterials, and construction of hierarchic structures. In this section, these aspects are introduced with recent enzyme-related examples.

### 4.1 *Integration into Device Structures*

Integration of LbL structures into man-made microdevices such as microchips has recently been investigated. Yang, Liu, and coworkers demonstrated modification

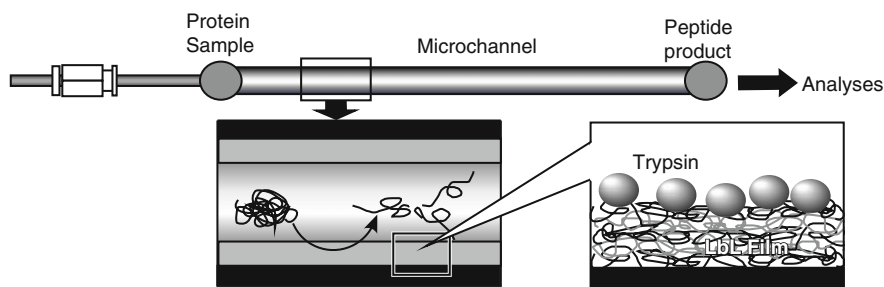


**Fig. 15** Microchip channel modified by the LbL film for detection of protein digestion

of microchip channels by using the LbL technique (Fig. 15) [258]. The microchip reactor modified with the LbL films were used for sensitive detection of protein digestion. Natural polysaccharides, positively charged chitosan and negatively charged hyaluronic acid (HA), were assembled into multi-layers onto the surface of a poly(ethylene terephthalate) (PET) microfluidic chip in order to form a microstructured and biocompatible network for enzyme immobilization. The controlled adsorption of trypsin in the multilayer membrane was monitored using a QCM technique and an enzymatic activity assay. The peptide resulting from digestion was analyzed by matrix-assisted laser desorption ionization time-of-flight mass spectrometry. The maximum proteolytic velocity of the adsorbed trypsin was thousands of times faster than that in solution. BSA, myoglobin, and cytochrome *c* were used as model substrates for the tryptic digestion. This simple technique may offer a potential solution for low-level protein analysis. They also used a similar system for biological samples such as casein extracted from bovine milk and attenuated hepatitis A virus vaccine [259]. The LbL-modified microreactor provides a large surface-area-to-volume ratio and a confined microenvironment, resulting in an increased reaction rate. Within a few seconds, the peptides derived from digestion of proteins are detected with high sequence coverage.

Palmer and coworkers immobilized organophosphorus hydrolase (OPH) enzyme onto the walls of silicon microchannels manufactured by the LbL technique [260]. Enzyme microreactors were constructed with one and two layers of enzyme to compare activity performance where hydrolysis of methyl-parathion by the OPH enzyme into *p*-nitrophenol was investigated. The microreactors with two channel dimensions were tested, one with 98 parallel channels 60  $\mu\text{m}$  wide and another with 1,000 parallel channels 5  $\mu\text{m}$  wide. The microreactor with the smaller channel width demonstrated superior performance that was proportional to the increase in available surface area. Xu et al. developed an enzyme field-effect transistor (ENFET) through immobilizing lactate oxidase (LOD) and  $\text{MnO}_2$  nanoparticles in PDDA films using LbL assembly to construct  $(\text{PDDA}/\text{MnO}_2/\text{PDDA}/\text{LOD})_n$  multilayer films on the surface of ion-sensitive field-effect transistors (ISFET) (Fig. 16) [261].  $\text{MnO}_2$  nanoparticles were introduced as an oxidant to react with  $\text{H}_2\text{O}_2$ , resulting in a pH change in the sensing membrane of the ISFET with the addition of lactate with high sensitivity even to low lactate concentration. Dong and coworkers reported a

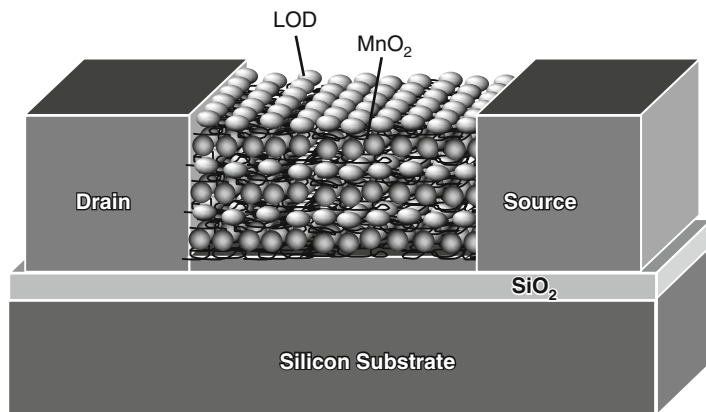


**Fig. 16** Enzyme field-effect transistor (ENFET) based on LbL assembly of enzymes with  $\text{MnO}_2$  nanoparticle and polyelectrolyte on the surface of ion-sensitive field-effect transistor (ISFET)

one-compartment glucose/ $\text{O}_2$  biofuel cell based on the LbL technique on 3D ordered macroporous gold electrodes [262]. The macroporous gold electrodes were functionalized with Au nanoparticles and enzyme, glucose dehydrogenase (GDH), or laccase. The macroporous gold electrode modified with LbL multilayer of gold nanoparticle showed excellent bioelectrocatalytic activity towards glucose where the direct electroreduction towards oxygen was realized. The maximum power output of this biofuel cell was almost 16 times larger than that based on the flat electrode. The performance can be greatly enhanced by the integration of 3D ordered macroporous electrode and LbL technique. De Smedt and coworkers reported a unique labeling system of LbL-based drug delivery [263]. They introduced the barcode concept to LbL drug delivery by using encoded fluorescent polystyrene with captured antibodies. With this system, quantification of proteins in serum plasma samples should become possible.

## 4.2 Advanced Medical Applications

Advanced medical uses are attractive targets for forefront applications of LbL films. Lee and Kotov used the LbL technique for stem cell culture [264]. Delta-like1 (DL-1) notch ligand was immobilized through the LbL assembly on the surface of 3D inverted colloidal crystal pores since the solution-based LbL coating procedure can be readily applied to the surface coating of complex 3D porous substrates while minimizing distortion of protein structures. The effectiveness of topology of D inverted colloidal crystal pores and the bioactivity of LbL-immobilized DL-1 notch ligands in ex vivo T-cell development of human hematopoietic stem cells. The LbL technique showed substantial advantages for creating an artificial 3D thymic stromal cell layer such as convenience, versatility, high controllability with nanoscale

resolution, and capacity to build a multifunctional complex structure. McShane and coworkers constructed micropatterned structures for neuronal cell cultures [265]. On combining photolithography and LbL self-assembly, precise construction of nanocomposite films of potentially complex architectures and patterning of these films on substrates becomes possible using a modified lift-off procedure. Using neuronal cells as a model biological system, comparison chips were produced with secreted phospholipase A2 (sPLA2), a known membrane-active enzyme for neurons, for direct comparison with gelatin, PLL, or bovine serum albumin (BSA). Cell culture studies showed that neurons respond and bind specifically to the sPLA2 enzyme embedded in the polyelectrolyte LbL films. These findings point to the potential of this method to be applied in developing test substrates for a broad array of studies aimed at identifying important biological structure-function relationships. Patterned co-cultures of primary neurons and astrocytes on LbL films of conventional polyelectrolytes without the aid of adhesive proteins/ligands were demonstrated by Kidambi et al. [266]. De Smedt and coworkers conducted in vivo studies on cellular uptake, degradation, and biocompatibility of LbL polyelectrolyte microcapsules that were fabricated from dextran sulfate and poly(L-arginine) layers [267]. Control of cellular apoptosis by bone morphogenetic protein and its antagonist, noggin, embedded in LbL films was examined by Benkirane-Jessel and coworkers [268]. Ogier and coworkers investigated doping of biologically active adenoviral vector in various LbL films [269]. LbL coating of biological cells, such as blood platelets and stem cells, which have dimensions of tens of micrometers, and of much smaller microbes of around 1–2  $\mu\text{m}$  was realized by Lvov and coworkers [270, 271]. Such coating allows varying of cell surface charge, preserving them alive and regulation of cell nutrition uptake. Interestingly, cell division was possible, and both resulting cells possessed LbL shells.

### **4.3 Hybridization with Nanomaterials Toward Hierarchic Assemblies**

LbL assemblies on functional nanomaterials should create novel possibilities in nanotechnology and nano-bio fields. In particular, LbL assembly on carbon nanotubes (CNT) is an attractive research target. Wang and coworkers utilized the concept of signal amplification to achieve a remarkably sensitive electrochemical detection of biomaterials using enzyme LbL multilayers on CNT [272]. As shown in Fig. 17, the LbL multilayer films of ALP were prepared by alternate electrostatic deposition of oppositely charged PDDA onto oxidized and shortened single-wall CNT (SWNT). Because the sonication-induced acid oxidation process resulted in negatively charged carboxylate groups on the CNT surface, adsorption of cationic PDDA becomes possible, which was followed by sequential adsorption of ALP and PDDA. The unique properties of CNT, particularly their huge surface area-to-weight ratio, make them extremely attractive amplification platforms. Such amplified bioelectronic assays allow detection of DNA and proteins down to 80 copies (5.4 aM) and

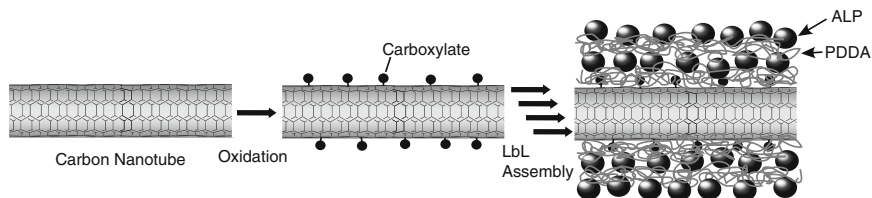


**Fig. 17** LbL assembly of enzyme and polyelectrolyte on oxidized carbon nanotube

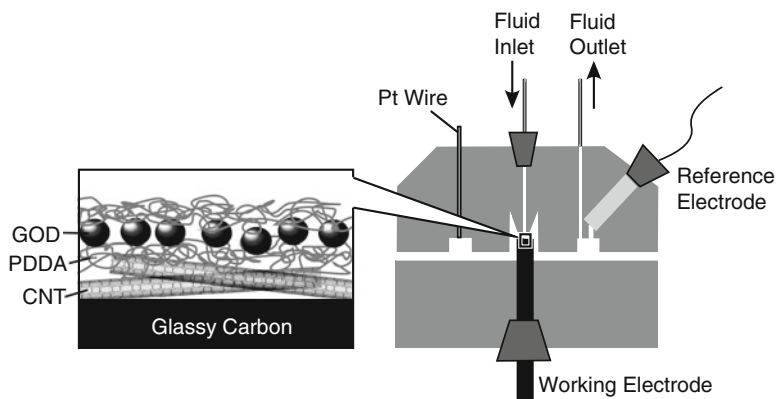


**Fig. 18** Flow injection amperometric glucose biosensor based on LbL assembly of GOD on a CNT-modified glassy carbon transducer

2,000 protein molecules (67 aM), respectively. Liu and Lin prepared a flow injection amperometric glucose biosensor based on electrostatic self-assembling GOD on a CNT-modified glassy carbon transducer (Fig. 18) [273]. The mechanical and electrical properties of CNTs enable sensitive determination of glucose concentration. The sensor showed an excellent detection limit, wide linear range, good precision, and operational stability as well as being free of interference from co-existing electroactive species. The same research team made similar amperometric sensors using LbL assemblies with CNT and appropriate enzymes such as choline oxidase (ChO), and acetylcholinesterase (AChE) as well as a bi-enzyme system of ChO and HRP [274].

Coating of various materials with enzymes by the LbL method has been widely investigated. Coating of useful and conventional materials with LbL enzyme films often creates practical applications. Lvov and coworkers immobilized laccase and urease on cellulose fibers through electrostatic LbL assembly to fabricate functional biocomposites [275]. With laccase-fiber composites, around 50% of the initial enzyme activity was preserved after 14 days of storage in water. Urease-fiber composites were successfully applied for biomineralization to grow calcium carbonate microparticles needed for paper whitening. The strategy presented could be used for the creation of cellulose fiber-based biocomposites with various functions that can be precisely controlled by the film nanoarchitecture. Bhattacharyya and



coworkers immobilized enzymes on microfiltration membranes through the LbL assembly technique. Either PLGA or PLL was covalently attached to the membrane surface [276]. Subsequently, PAH and PSS were alternately assembled then protein adsorbed depending on surface charge. Accessibility to the active site in the immobilized proteins was comparable to that obtained in the homogeneous phase, which was confirmed by affinity interaction (avidinbiotin) and two enzymatic reactions (catalyzed by GOD and ALP). The results obtained suggest that only minor conformational changes occur after biomolecule immobilization as well as some advantages such as reusability and the ease of regeneration. Shi et al. reported composite layered films of Hb and SiO<sub>2</sub> prepared by combined use of LbL assembly and vapor-surface sol-gel deposition [277]. The vapor-surface deposition technique was employed to develop an SiO<sub>2</sub> sol-gel matrix on GCE. The modified GCE was soaked in Hb solution, allowing the adsorption of the protein to form a SiO<sub>2</sub>/Hb bilayer. Through repetition of these processes, controlled thickness multilayer films of SiO<sub>2</sub>/Hb were fabricated. Catalytic activity for H<sub>2</sub>O<sub>2</sub> reduction was observed for the SiO<sub>2</sub>/Hb LbL film modified electrode with an apparent heterogeneous electron-transfer rate constant of 1.02 s<sup>-1</sup> and a Michaelis-Menten constant of 0.155 mM.

Mesoporous materials can be attractive materials for many kinds of applications [278–280], because these materials provide huge surface areas and pore volumes as well as well-defined pore geometries [281–288]. Research on mesoporous materials is currently extremely popular and detailed descriptions can be found in several reviews [289–295] and reports on advanced functions [296–299]. Such mesoporous materials provide excellent media for LbL assembly in the preparation of hierarchic nanostructures [300–302]. Several modifications of the preparation procedures have permitted syntheses of mesoporous silicates with designed pore geometries in various forms including powders and films [303–306]. Mesoporous materials are known as effective media to adsorb biomaterials such as proteins [307–312] and amino acids [313–316]. Therefore, combination of two powerful concepts of mesoporous materials and LbL assembly is anticipated to result in bio-functional nanostructures. Wang and Caruso demonstrated coating of mesoporous microspheres by using LbL assembly for effective biocomponent immobilization (Fig. 19) [317,318]. Densely enzyme-loaded particles were prepared through loading of the enzymes into mesoporous silica spheres followed by coating of the spheres with LbL multilayers. Following enzyme loading, a polyelectrolyte/nanoparticle LbL shell was assembled on the surface of porous spheres, thus preventing enzyme leakage. The encapsulated catalase can be recycled 25 times with an associated loss of activity of 30%, as compared to the 65% loss in activity for catalase immobilized in mesoporous silica spheres lacking the LbL coating. The same research team demonstrated immobilization of enzymes in interconnected macropores of three-dimensional zeolite membranes [319]. The composite membranes were amenable to surface modification with a variety of silane-coupling reagents for various application purposes. Yu and coworkers developed an immuno-labeling system with a



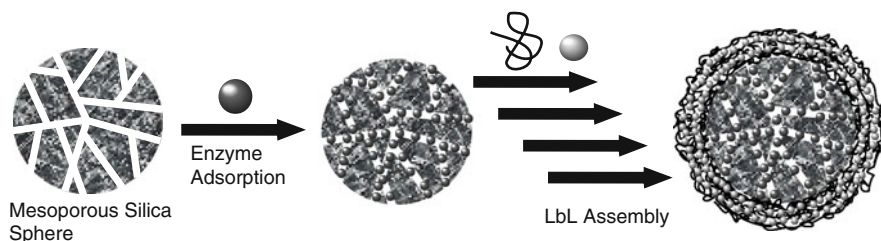


**Fig. 19** Entrapment of enzymes into mesoporous silica sphere covered with LbL films of polyelectrolyte and silica nanoparticle

high fluorescence/protein ratio through loading the organic dye fluorescein diacetate into hollow periodic mesoporous organosilica particles followed by polyelectrolyte LbL encapsulation and antibody attachment [320].

Composites of mesoporous materials and LbL films can be converted to novel nanostructured materials based on concepts of template synthesis [321–327]. For example, Caruso and coworkers demonstrated that the LbL coating of mesoporous silica spheres with polyelectrolytes and the subsequent removal of the silica templates results in formation of micrometre-sized nanoporous polyelectrolyte spheres [328, 329]. Wang and Caruso further applied this strategy to protein-based LbL films [330]. Proteins such as lysozymes were first adsorbed into mesopores of silica spheres, followed by several washing cycles to remove loosely adsorbed protein. The protein-loaded mesoporous silica spheres were dispersed in an aqueous solution of PAA, which most likely associates with the proteins through electrostatic interactions. This assembly was further stabilized through cross-linking using 1-ethyl-3-(3-dimethylaminopropyl) carbodiimide hydrochloride. Exposure of the composite to an HF/NH<sub>4</sub>F buffer induced selective removal of the silica component, finally resulting in nanoporous protein spheres. The spheres obtained have a large surface area and provide opportunities for easy approach of substrate molecules to proteins including enzymes. For example, Caruso and coworkers also demonstrated preparation of capsule-type reactors, similarly by LbL assembly on mesoporous silica spheres and subsequent template removal, in which a triggered enzymatic reaction with a nucleic acid substrate was realized [331]. In their system, bimodal mesoporous silica (BMS) particles were used as template for LbL assembly, where primary amine groups introduced at the silica surface provided positive charges for efficient electrostatic attraction with fluorescently labeled dsDNA. Infiltration of deoxyribonuclease (DNase) proceeded for 1 h following charge reversal by PMA. Coencapsulation of DNase I and dsDNA enabled the degradation of the DNA within LbL-assembled polymer capsules under the control of an external stimulus. High-throughput monitoring of the encapsulated, fluorescently labeled DNA provided a novel means of measuring the kinetics of the reaction.

## 5 Perspectives

Because conditions required for LbL assembly are very mild, this method is suitable for immobilization of biomaterials. Among biomaterials, enzymes have high-level functions, and can perform highly specific material conversion with incredible efficiency. Enzymes and their clusters can be regarded as ultrasmall machines and factories, respectively. Therefore, immobilizing them in organized nanostructures should lead to preparation of highly functional devices. As described above, enzyme-embedded and/or enzyme-encapsulated LbL structures provide various opportunities for device applications such as sensors and reactors. Most published research trials appear very successful. However, we would like to pose some questions here. *Have we reached the limits of the potential of LbL assemblies? Do the current functions represent the pinnacle of LbL technology? Are you satisfied with the current level of research?* We must answer *no* to these questions. Functions developed using LbL technology, such as sensing and reactor applications, lag far behind similar functions seen in the biological world. Functionality in naturally occurring systems is autonomous, self-regulated, and multi-responsive. One might say that biological systems contain the ultimate functional devices. A significant difference between biological systems and LbL assemblies lies in the complexity of their structures. In nature, several functional units are organized in sophisticated and/or hierarchic structures in which several functions are integrated, as seen in photosynthetic and signal transduction systems. If we construct such well-developed structures then we might realize the ultimate nanodevices. The LbL technique permits various creative possibilities in preparation of nanostructures. It is also flexible in terms of materials' selection, widely applicable to various structures, and enables coupling with man-made devices such as electrodes and transistors. These features are not available in most other fabrication techniques in either top-down or bottom-up disciplines. Therefore, we believe that LbL assembly is the most promising method for creation of the ultimate nanodevices.

**Acknowledgement** This work was partly supported by World Premier International Research Center Initiative (WPI Initiative), MEXT, Japan and Core Research for Evolutional Science and Technology (CREST) program of Japan Science and Technology Agency (JST), Japan.

## References

1. Lehn JM (1988) *Angew Chem Int Ed* 27:89
2. Mann S (1993) *Nature* 365:499
3. Niemeyer CM (2001) *Angew Chem Int Ed* 40:4128
4. Daniel MC, Astruc D (2004) *Chem Rev* 104:293
5. Ariga K, Nakanishi T, Hill JP (2007) *Curr Opin Colloid Interface Sci* 12:106
6. Sukhorukov GB, Möhwald H (2007) *Trend Biotechnol* 25:93
7. Xu A-W, Ma Y, Cölfen H (2007) *J Mater Chem* 17:415
8. Anslyn EV (2007) *J Org Chem* 72:687
9. Ma PX (2008) *Adv Drug Deliv Rev* 60:184

10. Ariga K, Hill JP, Lee MV, Vinu A, Charvet R, Acharya S (2008) *Sci Technol Adv Mater* 9:014109
11. Hembury GA, Borovkov VV, Inoue Y (2008) *Chem Rev* 108:1
12. Ariga K, Ji Q, Hill JP, Kawazoe N, Chen G (2009) *Expert Opin Biol Ther* 9:307
13. Cashion MP, Long TE (2009) *Acc Chem Res* 42:1016
14. Sathish M, Miyazawa K, Hill JP, Ariga K (2009) *J Am Chem Soc* 131:6372
15. He Q, Cui Y, Li J (2009) *Chem Soc Rev* 38:2292
16. Shundo A, Labuta J, Hill JP, Ishihara S, Ariga K (2009) *J Am Chem Soc* 131:9494
17. Harada A, Takashima Y, Yamaguchi H (2009) *Chem Soc Rev* 38:875
18. Shundo A, Hill JP, Ariga K (2009) *Chem Eur J* 15:2486
19. Kudernac T, Lei S, Elemans JAAW, De Feyter S (2009) *Chem Soc Rev* 38:402
20. Shen Y, Wang J, Kuhlmann U, Hildebrandt P, Ariga K, Möhwald H, Kurth DG, Nakanishi T (2009) *Chem Eur J* 15:2763
21. Breslow R (1995) *Acc Chem Res* 28:146
22. Ariga K, Nakanishi T, Hill JP, Shirai M, Okuno M, Abe T, Kikuchi J (2005) *J Am Chem Soc* 127:12074
23. Darbre T, Reymond J-L (2006) *Acc Chem Res* 39:925
24. Knör G (2009) *Chem Eur J* 15:568
25. Breslow R, Czarniecki MF, Emert J, Hamaguchi H (1980) *J Am Chem Soc* 102:762
26. Breslow R, Dong SD (1998) *Chem Rev* 98:1997
27. Ariga K, Anslyn EV (1992) *J Org Chem* 57:417
28. Smith J, Ariga K, Anslyn EV (1993) *J Am Chem Soc* 115:362
29. Kneeland DM, Ariga K, Lynch VM, Huang C-Y, Anslyn EV (1993) *J Am Chem Soc* 115:10042
30. Okahata Y, Tsuruta T, Ijio K, Ariga K (1989) *Thin Solid Films* 180:65
31. Okahata Y, Tsuruta T, Ijio K, Ariga K (1988) *Langmuir* 4:1373
32. Kikuchi J, Ariga K, Ikeda K (1999) *Chem Commun* 547
33. Kikuchi J, Ariga K, Miyazaki T, Ikeda K (1999) *Chem Lett* 253
34. Fukuda K, Sasaki Y, Ariga K, Kikuchi J (2001) *J Mol Catal B Enzym* 11:971
35. Kikuchi J, Ariga K, Sasaki Y, Ikeda K (2001) *J Mol Catal B Enzym* 11:977
36. Kurihara K, Ohto K, Tanaka Y, Aoyama Y, Kunitake T (1991) *J Am Chem Soc* 113:444
37. Cha X, Ariga K, Onda M, Kunitake T (1995) *J Am Chem Soc* 117:11833
38. Onda M, Yoshihara K, Koyano H, Ariga K, Kunitake T (1996) *J Am Chem Soc* 118:8524
39. Cha X, Ariga K, Kunitake T (1996) *J Am Chem Soc* 118:9545
40. Shinkai S, Murata K (1998) *J Mater Chem* 8:485
41. Ariga K, Kunitake T (1998) *Acc Chem Res* 31:371
42. Ariga K, Terasaka Y, Sakai D, Tsuji H, Kikuchi J (2000) *J Am Chem Soc* 122:7835
43. Estroff LA, Hamilton AD (2001) *Chem Mater* 13:3227
44. Castner DG, Ratner BD (2002) *Surf Sci* 500:28
45. Ariga K, Nakanishi T, Terasaka Y, Tsuji H, Sakai D, Kikuchi J (2005) *Langmuir* 21:976
46. Michinobu T, Shinoda S, Nakanishi T, Hill JP, Fujii K, Player TN, Tsukube H, Ariga K (2006) *J Am Chem Soc* 128:14478
47. Ariga K, Nakanishi T, Michinobu T (2006) *J Nanosci Nanotechnol* 6:2278
48. Ariga K, Nakanishi T, Hill JP (2006) *Soft Matter* 2:465
49. Fujita N, Shinkai S, James TD (2008) *Chem Asian J* 3:1076
50. Ariga K, Michinobu T, Nakanishi T, Hill JP (2008) *Curr Opin Colloid Interface Sci* 13:23
51. Ishihara K, Takai M (2009) *J R Soc Interface* 6:S129
52. Porter MD, Bright TB, Allara DL, Chidsey CED (1987) *J Am Chem Soc* 109:3559
53. Okahata Y, Ariga K, Shimizu O (1986) *Langmuir* 2:538
54. Ulman A (1996) *Chem Rev* 96:1533
55. Mrksich M, Whitesides GM (1996) *Ann Rev Biophys Biochem Struct* 25:55
56. Moldovan C, Mihailescu C, Stan D, Ruta L, Iosub R, Gavrilă R, Purica M, Vasilica S (2009) *Appl Surf Sci* 255:8953
57. Roberts GG (1985) *Adv Phys* 34:475

58. Zasadzinski JA, Viswanathan R, Madsen L, Garnaes J, Schwartz DK (1994) *Science* 263:1726
59. Ariga K, Tanaka K, Katagiri K, Kikuchi J, Ohshima E, Hisaeda Y (2000) *Colloid Surf A Physicochem Eng Asp* 169:47
60. Ariga K, Tanaka K, Katagiri K, Kikuchi J, Shimakoshi H, Ohshima E, Hisaeda Y (2001) *Phys Chem Chem Phys* 3:3442
61. Girard-Egrot AP, Godoy S, Blum LJ (2005) *Adv Colloid Interface Sci* 116:205
62. Chen X, Lenhart S, Hirtz M, Lu N, Fuchs H, Chi L (2007) *Acc Chem Res* 40:393
63. Talham DR, Yamamoto T, Meisel MW (2008) *J Phys Condes Matter* 20:184006
64. Acharya S, Hill JP, Ariga K (2009) *Adv Mater* 21:2959
65. Acharya S, Shundo A, Hill JP, Ariga K (2009) *J Nanosci Nanotechnol* 9:3
66. Decher G (1997) *Science* 277:1232
67. Decher G, Eckle M, Schmitt J, Struth B (1998) *Curr Opin Colloid Inter Sci* 3:32
68. Hammond PT (2004) *Adv Mater* 16:1271
69. Ostrander JW, Mamedov AA, Kotov NA (2001) *J Am Chem Soc* 123:1101
70. Tang Z, Wang Y, Podsiadlo P, Kotov NA (2006) *Adv Mater* 18:3203
71. Ariga K, Hill JP, Ji Q (2007) *Phys Chem Chem Phys* 9:2319
72. Quinn JF, Johnston APR, Such GK, Zelikin AN, Caruso F (2007) *Chem Soc Rev* 36:707
73. Ariga K, Hill JP, Ji Q (2008) *Macromol Biosci* 8:981
74. Lutkenhaus JL, Hammond PT (2007) *Soft Matter* 3:804
75. Ariga K, Vinu A, Ji Q, Ohmori O, Hill JP, Acharya S, Koike J, Shiratori S (2008) *Angew Chem Int Ed* 47:7254
76. Ji Q, Yoon SB, Hill JP, Vinu A, Yu J-S, Ariga K (2009) *J Am Chem Soc* 131:4220
77. Mattoussi H, Rubner MF, Zhou F, Kumar J, Tripathy SK, Chiang LY (2000) *Appl Phys Lett* 77:1540
78. Tokuhisa H, Hammond PT (2003) *Adv Funct Mater* 13:831
79. Kniprath R, McLeskey JT Jr, Rabe JP, Kirstein S (2009) *J Appl Phys* 105:124313
80. Ogawa M, Tamanoi M, Ohkita H, Benten H, Ito S (2009) *Sol Energy Mater Sol Cells* 93:369
81. Sgobba V, Troeger A, Cagnoli R, Mateo-Alonso A, Prato M, Parenti F, Mucci A, Schenetti L, Guldi DM (2009) *J Mater Chem* 19:4319
82. Liu S, Kurth DG, Möhwald H, Volkmer D (2002) *Adv Mater* 14:225
83. DeLongchamp DM, Kastantin M, Hammond PT (2003) *Chem Mater* 15:1575
84. Jain V, Sahoo R, Jinschek JR, Montazami R, Yochum HM, Beyer FL, Kumar A, Heflin JR (2008) *Chem Commun* 3663
85. Jain V, Khiterer M, Montazami R, Yochum HM, Shea KJ, Heflin JR (2009) *ACS Appl Mater Interface* 1:83
86. Jiang SP, Liu Z, Tian ZQ (2006) *Adv Mater* 18:1068
87. Daiko Y, Sakakibara S, Sakamoto H, Katagiri K, Muto H, Sakai M, Matsuda A (2009) *J Am Ceram Soc* 92:S185
88. Lee SW, Kim B-S, Chen S, Shao-Horn Y, Hammond PT (2009) *J Am Chem Soc* 131:671
89. Nolte AJ, Rubner MF, Cohen RE (2004) *Langmuir* 20:3304
90. Iler RK (1966) *J Colloid Interface Sci* 21:569
91. Decher G, Hong JD (1991) *Macromol Chem Macromol Symp* 46:321
92. Decher G, Hong JD (1991) *Ber Bunsen-Ges Phys Chem* 95:1430
93. Decher G, Hong JD, Schmitt J (1992) *Thin Solid Films* 210, 831
94. Lvov Y, Decher G, Möhwald H (1993) *Langmuir* 9:481
95. Lee H, Kepley LJ, Hong HG, Mallouk TE (1988) *J Am Chem Soc* 110:618
96. Lee H, Kepley LJ, Hong HG, Akhter S, Mallouk TE (1988) *J Phys Chem* 92:2597
97. Keller SW, Kim N-H, Mallouk TE (1994) *J Am Chem Soc* 116:8817
98. Yoo D, Shiratori SS, Rubner MF (1998) *Macromolecules* 31:4309
99. Shiratori SS, Rubner MF (2000) *Macromolecules* 33:4213
100. Lvov Y, Ariga K, Onda M, Ichinose I, Kunitake T (1999) *Colloid Surf A Physicochem Eng Asp* 146:337
101. Cheng JH, Fou AF, Rubner MF (1994) *Thin Solid Films* 244:985
102. Fou AC, Onitsuka O, Ferreira M, Rubner MF, Hsieh BR (1996) *J Appl Phys* 79:7501

103. Bouvree A, Feller J-F, Castro M, Grohens Y, Rinaudo M (2009) *Sens Actuator B Chem* 138:138
104. Lu J, Kumar B, Castro M, Feller J-F (2009) *Sens Actuator B Chem* 140:451
105. Tsukruk VV, Rinderspacher F, Bliznyuk VN (1997) *Langmuir* 13:2171
106. Tsukruk VV (1998) *Adv Mater* 10:253
107. Appoh FE, Kraatz H-B (2009) *J Appl Polym Sci* 111:709
108. Lvov Y, Ariga K, Kunitake T (1994) *Chem Lett* 2323
109. Caruso F, Furlong DN, Ariga K, Ichinose I, Kunitake T (1998) *Langmuir* 14:4559
110. Ai H, Jones SA, Lvov YM (2003) *Cell Biochem Biophys* 39:23
111. Matsusaki M, Akashi M (2009) *Exp Opin Drug Deliv* 6:1207
112. Decher G, Lehr B, Lowack K, Lvov Y, Schmitt J (1994) *Biosens Bioelectron* 9:677
113. Jessel N, Oulad-Abdelghani M, Meyer F, Lavalle P, Haïkel Y, Schaaf P, Voegel J-C (2006) *Proc Natl Acad Sci USA* 103:8618
114. Lvov Y, Onda M, Ariga K, Kunitake T (1998) *J Biomater Sci Polym Ed* 9:345
115. Richert L, Lavalle P, Payan E, Shu XZ, Prestwich GD, Stoltz J-F, Schaaf P, Voegel J-C, Picart C (2004) *Langmuir* 20:448
116. Fukui Y, Fujimoto K (2009) *Langmuir* 25:10020
117. Lvov Y, Haas H, Decher G, Möhwald H, Mikhailov A, Mchedlishvili B, Morgunova E, Vainshtein B (1994) *Langmuir* 10:4232
118. Kotov NA, Dekany I, Fendler JH (1995) *J Phys Chem* 99:13065
119. Ariga K, Lvov Y, Onda M, Ichinose I, Kunitake T (1997) *Chem Lett* 125
120. Lvov Y, Ariga K, Onda M, Ichinose I, Kunitake T (1997) *Langmuir* 13:6195
121. Sarathy KV, Thomas PJ, Kulkarni GU, Rao CNR (1999) *J Phys Chem B* 103:399
122. Tomczak N, Jańczewski D, Han M, Vancso GJ (2009) *Prog Polym Sci* 34:393
123. Lvov Y, Ariga K, Ichinose I, Kunitake T (1996) *Langmuir* 12:3038
124. Sasaki T, Ebina Y, Tanaka T, Harada M, Watanabe M, Decher G (2001) *Chem Mater* 13:4661
125. Liu Z, Ma R, Osada M, Iyi N, Ebina Y, Takada K, Sasaki T (2006) *J Am Chem Soc* 128:4872
126. Umemura Y, Shinohara E, Koura A, Nishioka T, Sasaki T (2006) *Langmuir* 22:3870
127. Sasaki T (2007) *J Ceram Soc Jpn* 115:9
128. Osada M, Akatsuka K, Ebina Y, Funakubo H, Kiguchi T, Takada K, Sasaki T (2007) *Jpn J Appl Phys Part 1* 46:6979
129. Akatsuka K, Takanashi G, Ebina Y, Sakai N, Haga M, Sasaki T (2008) *J Phys Chem Solid* 69:1288
130. Vial S, Pastoriza-Santos I, Pérez-Juste J, Liz-Marzán LM (2007) *Langmuir* 23:4606
131. Gole A, Murphy CJ (2005) *Chem Mater* 17:1325
132. Park H, Lee S, Chen L, Lee EK, Shin SY, Lee YH, Son SW, Oh CH, Song JM, Kang SH, Choo J (2009) *Phys Chem Chem Phys* 11:7444
133. Srivastava S, Kotov NA (2008) *Acc Chem Res* 41:1831
134. Suzuki Y, Pichon BP, D'Elia D, Beauger C, Yoshikawa S (2009) *J Ceram Soc Jpn* 117:381
135. Jiang C, Tsukruk VV (2006) *Adv Mater* 18:829
136. Ma R, Sasaki T, Bando Y (2004) *J Am Chem Soc* 126:10382
137. Cooper TM, Campbell AL, Crane RL (1995) *Langmuir* 11:2713
138. Ariga K, Lvov Y, Kunitake T (1997) *J Am Chem Soc* 119:2224
139. Ariga K, Onda M, Lvov Y, Kunitake T (1997) *Chem Lett* 25
140. Ma N, Zhang H, Song B, Wang Z, Zhang X (2005) *Chem Mater* 17:5065
141. Cho J, Hong J, Char K, Caruso F (2006) *J Am Chem Soc* 128:9935
142. Kim TG, Lee H, Jang Y, Park TG (2009) *Biomacromolecules* 10:1532
143. Michel M, Vautier D, Voegel J-C, Schaaf P, Ball V (2004) *Langmuir* 20:4835
144. Volodkin DV, Schaaf P, Möhwald H, Voegel J-C, Ball V (2009) *Soft Matter* 5:1394
145. Lvov Y, Essler F, Decher G (1993) *J Phys Chem* 97:13773
146. Ichinose I, Fujiyoshi K, Mizuki S, Lvov Y, Kunitake T (1996) *Chem Lett* 257
147. Bunge A, Fischlechner M, Loew M, Arbuzova A, Herrmann A, Huster D (2009) *Soft Matter* 5:3331
148. Berndt P, Kurihara K, Kunitake T (1992) *Langmuir* 8:2486

149. Hatzor A, Moav T, Cohen H, Matlis S, Libman J, Vaskevich A, Shanzler A, Rubinstein I (1998) *J Am Chem Soc* 120:13469
150. Altman M, Shukla AD, Zubkov T, Evmenenko G, Dutta P, van der Boom ME (2006) *J Am Chem Soc* 128:7374
151. Gao S, Yuan D, Lue J, Cao R (2010) *J Colloid Interface Sci* 341:320
152. Haga M, Kobayashi K, Terada K (2007) *Coord Chem Rev* 251:2688
153. Stockton WB, Rubner MF (1997) *Macromolecules* 30:2717
154. Sukhishvili SA, Granick S (2002) *Macromolecules* 35:301
155. Kharlampieva E, Kozlovskaya V, Sukhishvili SA (2009) *Adv Mater* 21:3053
156. Shimazaki Y, Mitsuishi M, Ito S, Yamamoto M (1998) *Langmuir* 14:2768
157. Shimazaki Y, Nakamura R, Ito S, Yamamoto M (2001) *Langmuir* 17:953
158. Shimazaki Y, Ito S, Tsutsumi N (2000) *Langmuir* 16:9478
159. Ikeda A, Hatano T, Shinkai S, Akiyama T, Yamada S (2001) *J Am Chem Soc* 123:4855
160. Lvov Y, Ariga K, Ichinose I, Kunitake T (1996) *Thin Solid Films* 284:797
161. Anzai J, Kobayashi Y, Nakamura N, Nishimura M, Hoshi T (1999) *Langmuir* 15:221
162. Sato K, Kodama D, Endo Y, Anzai J (2009) *J Nanosci Nanotechnol* 9:386
163. Serizawa T, Hamada K, Kitayama T, Fujimoto N, Hatada K, Akashi M (2000) *J Am Chem Soc* 122:1891
164. Serizawa T, Hamada K, Akashi M (2004) *Nature* 429:52
165. Lvov YM, Rusling JF, Thomsen DL, Papadimitrakopoulos F, Kawakami T, Kunitake T (1998) *Chem Commun* 1229
166. Ariga K, Lvov Y, Ichinose I, Kunitake T (1999) *App Clay Sci* 15:137
167. Onda M, Lvov Y, Ariga K, Kunitake T (1997) *Jpn J Appl Phys Part 2* 36:L1608
168. Clark SL, Hammond PT (1998) *Adv Mater* 10:1515
169. Shiratori SS, Yamada M (2000) *Polym Adv Technol* 11:810
170. Yamada M, Shiratori SS (2000) *Sens Actuator B-Chem* 64:124
171. Shiratori SS, Ito T, Yamada T (2002) *Colloids Surf A* 198:415
172. Lvov Y, Ariga K, Ichinose I, Kunitake K (1995) *J Am Chem Soc* 117:6117
173. Sauerbrey G (1959) *Z Phys* 155:206
174. Ariga K, Okahata Y (1994) *Langmuir* 10:2272
175. Ariga K, Isoyama K, Hayashida O, Aoyama Y, Okahata Y (1998) *Chem Lett* 1007
176. Matsuura K, Ariga K, Endo K, Aoyama Y, Okahata Y (2000) *Chem Eur J* 6:1750
177. Marx KA (2003) *Biomacromolecules* 4:1099
178. Onda M, Lvov Y, Ariga K, Kunitake T (1996) *Biotechnol Bioeng* 51:163
179. Onda M, Lvov Y, Ariga K, Kunitake T (1996) *J Ferment Bioeng* 82:502
180. Onda M, Ariga K, Kunitake T (1999) *J Biosci Bioeng* 87:69
181. Lvov Y, Ariga K, Ichinose I, Kunitake T (1995) *J Chem Soc Chem Commun* 2313
182. Anzai J, Kobayashi Y, Nakamura N, Nishimura M, Hoshi T (1999) *Langmuir* 15:221
183. Ngankam AP, Mao G, Van Tassel PR (2004) *Langmuir* 20:3362
184. Matsuno H, Nagasaka Y, Kurita K, Serizawa T (2007) *Chem Mater* 19:2174
185. Shutava TG, Kommireddy DS, Lvov YM (2006) *J Am Chem Soc* 128:9926
186. Lu H, Rusling JF, Hu N (2007) *J Phys Chem B* 111:14378
187. Constantine CA, Mello SV, Dupont A, Cao X, Santos D Jr, Oliveira ON Jr, Strixino FT, Pereira EC, Cheng T-C, Defrank JJ, Leblanc RM (2003) *J Am Chem Soc* 125:1805
188. Lvov YM, Lu Z, Schenkman JB, Zu X, Rusling JF (1998) *J Am Chem Soc* 120:4073
189. Zhou L, Yang J, Estavillo C, Stuart JD, Schenkman JB, Rusling JF (2003) *J Am Chem Soc* 125:1431
190. Liang M, Jia S, Zhu S, Guo L-H (2008) *Environ Sci Technol* 42:635
191. Ram MK, Adami M, Paddeu S, Nicolini C (2000) *Nanotechnology* 11:112
192. Spricigo R, Dronov R, Rajagopalan KV, Lisdat F, Leimkühler S, Scheller FW, Wollenberger U (2008) *Soft Matter* 4:972
193. Balkenhohl T, Adelt S, Dronov R, Lisdat F (2008) *Electrochem Commun* 10:914
194. Zhao G, Xu J-J, Chen H-Y (2006) *Electrochem Commun* 8:148
195. Zhang S, Yang W, Niu Y, Li Y, Zhang M, Sun C (2006) *Anal Bioanal Chem* 384:736



196. Wu B-Y, Hou S-H, Yin F, Li J, Zhao Z-X, Huang J-D, Chen Q (2007) *Biosens Bioelectron* 22:838
197. Guo X, Zheng D, Hu N (2008) *J Phys Chem B* 112:15513
198. Zhuo Y, Yuan R, Chai Y, Zhang Y, Li X, Wang N, Zhu Q (2006) *Sens Actuator B-Chem* 114:631
199. Sun Y, Bai Y, Yang W, Sun C (2007) *Electrochim Acta* 52:7352
200. Camacho C, Matías JC, Cao R, Matos M, Chico B, Hernández J, Longo MA, Sanromán MA, Villalonga R (2008) *Langmuir* 24:7654
201. Frago A, Sanromá B, Ortiz M, O'Sullivan CK (2009) *Soft Matter* 5:400
202. Tomalia DA, Naylor AM, Goddard WA III (1990) *Angew Chem Int Ed Engl* 29:138
203. Zeng FW, Zimmerman SC (1997) *Chem Rev* 97:1681
204. Bosman AW, Janssen HM, Meijer EW (1999) *Chem Rev* 99:1665
205. Ariga K, Urakawa T, Michiue A, Sasaki Y, Kikuchi J (2000) *Langmuir* 16:9147
206. Hecht S, Frechet MJM (2001) *Angew Chem Int Ed* 40:74
207. Higuchi M, Shiki S, Ariga K, Yamamoto K (2001) *J Am Chem Soc* 123:4414
208. Ariga K, Urakawa T, Michiue A, Kikuchi J (2004) *Langmuir* 20:6762
209. Jiang DL, Aida T (2005) *Prog Polym Sci* 30:403
210. Yoon HC, Hong M-Y, Kim H-S (2000) *Anal Chem* 72:4420
211. Zucolotto V, Pinto APA, Tumolo T, Moraes ML, Baptista MS, Riul A Jr, Araújo APU, Oliveira ON Jr (2006) *Biosens Bioelectron* 21:1320
212. Perinotto AC, Caseli L, Hayasaka CO, Riul A Jr, Oliveira ON Jr, Zucolotto V (2008) *Thin Solid Films* 516:9002
213. Ferreira M, Fiorito PA, Oliveira ON Jr, Córdoba de Torresi SI (2004) *Biosens Bioelectron* 19:1611
214. Li Y, Chen Z, Jiang X, Lin X (2004) *Chem Lett* 33:564
215. Yan XB, Chen XJ, Tay BK, Khor KA (2007) *Electrochem Commun* 9:1269
216. Wang Y, Joshi PP, Hobbs KL, Johnson MB, Schmidtke DW (2006) *Langmuir* 22:9776
217. Calvo EJ, Etchenique R, Pietrasanta L, Wolosiuk A, Danilowicz C (2001) *Anal Chem* 73:1161
218. Calvo EJ, Danilowicz CB, Wolosiuk A (2005) *Phys Chem Chem Phys* 7:1800
219. Li W, Wang Z, Sun C, Xian M, Zhao M (2000) *Anal Chim Acta* 418:225
220. Caruso F, Caruso RA, Möhwald H (1998) *Science* 282:1111
221. Tiourina OP, Antipov AA, Sukhorukov GB, Larionova NL, Lvov Y, Möhwald H (2001) *Macromol Biosci* 1:209
222. Caruso F (2001) *Adv Mater* 13:11
223. Johnston APR, Cortez C, Angelatos AS, Caruso F (2006) *Curr Opin Colloid Interface Sci* 11:203
224. Lvov Y, Antipov AA, Mamedov A, Möhwald H, Sukhorukov GB (2001) *Nano Lett* 1:125
225. Caruso F, Trau D, Möhwald H, Renneberg R (2000) *Langmuir* 16:1485
226. Tian Y, He Q, Cui Y, Tao C, Li J (2006) *Chem Eur J* 12:4808
227. Lu G, Ai S, Li J (2005) *Langmuir* 21:1679
228. He Q, Cui Y, Ai S, Tian Y, Li J (2009) *Curr Opin Colloid Interface Sci* 14:115
229. Schüler C, Caruso F (2000) *Macromol Rapid Commun* 21:750
230. Caruso F, Schüler C (2000) *Langmuir* 16:9595
231. Derbal L, Lesot H, Voegel JC, Ball V (2003) *Biomacromolecules* 4:1255
232. Wiemann LO, Buthe A, Klein M, van den Wittenboer A, Dähne L, Ansorge-Schumacher MB (2009) *Langmuir* 25:618
233. Zhu H, Srivastava R, Brown JQ, McShane MJ (2005) *Bioconjugate Chem* 16:1451
234. Bajrami B, Hvastkovs EG, Jensen GC, Schenkman JB, Rusling JF (2008) *Anal Chem* 80:922
235. Viswanathan S, Ho JAA (2007) *Biosens Bioelectron* 22:1147
236. Trau D, Yang W, Seydack M, Caruso F, Yu N-T, Renneberg R (2002) *Anal Chem* 74:5480
237. Wang C, Ye S, Dai L, Liu X, Tong Z (2007) *Biomacromolecules* 8:1739
238. Ghan R, Shutava T, Patel A, John VT, Lvov Y (2004) *Macromolecules* 37:4519
239. Stein EW, Volodkin DV, McShane MJ, Sukhorukov GB (2006) *Biomacromolecules* 7:710
240. Zhu H, McShane MJ (2005) *Langmuir* 21:424

241. Itoh Y, Matsusaki M, Kida T, Akashi M (2008) *Chem Lett* 37:238
242. Katagiri K, Ariga K, Kikuchi J (1999) *Chem Lett* 661
243. Katagiri K, Hamasaki R, Ariga K, Kikuchi J (2003) *J Sol Gel Sci Technol* 26:393
244. Katagiri K, Hashizume M, Ariga K, Terashima T, Kikuchi J (2007) *Chem Eur J* 13:5272
245. Katagiri K, Hamasaki R, Ariga K, Kikuchi J (2002) *Langmuir* 18:6709
246. Katagiri K, Hamasaki R, Ariga K, Kikuchi J (2002) *J Am Chem Soc* 124:7892
247. Ariga K, Vinu A, Miyahara M (2006) *Curr Nanosci* 2:197
248. Michel M, Izquierdo A, Decher G, Voegel J-C, Schaaf P, Ball V (2005) *Langmuir* 21:7854
249. Michel M, Arntz Y, Fleith G, Toquant J, Haïkel Y, Voegel J-C, Schaaf P, Ball V (2006) *Langmuir* 22:2358
250. Krishna G, Shutava T, Lvov Y (2005) *Chem Commun* 2796
251. Katagiri K, Caruso F (2005) *Adv Mater* 17:738
252. Duan L, He Q, Wang K, Yan X, Cui Y, Möhwald H, Li J (2007) *Angew Chem Int Ed* 46:6996
253. Qi W, Duan L, Wang K, Yan X, Cui Y, He Q, Li J (2008) *Adv Mater* 20:601
254. Städler B, Chandrawati R, Price AD, Chong S-F, Breheney K, Postma A, Connal LA, Zelikin AN, Caruso F (2009) *Angew Chem Int Ed* 48:4359
255. Agarwal A, Lvov Y, Sawant R, Torchilin V (2008) *J Control Release* 128:255
256. Lvov Y, Agarwal A, Sawant R, Torchilin V (2008) *Pharma Focus Asia* 36
257. Shutava TG, Balkundi SS, Vangala P, Steffan JJ, Bigelow RL, Cardelli JA, O'Neal DP, Lvov YM (2009) *ACS Nano* 3:1877
258. Liu Y, Lu H, Zhong W, Song P, Kong J, Yang P, Girault HH, Liu B (2006) *Anal Chem* 78:801
259. Liu Y, Zhong W, Meng S, Kong J, Lu H, Yang P, Girault HH, Liu B (2006) *Chem Eur J* 12:6585
260. Forrest SR, Elmore BB, Palmer JD (2007) *Catalysis Today* 120:30
261. Xu J-J, Zhao W, Luo X-L, Chen H-Y (2005) *Chem Commun* 792
262. Deng L, Wang F, Chen H, Shang L, Wang L, Wang T, Dong S (2008) *Biosens Bioelectron* 24:329
263. Derveaux S, Stubbe BG, Roelant C, Leblans M, De Geest BG, Demeester J, De Smedt SC (2008) *Anal Chem* 80:85
264. Lee JA, Kotov NA (2009) *Small* 5:1008
265. Mohammed JS, DeCoster MA, McShane MJ (2004) *Biomacromolecules* 5:1745
266. Kidambi S, Lee I, Chan C (2008) *Adv Funct Mater* 18:294
267. De Koker S, De Geest BG, Cuvelier C, Ferdinande L, Deckers W, Hennink WE, De Smedt S, Mertens N (2007) *Adv Funct Mater* 17:3754
268. Nadiri A, Kuchler-Bopp S, Mjahed H, Hu B, Haïkel Y, Schaaf P, Voegel J-C, Benkirane-Jessel N (2007) *Small* 3:1577
269. Dimitrova M, Arntz Y, Lavallo P, Meyer F, Wolf M, Schuster C, Haïkel Y, Voegel J-C, Ogier J (2007) *Adv Funct Mater* 17:233
270. Ai H, Fang M, Jones S, Lvov YM (2002) *Biomacromolecules* 3:560
271. Veerabadran NG, Goli PL, Stewart-Clark SS, Lvov YM, Mills DK (2007) *Macromol Biosci* 7:877
272. Munge B, Liu G, Collins G, Wang J (2005) *Anal Chem* 77:4662
273. Liu G, Lin Y (2006) *Electrochem Commun* 8:251
274. Liu G, Lin Y (2006) *Anal Chem* 78:835
275. Xing Q, Eadula SR, Lvov YM (2007) *Biomacromolecules* 8:1987
276. Smuleac V, Butterfield DA, Bhattacharyya D (2006) *Langmuir* 22:10118
277. Shi G, Sun Z, Liu M, Zhang L, Liu Y, Qu Y, Jin L (2007) *Anal Chem* 79:3581
278. Yanagisawa T, Shimizu T, Kuroda K, Kato C (1990) *Bull Chem Soc Jpn* 63:988
279. Kresge CT, Leonowicz ME, Roth WJ, Vartuli JC, Beck JS (1992) *Nature* 359:710
280. Zhao D, Feng J, Huo Q, Melosh N, Fredrickson GH, Chmelka BF, Stucky GD (1998) *Science* 279:548
281. Inagaki S, Guan S, Ohsuna T, Terasaki O (2002) *Nature* 416:304
282. Vinu A, Ariga K, Mori T, Nakanishi T, Hishita S, Golberg D, Bando Y (2005) *Adv Mater* 17:1648
283. Vinu A, Terrones M, Golberg D, Hishita S, Ariga K, Mori T (2005) *Chem Mater* 17:5887



284. Vinu A, Miyahara M, Sivamurugan V, Mori T, Ariga K (2005) *J Mater Chem* 15:5122
285. Jin H, Liu Z, Ohsuna T, Terasaki O, Inoue Y, Sakamoto K, Nakanishi T, Ariga K, Che S (2006) *Adv Mater* 18:593
286. Wan Y, Zhao D (2007) *Chem Rev* 107:2821
287. Vinu A, Srinivasu P, Sawant DP, Mori T, Ariga K, Chang J-S, Jhung S-H, Balasubramanian VV, Hwang YK (2007) *Chem Mater* 19:4367
288. Srinivasu P, Alam S, Balasubramanian VV, Velmathi S, Sawant DP, Böhlmann W, Mirajkar SP, Ariga K, Halligudi SB, Vinu A (2008) *Adv Funct Mater* 18:640
289. Ogawa M, Kuroda K (1995) *Chem Rev* 95:399
290. Corma A (1997) *Chem Rev* 97:2373
291. Vinu A, Hossain KZ, Ariga K (2005) *J Nanosci Nanotechnol* 5:347
292. Vinu A, Mori T, Ariga K (2006) *Sci Technol Adv Mater* 7:753
293. Vallet-Regi M, Balas F, Arcos D (2007) *Angew Chem Int Ed* 46:7548
294. Ariga K, Vinu A, Hill JP, Mori T (2007) *Coord Chem Rev* 251:2562
295. Yamauchi Y, Kuroda K (2008) *Chem Asia J* 3:664
296. Okabe A, Fukushima T, Ariga K, Aida T (2002) *Angew Chem Int Ed* 41:3414
297. Lu J, Liong M, Zink JJ, Tamanoi F (2007) *Small* 3:1341
298. Slowing II, Trewyn BG, Giri S, Lin VS-Y (2007) *Adv Funct Mater* 17:1225
299. Ariga K, Vinu A, Miyahara M, Hill JP, Mori T (2007) *J Am Chem Soc* 129:11022
300. Ji Q, Miyahara M, Hill JP, Acharya S, Vinu A, Yoon SB, Yu J-S, Sakamoto K, Ariga K (2008) *J Am Chem Soc* 130:2376
301. Ji Q, Acharya S, Hill JP, Vinu A, Yoon SB, Yu J-S, Sakamoto K, Ariga K (2009) *Adv Funct Mater* 19:1792
302. Ariga K, Ji Q, Hill JP, Vinu A (2009) *Soft Matter* 5:3562
303. Ogawa M, Ishikawa H, Kikuchi T (1998) *J Mater Chem* 8:1783
304. Ogawa M, Masukawa N (2000) *Microporous Mesoporous Mater* 38:35
305. Okabe A, Fukushima T, Ariga K, Niki M, Aida T (2004) *J Am Chem Soc* 126:9013
306. Yamauchi Y, Suzuki N, Gupta P, Sato K, Fukata N, Murakami M, Shimizu T, Inoue S, Kimura T (2009) *Sci Technol Adv Mater* 10:025005
307. Vinu A, Miyahara M, Ariga K (2005) *J Phys Chem B* 109:6436
308. Miyahara M, Vinu A, Hossain KZ, Nakanishi T, Ariga K (2006) *Thin Solid Films* 499:13
309. Vinu A, Miyahara M, Mori T, Ariga K (2006) *J Porous Mater* 13:379
310. Miyahara M, Vinu A, Ariga K (2006) *J Nanosci Nanotechnol* 6:1765
311. Vinu A, Hossain KZ, Srinivasu P, Miyahara M, Anandan S, Gokulakrishnan N, Mori T, Ariga K, Balasubramanian VV (2007) *J Mater Chem* 17:1819
312. Vinu A, Miyahara M, Ariga K (2006) *J Nanosci Nanotechnol* 6:1510
313. Zhang Q, Ariga K, Okabe A, Aida T (2004) *J Am Chem Soc* 126:988
314. Ariga K (2004) *Chem Rec* 3:297
315. Vinu A, Hossain KZ, Kumar GS, Ariga K (2006) *Carbon* 44:530
316. Otani W, Kinbara K, Zhang Q, Ariga K, Aida T (2007) *Chem Eur J* 13:1731
317. Wang Y, Caruso F (2004) *Chem Commun* 1528
318. Wang Y, Caruso F (2005) *Chem Mater* 17:953
319. Wang Y, Caruso F (2004) *Adv Funct Mater* 14:1012
320. Cai W, Gentle IR, Lu GQ, Zhu J-J, Yu A (2008) *Anal Chem* 80:5401
321. Martin CR (1995) *Acc Chem Res* 28:61
322. Jäger R, Vögtle F (1997) *Angew Chem Int Ed Engl* 36:930
323. Ariga K (2004) *J Nanosci Nanotechnol* 4:23
324. Wang Y, Angelatos AS, Caruso F (2008) *Chem Mater* 20:848
325. Ji Q, Acharya S, Hill JP, Richards GJ, Ariga K (2008) *Adv Mater* 20:4027
326. Crowley JD, Goldup SM, Lee A-L, Leigh DA, McBurney RT (2009) *Chem Soc Rev* 38:1530
327. Mandal S, Shundo A, Acharya S, Hill JP, Ji Q, Ariga K (2009) *Chem Asian J* 4:1055
328. Wang Y, Yu A, Caruso F (2005) *Angew Chem Int Ed* 44:2888
329. Wang Y, Caruso F (2006) *Chem Mater* 18:4089
330. Wang Y, Caruso F (2006) *Adv Mater* 18:795
331. Price AD, Zelikin AN, Wang Y, Caruso F (2009) *Angew Chem Int Ed* 48:329

# Non-Layer-by-Layer Assembly and Encapsulation Uses of Nanoparticle-Shelled Hollow Spheres

Gautam C. Kini, Sibani L. Biswal, and Michael S. Wong

**Abstract** Nanoparticles (NPs, diameter range of 1–100 nm) can have size-dependent physical and electronic properties that are useful in a variety of applications. Arranging them into hollow shells introduces the additional functionalities of encapsulation, storage, and controlled release that the constituent NPs do not have. This chapter examines recent developments in the synthesis routes and properties of hollow spheres formed out of NPs. Synthesis approaches reviewed here are recent developments in the electrostatics-based tandem assembly and interfacial stabilization routes to the formation of NP-shelled structures. Distinct from the well-established layer-by-layer (LBL) synthesis approach, the former route leads to NP/polymer composite hollow spheres that are potentially useful in medical therapy, catalysis, and encapsulation applications. The latter route is based on interfacial activity and stabilization by NPs with amphiphilic properties, to generate materials like colloidosomes, Pickering emulsions, and foams. The varied types of NP shells can have unique materials properties that are not found in the NP building blocks, or in polymer-based, surfactant-based, or LBL-assembled capsules.

**Keywords** Hollow spheres · Nanoparticles · Layer-by-layer assembly · Tandem assembly · Nanoparticle assembled capsule · Interfacial stabilization · Particle stabilized emulsion

---

G.C. Kini and S.L. Biswal  
Department of Chemical and Biomolecular Engineering, Rice University, Houston,  
TX, 77005, USA  
e-mail: [gck1@rice.edu](mailto:gck1@rice.edu); [biswal@rice.edu](mailto:biswal@rice.edu)

M.S. Wong (✉)  
Department of Chemical and Biomolecular Engineering, Rice University, Houston,  
TX, 77005, USA  
and  
Department of Chemistry, Rice University, Houston, TX, 77005, USA  
e-mail: [mswong@rice.edu](mailto:mswong@rice.edu)

## Contents

1	Introduction .....	91
2	Hollow Spheres from Electrostatic Assembly of Nanoparticles Through Tandem Assembly .....	92
2.1	Current Methods .....	92
2.2	Preparation of Two-Nanoparticle-Type Hollow Spheres .....	94
2.3	Preparation of One-Nanoparticle-Type Hollow Spheres .....	96
2.4	Applications and Properties of Tandem-Assembled Capsules .....	100
3	Interfacial Stabilization and Other Approaches to the Assembly of Nanoparticle-Shelled Hollow Structures as Emulsions and Foams .....	105
4	Conclusions and Future Work .....	108
	References .....	110

## Abbreviations

Cys	Cysteine
E	Energy of attachment
EDTA	Tetrasodium ethylenediamine tetraacetate
FDA	Food and Drug Administration
ICG	Indocyanine green
$k$	Boltzmann's constant
LBL	Layer-by-layer
Lys	Lysine
NAC	Nanoparticle assembled capsule
NIR	Near-infrared
NP	Nanoparticle
O/W	Oil-in-water
PAA	Poly(acrylic acid)
PAH	Poly(allylamine hydrochloride)
PE	Polyelectrolyte
PLL	Poly-L-lysine
QD	Quantum dot
$R$	$R$ ratio, defined as the total negative charge from a multivalent anion divided by the total positive charge from the polymer
$r$	Particle radius
SEM	Scanning electron microscope
$T$	Temperature
TEM	Transmission electron microscope
TGA	Thermogravimetric analysis
W/O	Water-in-oil

## 1 Introduction

The study of colloids and interfaces has resulted in identification of key short-range interactions and systematized understanding of colloidal interactions [1–5]. One of the tangibles that has emerged is the creation of assemblies with precision down to nanoscale levels, which hold promise as next-generation devices in technology-driven applications. Ranging from traditional areas such as agriculture and mining to the latest in cutting-edge fields that include nanotechnology and biotechnology, it is apparent that approaches to the control and creation of assemblies using building blocks with custom-designed functionalities are essential to sustain advancements in technology [6–20].

A class of colloidal assemblies that evokes interest in its synthesis approaches and physicochemical properties are “hollow spheres” or “capsules” [21]. Hollow spheres are discrete volume closures that have a well-defined boundary separating the interior from the bulk external environment [8, 22]. Popular routes for the synthesis of hollow spheres can be categorized into self-assembly, chemical reactions, sequential electrostatic assembly, and interfacial stabilization approaches [9, 13, 23–40].

The shell interior (hollow region) can be empty or filled (with a liquid but not a solid). The shell boundary is typically constituted of materials such as particles, polymers, charged polymers or polyelectrolytes (PEs), low-molecular-weight molecules such as enzymes, or their combinations [41]. These structures find wide applications in fields such as encapsulation, targeted and controlled drug delivery, personal care, biosensing, diagnostics, catalysis and paints [13, 32, 42, 43].

This review examines recent developments in the synthesis routes and properties of hollow spheres formed out of nanoparticles (NPs, diameter range 1–100 nm). Of specific interest to this review are cases where NPs (metal, metal oxide, and semiconductor compositions) constitute a part of the coating and can impart to the structures their optical, magnetic, and catalytic properties. To tailor next-generation devices with custom-built functionalities, methods for assembling NPs into controlled patterns and architectures are required and have resulted in areas of active research [7, 10, 44–46]. There are many excellent reviews that consider NPs as building blocks and describe methodologies to create functional NP assemblies [6, 47–53]. These include accounts that describe strategies and mechanisms for NP assemblies in one, two and three dimensions (1D, 2D and 3D), like wires, dyads, triads, rods, rings, clusters, strings, and spheres [54–64].

No review exists so far that examines the newest methodologies [apart from the popular layer-by-layer (LBL) assembly route] for forming hollow spheres or capsules where the shell is comprised of NPs, or describes the resultant properties of such assemblies. This is an area of immense significance as the utility of NPs in forming shell boundaries offers specific advantages over those formed by microparticles or polymers. Advantages include accurate control over shell thickness, resolvable to nanometer scales, and synergistic benefits gained through NP-exhibited “size-quantization effects” that give the system a host of new mechanical, optical, electrical, magnetic, and catalytic properties. Further, individual

NPs can be functionalized with chemical moieties (amino or mercapto groups or DNA), making them capable of binding to specific target sites through well-known amino or thio complexation chemistry or through Watson–Crick base pair interactions with DNA oligonucleotides. Thus, “smart” NP-shelled hollow spheres that are responsive to external triggers (pH, ionic strength, laser sources etc.) can be prepared [65–68]. Section 2 focuses on the electrostatic assembly approach to the synthesis of NP-shelled hollow spheres, specifically the NP–polymer tandem assembly route. Section 3 concerns interfacial stabilization methods for assembly of NP-shelled hollow spheres. Distinctions in properties that emerge from NP-shelled hollow spheres in comparison to their non-NP analogues will be highlighted [5, 19, 46, 69–73].

## 2 Hollow Spheres from Electrostatic Assembly of Nanoparticles Through Tandem Assembly

### 2.1 *Current Methods*

The use of colloidal templates has emerged as an elegant approach for the assembly of NPs into hollow spheres. Typically, hollow sphere synthesis begins by coating the core template with materials such as polymers and NPs using electrostatics or van der Waals attractive forces in conjunction with a reactive precursor. This is followed by a polymerization chemical reaction to form the shell. Removal of the core template by chemical dissolution or calcination results in hollow spheres [21, 74]. The term often used to describe this method – “sacrificial core templating” – can be somewhat misleading because it implies that other approaches do not involve the use and removal of a core template to form hollow spheres. To avoid any confusion, here we use the term “covalent assembly” in place of “sacrificial core templating” to distinguish its use of a reactive precursor to covalently bind the shell together.

An alternate route to assembly of nanoparticles as hollow spheres that does not require a polymerization reaction step is sequential electrostatic assembly. Electrostatic-mediated multilayer assembly of charged particles was first demonstrated by R. Iler on planar surfaces, wherein he established the proof-of-principle to deposit particles sequentially onto solid substrates [25]. Decher advanced this scheme by assembling alternately charged PEs (e.g., polycations and polyanions) onto solid supports. Ever since, this scheme has been used to form capsules by sequential electrostatic deposition of single or multiple coatings of materials on pre-formed colloidal templates and subsequent removal of the template by calcination or solvent dissolution. This constitutes the LBL method for assembly of hollow spheres.

Figure 1 depicts LBL assembly of hollow spheres. The first step involves surface modification of pre-formed solid colloidal templates (most commonly negatively charged) by depositing a layer of oppositely charged PE (here positive) through attractive electrostatic interactions. This step deposits the first layer of surface

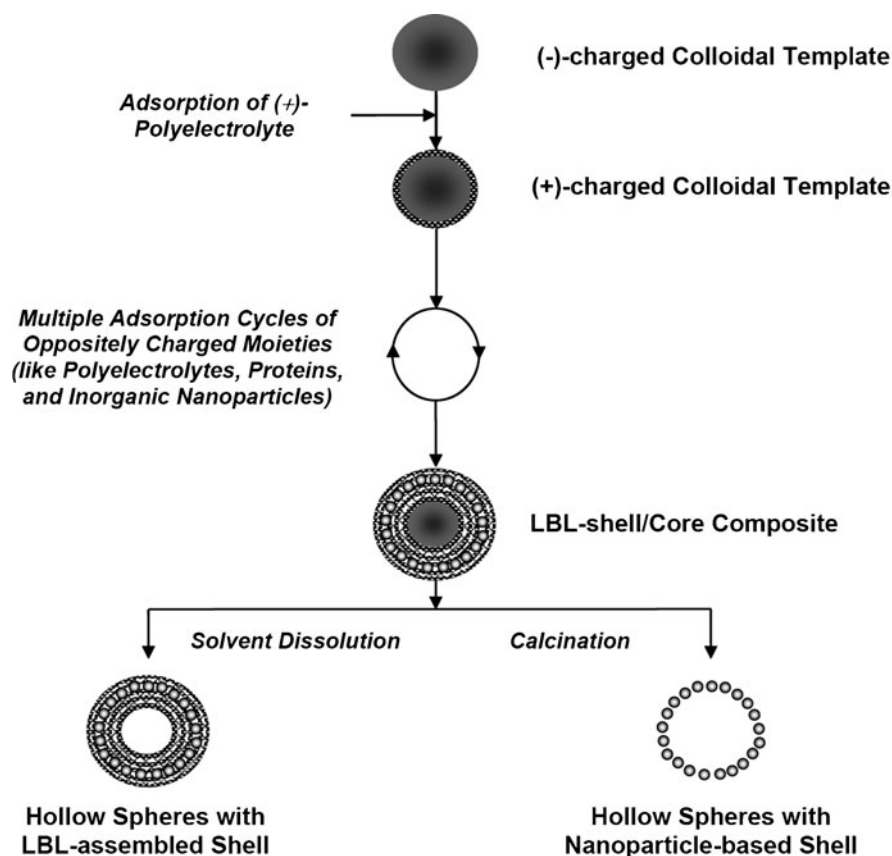


**Fig. 1** LBL assembly routes for formation of NP-shelled inorganic capsules

coating and results in charge reversal of the ensemble (in this case, positive). Following the first cycle of deposition, unadsorbed material is removed by centrifugation, wash, and filtration steps. Different combinations of charged moieties can be added, including PEs, proteins in the form of enzymes, organic dyes, and NPs. At the end of each cycle of deposition, unadsorbed material is removed by procedures described previously, and the process is repeated. Multiple repetitions lead to multi-layered composite structures, with each closed-shell layer made of a given charged moiety.

Capsules can then be formed by either a calcination or a dissolution step to create hollow structures. Calcination (typically carried out at a temperature of  $\sim 450^{\circ}\text{C}$ ) removes all the organic constituents (like the colloidal template core and the organic shell-forming moieties), leaving the constituent inorganic NPs slightly sintered to form robust shell walls. Solvent dissolution of the core material yields hollow spheres, which retain all the shell constituents. The LBL approach is thus a versatile route for creation of NP-shelled hollow spheres. Extensive reviews on forming

functional capsules by the LBL methods have been provided by Caruso and others and are beyond the scope of this chapter [13, 29, 30, 75].

A disadvantage common to both covalent and LBL assembly routes is the multiple steps involved in materials assembly. Automation of these layering steps provides an excellent approach to address this issue and leads to LBL-based manufacturing capabilities [76]. Also of concern are requirements of an incineration or solvent dissolution step to remove the core in order to form hollow spheres. It is a non-trivial challenge to selectively remove the inner core without degrading the shell properties and affecting structural integrity [13, 29, 30, 75]. Recent work demonstrates that liquid colloidal templates in the form of surfactant-stabilized liquid crystal droplets can be used successfully in the LBL assembly of capsules [77–79]. Such liquid droplets can further be used in continuous-flow production of LBL-assembled capsules via microfluidic technology.

Another recent development features the in situ formation of liquid colloidal templates. The assembly of NPs at the periphery of these templates is driven by electrostatics, resulting in the formation of robust NP-shelled hollow spheres, originally termed “nanoparticle-assembled capsules” (NACs). This scheme is called “tandem assembly”, “nanoparticle–polymer tandem assembly”, or “polymer-aggregate templating” and presents an alternate, simple and non-destructive route for formation of NP-shelled hollow spheres [6, 32–35, 40, 80, 81].

When comparing the time scales of transport of material to the hollow capsule interiors, the efficiency of encapsulation arising from assembly schemes featuring in situ encapsulation should be higher than for hollow structures formed by core-shell dissolution. Time requirements should be higher for hollow capsules contacted in a solution of material to be encapsulated, particularly when material transport is based on kinetically driven diffusion or absorption processes, as compared to an in situ encapsulation scheme. In the case of material transport governed by a thermodynamic phenomenon such as partitioning, the equilibrium quantity of material that needs to be transported across the shell will be dependent on the partition coefficient of the shell with respect to the material to be encapsulated [13, 32–35, 80–83].

## ***2.2 Preparation of Two-Nanoparticle-Type Hollow Spheres***

The origin to tandem assembly can be traced to the investigations by Stucky and coworkers on cooperative charge-based assembly of lysine (Lys)-cysteine (Cys) diblock copolypeptides with SiO<sub>2</sub> and Au NPs to result in robust hollow spheres. Diblock copolypeptides containing amphiphilic groups (hydrophilic Lys, pK<sub>a</sub>~9, hydrophobic Cys, pK<sub>a</sub>~8), upon reaction with Au NPs (diameter 10–12 nm), led to the formation of spherical aggregates of Au NPs (Fig. 2) [32]. On further reaction with SiO<sub>2</sub> NPs, micron-sized hollow spheres were seen to form. It is worthwhile re-emphasizing that aggregates emerge spontaneously and that the process is an electrostatically driven self-assembly process, which is different from entropy-driven molecular self-assembly schemes exhibited by surfactants, block copolymers, and vesicles.

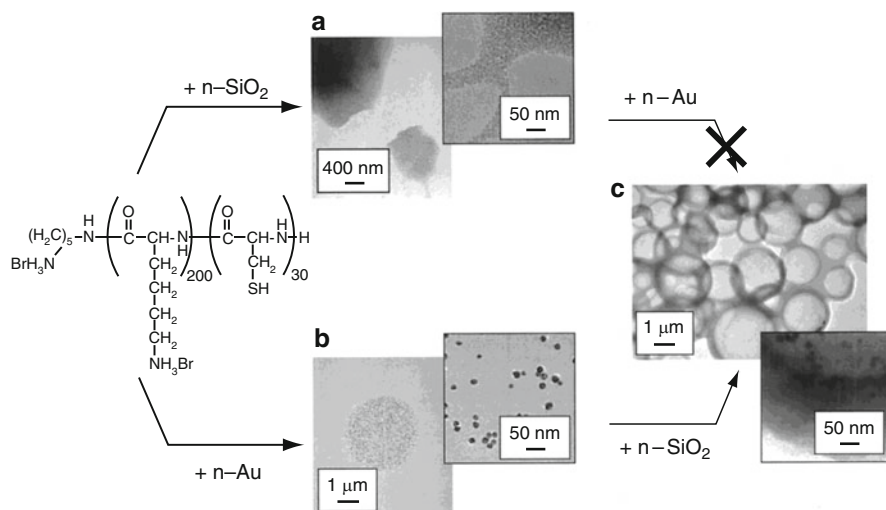


**Fig. 2** Formation of hollow spheres by tandem assembly of two NPs. (a) TEM images of  $\text{Lys}_{200}\text{Cys}_{30}/n\text{-SiO}_2$  precipitate. (b) TEM images of  $\text{Lys}_{200}\text{Cys}_{30}/n\text{-Au}$  precipitate. (c)  $\text{Lys}_{200}\text{Cys}_{30}/n\text{-Au}/n\text{-SiO}_2$  hollow spheres (*inset* shows areas of higher magnification). Structure in (c) is obtained only by adding  $\text{SiO}_2$  NPs to the  $\text{Lys}_{200}\text{Cys}_{30}/n\text{-Au}$  precipitate but is not formed when Au NPs are added to  $\text{Lys}_{200}\text{Cys}_{30}/n\text{-SiO}_2$  precipitate. Note:  $n\text{-Au}$  and  $n\text{-SiO}_2$  represent Au and  $\text{SiO}_2$  NPs, respectively. Reproduced from [32], with permission from the publisher

Noteworthy is the fact that hollow spheres did not form when diblock copolypeptides were reacted with  $\text{SiO}_2$  NPs first and then with Au NPs, thus indicating the crucial role of Au NPs in forming hollow spheres by binding copolypeptide chains into submicron- and micron-sized aggregates. Walls of the hollow spheres that formed consisted of a distinct layer of Au followed by an outer layer of  $\text{SiO}_2$  NPs with an average thickness of 250 nm. (as shown in Fig. 3). This indicates the flexibility and generic nature of the process, thus providing avenues for organization of multicompositional arrays of NPs. Also shown by a similar scheme was the formation of two-nanoparticle-type (2-NP) spheres from assembly of diblock copolypeptides poly-(L- $\text{Lys}_{200}$ -L- $\text{Cys}_{30}$ ) with citrate-stabilized CdSe/CdS quantum dots (QDs) followed by a layer of  $\text{SiO}_2$  NPs [84].

Stucky and coworkers furthered this work by studying citrate-stabilized CdSe QDs with single-block positively charged homopolymer PEs (poly-L-lysine, PLL) [33]. Macroscopic phase separation of initially water-soluble reactants were driven by molecular interactions between ligands on the inorganic phase (carboxylate groups of citric acid) and functional groups of the organic PEs (amino group on PLL), forming QD-PLL “vesicle”-like intermediates. The as-assembled QD NP vesicles collapsed on drying, but after addition of  $\text{SiO}_2$  NPs to the reaction mixture, stable 3D hollow spheres formed with distinct localization of the two NP types. QDs were located at the interior, whereas  $\text{SiO}_2$  NPs occupied the exterior of the shell wall, similar to the Au NP/ $\text{SiO}_2$  NP/diblock copolypeptide capsules.



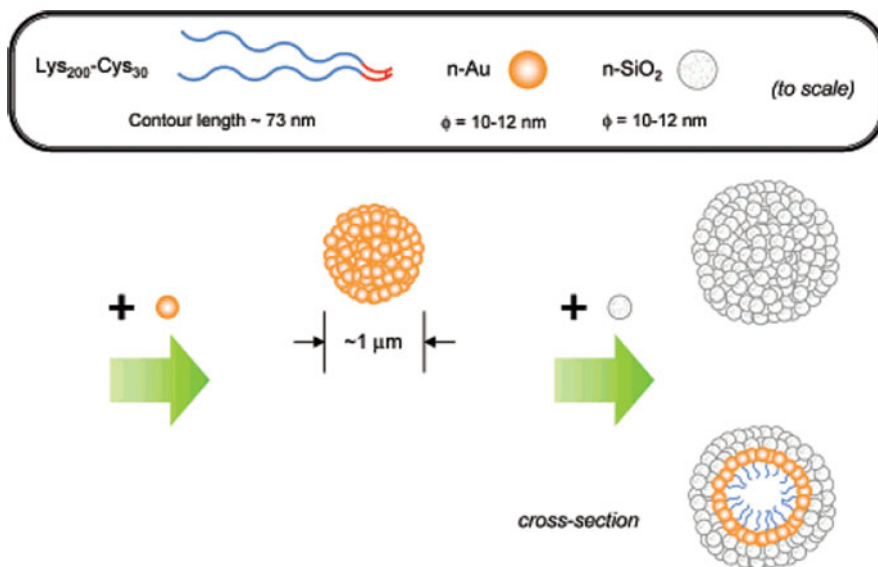


**Fig. 3** Hierarchical self-assembly of gold and silica NPs (n-Au and n-SiO<sub>2</sub>, respectively) into hollow spheres with a two-layer shell structure. Reproduced from [32], with permission from the publisher

The significant finding in this work was the establishment of the electrostatically driven mechanism behind self-assembly that did not depend on thiol–Au interactions.

Refining the NP vesicle formation model, Wong and coworkers developed a new model describing the formation of hollow microspheres in which polymer and NPs form spherical aggregate intermediates through particle/polymer flocculation [34]. An important finding was the establishment of a flocculation-driven mechanism of PLL-Au NP template growth, which led to a new understanding of how to control Au NP/SiO<sub>2</sub> NP hollow sphere sizes (Fig. 4). Dis-assembly of the shell was possible when the pH of the suspending fluid was made lower than the point of zero charge of SiO<sub>2</sub> ( $\sim 2$ ). The process was reversed on raising the pH.

### 2.3 Preparation of One-Nanoparticle-Type Hollow Spheres

In 2005, Rana et al. further expanded the scope of methods for forming colloidal templates in situ by devising a reaction scheme that utilized multivalent anions (such as tetrasodium ethylenediamine tetraacetate, EDTA) over previously used Au or CdSe NPs. The governing synthesis parameter is the “*R* ratio”, defined as the total negative charge from the multivalent anion divided by the total positive charge from the polymer. This new formation pathway relies on the counteranion condensation of EDTA and other multivalent anions with polyamines, to form polymer/salt

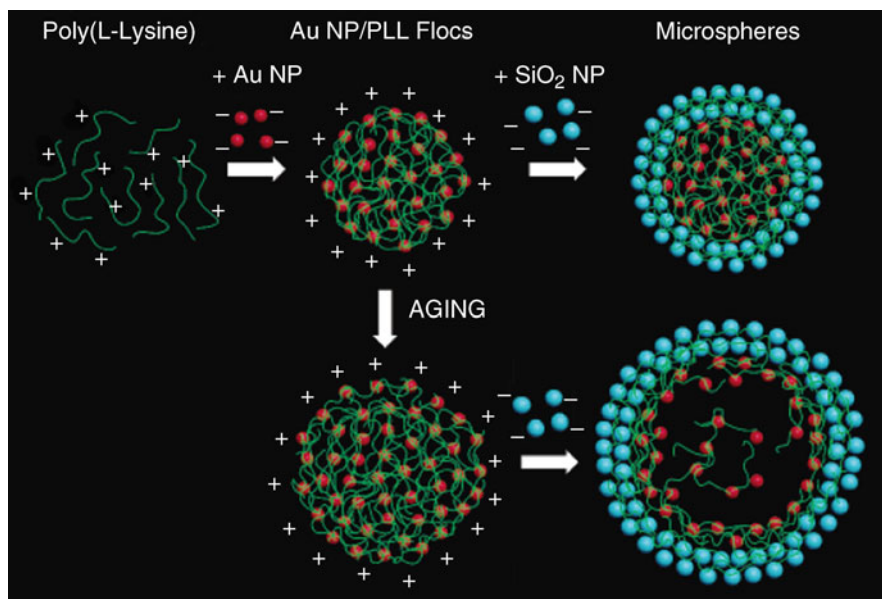


**Fig. 4** Flocculation-based self-assembly of organic-inorganic hollow spheres from PLL, Au NPs and SiO<sub>2</sub> NPs. Reproduced from [34], with permission from the publisher

aggregate colloidal templates. McKenna et al. reported similar aggregation behavior of polypeptides [85]. This salt-induced aggregation of polymer follows a very different mechanism from that in the cases of Au NP/PLL and CdSe QD/PLL. From a capsule synthesis point-of-view, salt-induced aggregation eventually yields materials composed of one NP composition whereas the other cases necessarily lead to materials composed of two NP compositions (Fig. 5).

Shell formation occurs when negatively charged SiO<sub>2</sub> NPs (at pH above its point of zero charge of 2) are contacted with the polymer/salt aggregates, such that the NPs adsorb to form a shell. Because the shell is many times thicker than the NP diameter, it has been proposed that the NPs penetrate into the polymer/salt aggregates before depositing, thereby forming a thick shell. This thick shell is responsible for the structural stability of these NACs on drying. Because the polymer/salt aggregates grow in time as metastable species (with growth rates a function of the *R* ratio), the capsule sizes can be controlled by both growth time and *R* ratio. Larger silica capsules are prepared with polymer/salt aggregates aged for longer times (30 min) rather than shorter times (3 min) (Fig. 6). The capsule material is essentially made of NPs and polymer in the shell, in which the polymer holds the oppositely charged NPs together. Interestingly, the NAC interior can contain either the polymer/salt aggregate or water, depending on the salt type used. Thus polymer-filled or water-filled capsules can be generated in one pot, merely by changing the precursor [35].

Subsequent investigations have established the general nature of the tandem assembly method using a host of linear cationic polymers [such as PLL and poly(allylamine hydrochloride), PAH] and multivalent salt variants (monosodium

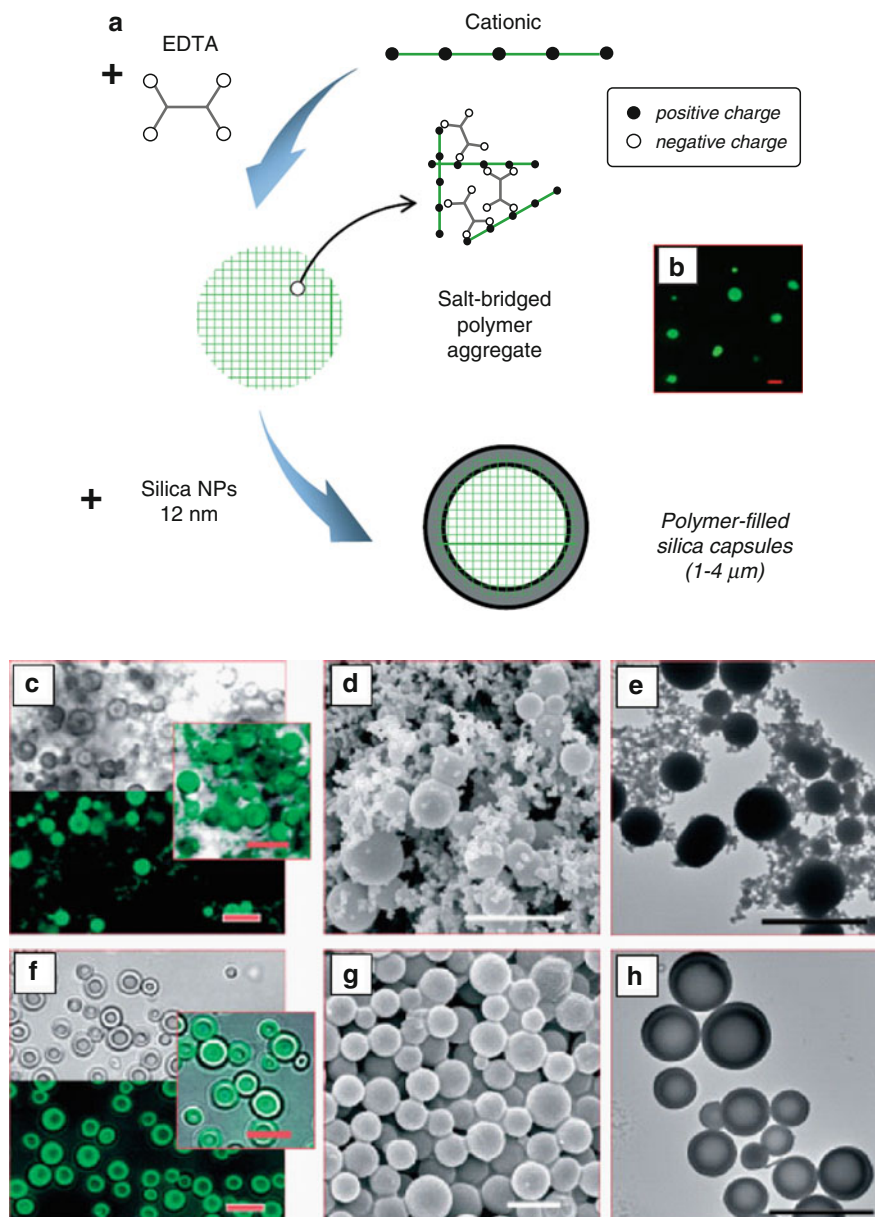
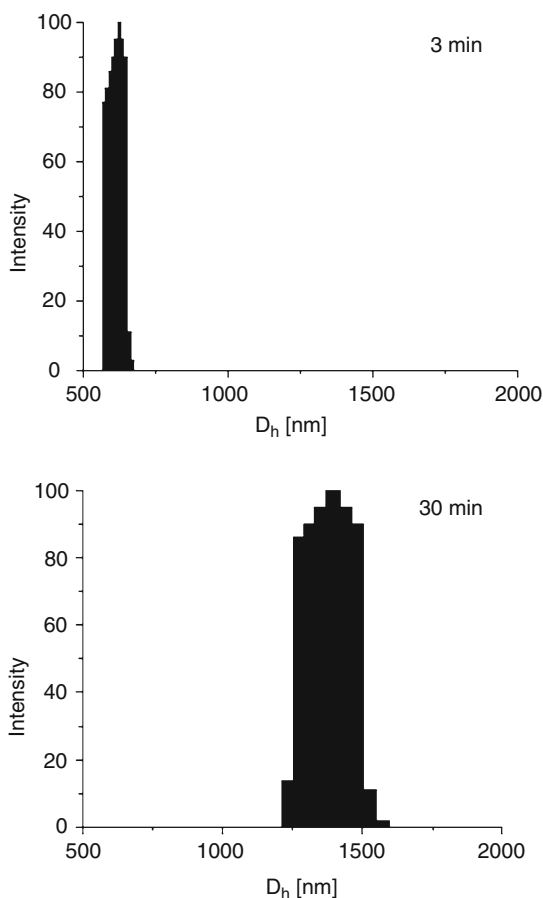


**Fig. 5** (a) Proposed schematic of the tandem self-assembly process in which positively charged polymer chains ionically cross-link with negatively charged multivalent anions, and silica nanoparticles subsequently deposit around the polymer aggregates. (b) Confocal image of EDTA-bridged PLL-FITC aggregates. (c, f) Bright field (top), confocal (bottom), and combined bright field/confocal (insets) of three different silica structures suspended in water. SEM (d, g) and TEM (e, h) images of silica structures correspond to structures in images (c and f), respectively. Scale bars: 5  $\mu\text{m}$ . Reproduced from [35], with permission from the publisher

**Fig. 6** Size distribution of citrate-bridged PAH aggregates ( $R = 10$ ) after aging for 3 min (*top*) and 30 min (*bottom*). Reproduced from [35], with permission from the publisher



citrate, disodium citrate, sodium acetate, trisodium citrate, sodium succinate, EDTA, and  $\text{Na}_2\text{HPO}_4$ ). Besides  $\text{SiO}_2$  NP capsules, capsules made of  $\text{SnO}_2$  NPs, ZnO NPs,  $\text{Fe}_2\text{O}_3$  NPs,  $\text{Fe}_3\text{O}_4$  NPs, CdSe QDs, polymer,  $\text{Al}_2\text{O}_3$ - $\text{SiO}_2$  NPs, and  $\text{SiO}_2$  NPs-silicic acid have been successfully synthesized [80, 81, 86–88]. A variation of tandem assembly was reported by Tropak et al. in which nanocomposite magnetic microspheres were formed through coascervates by reacting PLL with citrate-stabilized  $\text{Fe}_2\text{O}_3$  NPs and subsequent cross-linking with glutaraldehyde [89, 90]. In more recent developments, Murthy et al. describe formation of patchy or multicompartment capsules using a blend of polymers (PAH and PLL), citric acid and  $\text{SiO}_2$  NPs [91].

The unique selling proposition of the tandem-assembly process is its contribution to the field of green chemistry in obtaining closed-shell colloidal structures through an environmentally friendly route, as the entire synthesis is carried out in water, at near neutral pH, and at room temperature. Further, the size of the colloidal template can be controlled by the charge ratios of reactants, which results in structures with sizes ranging from 100 nm to 2  $\mu\text{m}$  [32–35, 80, 81].

## 2.4 Applications and Properties of Tandem-Assembled Capsules

### 2.4.1 Optical Properties

#### Photoresponsive Delivery Systems

In the fields of medicine and drug delivery, photoresponsive delivery systems have received much attention in recent years because irradiation with light provides a direct, non-invasive method for releasing active molecules. This offers significant advantages over conventional approaches of drug delivery that rely on altering local environments (through the use of triggers such as pH, ionic strength, and temperature) to release actives, often resulting in undesired side effects. Engineered photoresponsive systems with NPs or dyes that absorb in the near-infrared (NIR) region are advantageous because most body tissues show weak light absorption, thus protecting healthy tissue while selectively treating affected tissue. In advancing photoresponsive delivery technologies, metal–NP-shelled hollow spheres from tandem assembly can be engineered to provide suitable candidates [66].

One of the key features of tandem assembly is the ability to encapsulate compounds easily and without damage. In a demonstration of applications of optically functional NACs for medical applications, Yu et al. synthesized NIR NACs, where an FDA-approved photosensitizer dye called indocyanine green (ICG) was successfully incorporated into silica/polymer capsules with diameters ranging from 0.6 to 1.0  $\mu\text{m}$ . ICG loading was readily controlled, with a maximum attained loading of  $\sim 23$  wt%. Leakage tests carried out for over 24 h at room temperature indicated negligible ICG leakage in a phosphate buffer saline solution that demonstrated the robust nature of NACs. However, ICG-containing capsules were active (capable of heat generation) to NIR laser-induced irradiation and were stable to multiple photothermal heating cycles. Fibroblast cells exposed to these capsules remained viable even after 2 days of incubation, thus these NACs serve as a promising material for photothermal therapy, offering cost and processing advantages over LBL and reduction-reaction-based Au-NP capsules and Au-nanoshells (Fig. 7) [86].

#### Optical Stability and Targeted Fluorescence Imaging

ICG finds applications as a fluorescent probe in clinical imaging. Challenges to realizing ICG as a probe for targeted fluorescence imaging in vivo emerge from its optical instability and tendency to excessively accumulate in the liver. Yaseen et al. recently devised a versatile and inexpensive route to the encapsulation of ICG within NACs, and performed targeted fluorescence imaging in vivo for the first time ever. Negatively charged constructs, formed by a coating of magnetite ( $\text{Fe}_3\text{O}_4$ ) NPs and polyacrylic acid (PAA), were shown to predominantly accumulate in lungs, whereas neutrally charged capsules formed from PLL and ICG exhibited a prolonged circulation time in the bloodstream.

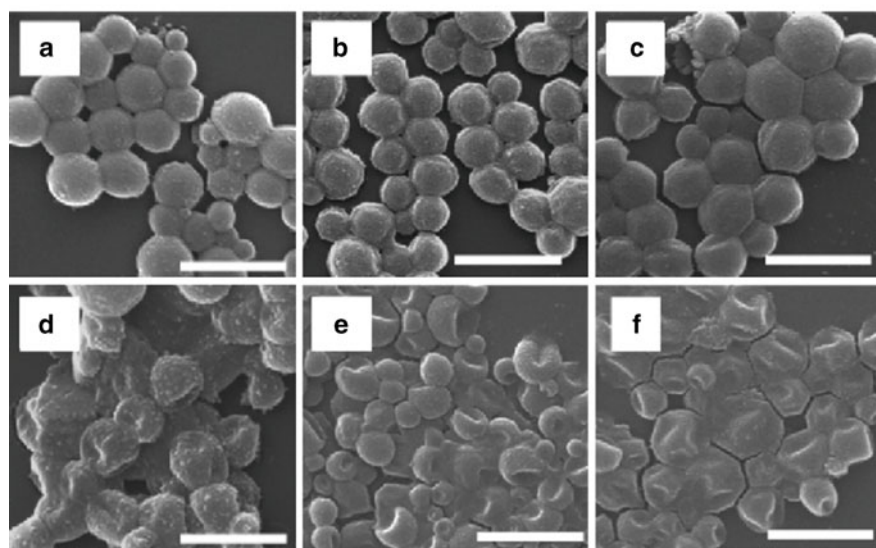
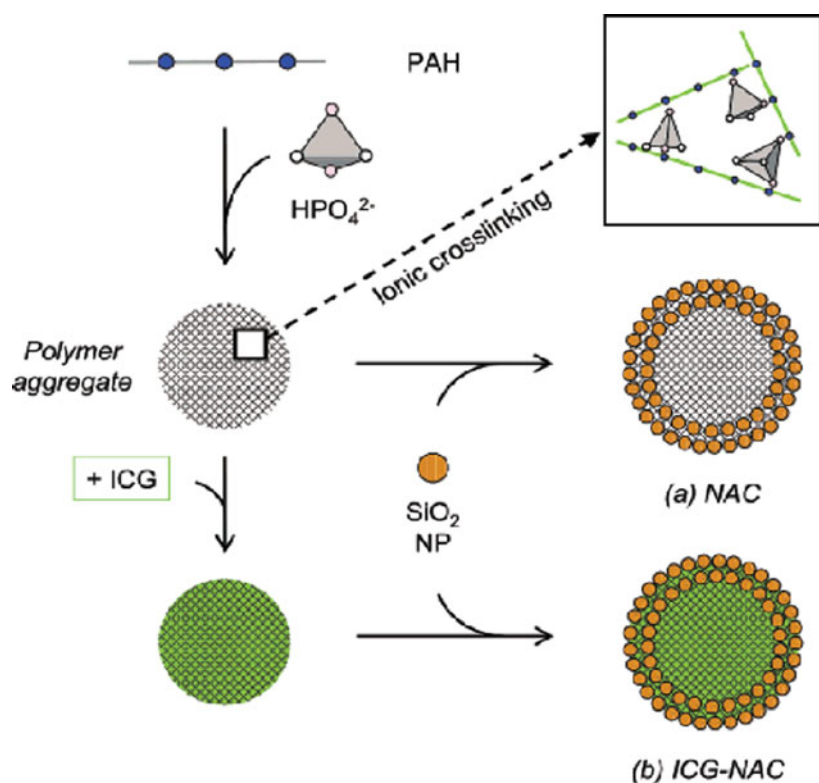


**Fig. 7** (Above) Formation mechanism of NACs and ICG-containing NACs (ICG-NACs). (Below) SEM images of ICG-NACs irradiated at different temperatures: (a) 23, (b) 40, (c) 50, (d) 60, (e) 70, (f) 73°C. Scale bars: 2  $\mu\text{m}$ . Reproduced from [86], with permission from the publisher



## Optical Devices

Semiconductor NPs such as QDs have successfully been utilized for their size-dependent optical properties and find applications as optical contrast agents for biological tagging, in photovoltaics, and in lasing. In the application of QDs for optical lasing, requirements are high volume fractions of QDs, rapid optical pumping, and an optical feedback media that stimulates spontaneously emitted photons. In this regard, spherical microcavities have been established to present the ideal feedback geometry for confining the propagation of light in 3D. Cha et al. showed that hollow spheres of CdSe/CdS QDs, formed with water-soluble diblock copolypeptides and SiO<sub>2</sub> NPs, could be used for microcavity lasing applications. These spheres have a high QD volume fraction and their hollow, 3D geometry provides an ideal combination of quantum and optical confinement properties, wherein electronic states of the confined QDs are coupled to the photonic states of the spherical microcavity [84].

Another variant of semiconductor NPs uses SnO<sub>2</sub>, with applications in displays, solar cells, sensors, and photocatalysis. Assembly of SnO<sub>2</sub> NPs in a spherical shell construct is desirable in that an optically active encapsulation device can be realized. Yu et al. recently reported preparation of semiconductor SnO<sub>2</sub> NACs, using PAH polymer and Na<sub>2</sub>HPO<sub>4</sub> polyelectrolyte, that exhibited the size-dependent optical properties of the SnO<sub>2</sub> NPs building blocks. Further, the size of the resulting SnO<sub>2</sub> NACs were easily controllable by the aging time of the PAH/Na<sub>2</sub>HPO<sub>4</sub> aggregates, demonstrating flexibility in creating optical constructs of desired size. The optical properties of SnO<sub>2</sub> NACs were measured using diffuse reflectance UV-vis spectroscopy and found to be similar to SnO<sub>2</sub> NPs, suggesting their application in light-responsive encapsulation devices (Fig. 8) [81].

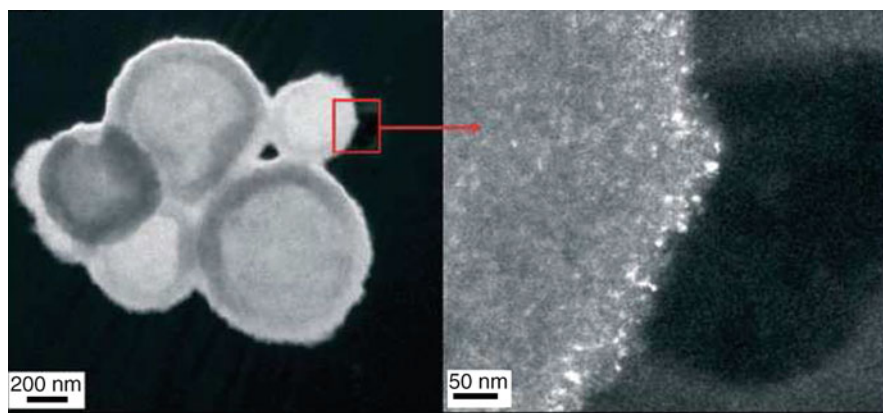


**Fig. 8** TEM image (*left*) of SnO<sub>2</sub> NACs, prepared with PAH and phosphate ions. TEM image of NAC walls (*right*) comprised of SnO<sub>2</sub> NPs. Reproduced from [81], with permission from the publisher

### 2.4.2 Mechanical Properties

The mechanical properties of microcapsules are characterized by parameters (mechanical strength, stiffness, buckling) that describe their resistance to deformation and structural change when subjected to an external load from mechanical stress or triggers such as pH, ionic strength, and temperature. Mechanical properties largely depend on the local microstructure of the capsule shell wall in terms of composition and thickness (based on its permeability or porosity), and of the core (water-filled or polymer-filled). It is useful to distinguish mechanical properties from structural stability, which in the parlance of microcapsules are changes associated with the structure of microcapsules during the drying step of synthesis. Depending on the anticipated application, structural collapse of capsules subjected to mechanical stress or triggers should either occur or be avoided.

#### Encapsulation and Release Properties

Rapid and facile generation of capsules from tandem assembly in aqueous media is amenable to encapsulation of water-soluble compounds. Encapsulation of ICG dye within PAH/ $\text{H}_2\text{PO}_4$  aggregates was shown by Yu et al. Enzyme encapsulation and the feasibility of capsules to serve as reaction vessels was demonstrated by Rana et al. In their study, they encapsulated acid phosphatase enzyme in PLL–citrate–silica sols and suspended the spheres in a solution containing fluorescein diphosphate. Fluorescence increased in intensity within the shell walls as fluorescein was formed by enzymatic cleavage of phosphate groups. This study showed that microcapsules could serve as reaction vessels that allow enzymatic action to take place in a protective environment and allow for reactants and/or products to diffuse through permeable shell walls.

Bagaria et al. developed new routes for controlling shell wall thickness by adding silicic acid to NACs formed by tandem assembly of PAH, citric acid, and  $\text{SiO}_2$  NPs. Diffusion of silicic acid through  $\text{SiO}_2$  NPs resulted in an inward thickening of shells walls, confirmed by thermogravimetric analysis (TGA) and decreased dye release [88].

To describe the concentration profiles and release kinetics of fluorescein from single NP-shelled capsules, Muñoz Tavera et al. solved a mathematical model that describes unsteady-state transport from multilayered spheres using the Sturm–Liouville approach [92]. Several aspects of dye release, such as the asymptotic plateau effect of diffusive release and the effects of capsule diameter and shell thickness distribution on dye release, were captured by the model and confirmed by experimental data.

In more recent developments, Murthy et al. report a novel variant of tandem assembly leading to the formation of patchy or multicompartment anisotropic microspheres from NP/polymer assembly and demixing of polyamine. On sequentially mixing a blend of PLL and PAH with citric acid and a silica source, PLL/PAH solution was seen to phase-separate as heterogeneous domains. Addition of  $\text{SiO}_2$  NPs



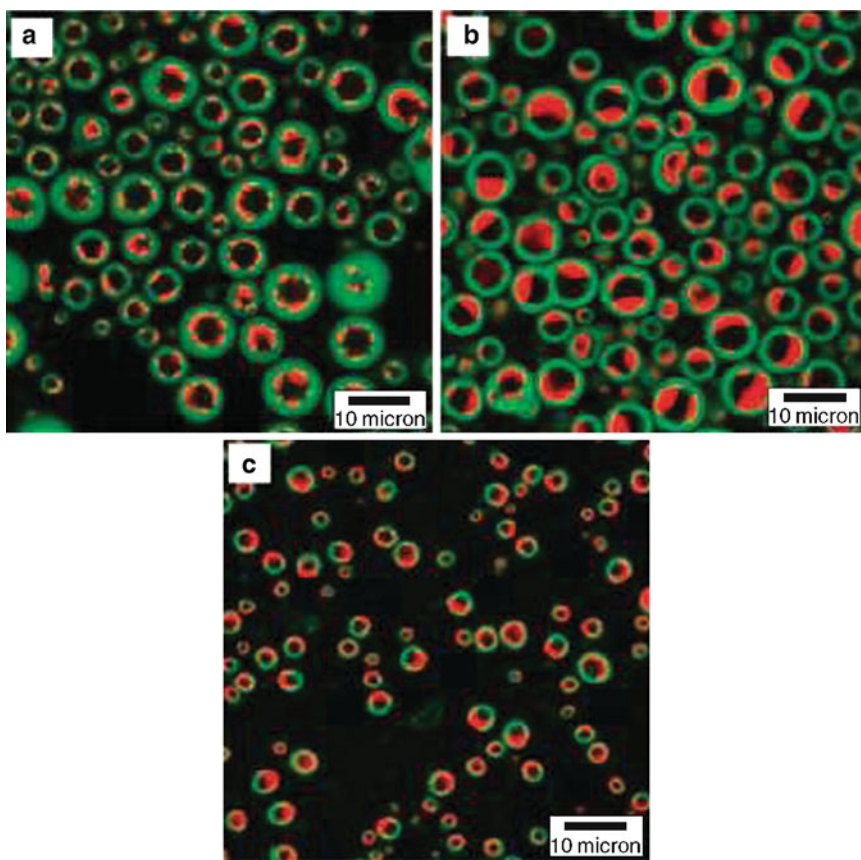


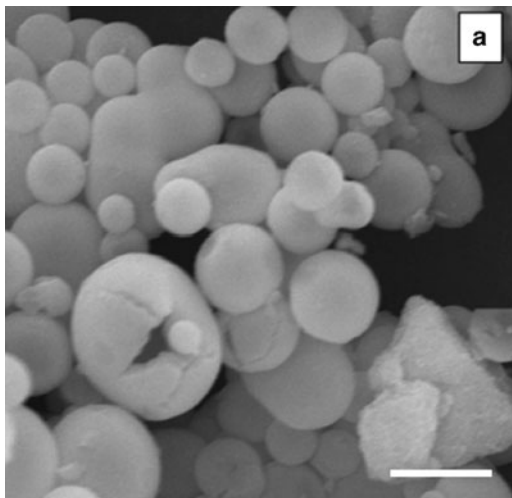
**Fig. 9** Patchy particles synthesized by stabilizing PLL-PAH/citrate aggregates with SiO<sub>2</sub> NPs at various PLL:PAH ratios: (a) 75:25, (b) 50:50, (c) 25:75. Reproduced from [91], with permission from the publisher

resulted in hollow, water-filled capsules with PAH-citrate domains attached to the cell walls. Addition of silicic acid resulted in solid spheres with PAH and PLL present in discrete domains. This method of generating compartmentalized microspheres promises to hold great potential for targeted delivery and triggered chemical release applications (Fig. 9) [91].

### Catalytic Properties

Kadali et al. demonstrated another useful application of NACs prepared by tandem assembly in the formation of catalyst support materials. NACs can be calcined to remove the polymer without collapsing the hollow sphere structure (Fig. 10). Such stability is more difficult to achieve with LBL-assembled capsules. On calcination,

**Fig. 10** SEM image of PAH-citrate and silica NACs calcined at 600°C while retaining structural stability. Scale bar: 5  $\mu\text{m}$ . Reproduced from [87], with permission from the publisher



the specific surface area of the microcapsules was found to be at  $259\text{ m}^2/\text{g}$ , with a pore size of 4 nm and pore volume of  $0.38\text{ cm}^3/\text{g}$ . The surface area was similar to that of dried, calcined NPs but the porosity and pore volume were found to be significantly higher. These are useful attributes for a catalyst support. Since the material is aluminosilicate in composition, these capsules could also have applications as an acid catalyst [87].

### 3 Interfacial Stabilization and Other Approaches to the Assembly of Nanoparticle-Shelled Hollow Structures as Emulsions and Foams

The previous sections reviewed recent advancements in sequential electrostatic assembly to form NP-shelled structures. An alternate route to NP assembly arises from interfacial activity and stabilization of NPs. Colloidal particles with partial hydrophilic and hydrophobic character are known to behave like surface-active molecules (surfactants), particularly when adsorbed to a fluid–fluid interface. The assembly of small particles at interfaces is of relevance to advance fields that traditionally feature emulsions, foams, and flotation systems. It is also of pertinence to the development of new fields such as the synthesis of novel materials that include Janus particles, colloidosomes, porous solids, and anisotropic particles, all recently prepared by particle assembly at interfaces [36, 38].

Finely divided solid particles have been known since the turn of the last century to act as stabilizers in emulsions. In a seminal paper, Pickering reported that particles that preferentially wetted water over oil formed oil-in-water (O/W) emulsions through assembly at the interface [93]. This idea has been extended to the

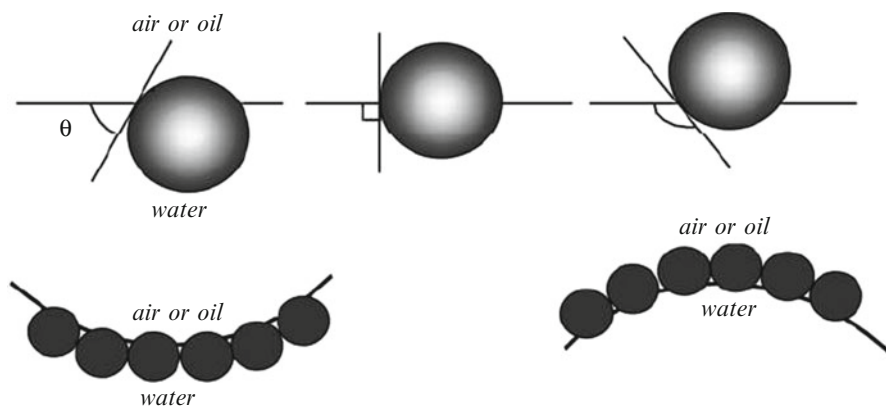


**Fig. 11** (Top) Position of a spherical (colloidal) particle at a planar fluid–water interface for a contact angle ( $\theta$ , measured through the aqueous phase)  $< 90^\circ$  (left),  $90^\circ$  (center), and  $> 90^\circ$  (right). (Bottom) Corresponding probable positioning of particles at a curved fluid–water interface. For  $\theta < 90^\circ$ , solid-stabilized aqueous foams or O/W emulsions may form (left). For  $\theta > 90^\circ$ , solid-stabilized aerosols or W/O emulsions may form (right). Reproduced from [37], with permission from the publisher

assembly of NPs at interfaces. There exist analogies between the interfacial assembly of colloidal particles and NPs with surfactants, in terms of their water- or oil-liking tendencies, wherein their behavior can be described in terms of wettability. This is defined by the contact angle ( $\theta$ ) formed at the fluid–fluid interface (Fig. 11). The result of this wetting behavior is the formation of either O/W or W/O emulsions with interfaces decorated by particles.

NPs, like surfactants, can facilitate phase transformation of emulsions from O/W to W/O type through change in surface wettability by altering field variables such as pH or electrolyte concentration. There are, however, important differences between stabilization of interfaces by surfactants and by particles, particularly in terms of emulsion stability. Binks has provided a comprehensive review highlighting the differences between surfactant- and particle-stabilized emulsions [37]. A key development in the latter has occurred through investigations of NP assembly at liquid–liquid interfaces, where emulsions have remarkably different properties to those formed using micron-sized particles [94]. The stability of emulsions prepared by particles is dependent on the ability of the particle to partially wet both fluid phases and to exist as a weakly flocculated state. In this regard, the energy of attachment ( $E$ ) of a particle to an interface is given by:

$$E = \pi r^2 \gamma_{\alpha\beta} (1 \pm \cos \theta)^2 \quad (1)$$

where  $r$  is the radius of the particle,  $\gamma_{\alpha\beta}$  is the interfacial tension between phases  $\alpha$  and  $\beta$ , and  $\theta$  is the contact angle of the particle defined with respect to one of the phases as the reference. It can be seen that  $E$  varies as the square of radius;

hence, NPs readily stabilize interfaces, assuming favorable wetting conditions (favorable  $\theta$ ). In contrast, micron-sized particles have to overcome an initially high energetic penalty arising from steric factors. However, once formed, the emulsions obtained are highly stable because  $E$  well exceeds the thermal energy ( $kT$ ,  $k$  being Boltzmann's constant and  $T$  temperature), so they are not easily destabilized by thermal fluctuations. At very low size ranges ( $<10$  nm), NPs tend to behave in a manner analogous to surfactants in that thermal fluctuations facilitate easy adsorption and desorption from interfaces. Thus, an optimum NP size (10–100 nm) is suitable for formation of stable emulsions [37].

Stability of NP-assembled emulsions can be controlled further in the presence of surfactants. Binks and coworkers report synergistic benefits when negatively charged silica NPs and cationic surfactants, or positively charged silica NPs and anionic surfactants, were used to create O/W emulsions. These emulsions demonstrated high kinetic stability to creaming and coalescence, due to synergistic lowering of interfacial tension by surfactants and of wetting behavior by NPs [94,95]. The stability of emulsions prepared using NPs and uncharged nonionic surfactants was seen to be strongly dependent on the protocol of preparation, where the absence of electrostatic interactions between NPs and surfactants resulted in scenarios in which either interfacial tension or wettability effects dominated, thus resulting in unstable or stable emulsions, respectively [94,96].

Binks and Murakami report unique behavior in NP-induced phase transformation in particle-stabilized air–water systems that is not demonstrated by surfactants. It was seen that by altering silica-NP (20–30 nm) hydrophobicity at constant air:water ratio or by changing the air:water ratio at fixed NP wettability, phase inversion could be induced from air-in-water to water-in-air foams (Fig. 12) [36]. This investigation thus demonstrates that control over interfacial assembly of NPs leads to the formation of stable NP-shelled hollow spheres, thus resulting in the formation of stable foams, dispersions, and powders with far reaching consequences in opening new avenues for advanced encapsulation (Fig. 13).

In other unique structures that emerge from interfacial NP assembly, Weitz and coworkers report formation of solid capsules with precise size control over permeability and mechanical strength through self-assembly of 0.9- $\mu$ m colloidal particles at the interface of emulsion droplets. Particles are locked to form elastic shells and then transferred to a continuous-phase fluid that is of similar composition to the fluid inside the droplets, resulting in colloidosomes with characteristics of high structural robustness [38,40]. Duan et al. report interfacial assembly of magnetic NPs and formation of water-dispersible NP colloidosomes with permeable shells, while He and Yu report formation of silica NP-armored polyaniline microspheres in particle-stabilized emulsions [97,98]. In all such cases, the driving force for assembly at interfaces is stabilization through minimization of exposed interfacial area [36,37,39,40,53,57,58,73,94–96,98–110].

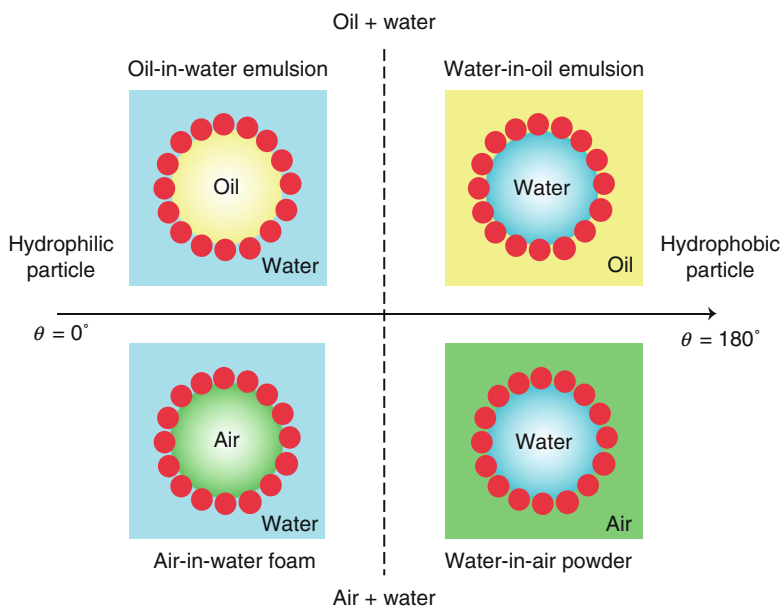


**Fig. 12** Dispersed systems prepared from fluid mixtures and colloidal particles/nanoparticles. For oil–water mixtures (*top*), emulsion drops of O/W emulsions and W/O emulsions are stabilized with hydrophilic or hydrophobic particles, respectively. For air–water mixtures (*bottom*), air-in-water foams or water-in-air powders can be likewise stabilized through the use of nanoparticles. Reproduced from [36], with permission from the publisher

## 4 Conclusions and Future Work

This chapter describes the non-LBL approaches of tandem assembly and interfacial stabilization for the formation of closed shell structures, with an emphasis on ensembles in which NPs constitute the shell. Tandem assembly is a versatile and environmentally friendly route to the formation of useful NP-shelled capsules. In contrast to sacrificial core templating and LBL assembly methods, tandem assembly has the important differentiating feature that it avoids the incineration or solvent dissolution step to generate the hollow interior of the capsule. Enhancements in optical, mechanical, catalytic, and release properties of such materials hold great promise for their application in photoresponsive delivery systems, catalysis, and encapsulation. Interfacial stabilization routes are found to yield NP-shelled structures in the form of emulsions and foams that have enhanced stability over those from conventional, surfactant-based approaches. Unusual interactions of the NP with fluid interfaces have made possible new structures, such as water-in-air foams, colloidosomes, and anisotropic particles.

As a future direction of research, capsule walls comprised of amphiphilic NPs (Janus capsules) could give rise to a new class of material that has the dual properties of interfacial activity and targeted materials delivery. LBL assembly has previously

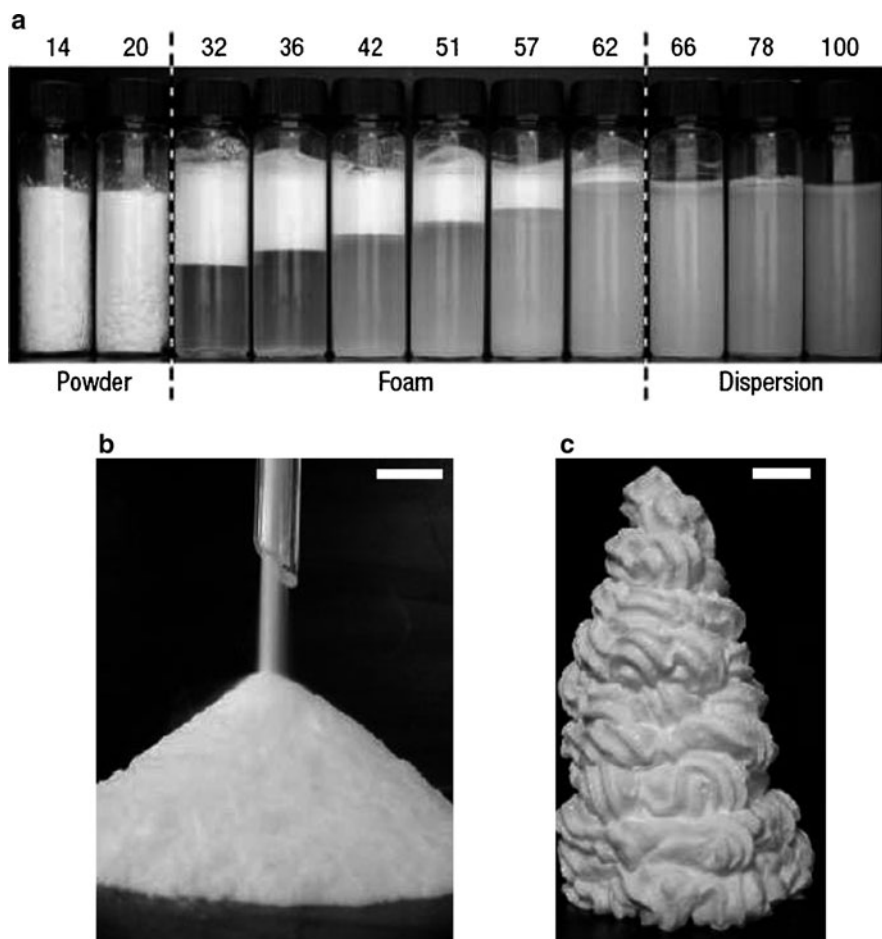


**Fig. 13** Transitional inversion of the curvature of air-water surfaces with respect to particle hydrophobicity. **(a)** Vessels containing 2 wt% (relative to water) of dichloromethylsilane-coated silica particles with fixed volume fraction of water ( $\phi_w = 0.056$ ) 2 weeks after mixing and aeration, for particles of different wettability. The % SiOH content on particle surfaces (given along the top) decreases from right to left as particles become more hydrophobic; the mixtures change from aqueous dispersions to air-in-water foams (with drained water) to water-in-air powders. Inversion occurs on moving either side of the *left dashed line*. **(b)** Free-flowing powder passing through a glass funnel made by aerating 5 g of silica particles possessing 20% SiOH and 95 g of water ( $\phi_w = 0.056$ ). **(c)** Foam extruded through a serrated metal nozzle prepared by aerating 5 g of silica particles possessing 32% SiOH and 95 g of water ( $\phi_w = 0.056$ ). Scale bars: 1 cm. Reproduced from [36], with permission from the publisher

been used to make hollow Janus structures with amphiphilic submicron particles, and tandem assembly has until recently resulted in 1- or 2-NP-shelled capsules. This approach could be revisited wherein NPs with differing levels of hydrophilic or hydrophobic nature (such as silica NPs) could be deposited at precise locations

on templates to create Janus capsules [31, 111–113]. The use of biological hollow particles called “vaults” ( $\sim 40$ – $70$  nm) could be incorporated into tandem assembly chemistry to generate multifunctional microcapsules comprised of biocompatible nanocapsules [114]. Continued development in top-down approaches of microfabrication (such as lithography and reactive-ion etching) could provide novel avenues for assembly of NP-shelled capsules into well-defined patterned macrostructured films [108].

**Acknowledgement** We acknowledge the financial support of National Science Foundation (CBET-0652073) and the Rice University Institute of Biosciences and Bioengineering Medical Innovations Award.

## References

1. Evans DF, Wennerström H (1999) The colloidal domain: where physics, chemistry, biology and technology meet, 2 edn. Wiley, New York
2. Israelachvili JN (1991) Intermolecular and surface forces. Academic, New York
3. Claesson PM, Ederth T, Bergeron V et al (1996) Techniques for measuring surface forces. *Adv Colloid Interface Sci* 67:119–183
4. Grabar KC, Brown KR, Keating CD et al (1997) Nanoscale characterization of gold colloid monolayers: a comparison of four techniques. *Anal Chem* 69(3):471–477
5. Schatz GC (2007) Using theory and computation to model nanoscale properties. *Proc Natl Acad Sci* 104(17):6885–6892
6. Tang ZY, Kotov NA (2005) One-dimensional assemblies of nanoparticles: preparation, properties, and promise. *Adv Mater* 17(8):951–962
7. Shipway AN, Katz E, Willner I (2000) Nanoparticle arrays on surfaces for electronic, optical, and sensor applications. *Chem Phys Chem* 1(1):18–52
8. Caruso F (2003) Nanoscale surface modification via sequential electrostatic assembly. In: Caruso F (ed) *Colloids and colloid assemblies*. Wiley, Weinheim
9. Parviz BA, Ryan D, Whitesides GM (2003) Using self-assembly for the fabrication of nanoscale electronic and photonic devices. *IEEE Trans Adv Packaging* 26(3):233–241
10. Chane-Ching JY, Cobo F, Aubert D et al (2005) A general method for the synthesis of nanostructured large-surface-area materials through the self-assembly of functionalized nanoparticles. *Chem Eur J* 1(3):979–987
11. Huang MH, Mao S, Feick H et al (2001) Room-temperature ultraviolet nanowire nanolasers. *Science* 292(5523):1897–1899
12. Han MY, Gao XH, Su JZ et al (2001) Quantum-dot-tagged microbeads for multiplexed optical coding of biomolecules. *Nat Biotechnol* 19(7):631–635
13. Caruso F (2001) Nanoengineering of particle surfaces. *Adv Mater* 13(1):11–22
14. Connolly S, Fitzmaurice D (1999) Programmed assembly of gold nanocrystals in aqueous solution. *Adv Mater* 11(14):1202–1205
15. Bruchez M, Moronne M, Gin P et al (1998) Semiconductor nanocrystals as fluorescent biological labels. *Science* 281(5385):2013–2016
16. Chan WCW, Nie SM (1998) Quantum dot bioconjugates for ultrasensitive nonisotopic detection. *Science* 281(5385):2016–2018
17. Alivisatos AP, Johnsson KP, Peng XG et al (1996) Organization of ‘nanocrystal molecules’ using DNA. *Nature* 382(6592):609–611
18. Mirkin CA, Letsinger RL, Mucic RC et al (1996) A DNA-based method for rationally assembling nanoparticles into macroscopic materials. *Nature* 382(6592):607–609



19. El-Sayed MA (2001) Some interesting properties of metals confined in time and nanometer space of different shapes. *Acc Chem Res* 34(4):257–264
20. Grieve K, Mulvaney P, Grieser F (2000) Synthesis and electronic properties of semiconductor nanoparticles/quantum dots. *Curr Opin Colloid Interface Sci* 5(1–2):168–172
21. Wilcox DL Sr, Berg M, Bernat T et al (1995) Hollow and solid spheres and microspheres: science and technology associated with their fabrication and application. Materials Research Society, Pittsburgh, PA
22. Yang M, Ma J, Zhang CL et al (2005) General synthetic route toward functional hollow spheres with double-shelled structures. *Angew Chem Int Ed.* 44(41):6727–6730
23. Huie JC (2003) Guided molecular self-assembly: a review of recent efforts. *Smart Mater Struct* 12(2):264–271
24. Boncheva M, Bruzewicz DA, Whitesides GM (2003) Millimeter-scale self-assembly and its applications. *Pure Appl Chem* 75(5):621–630
25. Iler RK (1966) Multilayers of colloidal particles. *J Colloid Sci* 21(6):569–594
26. Caruso RA, Antonietti M (2001) Sol-gel nanocoating: an approach to the preparation of structured materials. *Chem Mater* 13(10):3272–3282
27. Decher G, Hong JD (1991) Buildup of ultrathin multilayer films by a self-assembly process. 1. Consecutive adsorption of anionic and cationic bipolar amphiphiles on charged surfaces. *Makromol Chem Macromol Sym* 46:321–327
28. Decher G (1997) Fuzzy nanoassemblies: toward layered polymeric multicomposites. *Science* 277(5330):1232–1237
29. Caruso F, Caruso RA, Mohwald H (1998) Nanoengineering of inorganic and hybrid hollow spheres by colloidal templating. *Science* 282(5391):1111–1114
30. Caruso F (2000) Hollow capsule processing through colloidal templating and self-assembly. *Chem Eur J* 6(3):413–419
31. Jiang CY, Tsukruk VV (2006) Freestanding nanostructures via layer-by-layer assembly. *Adv Mater* 18(7):829–840
32. Wong MS, Cha JN, Choi KS et al (2002) Assembly of nanoparticles into hollow spheres using block copolypeptides. *Nano Lett* 2(6):583–587
33. Cha JN, Birkedal H, Euliss LE et al (2003) Spontaneous formation of nanoparticle vesicles from homopolymer polyelectrolytes. *J Am Chem Soc* 125(27):8285–8289
34. Murthy VS, Cha JN, Stucky GD et al (2004) Charge-driven flocculation of poly(l-lysine)-gold nanoparticle assemblies leading to hollow microspheres. *J Am Chem Soc* 126(16):5292–5299
35. Rana RK, Murthy VS, Yu J et al (2005) Nanoparticle self-assembly of hierarchically ordered microcapsule structures. *Adv Mater* 17(9):1145–1150
36. Binks BP, Murakami R (2006) Phase inversion of particle-stabilized materials from foams to dry water. *Nat Mater* 5(11):865–869
37. Binks BP (2002) Particles as surfactants - similarities and differences. *Curr Opin Colloid Interface Sci* 7(1–2):21–41
38. Dinsmore AD, Hsu MF, Nikolaides MG et al (2002) Colloidosomes: selectively permeable capsules composed of colloidal particles. *Science* 298(5595):1006–1009
39. Horozov TS, Binks BP (2006) Particle-stabilized emulsions: a bilayer or a bridging monolayer? *Angew Chem Int Ed.* 45(5):773–776
40. Hsu MF, Nikolaides MG, Dinsmore AD et al (2005) Self-assembled shells composed of colloidal particles: fabrication and characterization. *Langmuir* 21(7):2963–2970
41. Johnston APR, Cortez C, Angelatos AS et al (2006) Layer-by-layer engineered capsules and their applications. *Curr Opin Colloid Interface Sci* 11(4):203–209
42. Gibbs BF, Kermasha S, Alli I et al (1999) Encapsulation in the food industry: a review. *Int J Food Sci Nutr* 50(3):213–224
43. Park J, Fouche LD, Hammond PT (2005) Multicomponent patterning of layer-by-layer assembled polyelectrolyte/nanoparticle composite thin films with controlled alignment. *Adv Mat* 17(21):2575–2579
44. Nikolic K, Murugesan M, Forshaw M et al (2007) Self-assembly of nanoparticles on the surface of ionic crystals: structural properties. *Surf Sci* 601(13):2730–2734

45. Davies P, Schurr GA, Meenan P et al (1998) Engineered particle surfaces. *Adv Mat* 10(15):1264–1270
46. Niemeyer CM (2001) Nanoparticles, proteins, and nucleic acids: biotechnology meets materials science. *Angew Chem Int Ed* 40(22):4128–4158
47. Davis SA, Breulmann M, Rhodes KH et al (2001) Template-directed assembly using nanoparticle building blocks: a nanotectonic approach to organized materials. *Chem Mater* 13(10):3218–3226
48. Huwiler C, Halter M, Rezwan K et al (2005) Self-assembly of functionalized spherical nanoparticles on chemically patterned microstructures. *Nanotechnology* 16(12):3045–3052
49. Maury PA, Reinhoudt DN, Huskens J (2008) Assembly of nanoparticles on patterned surfaces by noncovalent interactions. *Curr Opin Colloid Interface Sci* 13(1–2):74–80
50. Jana NR (2004) Shape effect in nanoparticle self-assembly. *Angew Chem Int Ed* 43(12):1536–1540
51. Bognolo G (2003) The use of surface-active agents in the preparation and assembly of quantum-sized nanoparticles. *Adv Colloid Interface Sci* 106:169–181
52. Barrero A, Loscertales IG (2007) Micro- and nanoparticles via capillary flows. *Annu Rev Fluid Mech* 39:89–106
53. Hua F, Shi J, Lvov Y et al (2002) Patterning of layer-by-layer self-assembled multiple types of nanoparticle thin films by lithographic technique. *Nano Lett* 2(11):1219–1222
54. Gao JH, Zhang B, Zhang XX et al (2006) Magnetic-dipolar-interaction-induced self-assembly affords wires of hollow nanocrystals of cobalt selenide. *Angew Chem Int Ed*. 45(8): 1220–1223
55. Sayle DC, Feng XD, Ding Y et al (2007) “Simulating synthesis”: ceria nanosphere self-assembly into nanorods and framework architectures. *J Am Chem Soc* 129(25):7924–7935
56. Shi ZT, Pan DY, Zhao SF et al (2006) Self-assembly of ordered silver nanoparticle chains on triblock copolymer templates. *Mod Phys Lett B* 20(20):1261–1266
57. Govor LV, Reiter G, Parisi J et al (2004) Self-assembled nanoparticle deposits formed at the contact line of evaporating micrometer-size droplets. *Phys Rev E* 69(6):061609
58. Govor LV, Reiter G, Bauer GH et al (2004) Nanoparticle ring formation in evaporating micron-size droplets. *Appl Phys Lett* 84(23):4774–4776
59. Tripp SL, Dunin-Borkowski RE, Wei A (2003) Flux closure in self-assembled cobalt nanoparticle rings. *Angew Chem Int Ed* 42(45):5591–5593
60. Haryono A, Binder WH (2006) Controlled arrangement of nanoparticle arrays in block-copolymer domains. *Small* 2(5):600–611
61. Osterloh FE, Martino JS, Hiramatsu H et al (2003) Stringing up the pearls: self-assembly, optical and electronic properties of cdse- and Au-limo<sub>3</sub>se<sub>3</sub> nanoparticle-nanowire composites. *Nano Lett* 3(2):125–129
62. Osterloh FE (2006) Directional superparamagnetism and photoluminescence in clusters of magnetite and cadmium selenide nanoparticles. *Comments Inorg Chem* 27(1–2):41–59
63. Arumugam P, Xu H, Srivastava S et al (2007) ‘Bricks and mortar’ nanoparticle self-assembly using polymers. *Polym Int* 56(4):461–466
64. Kakkassery JJ, Abid JP, Carrara M (2004) Electrochemical and optical properties of two dimensional electrostatic assembly of Au nanocrystals. *Faraday Discuss* 125:157–169
65. Angelatos AS, Radt B, Caruso F (2005) Light-responsive polyelectrolyte/gold nanoparticle microcapsules. *J Phys Chem B* 109(7):3071–3076
66. Angelatos AS, Katagiri K, Caruso F (2006) Bioinspired colloidal systems via layer-by-layer assembly. *Soft Matt* 2(1):18–23
67. Dokoutchaev A, James JT, Koene SC et al (1999) Colloidal metal deposition onto functionalized polystyrene microspheres. *Chem Mater* 11(9):2389–2399
68. De Geest BG, Skirtach AG, De Beer TRM et al (2007) Stimuli-responsive multilayered hybrid nanoparticle/polyelectrolyte capsules. *Macromol Rapid Commun* 28(1):88–95
69. Efros AL, Rosen M (2000) The electronic structure of semiconductor nanocrystals. *Annu Rev Mater Sci* 30:475–521
70. Fukumori Y, Ichikawa H (2006) Nanoparticles for cancer therapy and diagnosis. *Adv Powder Technol* 17(1):1–28

71. Wang WT, Wang YM, Dai ZH et al (2007) Nonlinear optical properties of periodic gold nanoparticle arrays. *Appl Surf Sci* 253(10):4673–4676
72. Zhang H, Edwards EW, Wang DY et al (2006) Directing the self-assembly of nanocrystals beyond colloidal crystallization. *PCCP* 8(28):3288–3299
73. Barsotti RJ, Vahey MD, Wartena R et al (2007) Assembly of metal nanoparticles into nanogaps. *Small* 3(3):488–499
74. Hofman-Caris CHM (1994) Polymers at the surface of oxide nanoparticles. *New J Chem* 18(10):1087–1096
75. Caruso F (2003) Hollow inorganic capsules via colloid-templated layer-by-layer electrostatic assembly. In *Colloid Chem II*, Vol. 227, pp 145–168
76. Capsulation (2009) Turning ideas into reality. <http://www.capsulation.com/en/home.html>
77. Priest C, Quinn A, Postma A et al (2008) Microfluidic polymer multilayer adsorption on liquid crystal droplets for microcapsule synthesis. *Lab Chip* 8(12):2182–2187
78. Tjijto E, Cadwell KD, Quinn JF et al (2006) Tailoring the interfaces between nematic liquid crystal emulsions and aqueous phases via layer-by-layer assembly. *Nano Lett* 6(10):2243–2248
79. Wang Y, Angelatos AS, Caruso F (2008) Template synthesis of nanostructured materials via layer-by-layer assembly. *Chem Mater* 20(3):848–858
80. Murthy VS, Rana RK, Wong MS (2006) Nanoparticle-assembled capsule synthesis: Formation of colloidal polyamine-salt intermediates. *J Phys Chem B* 110(51):25619–25627
81. Yu J, Murthy VS, Rana RK, Wong MS (2006) Synthesis of nanoparticle-assembled tin oxide/polymer microcapsules. *Chem Commun* 10:1097–1099
82. Parth R (1997) Materials synthesis and characterization. In: Perry D (ed) Plenum, New York, pp 1–17
83. Atwood JL, Davies JED, Macnicol DD et al (1996) Templating, self assembly and self-organization. In: Sauvage JP, Hosseini MW (eds) *Comprehensive supramolecular chemistry*, Vol. 35b. Pergamon, Oxford, pp 507–528
84. Cha JN, Bartl MH, Wong MS et al (2003) Microcavity lasing from block peptide hierarchically assembled quantum dot spherical resonators. *Nano Lett* 3(7):907–911
85. McKenna BJ, Birkedal H, Bartl MH et al (2004) Micrometer-sized spherical assemblies of polypeptides and small molecules by acid-base chemistry. *Angew Chem Int Ed* 43(42):5652–5655
86. Yu J, Yaseen MA, Anvari B, Wong MS (2007) Synthesis of near-infrared-absorbing nanoparticle-assembled capsules. *Chem Mater* 19(6):1277–1284
87. Kadali SB, Soutanidis N, Wong MS (2008) Assembling colloidal silica into porous hollow microspheres. *Top Catal* 49:251–258
88. Bagaria HG, Kadali SB, Wong MS (2009) Shell thickness control of nanoparticle/polymer composite microcapsules (unpublished)
89. Toprak MS, McKenna BJ, Mikhaylova M et al (2007) Spontaneous assembly of magnetic microspheres. *Adv Mater* 19(10):1362–1368
90. Toprak MS, McKenna BJ, Waite JH et al (2007) Control of size and permeability of nanocomposite microspheres. *Chem Mater* 19(17):4263–4269
91. Murthy VS, Kadali SB, Wong MS (2009) Polyamine-guided synthesis of anisotropic, multi-compartment microparticles. *ACS Appl Mat Interfaces* 1(3):590–596
92. Tavera EM, Kadali SB, Bagaria HG et al (2009) Experimental and modeling analysis of diffusive release from single-shell microcapsules. *AIChE J* 55(11):2950–2965
93. Pickering SU (1907) Emulsions. *J Chem Soc* 91:2001–2021
94. Binks BP, Whithy CP (2005) Nanoparticle silica-stabilized oil-in-water emulsions: improving emulsion stability. *Colloids Surf A* 253(1–3):105–115
95. Binks BP, Rodrigues JA, Frith WJ (2007) Synergistic interaction in emulsions stabilized by a mixture of silica nanoparticles and cationic surfactant. *Langmuir* 23(7):3626–3636
96. Binks BP, Desforges A, Duff DG (2007) Synergistic stabilization of emulsions by a mixture of surface-active nanoparticles and surfactant. *Langmuir* 23(3):1098–1106
97. Duan HW, Wang DY, Sobal NS et al (2005) Magnetic colloidosomes derived from nanoparticle interfacial self-assembly. *Nano Lett* 5(5):949–952

98. He YJ, Yu XY (2007) Preparation of silica nanoparticle-armored polyaniline microspheres in a Pickering emulsion. *Mater Lett* 61(10):2071–2074
99. Binks BP, Clint JH, Fletcher PDI et al (2006) Growth of gold nanoparticle films driven by the coalescence of particle-stabilized emulsion drops. *Langmuir* 22(9):4100–4103
100. Binks BP, Duncumb B, Murakami R (2007) Effect of pH and salt concentration on the phase inversion of particle-stabilized foams. *Langmuir* 23(18):9143–9146
101. Binks BP, Kirkland M (2002) Interfacial structure of solid-stabilized emulsions studied by scanning electron microscopy. *PCCP* 4(15):3727–3733
102. Binks BP, Rodrigues JA (2007) Double inversion of emulsions by using nanoparticles and a di-chain surfactant. *Angew Chem Int Ed* 46(28):5389–5392
103. Binks BP, Rodrigues JA (2007) Enhanced stabilization of emulsions due to surfactant-induced nanoparticle flocculation. *Langmuir* 23(14):7436–7439
104. Nie YR, Li W, An LJ et al (2006) Fabricating ordered 2D arrays of magnetic rings on patterned self-assembly monolayers via dewetting and thermal decomposition. *Colloids Surf A* 278(1–3):229–234
105. Schacht S, Huo Q, VoigtMartin IG et al (1996) Oil-water interface templating of mesoporous macroscale structures. *Science* 273(5276):768–771
106. Madou M (1998) *Fundamentals of microfabrication*. CRC, Boca Raton
107. Cui TH, Hua F, Lvov Y (2004) Lithographic approach to pattern multiple nanoparticle thin films prepared by layer-by-layer self-assembly for microsystems. *Sens Actuators A* 14(2–3):501–504
108. Choi DG, Jang SG, Kim S et al (2006) Multifaceted and nanobored particle arrays sculpted using colloidal lithography. *Adv Funct Mater* 16(1):33–40
109. Barry CR, Lwin NZ, Zheng W et al (2003) Printing nanoparticle building blocks from the gas phase using nanoxerography. *Appl Phys Lett* 83(26):5527–5529
110. Barry CR, Steward MG, Lwin NZ et al (2003) Printing nanoparticles from the liquid and gas phases using nanoxerography. *Nanotechnology* 14(10):1057–1063
111. Zharov VP, Galitovskaya EN, Johnson C et al (2005) Synergistic enhancement of selective nanophotothermolysis with gold nanoclusters: potential for cancer therapy. *Laser Surg Med* 37(3):219–226
112. Choi WS, Koo HY, Park JH et al (2005) Synthesis of two types of nanoparticles in poly-electrolyte capsule nanoreactors and their dual functionality. *J Am Chem Soc* 127(46):16136–16142
113. Perro A, Reculosa S, Ravaine S et al (2005) Design and synthesis of Janus micro and nanoparticles. *J Mater Chem* 15(35–36):3745–3760
114. Kickhoefer VA, Garcia Y, Mikiyas Y et al (2005) Engineering of vault nanocapsules with enzymatic and fluorescent properties. *Proc Natl Acad Sci* 102(12):4348–4352

# Polymersomes: A Synthetic Biological Approach to Encapsulation and Delivery

Marzia Massignani, Hannah Lomas, and Giuseppe Battaglia

**Abstract** Compartmentalization, i.e. the ability to create controlled volumes and separate molecules one from another is possibly the most important requisite for complex manipulations. Indeed, compartmentalization has been the first step to isolate the building blocks of life and ensure the dynamic nature that today makes the complexity of any living system. For decades scientists have tried using many synthetic approaches to imitate such ability and one the most successful comes from mimicking the biological component responsible for the compartmentalization: the phospholipid. We are now able to synthesize macromolecular analogues of the phospholipid using advanced co-polymerization techniques. Copolymers that comprise hydrophilic and hydrophobic components (i.e. amphiphilic) can be designed to self assemble into membrane enclosed structures. The simplest of those is represented by a sac resulting from the enclosure of a membrane into a sphere: the vesicle. Vesicles made of amphiphilic copolymers are commonly known as polymersomes and are now one of the most important nanotechnological tool for many applications spanning from drug delivery, gene therapy, medical imaging, electronics and nanoreactors. Herein we review the molecular properties, the fabrication processes and the most important applications of polymersomes.

**Keywords** Encapsulation · Membrane · Polymersomes

---

M. Massignani, H. Lomas, and G. Battaglia (✉)  
Department of Biomedical Science, The University of Sheffield,  
Western Bank, S10 2TN, Sheffield, UK  
e-mail: [g.battaglia@sheffield.co.uk](mailto:g.battaglia@sheffield.co.uk)

M. Massignani and H. Lomas  
Department of Engineering Materials, The Kroto Research Institute,  
The University of Sheffield, S3 7HQ, Sheffield, UK

## Contents

1	Introduction .....	116
2	Polymersomes Formulations .....	117
2.1	The Membrane Conformation .....	117
2.2	Responsive Polymersomes .....	129
2.3	Polymersomes Surface Chemistry .....	131
3	Polymersomes Preparation .....	133
3.1	Polymersome Formation Kinetics .....	133
3.2	Solvent Free Methods .....	135
3.3	Organic Solvent Based Methods .....	136
3.4	Size Control .....	136
4	Polymersome Loading .....	138
4.1	Hydrophobic Molecules Encapsulation .....	138
4.2	Amphiphilic Molecules Encapsulation .....	139
4.3	Hydrophilic Molecules Encapsulation .....	139
5	Polymersomes Applications .....	141
6	Conclusions .....	146
	References .....	147

## 1 Introduction

The chemical and physical transformation of molecules and macromolecules such as proteins, nucleic acids, carbohydrates, lipids, etc. are the central dogma of life. All the transformations need to take place in highly organised compartments. Biological compartmentalization is achieved by exploiting the formation of membranes with thickness of few nanometres that enclose aqueous environments in structures whose size varies from a few tens of nanometres (e.g. trafficking vesicles) up to even metres (e.g. motoneuron plasma membranes) [1]. These membranes result from the self-assembly of amphiphilic molecules known as phospholipids. Amphiphiles have a dual nature that comprises both hydrophilic (water soluble) parts and hydrophobic (water insoluble) parts. In the presence of water the hydrophobic parts tend to minimize the contact with water, attracting each other, while the hydrophilic parts prefer contact with water and repel each other. The membrane assembly is clearly the perfect building block for generating confined aqueous compartments. Indeed, this two-dimensional structure increases the efficiency considerably and opens up the opportunity for irreversible charge separation and transitory storage of energy in the form of chemical potential gradients [1]. Certainly, this modular design has been a crucial evolutionary step to produce some order within the cell and to control such a complex machine [2]. Numerous different molecules are distributed among the organized cellular subspaces. The differences in concentration and composition between the sub-cellular compartments generate a composition and concentration gradient vital for the directed flow of freshly synthesized material from one intracellular organelle to other organelles or to the plasma membrane.

The extraordinary ability of nature to engineer functional and dynamic supramolecular structures with tuneable size has been mimicked by synthetic

amphiphiles. In particular, recent new advances in controlled polymerisation techniques [3,4] have allowed the design of a new class of amphiphilic membranes based on block copolymers. Block copolymers are macromolecules comprising two or more different polymers (see Table 1). The combination of different polymer backbones gives a range of properties defined by the designed molecules. Polymeric amphiphiles can be considered as “super” amphiphiles as they have molecular weights up to several orders of magnitude higher than phospholipids. As a consequence of such macromolecular nature [5] they are able to self-assemble into highly entangled membranes providing the final structure with improved mechanical properties [6] and stability compared to membrane based on phospholipids. The simplest structure that membranes can form is a core shell sphere known as vesicle or “polymersome” (“some” from Greek “body of”). Polymersomes can be formed with sizes ranging from tens of nanometres to tens of micrometres with relatively high control on the size distribution. This flexibility has attracted the attention of several scientists and engineers in studying polymersomes for different applications from biomedical devices to electronics.

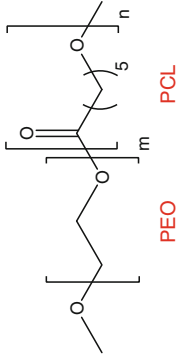
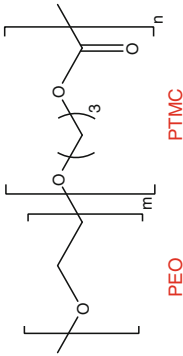
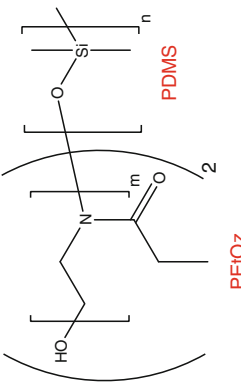
## 2 Polymersomes Formulations

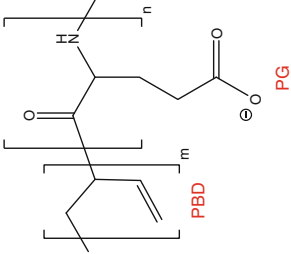
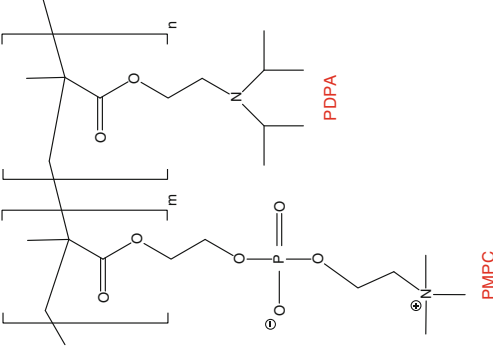
### 2.1 *The Membrane Conformation*

The synthetic nature of block copolymers allows the application of different compositions and functionalities over a limitless range of molecular weights and consequently of membrane thickness [5]. Polymersome membranes comprise a highly entangled hydrophobic layer with thickness  $t$ , and two hydrophilic polymer brushes, with thickness  $d$ , that stabilize the membrane (Fig. 1). We have recently calculated [7] the electron density distribution of polyethylene oxide based polymersomes combining small angle X-ray scattering (Fig. 1) and electron microscopy (Fig. 1) and it has been proved that hydrophilic brush and membrane have similar sizes. As shown in Fig. 1, while the hydrophilic brush thickness scales almost linearly with the copolymer molecular weight [7], typical of dense polymer brushes in solution [8,9], the hydrophobic membrane follows a power law with exponent smaller than the unity [5,10], typical of bulk strongly segregated systems [11]. Different studies contributed to highlight that high molecular weights are related to thicker membranes; in particular, polymersomes membrane thickness,  $t$ , ranges approximately between 2 and 50 nm [6,12–15], whilst lipid membranes present  $t \approx 3\text{--}5\text{ nm}$  [16]. The power law  $t \sim M_w^b$  has been proved both experimentally and theoretically to be applicable for relating amphiphiles molecular weight to the membrane thickness [5,10,17–22]. According to the block copolymer theory [23] the two boundary conditions for the exponent are  $b = 1$  for fully stretched [5] and  $b = 1/2$  for random Gaussian coil conformation [12,22]. The former case is the theoretical limit approached by phospholipids, whilst the latter is known as “weak segregation” in block copolymer melts. In the intermediate condition, as in the polymersomes



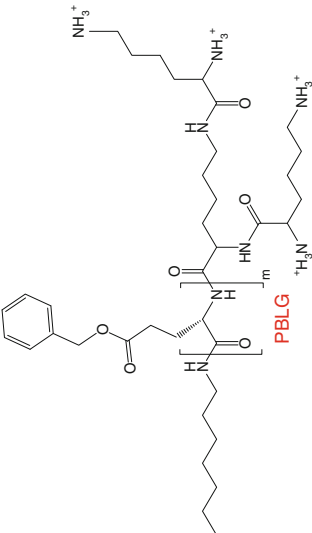
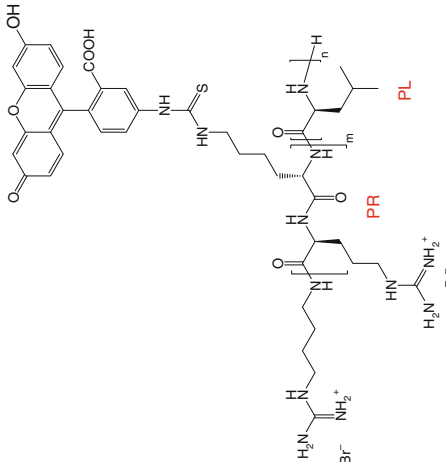
**Table 1** Chemical structure of polymeric block copolymers

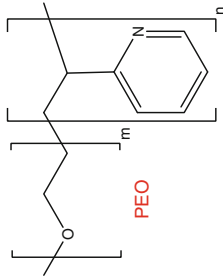
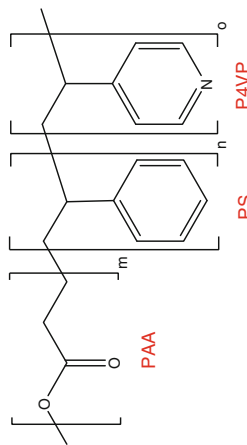
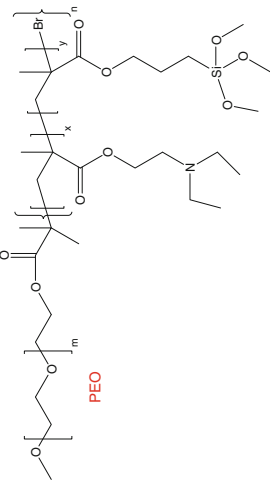
Copolymer		Properties	Applications
Poly(ethylene oxide)- Polycaprolactone		Biodegradability, slow release kinetics <sup>1,5</sup>	Anticancer drug delivery, delivery to the CNS
		Biodegradability, temperature-sensitivity <sup>1,5</sup>	<i>In situ</i> gel production for drug delivery/ tissue engineering
Poly(2-ethyl-2-oxazoline)- poly (dimethylsiloxane)- poly(2-ethyl-2-oxazoline)		Ability to incorporate membrane proteins within polymersomal membrane <sup>27</sup>	“Artificial cell”, nanoreactor

Polybutadiene-(poly-L-glutamate)		pH-sensitivity, ability to undergo helix-coil transitions without affecting polymersome morphology <sup>16</sup>	None reported
Poly(2-methacryloxyethyl phosphorylcholine)-poly(2-(diisopropylamino) ethyl methacrylate)		pH-sensitivity <sup>17</sup>	Gene and drug delivery

(continued)

Table 1 (continued)

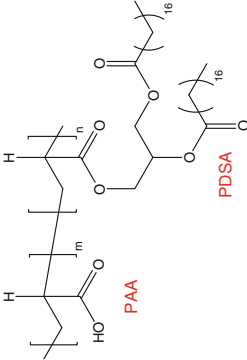
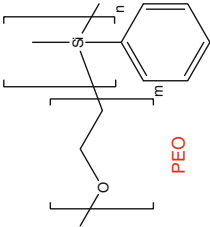
Copolymer	Properties	Applications
<div><p>Poly(<math>\gamma</math>-benzyl-L-glutamate)-poly(L-lysine)</p></div>	<p>Dendrimer, <math>\alpha</math>-helical conformation<sup>35</sup></p>	<p>Modelling of proteins tertiary structures</p>
<div><p>Poly(L-arginine)-poly(L-leucine)</p></div>	<p>pH sensitivity<sup>18</sup></p>	<p>Drug delivery</p>

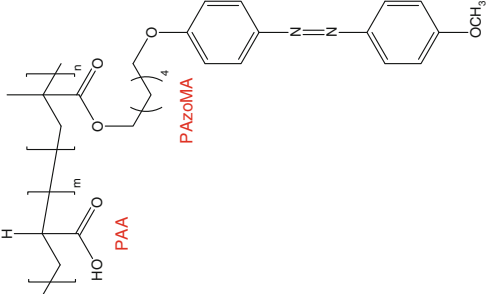
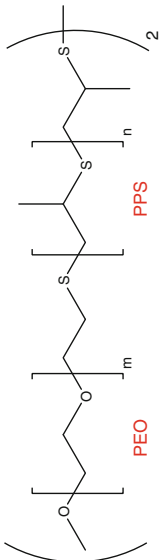
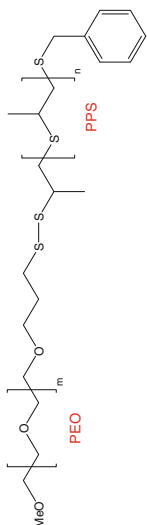
Poly(2-vinylpyridine)-poly(ethylene oxide)		pH sensitivity <sup>19</sup>	Controlled release
Poly(acrylic acid)-polystyrene-poly(4-vinyl pyridine)		pH-dependent vesicle surface chemistry <sup>20</sup>	None reported
Poly(ethylene oxide)-poly(2-(diethylamino)ethyl methacrylate- <i>stat</i> -3-(trimethoxysilyl) propyl methacrylate)		pH-tunable membrane permeability, self-cross-linkability <sup>21</sup>	Support for precious metal catalyst

P(DEA-*stat*-TMSPMA)

(continued)

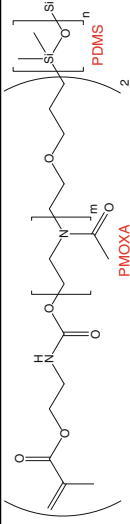
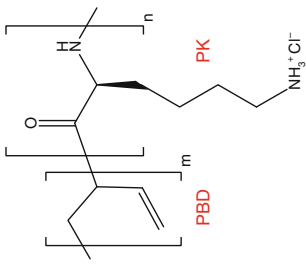
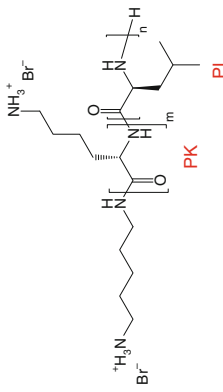
Table 1 (continued)

Copolymer	Properties	Applications
<div><p>Poly(acrylic acid)-poly(distearin acrylate)</p></div>	pH-tunable membrane permeability, generation of multivesicle assemblies <sup>22</sup>	Controlled release, model for eukaryotic cells and their internal organelles
<div><p>Poly(ethylene oxide)-poly(methylphenylsilane)</p></div>	Sensitivity to UV light <sup>23</sup>	None reported

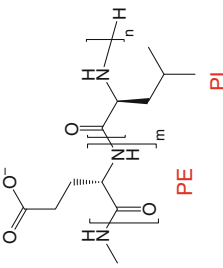
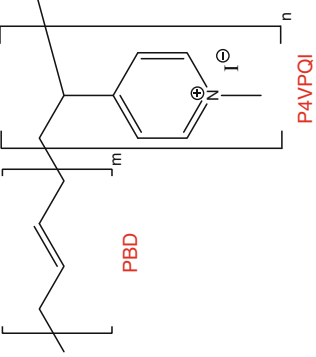
Azobenzene-containing poly(methacrylate)- poly(acrylic acid)		Sensitivity to UV light <sup>23</sup>	None reported
Poly(ethylene oxide)-poly(propylene sulphide)		Sensitivity to oxidation <sup>24</sup>	Oxidative species and glucose sensitive delivery
Poly(ethylene oxide)- SS-poly(propylene sulphide)		Sensitivity to reduction <sup>25</sup>	Drug delivery

(continued)

Table 1 (continued)

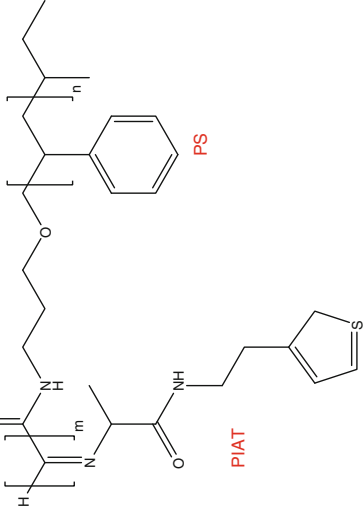
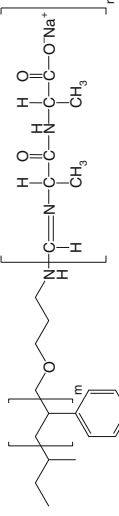
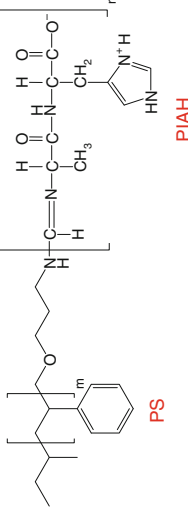
Copolymer	Properties	Applications
Poly(2-methyloxazoline)-poly(dimethylsiloxane)-poly(2-methyloxazoline)	 Ability to incorporate membrane proteins within polymersomal membrane <sup>26</sup>	Nanoreactor
Poly(butadiene)-poly(L-lysine)	 Helical morphologies copolymer blocks <sup>32–34</sup>	Drug delivery
Poly(L-lysine)-poly(L-leucine)	 Controllable vesicle diameter, degradability <sup>29</sup>	Mimicking tertiary structures of proteins



<p>Poly(L-glutamic acid)-poly(L-leucine)</p>		<p>Controllable vesicle diameter, degradability, stability in presence of serum proteins<sup>29</sup></p>	<p>None reported</p>
<p>Poly(butadiene)-poly(N-methyl-4-vinylpyridinium iodide)</p>		<p>Polymersomes formation through using a “single emulsion technique”<sup>30</sup></p>	<p>DNA delivery</p>

(continued)

Table 1 (continued)

Copolymer	Properties	Applications
	Selective permeability <sup>28</sup>	Nanoreactor
Polystyrene-poly(L-isocyanoalanine (2-thiophen-3-ylethyl)amide)		None reported
Polystyrene-poly(isocyano-L-alanine-L-alanine)		None reported
Polystyrene-poly(isocyano-L-alanine-L-histidine)		None reported

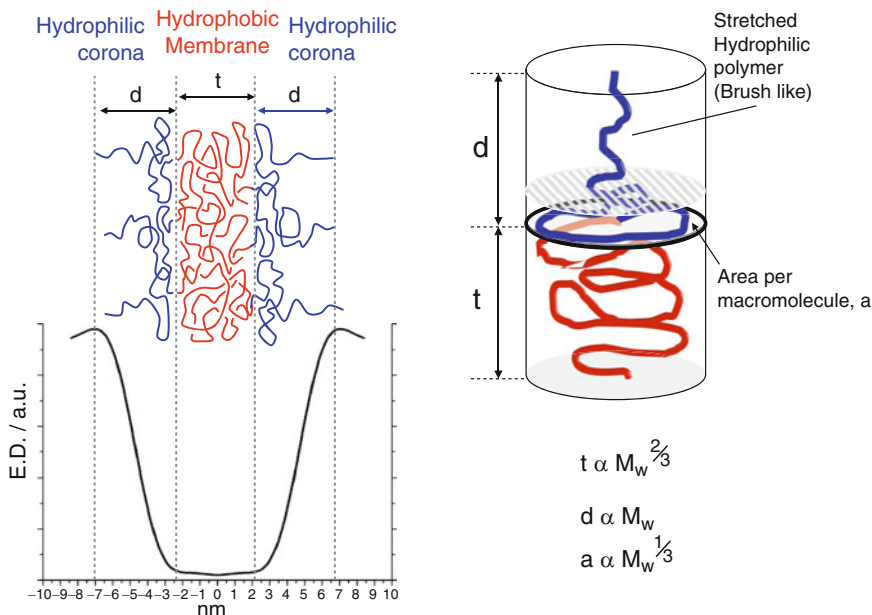


**Fig. 1** Electron density profile for a polymersome membrane calculated from SAXS and cartoon to schematize the conformation of the hydrophobic and hydrophilic blocks. Scaling relations for the hydrophobic membrane,  $t$ , the hydrophilic corona thickness,  $d$ , and the area per molecule,  $a$ , as a function of the copolymer molecular weight

case, the exponent was found to be  $b = 2/3$  [5, 10, 23]. That is the result of the “interdigitation” of hydrophobic copolymer chains that has been demonstrated to occur at the bilayer midplane also computationally [23]. Elastic bending, stretching and shear of polymersomes have been measured by micropipette aspiration and compared to liposomes corresponding values; both liposomes and polymersomes present similar elastic properties but the latter are able to undergo higher tension and area strain before rupture [6, 15, 17, 24, 25]; in fact the low thickness makes liposomes more susceptible to defects and fluctuations with respect to polymersomes [26].

It is possible to prepare diblock, triblock, multiblock, random block, star and graft copolymers simply by controlling their synthesis [7]. Such diversity of chemical architecture can be exploited for the design of different polymersomes membranes with diverse degree of entanglements and sub-structures. Figure 2 emphasizes the potential bilayer assembly depending on the molecular architecture of the copolymer utilized.

Polymersomes generated from simple AB block copolymers display interdigitated membrane. The robust entanglement within the hydrophobic layer can be considered as a physical cross-link able to enhance the mechanical properties of those aggregates compared to liposomes [5]. Tri-block (BAB) hydrophobic–hydrophilic–hydrophobic copolymers are similar to diblock copolymers since there

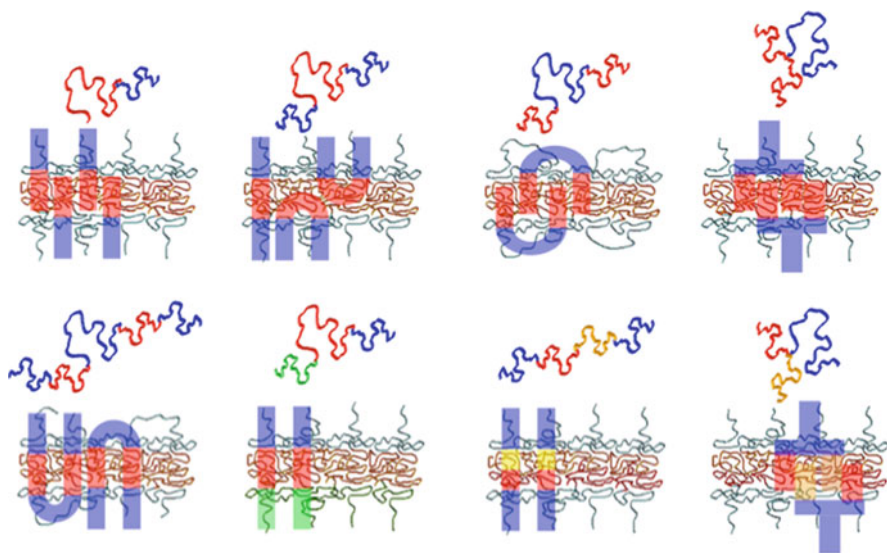


**Fig. 2** Membrane conformation of polymersomes formed by diblock (AB), triblock (ABA, BAB, ABC), multiblock copolymers and milk-to-arm copolymers

is only one molecular conformation that can lead to membrane formation: the hydrophobic chain ends must assemble into a membrane and the hydrophilic block must form a loop (U-shape). No looping is allowed in BAB block copolymers where two hydrophobic blocks B are attached to the same end of the hydrophilic block A. This molecular architecture known as star-copolymer or milk-to-arm copolymer reassembles the double tailed conformation of the phospholipid [27]. In contrast, hydrophilic–hydrophobic–hydrophilic copolymers (ABA) can have two possible conformations: the hydrophobic block can either form a loop so as the hydrophilic chains are on the same side of the membrane (U-shape) or they can stretch forming a monolayer with the two hydrophilic blocks at the opposite sides of the membrane (I-shape) [28–32]. Similar conformation can be formed by pentablock copolymers [33].

The membrane conformation can be further engineered employing multiblocks that contain different polymers undergoing phase separation after assembly. Several studies have already demonstrated that ABC copolymers, where A and C are hydrophilic and B is hydrophobic, assemble into asymmetric “Janus” (as the double-faced Roman god) particles [34]. When the hydrophobic/hydrophilic ratio is such as to favour the membrane formation, ABC copolymers assemble into asymmetric membranes [31,35,36] that form polymersomes whose internal and external surface chemistry are different from one another in order to minimise interfacial tension and enhance vesicle curvature. Studies suggest that hydrophobic block B tends to form bridges across the membrane increasing their molecular weight [5]. Moreover, it was observed that the relative sizes of the hydrophilic blocks A and C controlled

their final location of the two coronas (i.e. internal or external lumen) [31, 36]. ABC star polymers where B and C block are both hydrophobic have been used to generate membranes with an internal nanoscopic structure whose morphology is controlled by the interaction between B and C [37, 38]. Similarly, level of control was demonstrated by Brannan et al. [39] using ABCA tetrablock copolymers, where A is hydrophilic and B and C are both hydrophobic. The multi-block copolymers assemble into vesicles whose membrane has an internal morphology that changes from lamellae to cylinders changing the volume fraction between B and C.

## 2.2 *Responsive Polymersomes*

One of the advantages of polymers compared to their smaller molecular weight counterparts is that the polymer solution properties are strictly controlled by the side group chemistry. The same polymeric chain can comprise soluble and insoluble parts and their balance dictates the overall solubility. Therefore polymer solubility can be altered by external stimuli such as temperature, pH, ionic strength, light, etc. This approach has been largely exploited in polymer engineering and several devices based on polymer solubility have been devised [40]. When it comes to polymersomes these properties can be utilised to generate structures able to dissolve under certain environmental conditions.

The simplest approach has been achieved by coupling hydrophilic polymers with hydrolysable polymers such as poly(lactic acid) [41–44] or poly( $\epsilon$ -caprolactone). In proximity to water these polymers will degrade leading to a non-reversible disassembling of polymersome and hence the release of its content. The ability to degrade after a definite time or upon stimuli seems to be critical for the design of new carriers as well as controllable vesicle diameter. Those needs are satisfied by amphiphilic polypeptide like poly(L-lysine)-poly(L-leucine) (PK-PL) and poly(L-glutamic acid)-poly(L-leucine) (PE-PL) [45]. Similarly, non-reversible transitions can be achieved using block copolymers based on poly(propylene sulfide) (PPS) as the hydrophobic block [32, 46]. In this case the change in the hydrophilic/hydrophobic balance is due to the oxidation of PPS into more hydrophilic sulfoxides and sulfones upon exposure to oxidative environments, such as  $H_2O_2$ , leading first to the transition of vesicles to cylindrical micelles, spherical micelles and eventually into non-associating unimers. Such an approach in combination with specific enzymes opens new perspectives in the field of biosensors for the detection of molecules of interest (such as glucose, inflammatory signals, etc). An alternative approach to oxidation sensitive polymersomes was reported by Cerritelli et al. [47] who have synthesized block copolymers comprising the hydrophilic poly(ethylene oxide) (PEO) and the hydrophobic poly(propylene sulfide) (PPS) linked via a disulfide bond. Copolymers that contain sulfur–sulfur bonds are receiving more attention in recent research due to the strong preference for block copolymer delivery vectors to be biodegradable [41, 48]. Such vectors are chemically stable in the bloodstream, but their reductive degradation is triggered within cells due to the presence

of glutathione (GSH), which can reduce sulfur–sulfur bonds. This is in contrast to copolymers which are sensitive to hydrolysis, for examples polyesters and polycarbonates, whereby degradation occurs slowly and is not exclusive to intracellular environments [41, 47, 48].

Reversible disassembling can be obtained by combining hydrophilic polymers with polymers having solubility strongly dependent on pH, temperature and UV light. For example, pH-responsive polymersomes based on poly(L-glutamic acid)-poly(L-lysine) have been reported [49] that can be reversibly formed in weak acidic or basic aqueous solutions. Armes and co-workers [50] showed the spontaneous formation of biocompatible vesicles when the pH of the solution is increased from 2 to over 6 using a diblock copolymer made of poly(2-(methacryloyloxy)ethyl phosphorylcholine) (PMPC), a hydrophilic and highly biocompatible block, and poly(2-(diisopropylamino)ethyl methacrylate) (PDPA), a hydrophobic block able to be protonated. The protonation of the PDPA bit at pHs lower than its  $pK_a$  value turns the polymer into hydrophilic, leading to the dissolution of the vesicles [51]. Similarly, poly(2-vinylpyridine-*b*-ethylene oxide) (P2VP-PEO) block copolymer vesicles have been reported [52] to undergo similar transition at pH around 5. Similar responsiveness can be obtained by having the hydrophilic block such as weak polyacids and polybases that change their macromolecular conformation as a function of pH. As the acid or the basic groups get protonated and deprotonated the polyelectrolyte undergo transitions from hypercoiled to stretched configuration [53]. When attached to a hydrophobic block this transition changes the assembly properties resulting in the formation of vesicles and micelles depending on the pH of the solution [54–56, 150]. Similar transitions have been observed as a function of temperature using poly[*N*-(3-aminopropyl)-methacrylamide hydrochloride]-poly(*N*-isopropylacrylamide) (PAPMA-PNIPAM) diblock copolymers. McCormick and co-worker [37] obtained vesicles reversibly forming at temperatures higher than the lower critical solution temperature of the pure PNIPAM block. Similar approach was used using PEO-PNIPAM temperature responsive polymersomes [57]. Rank and co-workers have also shown that temperature can be exploited to trigger the transition from micelles to vesicles [58]. Polymersomes from PEO-poly(2-vinyl pyridine) (PEO-P2VP) block copolymers, were reversibly converted into cylindrical micelles when the temperature was lowered to 4 °C [58]. This temperature-sensitive behaviour was attributed to the effect of temperature on PEO solubility in polar solvents. PEO water solubility decreases as the temperature is raised, resulting in decreased penetration of water into the PEO brush.

Finally similar transition can be induced by using UV-sensitive groups such as poly(ethylene oxide)-poly(methylphenylsilane) (PEO-PMPS) and azobenzene-containing poly(methacrylate)-poly(acrylic acid) (PAA-PAzoMA) [59]. More recently Mabrouk et al. [60] have shown an asymmetric polymersomes whose membrane has only one leaflet composed of UV-sensitive liquid-crystalline copolymer Poly(ethylene glycol)-poly(4-butyloxy-2-(4-(methacryloyloxy)butyloxy)-4-(4-butyloxybenzoyloxy)azobenzene) (PEG-*b*-PMAazo444). Once exposed to UV light these polymersome burst due to changes in the spontaneous curvature of the membrane.

## 2.3 *Polymersomes Surface Chemistry*

Polymersomes membrane is the result of the self-assembly in water of amphiphilic block copolymers and, as discussed above, almost any chemistry can be used provided the necessary hydrophilic/hydrophobic conditions for the assembly are maintained. As discussed in detail in Sect. 2.1, the hydrophilic blocks assemble into a dense brush configuration, that, depending on the polymer nature (i.e. cationic, anionic, or neutral), will control the surface characteristics of the polymersome and hence its interaction with the environment. For example, PEO containing block copolymers assemble into polymersomes with a highly hydrated and yet neutral polymer brush [61] which has very limited interaction with proteins [62, 63]. Such non-fouling nature allowed the PEO-polymersomes to withstand biological fluids almost without interacting with the immune system [64]. The ability to “hide” from the immune system known as “stealth” has been largely exploited for enhancing the circulation life time of liposomes and other nanoparticles [65, 66]. The brush thickness and conformation is crucial for the stealthiness of polymersomes, as already demonstrated by Photos et al. that found different circulation times for different molecular weight PEO polymersomes [67]. PEG and other non-fouling polymers are highly desirable for applications involving extended time in contact with biological fluids. The translation of these design principles can help significantly the synthesis of many ad hoc chemistries for new specific applications [68]. In addition we have recently demonstrated that polymersomes surface can be further modified introducing domains of different chemistry. This can be achieved by mixing different polymersome forming copolymers so as to induce polymersome-confined polymer-polymer phase separation. As shown in Fig. 3a–e, different surface topology can be identified as a function of the PMPC-PDPA/PEG-PDPA ratio [69]. Furthermore, studies on polymersomes phase separation (Fig. 3f) have been recently carried out by Discher and colleagues on PAA-PBD/PEO-PBD copolymers couples [70]. Here the ability of phase separation has also been combined with the responsive nature of the PAA showing ion and pH induced transitions from patchy polymersomes to patchy micelles.

On a second level of complexity, polymersomes surfaces can be decorated with active moieties such as proteins, antibodies, vitamins, carbohydrates, etc. (Fig. 4). One of the simplest methods to decorate polymersomes is by exploiting biotin avidin complex [71]. The linkage of biotin moieties to the hydrophilic block of the copolymer is used to attach avidin groups to pre-formed polymersomes, which in turn can bind to biotinylated targeting ligands, as each avidin group has four binding sites for biotin [72–74]. Broz et al. have taken advantage of biotin–avidin chemistry to attach polyG, specific to the scavenger receptor A1 (SRA1) of macrophage cells to polymersomes formed from an “ABA” PMOXA-PDMS-PMOXA triblock copolymer [72]. Using a similar approach, polymersomes conjugated with anti-ICAM-1 antibody were tested to treat endothelial cells undergoing inflammation. In those cells the molecules ICAM-1 is over expressed during intracellular adhesion. This work highlights the importance of tag-orientation on polymersomes surface [73]. Other conjugation strategies have been performed coupling thiolated antibodies

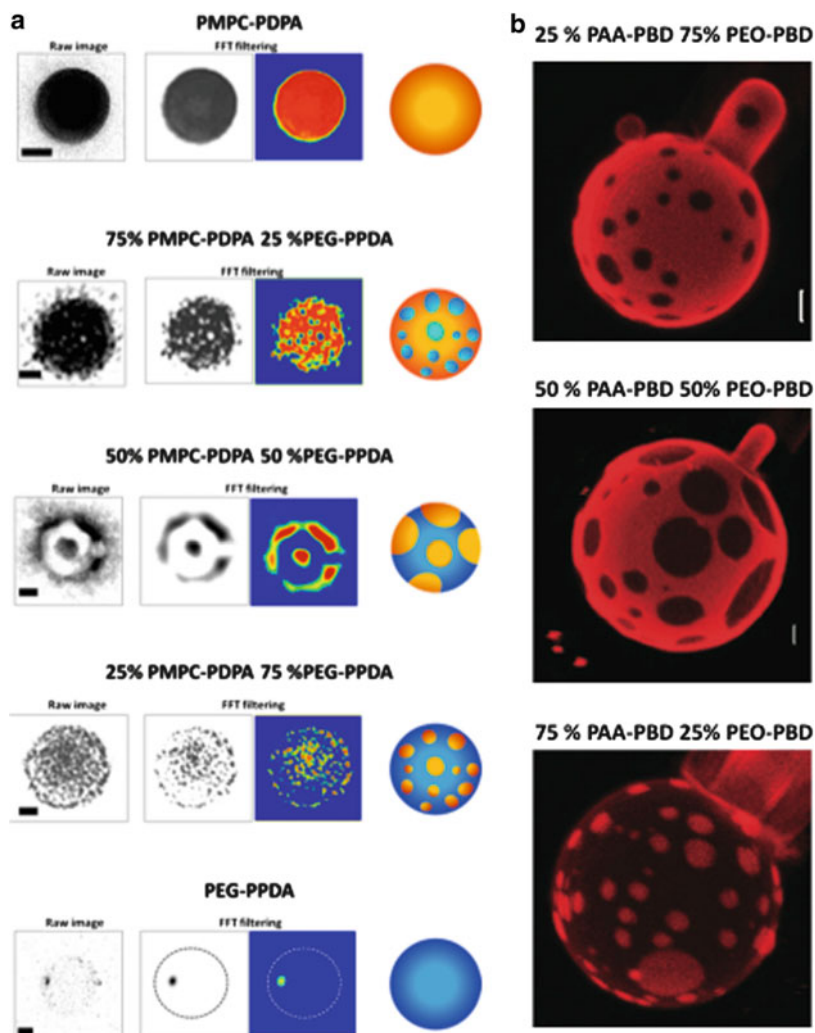


**Fig. 3** (a) Nanometer-sized polymersomes imaged by transmission electron microscopy (TEM) and analysed using fast fourier transform (FFT) filtering. Phase segregation generated by binary different ratio mixtures of PMPC-PDPA and PEG-PDPA copolymers forming patchy polymersomes that displays surface domains highlighted by selective staining of the PMPC chain by phosphotugstenic acid (selective for ester groups). Scale bar = 50 nm [69]. (b) Micrometer-sized polymersomes phase separation at the generated by mixing different ratio of PEO-PBD and PAA-PBD copolymers and imaged by confocal microscopy during micropipette aspiration. The red fluorescence is from the tetraethyl rhodamine-5 carbonyl azide chemically conjugated to the PEO-PBD copolymer. Scale bar = 2  $\mu$ m [70]

with maleimide functionalised PEO-poly(caprolactame) copolymers [75]. These antibody functionalised polymersomes were shown to target the OX21 receptor expressed on the blood brain barrier facilitating the delivery of therapeutic peptides



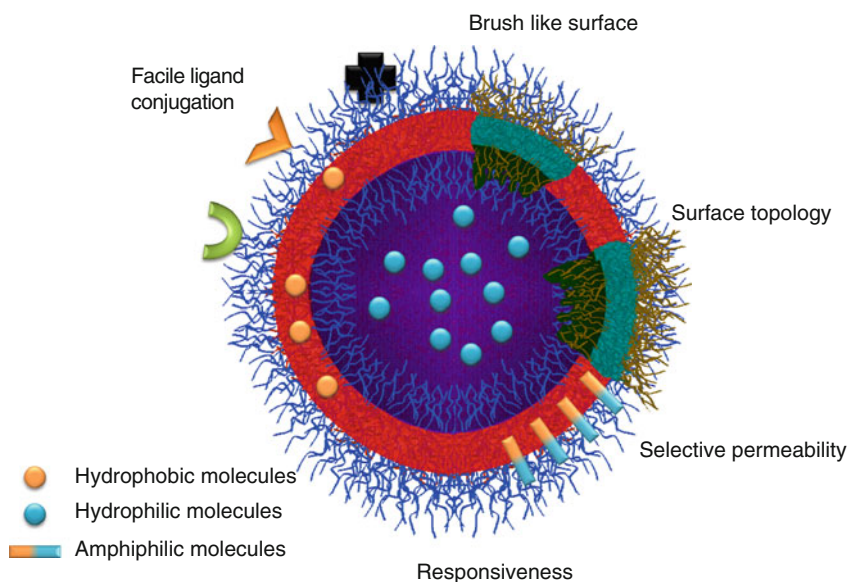


**Fig. 4** Scheme of responsive polymersome with its properties

within the brain [75]. A similar chemical approach was used by Christian et al. to functionalize polymersomes with cell permeable peptide, TAT to enhance cellular uptake [76].

Upadhyay et al. have also show that the targeting moiety can be engineered so as to act as hydrophilic block of the copolymer. They synthesized hyaluronan-*b*-poly( $\gamma$ -benzyl-L-glutamate) copolymer exploiting the hyaluronan ability to target type 1 transmembrane glycoprotein CD44 upregulated in certain tumours [77].

### 3 Polymersomes Preparation

#### 3.1 Polymersome Formation Kinetics

Polymersome forming block copolymers, like any other amphiphiles [151], assemble into lyotropic phases with liquid crystalline nature such as inverse hexagonal structures, lamellae, hexagonal perforated membranes, sponge phases, etc. [78–81]. The details of the phase diagram can be found in Fig. 5, where the morphology formed is plotted as a function of the molecular weight and concentration in water [78]. The size of the amphiphile significantly affects both the formation of lyotropic phases and dispersed vesicles. The evolution from the bulk solid to lyotropic liquid shows that the low molecular weight copolymer assembles first into an inverted hexagonal structure and then lamellae, whereas the high molecular weight dissolves

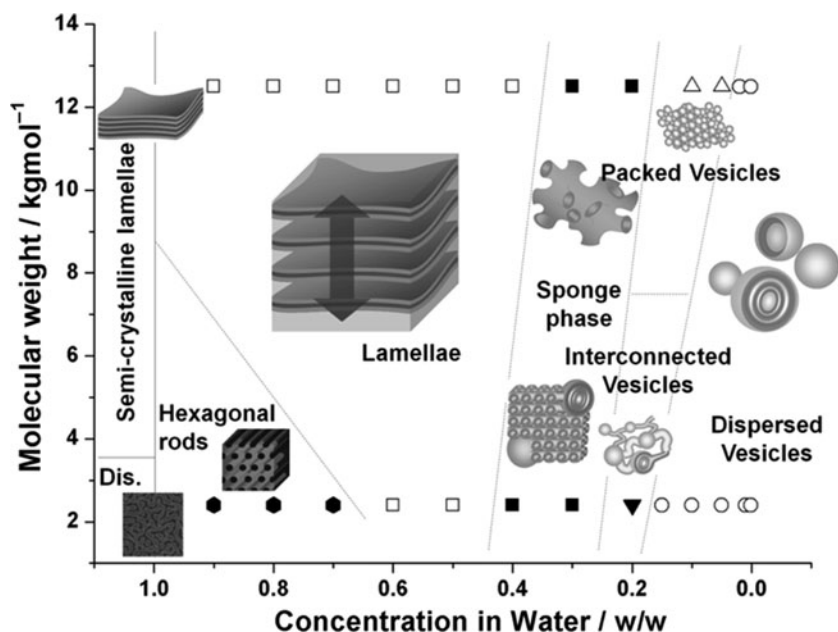


Fig. 5 Isothermal phase diagrams of PEO-PBO copolymers/water [78]

directly to the lamellar phase. The transition from lamellae to the sponge phase is essentially unaffected by the molecular weight of the amphiphiles. In contrast, the evolution of the sponge phase into vesicles is qualitatively different depending on the size of the amphiphilic block copolymer. Smaller copolymers form dispersed vesicles at quite high concentrations, whereas high molecular weight copolymers initially form vesicular gel clusters, which eventually break up into dispersed vesicles. The amphiphile molecular weight affects also the nature of the vesicles formed, the larger amphiphiles forming exclusively unilamellar vesicles on dilution and the smaller copolymers giving rise to multilamellar vesicles.

The molecular weight of the copolymers not only affects the phase transition but it has a quite substantial effect on the kinetics from one phase to the other. Indeed one of the most interesting characteristics of block copolymer assemblies is their no-ergodic nature [82, 152]. This means that there is almost no exchange between micelle and/or vesicles and the bulk solution, indicating a critical aggregation concentration close to zero [83]. This is a quite desirable property for polymersome and accounts for the long shelf life observed [5, 51]. Yet the lack of unimers in solution complicates the phase transition from high to low concentrations, permitting only the route through the copolymer rearrangement within the aggregate and water diffusion. As evident in Fig. 5, the polymersome-forming copolymer phase diagram is dominated by a lamellar phase. As the water content increases this swells up to a point where it undergoes a complete and drastic unbinding. The amphiphilic membranes therefore require all the time necessary to evolve into the most stable

structure. We have shown that the polymersomes forming block copolymers swell in water according to two qualitatively different regimes [84]. Initially, water and copolymer diffuse into each other following a sub-diffusional regime as a result of the molecular-level arrangement of the amphiphilic membranes. After a critical time, which changes exponentially with the polymer molecular weight, the amphiphilic membranes reach their equilibrium morphology and, consequently, the growth starts to follow a more typical Fickian diffusion. Such complex kinetics would explain why polymersomes started to be studied much later than copolymer micelles. Quite likely most of the polymersomes forming copolymers were simply discarded as water-insoluble.

### 3.2 *Solvent Free Methods*

Upon hydration of the copolymer the driving force for polymersome formation is the concentration gradient between the copolymer front, diffusing in water, and the water front, diffusing in the copolymer. Under simple hydration the concentration gradient decreases almost linearly with time. As the concentration gradient changes, the lamellar structures may not have sufficient time to unbind completely [84]. In order to ensure the mutual diffusion and hence to keep the concentration gradient constant, an external energy source needs to be applied [85]. The most common method used for polymersome formation, film hydration, overcomes this kinetical barrier by hydration of pre-casted thin copolymer film under mechanical stirring. [5, 6, 39, 86, 87]. Typically this method produces polymersome suspensions with large size distribution and often with large quantities of other metastable phases [88]. An alternative method was proposed by adapting the electroformation of liposomes originally proposed by Angelova et al. [89] which is based on the hydration of the amphiphilic film under an a.c. electrical field that enhances water diffusion across the bulk copolymer [5, 51, 84, 86]. This method, although guaranteeing almost exclusively the formation of unilamellar polymersomes, does not allow high volume production and is mostly relegated as an experimental tool. Recently we have reported a method for the production of controlled size distributions of micrometre-sized vesicles combining photolithography with bulk phase dewetting. This enables the spontaneous creation of unilamellar polymersomes with a narrow size distribution controlled by the pre-patterned substrate [90]. An alternative direct rehydration process was recently proposed by O'Neil and co-workers [91]. They showed an effective polymersome formation by speeding up the formation of sponge phase at high temperatures. This is then stirred and left cooling down at room temperature while a solution containing another polymer soluble both in the hydrophilic phase of the diblock and in the aqueous environment is added dropwise. During the slow rehydration the synthetic amphiphiles cross the phase diagram described in Fig. 5 from sponge phase to the desired dispersed polymersomes. This method seems attractive, especially to enhance the encapsulation efficiency that will be described later in this review. However, it is not suitable for those polymers sensitive to high temperatures due to their potential degradation.

### 3.3 Organic Solvent Based Methods

Direct hydration is normally limited to polymers with relatively high chain flexibility and becomes kinetically impossible for glassy and crystalline copolymers. Polymersomes from such polymers can be prepared by dissolution of the block copolymer in an organic solvent that dissolves both blocks, followed by the hydration in water. The “phase inversion” technique involves first forming a solution of the block copolymer in an organic phase which is a suitable solvent for all the blocks, followed by the injection of an aqueous phase, which causes the non-polar block to become insoluble, triggering copolymer self-assembly into polymersomes [54,92,93]. This technique can trigger a transition from spherical micelles to cylindrical micelles and finally to vesicles upon the addition of an aqueous medium [94], as a result of greater hydrophobe-water interfacial tension with increasing water content [26,68]. The liquid nature of the reagents permits development of high throughput methodologies. A good example is the preparation of unilamellar and narrow size polymersomes using inkjet printers where organic solutions of copolymers are injected drop-wise into water using the same technology used by inkjet printer [95].

Another polymersomes formation method based on organic solvents makes use of “water-in-oil-in-water” (W/O/W) double emulsions as template [96–98]. This allows the formation of polymersomes with asymmetric membrane where the internal and the external leaflets have different compositions. This is achieved by stabilizing a water-in-oil emulsion using the copolymer for the inner leaflet and produce vesicles by passing the water droplets through a second oil-water interface containing the copolymer to form the outer leaflet of the membrane, where they become coated with the outer leaflet. The polymersomes assembly is eventually obtained by controlled dewetting of the organic phase using dialysis [60,99]. Furthermore, Weitz and co-workers have recently adapted this method using microfluidic devices for the preparation of monodisperse distributions of PEO-PLA polymersomes [100] (see Fig. 6 in the following paragraph).

The drawback of any organic solvent based technique is that residual organic solvent can induce biological toxicity, thereby restricting the application of polymersomes formed by using this method in biomedical research [68]. Furthermore, traces of organic solvent can considerably reduce the colloidal stability of polymersomes and extensive dialysis against water should be undertaken, to ensure complete removal of organic solvent [41].

### 3.4 Size Control

Polymersomes size is crucial for the design of drug delivery systems. Size governs the fate of particles both in vitro and in vivo. Cellular internalisation can drop by three orders of magnitude, going from 100 to 400 nm [70]. In vivo the size determines the particles circulation times, their ability to reach specific target, the

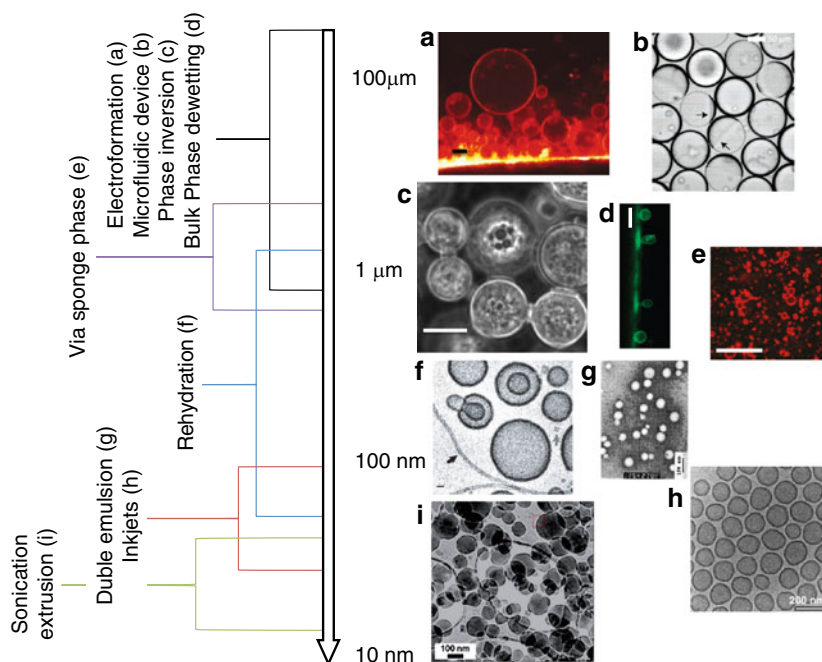


**Fig. 6** Schematic representation of polymersomes size distribution associated with their preparation technique. **(a)** Confocal laser scanning microscopy (CLSM) micrograph showing a PEO-PBO polymersome formed via electroformation. Scale bar = 50  $\mu\text{m}$  [68]; **(b)** Bright-field microscope image of a dried capsule formed by microfluidic devices from the PEG-b-PLA diblock copolymer. The red arrows indicate aggregates of excess diblock copolymer. Scale bar = 50  $\mu\text{m}$  [100]; **(c)** PABu-PAM Polymersomes prepared by phase inversion technique. Scale bar = 5  $\mu\text{m}$  [98]; **(d)** A single CLSM vertical slice showing a series of PEO-PBO polymersomes “budding” from the surface using photolithography coupled with bulk phase dewetting. Scale bar = 10  $\mu\text{m}$  [90]; **(e)** Confocal microscopy images of polymersomes produced from direct hydration (via sponge phase) using PEO-PS labelled with rhodamine B-labeled PEO-PS, at a ratio of 10:1. Scale bar = 15  $\mu\text{m}$  [91]; **(f)** Cryo-TEM micrograph of polymersomes generated by rehydration of a PEO-PEE polymer film. Scale bar = 50 nm [6]; **(g)** TEM micrograph of PLA-PEG polymersomes generated via double emulsion. Scale bar = 150 nm [96]; **(h)** Cryo-TEM micrograph of P2VP-PEG polymersomes prepared with a HP890 printer. Scale bar = 200 nm [95]; **(i)** Cryo-TEM micrograph of PEO-PBO vesicles formed via rehydration followed by extrusion and sonication. Scale bar = 100 nm [5]

possibility of extravasation, their flow properties and their eventual degradation or clearance. As discussed in Sect. 2.1 the membrane and corona thickness can be easily predicted using scaling relations. The same thing cannot be said regarding the polymersomes size. It is still very unclear what controls the size and yet most of the methods discussed above result in polymersomes dispersions with sizes ranging from tens to thousands of nanometres. We have recently observed on polybutadiene-poly(methacrylic acid) (PMAA-PBd) copolymers that, as the hydrophilic PMAA coils as a function of the pH, the overall hydrophilic/hydrophobic ratio changes, influencing the final morphology [56]. Particularly in the polymersome forming

region, we observed that as the copolymer hydrophilic/hydrophobic ratio approaches the micelle region (i.e. the overall copolymer is more hydrophilic) the average vesicle diameter drops by three orders of magnitude. This can be simply ascribed to curvature argumentations; clearly the more hydrophilic the copolymer the more curved structures are stabilized. On the other hand, using crystals growth arguments, we can show that the dimensions of polymersomes are inversely proportional to the concentration gradient [84]; thus, under conditions of mixing, where the concentration gradient is kept high, vesicles are shown to have diameters of the orders of nanometres, whilst in mild diffusion conditions (e.g. electroformation) the diameter is of the order of micrometers. Experimentally, the polymersome size is strictly controlled by the methodology used. Indeed, to date single step formation of monodisperse polymersomes was only achieved by phase inversion technique where the hydrophobic hydrophilic interface can be easily controlled such as in inkjet printing [95] and microfluidic devices [100]. On the other hand, the supramolecular nature of polymersomes allows post formation control of the size by controlled destabilisation methods such as freeze-thaw cycles, sonication and extrusion [68, 86]. During sonication, polymersomes solution is submerged into a water bath of a sonicator for 15-30 min. More disruption is involved with a freeze-thaw cycle where a vial containing polymersomes solution is submerged in liquid nitrogen for 1 min followed by 1 min in a 50 °C water bath [86]. However, polymersomes require several cycles times before reaching monodisperse population. A more versatile technique is based on the extrusion of polymersomes through controlled size membranes. This can be performed by introducing the polymersome suspension in a thermally controlled steel cylinder connected to pressurized nitrogen gas. The suspension is then pushed through a 100- to 400-nm polycarbonate membrane or filter supported by a circular steel sieve at the bottom of the cylinder, where the vesicle solution is collected after extrusion. The same process can be done manually by pushing the sample back and forth between two syringes passing through a polycarbonate membrane. This is typically repeated for a certain number of times (over 21) depending on the block copolymer studied. Thus, the final size of formed vesicles in a given solution is dictated more by kinetics aspects than thermodynamics [26].

## 4 Polymersome Loading

### 4.1 *Hydrophobic Molecules Encapsulation*

Like any other aggregate formed exploiting hydrophobic interaction, polymersomes have the ability to encapsulate relatively large amount of water insoluble molecule within their membranes. Several examples of polymersomes loaded with hydrophobic drugs have been reported by Discher and colleagues [101, 153]. Ghoroghchian et al. have incorporated large hydrophobic multi-porphyrin-based fluorophores non-covalently [102, 103] within PEO-PBD polymersomes without compromising polymersome colloidal or mechanical stability, as assessed by cryo-TEM

and micropipette aspiration techniques, respectively [104]. The absorption and emission spectra of the fluorophores changed with fluorophore size, allowing the degree of polymersome membrane loading to be determined. The authors demonstrated that the fluorophores could be incorporated within the polymersomes up to a maximum concentration of 10 mol/wt%. The size of the fluorophores that were successfully incorporated were similar to the size of hydrophobic drugs/active molecules that are used in the pharmaceutical industry, “(e.g. 1.4–5.4 nm in length and  $MW = 0.7\text{--}5.4\text{ kg mol}^{-1}$ )” [104]. The inclusion of hydrophobic species within polymersomes prevents their self-aggregation which occurs when they are free in aqueous media, whilst also protecting such species from interaction with biological components.

## 4.2 *Amphiphilic Molecules Encapsulation*

The amphiphilic nature of polymersomes allows the introduction of other amphiphilic species into the membrane. Pata et al. demonstrated that the macromolecular nature of polymersome makes them particularly resistant to detergent solubilization and suggested the inclusion of the surfactant within the polymersome membrane [105]. Similarly Ruyschaert et al. observed that hybrid structure introducing large amount of phospholipids within polymersomes [106]. Amphiphilic fluorescent dyes have also been encapsulated within various polymersomes; for example, octadecyl rhodamine B has been loaded into the membranes of PEO-PBO [5, 51, 107], PMPC-PDPA [51, 70] and PEO-PDPA-PDMA [36] polymersomes; these are just a few of the examples in the literature. The generation of polymersomes using this method should result in a very high (virtually 100%) loading efficiency for amphiphilic molecules. Probably the most interesting example of amphiphilic molecules stabilization is the possibility to use polymersome as a scaffold for membrane proteins. Membrane proteins such as OmpF, LamB, FhuA and Complex I have all been demonstrated to be encapsulated within polymersomes and still maintain their functionality. [31].

## 4.3 *Hydrophilic Molecules Encapsulation*

The ability to encapsulate large aqueous volumes and consequently whatever is dissolved in it is one prerogative of polymersomes and represents their most promising ability. Nevertheless, while for hydrophobic and amphiphilic molecules the encapsulation process is more or less straightforward, the complex kinetics of polymersomes formations hampers the encapsulation of hydrophilic molecules. Clearly the most important parameter to consider in encapsulating water-soluble molecules is the polymersome membrane permeability. Early work carried out by Discher and co-workers [6] showed that the water permeability of PEO-PEE polymersomes was established by measuring the reduction in polymersome swelling as a function



of small alterations to the osmolarity of the surrounding milieu. The obtained permeability coefficient of  $\sim 2.5 \mu\text{m s}^{-1}$  is an order of magnitude lower than that typically observed for phospholipid membranes, indicating that polymeric membranes display much lower levels of permeability, in accordance with their larger core thickness and ability to yield an interdigitated conformation of the hydrophobic chains [6]. In a separate study carried out by Eisenberg and co-workers on polystyrene-poly(acrylic acid) (PS-PAA) polymersomes, the copolymer membrane permeability to protons was controlled by the addition of dioxane to the aqueous medium containing the polymersomes [108]. The concentration of protons in the external milieu was determined by following the change in the fluorescence emission spectrum of a pH-sensitive fluorescent dye, 8-hydroxypyrene-1,3,6-trisulfonate. The apparent diffusion coefficient of the protons rose with increasing dioxane content of the surrounding medium, showing the ability of this organic solvent to fluidise the membrane, and thereby control the degree and rate of diffusion across the membrane. The well-known ability of organic solvents to plasticize membranes is also demonstrated in a paper published by Feijen and co-workers [41], whereby the presence of chloroform in aqueous dispersions of polymersomes was found to stimulate spontaneous dissociation or aggregation of the polymersomes upon their storage, resulting in a relatively short shelf-life. Upon elimination of the organic solvent, the colloidal stability of the polymersomes was drastically improved, and the shelf-life of such dispersions was increased to a minimum of 1 month, as assessed by EM techniques.

The membrane permeability to a given molecule can be easily derived from the First Fick's law [85] and one can define the permeability of a specific molecule across polymersome membrane as  $p = s/t$  (1), where  $p$  is the permeability,  $s$  the solubility of the specific molecule within the membrane, and  $t$  is the membrane thickness. Assuming that the desired molecule to encapsulate is soluble in water, it appears evident that the higher molecule solubility within the polymersome membrane the higher its permeability precluding long retention time. As we demonstrated using a simple chemical essay, the opposite rule applies to the membrane thickness, and the thicker the membrane the lower is the permeability [85]. Indeed, both solubility and thickness are controlled by the chemistry of choice to make the polymersomes and therefore one can tailor-make polymersomes for the specific need. The Hammer/Therien research groups encapsulated doxorubicin within the aqueous lumen of PEO-PCL polymersomes [109]. It was discovered that rather than displaying a controlled, steady release of doxorubicin as a result of hydrolysis of the PCL hydrophobic component of the membrane, an initial burst release was observed, thought to be the result of diffusion across the membrane. To reduce this untimely release that occurred before membrane lysis, Katz and co-workers have increased the stability of the membrane by conjugating an acrylate functionality to the PCL block [154]. The incorporation of a separate hydrophobic moiety sensitive to UV light triggered the polymerisation of the acrylate groups upon exposure to UV light. This technique has also been used to stabilise polymersomes formed from Pluronic (PEO-PPO-PEO) triblock copolymers [155], whereby the authors proved that radical polymerisation of these acrylate groups was triggered by an



increase in temperature, in addition to UV light absorption. Similar chemical modifications addressed to the modulation of the membrane permeability were proposed by Du et al. [110]. They developed poly(2-(diethylamino)ethyl methacrylate-stat-3-(trimethoxysilyl) propyl methacrylate) PEO-DEA-stat-PMSPMA polymersomes with a pH-tunable membrane permeability that, when ionized by the environment, become selectively permeable to certain encapsulated molecules in solution. A similar approach was shown by Robbins et al. [111]. Here the release of model proteins encapsulated within PEO-PBD polymersome lumen, was found to be photoinduced when a light-sensitive porphyrin chromophore was loaded within the polymersome membrane. Polymersome morphology was altered in response to light, as a result of the porphyrin-protein system utilising the “light energy” to generate a local temperature increase, which triggered membrane fission.

Normally the water-soluble drug is added during the hydration process and subsequently the loaded polymersomes are purified by the original solution by either dialysis or size exclusion chromatography [68]. However, this method ensures relative high encapsulation efficiency only if combined with post processing by extrusion or sonication [51, 112]. Interaction between copolymers and the desired molecules certainly favours the efficiency. pH sensitive systems such as PMPC-PDPA showed efficient encapsulation efficiency due to the strong interaction between the polymers and the DNA prior to pH variation [51, 70, 113].

Encapsulation efficiency close to 100% were reported by organic solvent based methods of inkjet printing [95] and microfluidic devices [100]. These procedures permit a controlled and efficient *in situ* encapsulation enabling multi drugs loading into polymersomes incompatible with material sensitive to organic solvents (i.e. nucleic acids and proteins). More *ad hoc* methods are based on specific solubility properties of the molecule to encapsulate. This is the case of doxorubicin hydrochloride that can be encapsulated by ammonium sulfate transmembrane gradients protocol using preassembled polymersomes [114]. Additionally, Kim et al. [115] reported the application of non-ionic polymersomes for the delivery of siRNA and antisense oligonucleotides. In order to encapsulate those active polynucleotides a polymer mixed solution was prepared by mixing PEG-polycaprolactone with PEG-PBO (25:75 w/w) in a DMSO/PBS solution 15:85 v/v. This copolymer mixture was added to the oligonucleotide solution while vortexing and it was purified by dialysis in order to eliminate all organic solvent and the non-encapsulated materials. More recently Conlin et al. have reported high encapsulation efficiency by pre-loading proteins and drugs within sponge phase formed at high copolymer concentrations. In such a fashion polymersomes form already loaded with the desired molecule [91].

## 5 Polymersomes Applications

Some important applications of polymersomes span from imaging of tissues *in vivo* using near-infrared emissive polymersomes (NIR-polymersomes) [116], to the encapsulation of proteins, DNA and anti-cancer drugs for delivery applications. With

the advent of new imaging techniques [158], improving the current intracellular labelling procedure became fundamental. As an excellent delivery system the polymersome turns out to be extremely useful for imaging application. As an example, Peter Ghoroghchian [117] and co-workers recently showed how to apply simple diblock copolymer system such as poly(ethyleneoxide)-block-poly( $\epsilon$ -caprolactone) (PEO-*b*-PCL) and poly(ethyleneoxide)-block-poly( $\gamma$ -methyl- $\epsilon$ -caprolactone) (PEO-*b*-PMCL), to create polymersomes with special emissive properties. This can be achieved by incorporating porphyrin-based fluorophores within the polymeric membrane. The final structure shows optical properties similar to quantum dots from the visible to the infrared. Those studies have been expanded to poly(ethylene oxide)-block-poly(ethylene) PEO-*b*-PEE polymersomes as well [117]. NIR-polymersomes conjugated to a cell permeable peptide (TAT) have been used by Christian et al. [76] in order to enable efficient intracellular delivery for future dendritic cell tracking with these optical probes. With a similar purpose, the PMPC-PDPA polymersomes mediated delivery of fluorophores has been recently explored by our group [118]. In detail, fluorescent amphiphilic molecules have been incorporated to polymersomes membrane and delivered within cells in order to generate a revolutionary non-cytotoxic, non-immunogenic cellular tracking system [118]. Polymersomes loaded with such fluorophores are therefore promising candidates for use as “nanoscale imaging agents” [119]. In addition to the incorporation of fluorophores within polymersomes [117, 118], the potential of those carrier to the field of imaging has been further exemplified by the encapsulation of magnetic resonance imaging (MRI) contrast agents within porous PEO-PBD polymersomes, in research work carried out by Cheng and Tsourkas [116]. Polymersomes were prepared by hydration of a thin film of the PEO-PBD diblock copolymer mixed with 1-palmitoyl-2-oleoyl-*sn*-glycero-3-phosphocholine (POPC) phospholipid at a molar ratio of 85:15. A chelated gadolinium (Gd) covalently attached to a dendrimer was loaded within the polymersome lumen, and the diblock copolymer was then cross-linked by free radical polymerisation via the addition of a chemical initiator, to increase the stability of the polymersome membrane (see Fig. 7a). Upon the addition of a surfactant, such as Triton X-100, the phospholipid component of the polymersomal membrane was removed, generating holes in the membrane for a facile influx of water (see Fig. 7a). The strength of the signal provided by the Gd ions for imaging purposes is dependent on rapid exchange kinetics “between Gd-bound water molecules and the surrounding bulk water” [116], which is facilitated by the presence of pores in the polymersomal membrane. The conjugation of the Gd chelates to dendrimers inhibited their escape via the polymersome pores. Their encapsulation within polymersomes has the advantage of greatly increasing the signal intensity generated by the Gd ions compared with free Gd, since virtually 44,000 Gd ions were loaded into each polymersome on average. Furthermore, these polymersomes offer the potential to encapsulate both hydrophilic and hydrophobic active agents and add targeting ligands to their exterior, as discussed above, rendering the generation of targeted nanocarriers for “combined drug delivery and MR imaging” a viable area of research. Similarly, Yang and co-workers [122] utilized a binary mixture of amphiphilic folate-poly(ethylene glycol)-poly(D,L-lactide)

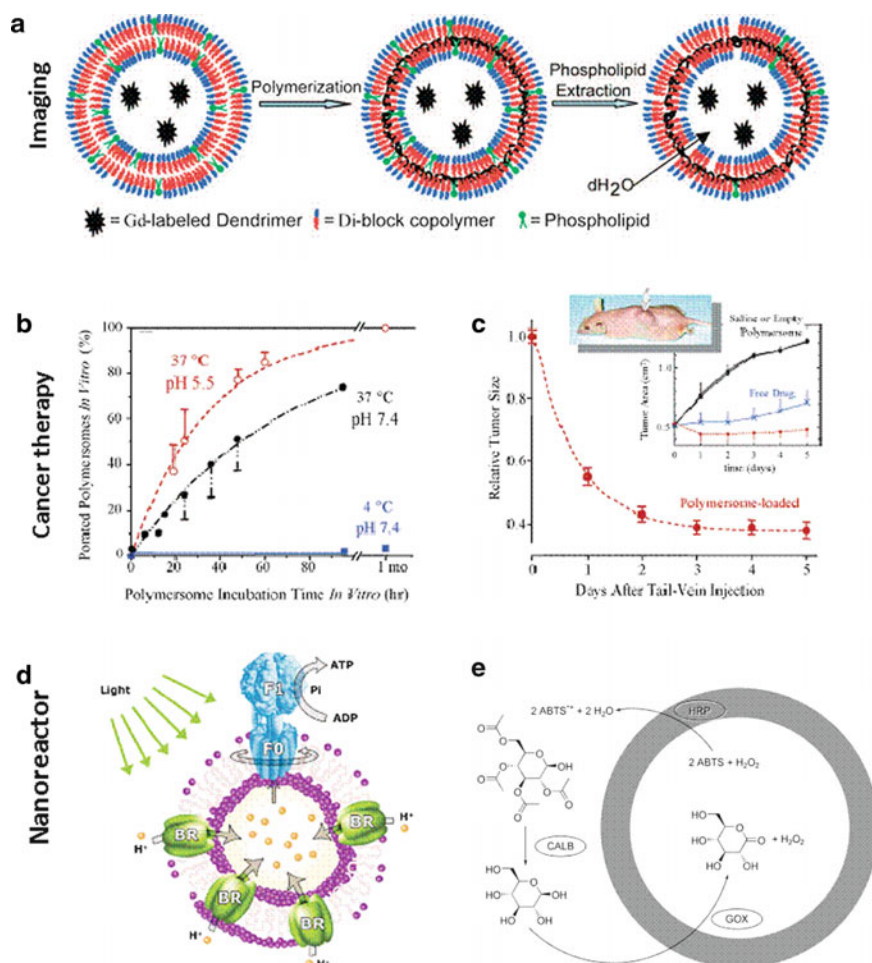


**Fig. 7** (a) [116] Schematic representation of the generation of porous polymersomes loaded with a Gd-chelated dendrimer for magnetic resonance imaging applications. (b) [43] Rate of poration of polymersomes formed from a 3:1 mol/mol mixture of PEO-PBD and PEO-PLA, following their incubation at both 37 °C and at 4 °C with buffered saline solutions. At 37 °C, the effect of pH was also investigated, by applying conditions of both physiological pH and mildly acidic pH conditions, analogous to the endocytotic environment. (c) Reduction in the size of a human breast tumour implanted into nude mice following successful delivery of the polymersomes loaded with both paclitaxel and doxorubicin anti-cancer drugs into the tumour tissue. In the control experiments whereby mice were injected with saline, unloaded polymersomes, or the free drug, growth of the tumour was not impeded. (d) [120] Schematic representation of the “proteopolymersome” nanoreactor, showing that the bacteriorhodopsin (BR) channels present within the polymersome membrane can transport H<sup>+</sup> ions into the polymersome interior in response to light, triggering the conversion of ADP to ATP in the presence of inorganic phosphate (Pi) by the action of the F<sub>0</sub>F<sub>1</sub>-ATP synthase rotary motor protein, which is also incorporated within the polymersome membrane. (e) [121] Schematic representation of a three step cascade reaction for the conversion of ABTS to ABTS<sup>•+</sup>, catalysed by enzymes positioned within different polymersome compartments

(folate-PEG-PDLLA) and NH<sub>2</sub>-PEG-PDLLA to generate polymersomes in order to encapsulate hydrophilic superparamagnetic iron oxide nanoparticles (SPIONs) via double emulsion. Those particles have a broad range of applications spanning from MRI (Baghi et al. 2005), drug delivery [123, 124], therapy [125] and cell labelling [126], but unfortunately they are hydrophobic and therefore applicability is limited *in vivo* without a proper carrier. Results demonstrate that the encapsulation enables a high loading level of SPION particles followed by their clustering within the aqueous core. The overall superparamagnetic property results increased giving an effective contrast probes for cancer diagnosis and treatment [122].

Another imaging application of PEO-PBD copolymers has been found by the Maskos research group which encapsulates quantum dots within polymersome membranes [127]. Quantum dot nanocrystals have been largely studied because of their broad imaging applications. Unfortunately, their inorganic nature induces cellular toxicity, limiting their biological application compared to organic-based fluorophores which are more biocompatible [119]. This is confirmed by studies performed on murine melanoma cells treated with polymersomes encapsulating porphyrin-based fluorophores [128].

Cancer therapy is another emerging application, due to the ability of polymersomes to load both hydrophilic and hydrophobic anti-cancer drugs within their lumen and membrane cores, respectively. Both hydrophilic (doxorubicin) and hydrophobic (paclitaxel) anti-cancer drugs have been loaded simultaneously within PEO-PLA and PEO-PCL polymersomes (generated by mixing these hydrolytically degradable block copolymers 1:3 mol/mol with inert PEO-PBD) by Ahmed and co-workers within the Discher research group [43, 129]. These polymersomes were not only able to deliver these drugs into a human breast tumour implanted into mice; growth retardation and a reduction of the tumour area were also observed (Fig. 7c). At a time point of 5 days after intravenous tail injection of the polymersomes into the mice, the tumour shrank to less than 50% of its original size. Due to the biodegradability of the ester blocks comprising these polymersomes, and the blending of a degradable block copolymer with a chemically inactive block copolymer, the drug release rate could be controlled, with the mildly acidic environment within cellular endosomes triggering faster ester hydrolysis and polymersome poration compared with the extracellular environment (Fig. 7b). Temperature was also found to have an effect on the rate of polymersome poration (see Fig. 7c).

The potentials of PEO-PBD as well as PMPC-PDPA as delivery vectors have been thoroughly investigated. Both have been applied for the encapsulation of different proteins. The former have been used by Arifin and Palmer that demonstrated its ability to encapsulate bovine haemoglobin (Hb) without perturbing its affinity for oxygen mimicking the red blood cells capability. This in turn can generate alternative *in vivo* oxygen therapeutics [87]. The latter have been studied by our group for the delivery of primary human antibodies in order to achieve not only “in live” immunolabelling [130], by using fluorescently labelled antibodies, but also to exploit the antibodies therapy potential [131]. Much work has also been undertaken by Meier and co-workers in the field of protein incorporation within polymersome walls to yield nanoreactors. An example of this is the

incorporation of ionophores (i.e. lipophilic molecules used to carry ions across membranes, for example, by forming channels to avoid contact of the ions with the hydrophobic membrane core, or by binding to the ions, thereby reducing their polarity) within poly(2-ethyl-2-oxazoline)-poly(dimethylsiloxane)-poly(2-ethyl-2-oxazoline) (PMOXA-PDMS-PMOXA) triblock copolymer polymersome membranes [132], to allow controlled calcium phosphate precipitation to occur within the polymersome aqueous cores. Anionic phosphates were encapsulated within the polymersomes, and the ion-carrier channels were successfully used to transport  $\text{Ca}^{2+}$  across the polymer membrane, allowing calcium phosphate precipitation to take place in the polymersome lumen. Various research groups have attempted to generate artificial cells/cell organelles by the incorporation of enzymes [121] or protein channels [133] within polymersome membranes, thereby creating nanoreactors. Montemagno and co-workers have developed a multiprotein polymersome system for ATP synthesis [120]. These polymersomes were formed from an ABA triblock copolymer, poly(2-ethyl-2-oxazoline)-poly(dimethylsiloxane)-poly(2-ethyl-2-oxazoline) (PEtOz-PDMS-PEtOz), and incorporated two different protein channels within the polymersome membrane; ATP synthetase, which is a rotary motor protein, and bacteriorhodopsin, which can act as a proton pump in response to light (Fig. 7d), resulting in an influx of hydrogen ions ( $\text{H}^+$ ) into the polymersome lumen. Through coupled reactions involving both protein channels, ATP was successfully synthesised in the presence of ADP and inorganic phosphate (Pi), giving this “hybrid proteopolymersome” a potential use in numerous applications, including the “in vitro investigation of cellular metabolism” [120].

Van Hest and co-workers have also extensively researched the incorporation of enzymes within PS-polyisocyanopeptide (PIAT) polymersomes for the generation of polymersome “nanoreactors” [121, 134, 135, 156]. These block copolymers comprise a mobile hydrophobic block (PS) and a rigid hydrophilic block (PIAT), and yield polymersomes that contain pores in the membrane, allowing diffusion of small solutes between the polymersome lumen and the external aqueous milieu whilst larger biomacromolecules stay entrapped [136]. Vriezema et al. have not only succeeded in encapsulating enzymes within these polymersomes, but have also imparted a high degree of control over their location within the polymersomes [121]. Three different enzymes involved in a multi-step reaction were incorporated; *Candida antarctica* lipase B (CALB), horseradish peroxidase (HRP) and glucose oxidase (GOX), which were placed outside the polymersomes, within the polymersome lumen and within the polymersome membrane, respectively. The coupled catalytic activity of these enzymes was found to be 100 times higher when located inside polymersome compartments rather than free in solution. A schematic representation of the nanoreactor and the catalytic conversion of glucose into lactone, releasing hydrogen peroxide for catalytic reaction with 2,2'-azinobis(3-ethylbenzothiazoline-6-sulfonic acid) (ABTS), yielding  $\text{ABTS}^{\cdot+}$ , is shown in Fig. 7e.

Finally, gene therapy is an area of research that is receiving significant attention due to its potential to replace or “switch off” the expression of particular genes. Intracellular delivery of naked genes lacks efficiency due to their negative charge and size, since they experience a repulsive interaction from the negatively charged

cell plasma membrane [137–141]. Various methods either to avoid interaction with the cell membrane (e.g. by direct injection of genes into the cell by electroporation techniques), or to use a vector to transport genes into the cell, have been investigated. Some of those methods involve the use of polymersomes.

Korobko and co-workers [142, 143] encapsulated DNA in polymersomes made of a cationic amphiphilic diblock copolymer poly-(butadiene-*b*-*N*-methyl-4-vinyl pyridinium) (PBDP4VPQI). DNA accumulation appeared in both the polymersome core and brush due to the preparation protocol followed. The final formulation results are very stable and therefore suitable for air purification and redispersion in aqueous PEG solution. Intracellular delivery is achieved by endosomal rupture due to the polymer charge [142, 143]. Poly(amino acid) (poly(AA))-based polymersomes have also been considered for transfection by Brown and co-workers. They utilized a triblock co-polymer generated by attaching methoxy-poly(ethylene glycol) and palmitic acid to a poly-L-lysine (PLL) or poly-L-ornithine (PO) backbone [144]. These slightly anionic polymersomes have shown improved results in transfection efficiency both in vitro and in vivo compared to basic poly(AA)/DNA complex or naked DNA. Unfortunately, they turn out to be cytotoxic at therapeutic concentration [145]. In contrast, the neutral system has been proved to be more effective as a gene delivery vector without generating any significant morbidity. As an example, the degradable PEG-PLA polymersomes displayed an encapsulation efficiency and delivery of siRNA in vitro comparable to levels achieved with the commonly used lipoplex of siRNA and Lipofectamine 2000 (LF2K) [157]. More in detail polymers were dissolved in dimethyl sulfoxide (DMSO) and added to an aqueous solution of fluorescently labelled siRNA. Furthermore, a siRNA, specific for the silencing of lamin A/C, was added. By the emulsion technique,  $93 \pm 7$  nm polymersomes were formed and subsequently purified via dialysis. Results in A549 cell lines confirmed a general 30% knock down of lamin expression. Even though the knock down results similar to that obtained by LF2K or lipoplex mediated delivery, PEG-PLA polymersomes are less cytotoxic and therefore more suitable for in vivo application.

Emphasizing the importance of stealth, PMPC-PDPA polymersomes were able to encapsulate DNA physically with high transfection efficiencies in both cell line and primary cells [51, 113], modestly affecting cell viability. Furthermore, the presence of the biocompatible PMPC chains on the external corona, coupled with the 200–400 nm vesicles dimensions, are likely to promote relatively long in vivo circulation times.

## 6 Conclusions

Polymersomes are, like any other vesicular structure, able to encapsulate hydrophilic, hydrophobic and amphiphilic molecules, but unlike other vesicular structure, their macromolecular nature makes them stronger and more stable with the intrinsic responsiveness of polymers. All these properties make polymersomes one of the most interesting supramolecular structures with potential applications in drug



delivery, gene therapy, protein delivery and medical imaging as well as a multifunctional platform for nanoreactor technology. The only requisite is to have the right balance of water soluble and insoluble components and then the rest is open to any combination of a limitless number of chemistries. This hierarchical structure indeed allows the design of the capsule, controlling the size and the interaction with its environment with exquisite molecular control. The increasing number of publications on polymersomes demonstrates such flexibility. Since 1995, when the very first example of polymer vesicles was reported [54], more than 2,000 papers have been published, with most of them published during the last 5 years. Furthermore, it is worth noting that, in analogy with biological systems, amphiphilic membranes can form more complex structures. Several examples of more complex block copolymer membrane enclosed structures have been reported, such as multilamellar structures [88, 146, 147], tubular myelin-like structures [107, 148, 149] and tissue-like structures [5, 79]. Finally, polymersomes can be imagined as a starting point of the scientific pathway towards the perspective of new synthetic biological intricate structures able to perform more complicated functions, such as the Golgi apparatus, the endoplasmic reticulum or neural axons.

## References

1. Alberts B, Johnson A, Lewis J, Raff M, Roberts K, Walter P (2002) Molecular biology of the cell. Garland Science, New York
2. Mansy SS, Schrum JP, Krishnamurthy M, Tobk S, Treco DA, Szostak JW (2008) Template-directed synthesis of a genetic polymer in a model protocell. *Nature* 454(7200):122–125
3. Matyjaszewski K, Spanswick J (2005) Controlled/living radical polymerization. *Mater Today* 8:26–33
4. Matyjaszewski K, Xia J (2001) Atom transfer radical polymerization. *Chem Rev* 101: 2921–2990
5. Battaglia G, Ryan AJ (2005) Bilayers and interdigitation in block copolymer Vesicles. *J Am Chem Soc* 127:8757–8764
6. Discher BM, Won YY, Ege DS, Lee JC-M, Bates FS, Discher DE, Hammer DA (1999) Polymersomes: tough vesicles made from diblock copolymers. *Science* 284:1143–1146
7. Smart T, Lomas H, Massignani M, Flores-Merino MV, Ruiz Perez L, Battaglia G (2008) Block copolymer nanostructures. *Nano Today* 3:38–46
8. De-Gennes PG (1980) Conformations of polymers attached to an interface. *Macromolecules* 13:1069–1075
9. De-Gennes PG (1980) Scaling concepts in polymer physics. Cornell University Press, New York
10. Jain S, Bates FS (2004) Consequences of nonergodicity in aqueous binary PEO-PB micellar dispersions. *Macromolecules* 37:1511–1523
11. Förster S, Hermsdorf N, Leube W, Schnablegger H, Regenbrecht M, Akari S (1999) Fusion of charged block copolymer micelles into toroid networks. *J Phys Chem B* 103:6657–6668
12. Bermudez H, Brannan AK, Hammer DA, Bates FS, Discher DE (2002) Molecular weight dependence of polymersome membrane structure, elasticity, and stability. *Macromolecules* 35:8203–8208
13. Disher DE, Ahmed F (2006) Polymersomes. *Annu Rev Biomed Eng* 8:323–341
14. Aranda-Espinoza H, Bermudez H, Bates FS, Disher DE (2001) Electromechanical limits of polymersomes. *Phys Rev Lett* 87:208301–208304

15. Dimova R, Seifert U, Pouligny B, Forster S, Dobereiner HG (2002) Hyperviscous diblock copolymer vesicles. *Eur Phys J E* 7:241–250
16. Cevc G, Marsh D (1987) Phospholipid bilayers: physical principles and models. Wiley, New York
17. Srinivas G, Discher DE, Klein M (2004) Self-assembly and properties of diblock copolymers by coarse-grain molecular dynamics. *Nat Mater* 3:6338–6344
18. Hadziioannou G, Skoulios A (1982) Molecular weight dependence of lamellar structure in styrene/isoprene two- and three-block copolymers. *Macromolecules* 15:258–262
19. Hashimoto T, Shibayama M, Kawai H (1980) Domain-boundary structure of styrene-isoprene block copolymer films cast from solution. Molecular-weight dependence of lamellar microdomains. *Macromolecules* 13:1237–1247
20. Richards RW, Thomason JL (1983) Small-angle neutron scattering study of block copolymer. *Macromolecules* 16(6):982–992
21. Ryan AJ, Mai SM, Fairclough JPA, Hamley IW, Booth C (2001) Ordered melts of block copolymers of ethylene oxide and 1,2-butylene oxide. *Phys Chem Chem Phys* 3:2961–2971
22. Ortiz V, Nielsen SO, Disher DE, Klein ML, Lipowsky R, Shillicock J (2005) *J Phys Chem B* 109:17708–17714
23. Matsen MW, Bates FS (1995) Testing the strong-stretching assumption in a block copolymer microstructure. *Macromolecules* 28:8884–8886
24. Bermudez H, Hammer DA, Disher DE (2004) Effect of bilayer thickness on membrane bending rigidity. *Langmuir* 20:540–543
25. Bermudez H, Aranda-Espinoza H, Hammer DA, Discher DE (2003) Pore stability and dynamics in polymer membranes. *Europhys Lett* 64:550–556
26. Discher DE, Eisenberg A (2002) Polymer vesicles. *Science* 297:967–973
27. Yin H, Kang SW, Bae YH (2009) Polymersome formation from AB<sub>2</sub>Type 3-miktoarm star copolymers. *Macromolecules* 42(19):7456–7464
28. Zhulina EB, Halperin A (1992) Lamellar mesogels and mesophases: a self-consistent-field theory. *Macromolecules* 25:5730–5741
29. Dai LM, Toprakcioglu C (1992) End-adsorbed triblock copolymer chains at the liquid-solid interface: bridging effects in a good solvent. *Macromolecules* 25(22):6000–6006
30. Levicky R, Koneripalli N, Tirrell M, Satija SK (1998) *Macromolecules* 31:3731–3734
31. Stoenescu R, Graff A, Meier W (2004) Asymmetric ABC-triblock copolymer membranes induce a directed insertion of membrane proteins. *Macromol Biosci* 4:930–935
32. Napoli A, Tirelli N, Wehrli E, Hubbell JA (2002) Lyotropic behavior in water of amphiphilic ABA triblock copolymers based on poly(propylene sulfide) and poly(ethylene glycol). *Langmuir* 18:8324–8329
33. Sommerdijk NAJM, Holder SJ, Hiorns RC, Jones RG, Nolte RJM (2000) Self-assembled structures from an amphiphilic multiblock copolymer containing rigid semiconductor segments. *Macromolecules* 33:8289–8294
34. Walther A, Muller AHE (2008) Janus particles. *Soft Matter* 4:663–668
35. Wittemann A, Azzam T, Eisenberg A (2007) Biocompatible polymer vesicles from bi-amphiphilic triblock copolymers and their interaction with bovine serum albumin. *Langmuir* 23:2224–2230
36. Blanazs A, Massignani M, Battaglia G, Armes SP, Ryan AJ (2009) Tailoring macromolecular expression at polymersome surfaces. *Adv Funct Mater* 19(18):2906–2914
37. Li C, Madsen J, Armes SP, Lewis AL (2006) A new class of biochemically degradable, stimulus-responsive triblock copolymer gelators. *Angew Chem Int Ed* 45:3510–3513
38. Li Z, Hillmyer MA, Lodge TP (2006) Morphologies of multicompartment micelles formed by ABC miktoarm star terpolymers. *Langmuir* 22:9409–9417
39. Brannan AK, Bates FS (2004) ABCA tetrablock copolymer vesicles. *Macromolecules* 37:8816–8819
40. De Las Heras Alarcon C, Pennadam S, Alexander C (2005) Stimuli responsive polymers for biomedical applications. *Chem Soc Rev* 34:276–285
41. Meng F, Hiemstra C, Engbers GHM, Feijen J (2003) Biodegradable polymersomes. *Macromolecules* 36:3004–3006



42. Ahmed F, Discher DE (2004) Self-porating polymersomes of PEG–PLA and PEG–PCL hydrolysis-triggered controlled release vesicles. *J Contr. Release* 96:37–53
43. Ahmed F, Pakunlu RI, Srinivas G, Brannan A, Bates F, Klein ML, Minko T, Discher DE (2006) Shrinkage of a rapidly growing tumor by drug-loaded polymersomes: pH-triggered release through copolymer degradation. *Mol Pharm* 3:340–350
44. Najafi F, Sarbolouki MN (2003) Biodegradable micelles/polymersomes from fumaric/sebacic acids and poly (ethylene glycol). *Biomaterials* 24:1175–1182
45. Holowka EP, Pochan DJ, Deming TJ (2005) Charged polypeptide vesicles with controllable diameter. *J Am Chem Soc* 127:12423–12428
46. Napoli A, Valentini M, Tirelli N, Martin M, Hubbell JA (2004) Oxidation-responsive polymeric vesicles. *Nat Mater* 3:183–189
47. Cerritelli S, Velluto D, Hubbell JA (2007) PEG-SS-PPS: reduction-sensitive disulfide block copolymer vesicles for intracellular drug delivery. *Biomacromolecules* 8:1966–1972
48. Meng F, Hennink WE, Zhong Z (2009) Reduction-sensitive polymers and bioconjugates for biomedical applications. *Biomaterials* 30:2180–2198
49. Rodriguez-Hernandez J, Lecommandoux S (2005) Reversible inside-out micellization of pH-responsive and water-soluble vesicles based on polypeptide diblock copolymers. *J Am Chem Soc* 127:2026–2027
50. Du J, Tang Y, Lewis AL, Armes SP (2005) pH-sensitive vesicles based on a biocompatible zwitterionic diblock copolymer. *J Am Chem Soc* 127:17982–17983
51. Lomas H, Massignani M, Abdullah AK, Presti CL, Canton I, MacNeil S, Du J, Blanz A, Madsen J, Armes SP, Lewis AL, Battaglia G (2008) Non-cytotoxic polymer vesicles for rapid and efficient intracellular delivery. *Faraday Discuss* 139:143–159
52. Borchert U, Lipprandt U, Bilanz M, Kimpfler A, Rank A, Peschka-Süss R, Schubert R, Lindner P, Förster S (2006) pH-induced release from P2VP-PEO block copolymer vesicles. *Langmuir* 22:5843–5847
53. Ruiz-Perez L, Pryke A, Sommer M, Battaglia G, Soutar I, Swanson L, Geoghegan M (2008) Conformation of poly(methacrylic acid) chains in dilute aqueous solution. *Macromolecules* 41(6):2203–2211
54. Zhang L, Eisenberg A (1995) Multiple morphologies of “crew-cut” aggregates of polystyrene-*b*-poly(acrylic acid) block copolymers. *Science* 268:1728–1731
55. Choucair AA, Lavigneur C, Eisenberg A (2004) Polystyrene-*b*-poly(acrylic acid) vesicle size control using solution properties and hydrophilic block length. *Langmuir* 20(10):3894–3900
56. Fernyhough C, Ryan AJ, Battaglia G (2009) pH controlled assembly of a polybutadiene-poly(methacrylic acid) copolymer in water: packing considerations and kinetic limitations. *Soft Matter* 5(8):1674–1682
57. Qin S, Geng Y, Discher DE, Yang S (2006) Temperature-controlled assembly and release from polymer vesicles of poly(ethylene oxide)-block- poly(*N*-isopropylacrylamide). *Adv Mat* 18:2905–2909
58. Rank A, Hauschild S, Forster S, Schubert R (2009) Preparation of monodisperse block copolymer vesicles via a thermotropic cylinder-vesicle transition. *Langmuir* 25:1337–1344
59. Wang G, Tong X, Zhao Y (2004) Preparation of azobenzene-containing amphiphilic diblock copolymers for light-responsive micellar aggregates. *Macromolecules* 37:8911–8917
60. Mabrouk E, Cuvelier D, Brochard-Wyart F, Nassoy P, Li MH (2009) Bursting of sensitive polymersomes induced by curling. *Proc Natl Acad Sci* 106:7294–7298
61. Smart T, Mykhaylyk OO, Ryan AJ, Battaglia G (2009) Polymersomes hydrophilic brush scaling relations. *Soft Matter* 5:3607–3610
62. Alcantar NA, Aydil ES, Israelachvili JN (2000) Polyethylene glycol-coated biocompatible surfaces. *J Biomed Mater Res* 51:343–351
63. Israelachvili JN, Wennerstrom H (1996) Role of hydration and water structure in biological and colloidal interactions. *Nature* 379:219–225
64. Vonarbourg A, Passirani C, Saulnier P, Benoit J-P (2006) Parameters influencing the stealthiness of colloidal drug delivery systems. *Biomaterials* 27:4356–4373
65. Lasic DD (1994) Sterically stabilized vesicles. *Angew Chem Int Ed* 33:1685–1698

66. Papahadjopoulos D, Allen TM, Gabizon A, Mayhew E, Matthay K, Huang SK, Lee K, Woodle MC, Lasic DD, Redemann C, Martin FJ (1991) Sterically stabilized liposomes: Improvements in pharmacokinetics and antitumor therapeutic efficacy. *Proc Natl Acad Sci USA*, 88:11460–11464
67. Photos PJ, Bacakova L, Discher B, Bates FS, Discher DE (2003) Polymer vesicles in vivo: correlations with PEG molecular weight. *J Contr Release* 90:323–334
68. LoPresti C, Lomas H, Massignani M, Smart T, Battaglia G (2009) Polymersomes: nature inspired nanometer sized compartments. *J Mater Chem* 19:3576–3590
69. Massignani M, LoPresti C, Blanz A, Madsen J, Armes SP, Lewis AL, Battaglia G (2009a) controlling cellular uptake by surface chemistry, size, and surface topology at the nanoscale. *Small* 5(21):2424–2432
70. Christian DA, Tian A, Ellenbroek WG, Levental I, Rajagopal K, Janmey PA, Liu AJ, Baumgart T, Discher DE (2009) Spotted vesicles, striped micelles and Janus assemblies induced by ligand binding. *Nat Mater* 8:843–849
71. Kuntz ID, Chen K, Sharp KA, Kollman PA (1999) The maximal affinity of ligands. *Proc Natl Acad Sci USA* 96:9997–10002
72. Broz P, Benito SM, Saw C, Burger P, Heider H, Pfisterer M, Marsch S, Meier W, Hunziker P (2005) Cell targeting by a generic receptor-targeted polymer nanocontainer platform. *J Contr Release* 102:475–488
73. Lin JJ, Ghoroghchian PP, Zhang Y, Hammer DA (2006) Adhesion of antibody-functionalized polymersomes. *Langmuir* 22:3975–3979
74. Hammer DA, Robbins GP, Haun JB, Lin JJ, Qi W, Smith LA, Ghoroghchian PP, Therien MJ, Bates FS (2008) Leukopolymersomes. *Faraday Discuss* 139:129–141
75. Pang Z, Lu W, Gao H, Hu K, Chen J, Zhang C, Gao X, Jiang X, Zhu C (2008) Preparation and brain delivery property of biodegradable polymersomes conjugated with OX26. *J Contr Release* 128:120–127
76. Christian NA, Milone MC, Ranka SS, Li G, Frail PR, Davis KP, Bates FS, Therien MJ, Ghoroghchian PP, June CH, Hammer DA (2007) Tat-functionalized near-infrared emissive polymersomes for dendritic cell labeling. *Bioconjugate Chem* 18:31–40
77. Upadhyay KK, Meins J-FL, Misra A, Voisin P, Bouchaud V, Ibarboure E, Schatz C, Lecommandoux S (2009) Biomimetic doxorubicin loaded polymersomes from hyaluronan-block-poly(benzyl glutamate) copolymers. *Biomacromolecules* 10(10):2802–2808
78. Battaglia G, Ryan AJ (2006) Effect of amphiphile size on the transformation from a lyotropic gel to a vesicular dispersion. *Macromolecules* 39:798–805
79. Battaglia G, Ryan AJ (2005) The evolution of vesicles from bulk lamellar gels. *Nat Mater* 4:869–876
80. Jain S, Gong X, Scriven LE, Bates FS (2006) Disordered network state in hydrated block-copolymer surfactants. *Phys Rev Lett* 96(13):138304
81. Jain S, Dyrda MHE, Gong X, Scriven LE, Bates FS (2008) Lyotropic phase behavior of poly(ethylene oxide)-poly(butadiene) diblock copolymers: evolution of the random network morphology. *Macromolecules* 41:3305–3316
82. Jain S, Bates FS (2003) On the origins of morphological complexity in block copolymer surfactants. *Science* 300(5618):460–464
83. Won YY, Davis HT, Bates FS (2003) Molecular exchange in PEO-PB micelles in water. *Macromolecules* 36:953–955
84. Battaglia G, Ryan AJ (2006) Pathways of polymeric vesicle formation. *J Phys Chem B* 110:10272–10279
85. Battaglia G, Ryan AJ, Tomas S (2006) Polymeric vesicle permeability: a facile chemical assay. *Langmuir* 22:4910–4913
86. Lee JC-M, Bermudez H, Discher BM, Sheehan MA, Won Y-Y, Bates FS, Discher DE (2001) Preparation, stability, and in vitro performance of vesicles made with diblock copolymers. *Biotech Bioeng* 73:135–145
87. Arifin DR, Palmer AF (2005) Polymersome encapsulated hemoglobin: a novel type of oxygen carrier. *Biomacromolecules* 6:2172–2181

88. Battaglia G, Tomas S, Ryan AJ (2007) Lamellarsomes: metastable polymeric multilamellar aggregates. *Soft Matter* 3:470–475
89. Angelova MI, Dimitrov DS (1986) Liposome electroformation. *Faraday Discuss* 81:303–311
90. Howse JR, Jones AR, Battaglia G, Ducker RE, Leggett GJ, Ryan AJ (2009) Templated formation of giant polymer vesicles with controlled size distributions. *Nat Mater* 8(6):507–511
91. O'Neil CP, Demurtas TSD, Finka A, Hubbell JA (2009) A novel method for the encapsulation of biomolecules into polymersomes via direct hydration. *Langmuir* 25:9025–9029
92. Luo L, Eisenberg A (2001) Thermodynamic size control of block copolymer vesicles in solution. *Langmuir* 17:6804–6811
93. Luo L, Eisenberg A (2001) Thermodynamic stabilization of mechanism of block copolymer vesicles. *J Am Chem Soc* 123(5):1012–1013
94. Shen H, Eisenberg A (1999) Morphological phase diagram for a ternary system of block copolymer PS310-*b*-PAA52/Dioxane/H<sub>2</sub>O. *J Phys Chem B*, 103:9473–9487
95. Hauschild S, Anja Rumpelcker UL, Borchert U, Rank A, Schubert R, Forster S (2005) Direct preparation and loading of lipid and polymer vesicles using inkjets. *Small* 1:1177–1180
96. Tobio M, Gref R, Sanchez A, Langer R, Alonso MJ (1998) Stealth PLA-PEG nanoparticles as protein carriers for nasal administration. *Pharm Res* 15:270–275
97. Yasugi K, Nagasaki Y, Kato M, Kataoka K (1999) Preparation and characterization of polymer micelles from poly(ethylene glycol)-poly(D,L-lactide) block copolymers as potential drug carrier. *J Contr Release* 62:89–100
98. Pautot S, Frisken BJ, Weitz DA (2003) Production of unilamellar vesicles using an inverted emulsion. *Langmuir* 19:2870–2879
99. Hayward R, Utada A, Dan NR, Weitz D (2006) Dewetting instability during the formation of polymersomes from block-copolymer-stabilized double emulsions. *Langmuir* 22(10):4457–4461
100. Cheung Shum H, Kim JW, Weitz DA (2008) Microfluidic fabrication of monodisperse biocompatible and biodegradable polymersomes with controlled permeability. *J Am Chem Soc* 130:9543–9549
101. Geng Y, Dalhaimer P, Cai S, Tsai R, Tewari M, Minko T, Discher DE (2007) Shape effects of filaments versus spherical particles in flow and drug delivery. *Nat Nanotech* 2:249–255
102. Ghoroghchian PP, Frail PR, Susumu K, Blessington D, Brannan AK, Bates FS, Chance B, Hammer DA, Therien MJ (2005) Near-infrared-emissive polymersomes: self-assembled soft matter for in vivo optical imaging. *Proc Natl Acad Sci USA* 102:2922–2927
103. Ghoroghchian PP, Frail PR, Susumu K, Park TH, WU SP, Uyeda HT, Hammer DA, Therien MJ (2005) Broad spectral domain fluorescence wavelength modification of visible and near-infrared emissive polymersomes. *J Am Chem Soc* 127:15388–15390
104. Ghoroghchian PP, Lin JJ, Brannan AK, Frail PR, Bates FS, Therien MJ, Hammer DA (2006) Quantitative membrane loading of polymer vesicles. *Soft Matter* 2:973–980
105. Pata V, Ahmed F, Discher DD, Dan N (2004) Membrane solubilization by detergent: resistance conferred by thickness. *Langmuir* 20(10):3888–3893
106. Ruysschaert T, Sonnen AFP, Haelele T, Meier W, Winterhalter M, Fournier D (2005) Hybrid nanocapsules: interactions of ABA block copolymers with liposomes. *J Am Chem Soc* 127(17):6242–6247
107. Battaglia G, Ryan AJ (2006) Neuron-like tubular membranes made of diblock copolymer amphiphiles. *Angew Chem Int Ed* 45:2052–2056
108. Wu J, Eisenberg A (2006) Proton diffusion across membranes of vesicles of poly(styrene-*b*-acrylic acid) diblock copolymers. *J Am Chem Soc* 128:2880–2884
109. Ghoroghchian PP, Li GZ, Levine DH, Davis KP, Bates FS, Hammer DA, Therien MJ (2006) Bioresorbable vesicles formed through spontaneous self-assembly of amphiphilic poly(ethyleneoxide)-block-polycaprolactone. *Macromolecules* 39:1673–1675
110. Du J, Armes SP (2005) pH-responsive vesicles based on a hydrolytically self-cross-linkable copolymer. *J Am Chem Soc* 127:12800–12801
111. Robbins GR, Jimbo M, Swift J, Therien MJ, Hammer DA, Dmochowski IJ (2009) Photoinitiated destruction of composite porphyrin-protein polymersomes. *J Am Chem Soc* 131:3872–3874

112. Parnell AJ, Tzokova N, Topham PD, Adams DJ, Adams S, Fernyhough CM, Ryan AJ, Jones RAL (2009) The efficiency of encapsulation within surface rehydrated polymersomes. *Faraday Discuss* 143:29–46
113. Lomas H, Canton I, MacNeil S, Du J, Armes SP, Ryan AJ, Lewis AL, Battaglia G (2007) Biomimetic pH sensitive polymersomes for efficient DNA encapsulation and delivery. *Adv Mater* 19:4238–4243
114. Zheng C, Qiu L, Zhu K (2009) Novel polymersomes based on amphiphilic graft polyphosphazenes and their encapsulation of water-soluble anti-cancer drug. *Polymer* 50:1173–1177
115. Kim Y, Tewari M, Pajeroski JD, Cai S, Sen S, Williams J, Sirsi S, Lutz G, Discher DE (2009) Polymersome delivery of siRNA and antisense oligonucleotides. *J Contr Release* 134:132–140
116. Cheng Z, Tsourkas A (2008) Paramagnetic porous polymersomes. *Langmuir* 24:8169–8173
117. Ghoroghchian PP, Frail PR, Li G, Zupancich JA, Bates FS, Hammer DA, Therien AMJ (2007) Controlling bulk optical properties of emissive polymersomes through intramembranous polymer-fluorophore interactions. *Chem Mater* 19:1309–1318
118. Massignani M, Canton I, Sun T, Hearnden V, MacNeil S, Blanz A, Armes SP, Lewis A, Battaglia G (2009) Enhanced fluorescence imaging of live cells by effective cytosolic delivery of probes. Under review
119. Duncan TV, Ghoroghchian PP, Rubtsov IV, Hammer DA, Therien MJ (2008) Ultrafast excited-state dynamics of nanoscale near-infrared emissive polymersomes. *J Am Chem Soc* 130:9773–9784
120. Choi H-J, Montemagno CD (2005) Artificial organelle: ATP synthesis from cellular mimetic polymersomes. *Nano Lett* 5:2538–2542
121. Vriezema DM, Garcia PML, Oltra NS, Hatzakis NS, Kuiper SM, Nolte RJM, Rowan AE, Hest JCMv (2007) Positional assembly of enzymes in polymersome nanoreactors for cascade reactions. *Angew Chem Int Ed* 46:7378–7382
122. Yang X, Pilla S, Grailer JJ, Steeber DA, Gong S, Chen Y, Chen G (2009) Tumor-targeting, superparamagnetic polymeric vesicles as highly efficient MRI contrast probes. *J Mater Chem* 19:5812–5817
123. Kohler N, Sun C, Wang J, Zhang M (2005) Methotrexate-modified superparamagnetic nanoparticles and their intracellular uptake into human cancer cells. *Langmuir* 21(19):8858–8864
124. Gupta AK, Curtis AS (2004) Surface modified superparamagnetic nanoparticles for drug delivery: interaction studies with human fibroblasts in culture. *J Mater Sci Mater Med* 15:493–496
125. Gupta K, Gupta M (2005) Synthesis and surface engineering of iron oxide nanoparticles for biomedical applications. *Biomaterials* 26:3995–4021
126. Song HT, Choi JS, Huh YM, Kim SJ, Jun YW, Suh JS, Cheon JW (2005) Surface modulation of magnetic nanocrystals in the development of highly efficient magnetic resonance probes for intracellular labeling. *J Am Chem Soc* 127:9992–9994
127. Mueller W, Koynov K, Fischer K, Hartmann S, Pierrat S, Basche T, Maskos M (2009) Hydrophobic shell loading of PB-*b*-PEO vesicles. *Macromolecules* 42:357–361
128. Wu SP, Lee I, Ghoroghchian PP, Frail PR, Zheng G, Glickson JD, Therien MJ (2005) Bio-conjugate Chem 16:542–550
129. Ahmed F, Pakunlu RI, Brannan A, Bates F, Minko T, Discher DE (2006) Biodegradable polymersomes loaded with both paclitaxel and doxorubicin permeate and shrink tumors, inducing apoptosis in proportion to accumulated drug. *J Contr Release* 116:150–158
130. Massignani M, Canton N, Warren SP, Armes AL, Battaglia G (2009) Live immunostaining of intracellular compartments. Under review
131. Cattaneo A, Biocca S (1997) Intracellular antibodies: development and applications. Springer, Berlin
132. Sauer M, Haefele T, Graff A, Nardin C, Meier W (2001) Ion-carrier controlled precipitation of calcium phosphate in giant ABA triblock copolymer vesicles. *Chem Commun* 2452–2453

133. Nallani M, Benito SM, Onaca O, Graff A, Lindemann M, Winterhalter M, Meier W, Schwaneberg U (2006) A nanocompartment system (synthosome) designed for biotechnological applications. *J Biotechnol* 123:50–59
134. Kuiper SM, Nallani M, Vriezema DM, Cornelissen JJLM, Van Hest JCM, Nolte RJM, Rowan AE (2008) Enzymes containing porous polymersomes as nano reaction vessels for cascade reactions. *Org Biomol Chem* 6:4315–4318
135. Van Dongen SFM, Nallani M, Cornelissen JJLM, Nolte RJM, Van Hest JCM (2009) A three-enzyme cascade reaction through positional assembly of enzymes in a polymersome nanoreactor. *Chem Eur J* 15:1107–1114
136. Vriezema DM, Hoogboom J, Velonia K, Takazawa K, Christianen PCM, Maan JanC, Rowan AE, Nolte RJM (2003) Vesicles and polymerized vesicles from thiophene-containing rod-coil block copolymers. *Angew Chem Int Ed* 42:772–776
137. Friedmann T (1989) Progress toward human gene therapy. *Science* 244:1275–1281
138. Friedmann T, Robin R (1972) Gene therapy for human genetic disease? *Science* 175:949–955
139. Kay MA, Liu D, Hoogerbrugge PM (1997) Gene therapy. *Proc Natl Acad Sci USA* 94:12744–12746
140. Laporte LD, Rea JC, Shea LD (2006) Design of modular non-viral gene therapy vectors. *Biomaterials* 27:947–954
141. Thomas CE, Ehrhardt A, Kay MA (2003) Progress and problems with the use of viral vectors for gene therapy. *Nat Rev Genet* 4:346–358
142. Korobko AV, Backendorf C, Van der Maarel JRC (2006) Plasmid DNA encapsulation within cationic diblock copolymer vesicles for gene delivery. *J Phys Chem B* 110:14550–14556
143. Korobko AV, Jesse W, Van der Maarel JRC (2005) Encapsulation of DNA by cationic diblock copolymer vesicles. *Langmuir* 21(1):34–42
144. Brown MD, Schatzlein A, Brownlie A, Jack V, Wang W, Tetley L, Gray AI, Uchegbu IF (2000) Preliminary characterization of novel amino acid based polymeric vesicles as gene and drug delivery agents. *Bioconjugate Chem* 11(6):880–891
145. Brown MD, Gray AI, Tetley L, Santovena A, Rene J, Schatzlein AG, Uchegbu IF (2003) In vitro and in vivo gene transfer with poly(amino acid) vesicles. *J Contr Release* 93(2):193–211
146. Zhang L, Bartels C, Yu Y, Shen H, Eisenberg A (1997) Mesosized crystal-like structure of hexagonally packed hollow hoops by solution self-assembly of diblock copolymers. *Phys Rev Lett* 79:5034–5037
147. Chen Y, Du J, Xiong M, Guo H, Jinnai H, Kaneko T (2007) Perforated block copolymer vesicles with a highly folded membrane. *Macromolecules* 40:4389–4392
148. Grumelard J, Taubert A, Meier W (2004) Soft nanotubes from amphiphilic ABA triblock macromonomers. *Chem Commun* 13:1462–1463
149. Reiner JE, Wells JM, Kishore RB, Pfefferkorn C, Helmersen K (2006) Stable and robust polymer nanotubes stretched from polymersomes. *Proc Natl Acad Sci USA* 103:1173–1177
150. Liu F, Eisenberg A (2003) Preparation and pH triggered inversion of vesicles from poly(acrylic acid)-block-polystyrene-block-poly(4-vinyl pyridine). *J Am Chem Soc* 125:15059–15064
151. Israelachvili JN, Mitchell DJ, Ninham BW (1976) Theory of self-assembly of hydrocarbon amphiphiles into micelles and bilayers. *J Chem Soc Faraday T* 1(72):1525–1568
152. Jain S, Bates FS (2004) Consequences of nonergodicity in aqueous binary PEO-PB micellar dispersions. *Macromolecules* 37:1511–1523
153. Ahmed F, Pakunlu RI, Brannan A, Bates F, Minko T, Discher DE (2006) Biodegradable polymersomes loaded with both paclitaxel and doxorubicin permeate and shrink tumors, inducing apoptosis in proportion to accumulated drug. *J Control Release* 116:150–158
154. Katz JS, Levine DH, Davis KP, Bates FS, Hammer DA, Burdick JA (2009) Membrane stabilization of biodegradable polymersomes. *Langmuir* 25:4429–4434

155. Li F, Ketelaar T, Marcelis ATM, Leermakers FAM, Cohen Stuart MA, Sudholter EJR (2007) Stabilization of polymersome vesicles by an interpenetrating polymer network. *Macromolecules* 40:329–333
156. Nallani M, De Hoog H-PM, Cornelissen JJLM, Palmans ARA, Van Hest JCM, Nolte RJM (2007) Polymersome nanoreactors for enzymatic ring-opening polymerization. *Biomacromol* 8:3723–3728
157. Kim Y, Tewari M, Pajeroski JD, Cai S, Sen S, Williams J, Sirsi S, Lutz G, Discher DE (2009) Polymersome delivery of siRNA and antisense oligonucleotides. *J Contr Release* 134:132–140
158. Hell SW (2007) Far-field optical nanoscopy. *Science* 316(5828):1153–1158. DOI: 10.1126/science.1137395

# Reaction Vessels Assembled by the Sequential Adsorption of Polymers

Andrew D. Price, Angus P.R. Johnston, Georgina K. Such, and Frank Caruso

**Abstract** Nanoengineered polymer carriers assembled by the layer-by-layer technique are being increasingly investigated as nano- to millimeter-sized, semi-permeable reactors. The reactors are assembled by the sequential adsorption of polymers that interact primarily via electrostatic forces, hydrogen bonding, or covalent bond formation onto a sacrificial colloidal template. Controlled permeability of molecular species is key to the functioning of these reactors and a number of techniques have been developed for measuring and controlling their permeability to both small molecules and larger macromolecules. The encapsulation of enzyme “machinery” into the carriers has produced a number of reactor examples capable of small molecule conversion. Advanced assembly techniques have been used to generate reactors with relevance to biomedicine, including biosensing, controlled drug release, and biopolymer synthesis.

**Keywords** Capsules · Layer-by-layer · Multilayer films · Reaction vessels · Self-assembly

---

A.D. Price, A.P.R. Johnston, G.K. Such, and F. Caruso (✉)  
Centre for Nanoscience and Nanotechnology, Department of Chemical and Biomolecular Engineering, The University of Melbourne, Parkville, Victoria 3010, Australia  
e-mail: [fcarus@unimelb.edu.au](mailto:fcarus@unimelb.edu.au)



## Contents

1	Introduction .....	156
2	Layer-by-Layer Assembly .....	157
2.1	Layer-by-Layer Assembly – Electrostatics .....	157
2.2	Layer-by-Layer Assembly – Hydrogen Bonding .....	158
2.3	Layer-by-Layer Assembly – Hydrogen-Bonding Stabilization .....	159
2.4	Layer-by-Layer Assembly – Covalent Bonding .....	160
3	Capsule Design .....	161
3.1	Methods for Determining Permeability .....	161
3.2	Methods for Controlling Permeability .....	163
4	Microreactors Formed by LbL Assembly .....	167
4.1	Microreactors by Enzyme Post-Loading .....	168
4.2	Microreactors by Enzyme Pre-Loading .....	168
4.3	Bienzymatic Microreactors .....	172
4.4	Controlled Release Microreactors .....	173
4.5	Encapsulated (Bio)Polymer Synthesis .....	174
5	Outlook .....	174
	References .....	176

## 1 Introduction

The capacity to design nanoengineered polymer carriers is of significant interest in a range of research areas, such as biomedicine and catalysis [1, 2]. A number of approaches have been used for the assembly of such carriers, most notably the self-assembly of polymer micelles and vesicles using engineered polymeric amphiphiles [3]. A complementary technique used for the assembly of polymer carriers is based on the layer-by-layer (LbL) approach. The LbL approach was initially developed by Decher et al. [4] for the electrostatically driven sequential deposition of polyelectrolytes onto planar substrates. Later work has expanded upon the interactions that can be used for LbL assembly to include a range of non-covalent forces as well as covalent bond formation [5]. The LbL approach has attracted significant attention, as it is a simple and versatile technique which affords precise control over film characteristics. In addition, LbL assembly can be performed on a range of templates, including colloidal particles for the synthesis of spherical polymeric carriers [6, 7]. This is achieved via the assembly of a polymer film onto a colloidal surface followed by removal of the core, leaving a hollow polymeric capsule. The engineering of polymeric components chosen for LbL assembly allows the design of capsules that are responsive to external stimuli such as pH, salt concentration, and temperature. Furthermore, the capsules may be used to encapsulate a range of particles or polymeric materials with potential utility in drug therapy or catalysis. Specifically, the capacity to tune reliably the retention of cargo within the capsules is fundamental for the development of advanced microreactor systems.

This chapter will discuss the progress in the design of micron- to submillimeter-sized LbL capsule reactors in three main sections. First will be an introduction to the fundamentals that underpin the assembly of LbL films, focusing on the

main interactions used for film design including electrostatic, hydrogen-bonding and covalent interactions. Second, we will discuss how the parameters of LbL assembly affect the retention of components within the assembled capsules. Finally, prominent examples of LbL assembled microreactors and potential applications of such technology in the fields of biomedicine and micro-encapsulated catalysis will be discussed.

## 2 Layer-by-Layer Assembly

### 2.1 Layer-by-Layer Assembly – Electrostatics

The majority of LbL systems employ oppositely charged polyelectrolytes for the adsorption of polymer layers driven by electrostatic forces (Fig. 1). The assembly relies on the sequential reversal of charge upon the adsorption of oppositely charged polyelectrolytes. Polyelectrolytes may be classified as either strong or weak, with the former maintaining its charge independent of the pH, while the latter exhibits pH-dependent charge due to the presence of ionizable moieties. One of the most

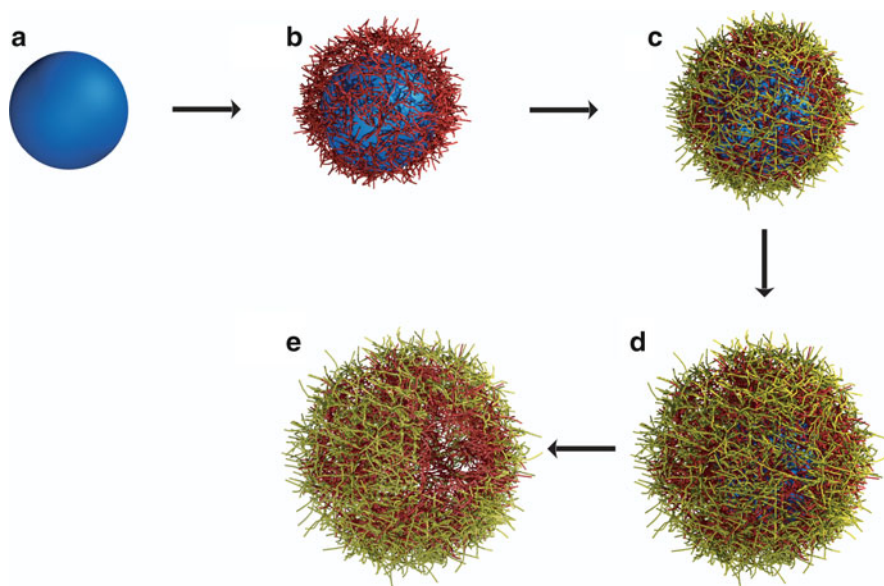


**Fig. 1** LbL assembly onto a colloidal substrate. (a) Electrostatic adsorption onto a charged template results in (b) charge reversal of the surface. (c) A second polymer layer, oppositely charged to the first, can then be deposited on the surface. (d) This process is repeated until the desired number of layers is deposited. (e) If a sacrificial template is used, the core can be removed to form a hollow capsule

commonly used polymer systems is the strong polyanion poly(styrene sulfonate) (PSS) and weak polycation poly(allylamine hydrochloride) (PAH) [8]. This particular polyelectrolyte pair has been used in numerous LbL studies due to its attractive assembly properties, including colloidal stability when assembled onto colloidal substrates [9]. Polyelectrolytes adopt a coiled conformation with increasing salt concentration due to the shielding effects on the charged groups. Correspondingly, this leads to changes in polymer deposition and the films produced. Multilayer films assembled with strong polyelectrolytes are characterized by high stability, requiring extremes in pH to disassemble. This can limit their use for some biomedical applications, as there is no inherent mechanism for degradation or controlled release. This problem may be addressed by assembling multilayer films from responsive components, such as pH responsive weak polyelectrolytes.

Weak polyelectrolytes, on the other hand, become ionized within a specific pH range, creating a mechanism for the disassembly of the polymer multilayers. The most common examples of weak polyelectrolytes include polyacids, such as poly(acrylic acid) (PAA) and poly(methacrylic acid) (PMA). A decrease in the pH below the  $pK_a$  of the polymer decreases the charge on the polymer, thus destabilizing the electrostatic interactions within the multilayers. The properties of films assembled from weak polyelectrolytes are highly dependent on the charge density, which can be tuned by both the salt concentration and pH [10].

While the majority of electrostatically assembled multilayers are stable, they may be adversely affected by conditions such as high ionic strength, extreme pH, and strong polar solvents [11]. Consequently, a variety of approaches to crosslink these films have been investigated using chemical [12], thermal [13], and photochemical [14, 15] techniques. Such stabilization can lead to changes in the film morphology and alter film permeability. For example, Möhwald [16] and coworkers crosslinked the primary amine groups of branched poly(ethyleneimine) (PEI) with glutaraldehyde (GA) assembled alternately with PAA to form capsules that possessed pH-dependent permeability. At pH 3 the walls were permeable to 2,000 kDa dextran, but above pH 6 the dextran could no longer permeate into the capsule interior.

## ***2.2 Layer-by-Layer Assembly – Hydrogen Bonding***

Another interaction that may be utilized for the assembly of LbL films is hydrogen bonding. Early work in this area was performed by both Stockton and Rubner [17] and Zhang and coworkers [18] and has become an area of intensive research with excellent reviews [19, 20]. Hydrogen bonding LbL assembly is based on the alternate deposition of polymers containing a hydrogen bond acceptor or donor. Commonly used hydrogen-bonding acceptors include poly(ethylene oxide) (PEO), where the oxygen atoms on the polymer backbone are hydrogen bonding acceptors, or poly(*N*-vinyl pyrrolidone) (PVPON), where the carbonyl groups are the acceptors. The most commonly used donors include protonated polyacids such as PMA and PAA, which

contain carboxylic acid groups that are the hydrogen bond donors. Compared to electrostatically interacting polymers, the pH range where hydrogen-bonding polymers can interact and form stable films is limited [21]. This range is dependent on the  $pK_a$  of the component polymers as well as the strength of the interaction between the hydrogen bonding pairs, as weaker hydrogen bonding in films requires a smaller number of bonds to be broken before films will disassemble. An illustration of this point are PMA/PEO and PMA/PVPON hydrogen-bonded multilayer films, the former disassembles at approximately pH 4 while the latter, being significantly more stable, disassembles at approximately pH 6.4 [19]. The strength of the hydrogen-bonding interaction also affects the thickness of the polymers deposited. Generally, in more weakly interacting polymers the growth of film thickness is exponential compared with a linear film thickness growth for strongly interacting polymers [19].

This ability to disassemble films at mild pH makes hydrogen-bonded films attractive for delivery applications, as biological cargo is often sensitive to the extremes of pH required to degrade electrostatically interacting films. Hydrogen-bonded systems also allow the incorporation of uncharged polymers such as polyethylene glycol (PEG) or PVPON, which have documented stealth properties in vivo and thus are attractive for biomedical applications [22,23]. Another class of materials that can be incorporated into hydrogen-bonded multilayers are temperature-responsive polymers such as poly(*N*-isopropylacrylamide) (PNIPAM), poly(*N*-vinylcaprolactam) (PVCL) and poly(vinyl methyl ether) (PVME). These polymers have a low critical solution temperature (LCST), a temperature at which the polymers undergo a dramatic change in solubility. The incorporation of these polymers into LbL multilayers offers the possibility to design temperature-responsive films and capsules within an appropriate range for biomedical applications. Interestingly, the deposition of thermally responsive materials has been shown to increase significantly as the temperature approaches the LCST of the polymer [24, 25].

Recently, DNA multilayer films have been designed by exploiting the unique hydrogen-bonding of DNA [26]. This approach is based on the assembly of di-block oligonucleotides, where one block of the oligonucleotide is complementary to DNA immobilized on the surface (either colloidal or planar) and the second block is free to hybridize to subsequent layers. Through rational design of the DNA sequences used in the assembly of the capsules, the specific properties of the films such as deposition [27], stability [28], and degradation [29] can be readily tuned.

### ***2.3 Layer-by-Layer Assembly – Hydrogen-Bonding Stabilization***

One potential limitation of hydrogen-bonded multilayers is that many of the polymer pairs employed in LbL assembly are not stable in the biological pH range. One approach to address this limitation is to crosslink these structures and use their pH-responsive properties to stimulate changes in the films or capsules. These films are stable over a wide pH range and often exhibit the swelling and shrinking characteristics of macroscopic hydrogels. LbL films have been crosslinked using a variety of chemical [30], thermal [31], and photochemical techniques. One

approach was introduced by Rubner et al. [30], where the PAA component of PAA/poly(acrylamide) (PAAm) multilayers was crosslinked with ethylenediamine using carbodiimide chemistry to create a PAA hydrogel. Sukhishvili and coworkers have extensively used a similar approach with polyacids such as PMA assembled with PVPON [21, 32]. In this system, when the pH was increased above the  $pK_a$  of the acid, the carboxylic acid groups became deprotonated, disrupting the hydrogen bonding. The non-crosslinked component was subsequently released from the system and a single-component hydrogel polyacid capsule was formed. These capsules underwent pH-tunable swelling and contraction due to their highly charged polymeric wall. Sukhishvili and coworkers have demonstrated the ability to tune the swelling capabilities of these capsules by the choice of the polyacid within the multilayers or by addition of a copolymer of PVPON or PVCL to create a two-phase system [21]. Photochemical crosslinking of PMA multilayers was also demonstrated by the use of thiol-ene chemistry [33].

An alternative approach to capsule stabilization was introduced by our group [34, 35]. Here, thiol-modified PMA was assembled with PVPON, which could be used to crosslink the PMA multilayers by oxidation of the thiols into disulfides. The disulfide linkages are of particular interest as they are expected to degrade upon cellular internalization due to the reductive capacity of the cellular cytosol [36]. The capacity of this material to load and release a range of biomaterials has been demonstrated, creating the foundation for a hydrogel-based microreactor system [37, 38]. The concept of disulfide-mediated degradation has been extended to other polymer systems. The assembly of alkyne-modified hydrogen-bonding polymers (PVPON<sub>ALK</sub>/PMA) followed by crosslinking with a disulfide-containing bis-azide crosslinker to form 1,2,3 triazole linkages was used to synthesize single-component PVPON capsules following release of the PMA component at elevated pH. Such hollow capsules combine the advantages of low-fouling properties and degradation within a cellular environment [39].

## ***2.4 Layer-by-Layer Assembly – Covalent Bonding***

The use of sequential covalent reactions to assemble LbL multilayers has been well studied on planar surfaces [40, 41]; however, it can be more challenging on a colloidal template due to a tendency for particle aggregation. Recently, our group developed a covalent LbL technique based on a highly quantitative click reaction between an alkyne and azide in the presence of copper to form a 1,2,3 triazole linkage. In this work, PAA was modified with either alkyne or azide groups and then the polymers were deposited sequentially in the presence of a copper catalyst [42, 43]. This approach has also been demonstrated successfully using PNIPAM [25], poly(glutamic acid) (PGA) [44], and nonlinear PEG [45]. Another approach is based on the sequential assembly of an amine-functional polymer such as PAH with glutaraldehyde [46].

### 3 Capsule Design

One of the key considerations when designing containers for encapsulated reactions is the ability to control the permeability of different components. Permeation of species through the capsule wall is primarily governed by two main factors: size exclusion (i.e., the physical entrapment) and electrostatic interactions between the encapsulated molecule and the capsule wall, although other interactions also exist. Permeability may be tailored through a combination of polymer selection (i.e., charge and  $pK_a$ ), multilayer thickness and crosslinking density. Understanding the permeability of molecular species through a polymer multilayer film is challenging, as such films do not have a well-defined “pore size.” Therefore, a number of approaches have been devised for measuring the permeability.

#### 3.1 Methods for Determining Permeability

Fluorescence Recovery After Photobleaching (FRAP) has been applied to determine the diffusion rate of fluorescently labeled low molecular weight species into polymer capsules [47, 48]. In this approach, a confocal microscope is used to image a cross-section of a capsule within a solution containing the fluorescent molecule (Fig. 2). Confocal microscopy enables the imaging of a thin optical cross section ( $\sim 400$  nm thick) by eliminating out of focus photons. A high powered laser is used to photobleach the contents of the capsule. The diffusion of fluorescent molecules into the capsule is determined by monitoring fluorescence recovery within the capsule over time. The diffusion of fluorescein [47, 48] and low molecular weight dextrans [49] into the capsules have been measured by FRAP. This technique is limited to studying

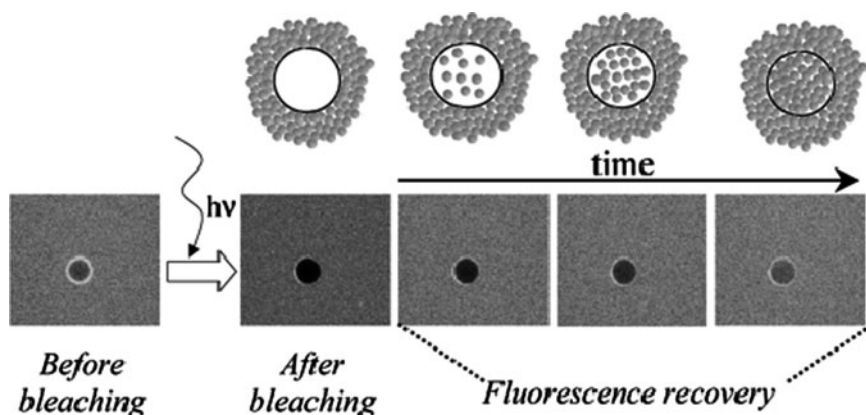


**Fig. 2** FRAP experiments to study the diffusion of low molecular weight fluorescent molecules into a capsule. Reprinted with permission from Chemistry of Materials [48]

the diffusion of relatively fast diffusing species (permeability  $>1 \times 10^{-9} \text{ m s}^{-1}$ ), as the slow diffusion of larger molecular weight species cannot be practically measured over the timeframe of a confocal microscopy experiment [49].

A qualitative measure of the permeability of the capsules can be made using confocal microscopy by simple observation of the fluorescently labeled diffusing species [50, 51]. In one study, PSS/PAH capsules were incubated in a concentrated solution of fluorescently labeled dextran and confocal microscopy was used to image a cross-section of the capsules [50]. If the fluorescent molecules permeate the capsules, a uniform fluorescence is observed both within and outside the capsules. Fluorescently labeled polydextrans of varying molecular weights have been employed to probe the permeability of capsules (see Sect. 2.2). Dextran is a highly flexible, uncharged sugar [52] that is commercially available in a wide range of molecular weights and as such is commonly used as a model molecule for examining the diffusion of different molecular weight species through a porous film. However, the uncharged nature of dextran, coupled with its high degree of flexibility and undefined tertiary structure, means that the diffusion of dextran is not necessarily similar to the diffusion of charged and/or structured molecules such as proteins and DNA.

The permeability of proteins is significantly more complicated than that of dextrans, as their permeability is affected not only by their molecular weight, but also their tertiary structure, charge, and hydrophobicity. Proteins with similar molecular weights can have significantly different diffusion rates through a polymer multilayer. Therefore, to assess the permeability of proteins through films, it is typically necessary to assess the permeability of each individual protein of interest for any particular capsule system. This method requires a significant concentration of the protein that is being investigated and is not always practical when investigating costly proteins. It is also possible to investigate the permeability by first encapsulating the protein within the capsule and examining the leakage of the protein from the capsule [53].

Another technique developed to investigate the permeability of capsules is to monitor the diffusion of DNA through the capsule wall using a molecular beacon (Fig. 3) [54, 55]. A molecular beacon is a single strand of DNA with a fluorophore and quencher at opposite ends [56]. The sequence is designed so that there are two complementary regions at either end of the strand, causing the opposite ends of the sequence to come together, forming a stem loop structure. In this conformation the fluorophore and quencher are in close proximity and the fluorescence is quenched. However, if a sequence of DNA complementary to the loop region is present, hybridization causes the separation of the fluorophore and quencher, resulting in a fluorescent signal. If the molecular beacon is immobilized inside the capsule, then the capsule can be incubated with different length DNA strands to determine the effect of strand length on the permeability through the capsule wall. One of the advantages of this technique is that it can be used to investigate the permeability of the DNA sequences without fluorescent labeling. Such modification can affect the permeability of the permeating species through the film. This system could be expanded to investigate the permeability of proteins by using aptameric beacons



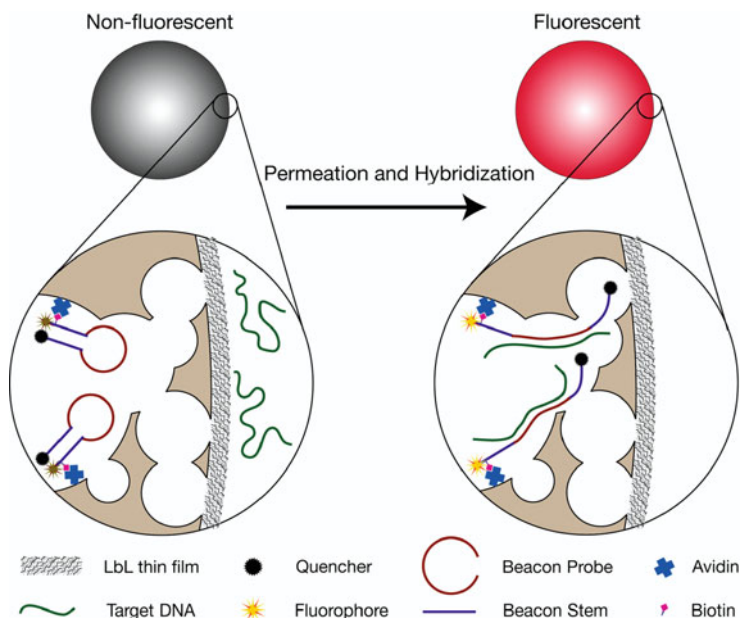


**Fig. 3** Molecular beacon approach for examining the permeability of thin films. A molecular beacon is immobilized in a porous template and the layers are assembled on the surface. The particles are incubated with DNA of different length sequences and the permeation of the DNA through the film is measured by an increase in the fluorescence of the particles. Reprinted with permission from the Journal of the American Chemical Society [55]

immobilized inside the capsule [57], and the permeability of nanoparticles could also be investigated by conjugating nucleic acid sequences to the surface of the particles.

## 3.2 Methods for Controlling Permeability

### 3.2.1 Low Molecular Weight Species

Typically, low molecular weight compounds [such as fluorescein isothiocyanate (FITC) and doxorubicin (DOX)] can freely diffuse through the capsule walls [47]. Therefore, if these molecules are to be encapsulated, additional strategies beyond standard LbL encapsulation are required. One approach for oil soluble molecules, such as DOX, is the infiltration of oil into the capsules to yield encapsulated emulsion droplets [38].

Another encapsulation method, which has been used for short peptides, involves linking them to a larger polymer by reversible disulfide linkages [37, 58]. The peptide/polymer conjugate can be either immobilized on the capsule wall or free

floating in the interior of the capsule, depending on the ability of the polymer conjugate to link covalently to the capsule.

The stable encapsulation of biological cargo is important for applications in drug delivery. However, for some applications, enhanced permeability can be advantageous, for example in the design of microreactors. In this case, diffusion of low molecular weight species can initiate and maintain reactions occurring inside the capsule (see Sect. 4).

### 3.2.2 High Molecular Weight Species

For larger molecules there are two principal factors that govern encapsulation: size and charge exclusion. Size exclusion of the cargo is directly related not only to the density of the capsule wall but also the flexibility of the permeating molecule. It is well known that single-stranded DNA (ssDNA) with a persistence length of around 1 nm [59] is a significantly more flexible molecule than double-stranded DNA (dsDNA), which has a persistence length of around 50 nm [60]. Thus ssDNA can more effectively diffuse through small pores than dsDNA.

Other properties of diffusing molecules also play an important role in their entrapment. In work by our group, it was found DNA oligomers can be effectively trapped inside negatively charged polymer capsules (Fig. 4) composed primarily of PMA [35, 61]; however, oligopeptides of a similar molecular weight freely diffuse through the capsule wall, as oligopeptides do not typically possess the same magnitude of charge as identical length oligonucleotides [58, 62]. This is principally due to the electrostatic repulsion between the negatively charged DNA and the negatively charged capsule wall. Uncharged species (like certain peptides or dextrans) can diffuse through the polymer membrane in a less hindered fashion. On the other hand, when large cargo is oppositely charged to the capsule wall, it typically electrostatically adsorbs to the capsule wall, thereby limiting its diffusion from the capsule.

There are a number of ways that permeability can be induced into the capsule wall. The most commonly exploited technique is by controlling the pH. Antipov and coworkers have shown that capsules assembled from the electrostatically interacting pair of PSS and PAH exhibit switchable porosity between the pH range 6–8 (Fig. 5) [50]. Using dextrans of different molecular weight (75 and 2,000 kDa) they found that capsules were permeable to dextran below pH 6. As the pH was increased to 7, a double population of capsules was observed with dextran excluded from some and permeating into others. Above pH 8, all capsules became impermeable. The higher molecular weight dextran (2,000 kDa) and albumin (a model protein, 65 kDa) showed a similar permeability trend to 75 kDa dextran; however, the point of exclusion into the capsule was decreased by between 0.1 and 1 pH unit. They also observed that a significant amount of dextran was lodged in the capsule wall (as observed by a bright ring of fluorescence), indicating significant adsorption to the capsule wall.

Similarly, pH can be used to control the permeability of the capsule wall in hydrogen-bonded LbL systems. Kozlovskaya et al. [32] have demonstrated in a number of studies the pH-responsive behavior of single-component polyacid

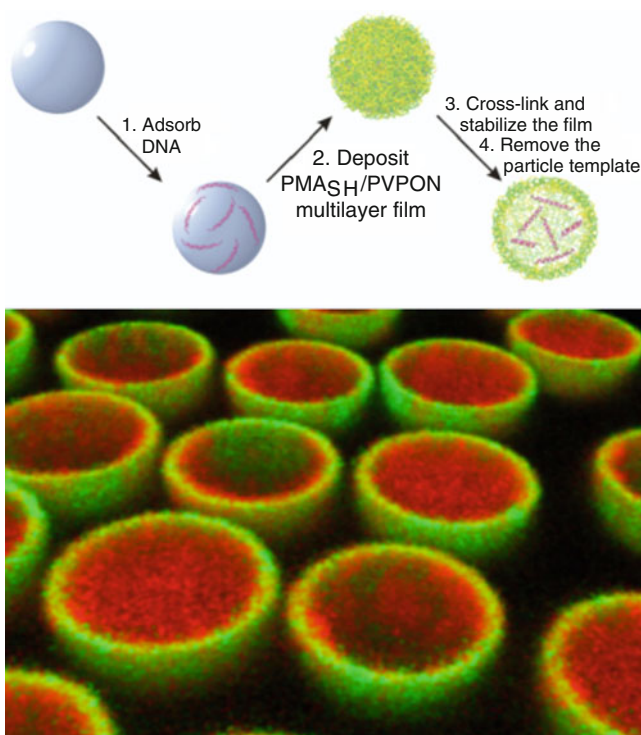


**Fig. 4** Schematic showing the assembly process used to encapsulate DNA within a thiol-modified PMA (PMA<sub>SH</sub>) (negatively charged) capsule. The DNA is electrostatically adsorbed to the silica particle surface, followed by multilayer deposition of PMA<sub>SH</sub> and PVPON at an acidic pH. Following the multilayer buildup, the PMA<sub>SH</sub> component of the layers is crosslinked by oxidation of the thiols into disulfides. Removal of the core and disruption of hydrogen-bonding by increasing the pH creates single-component PMA<sub>SH</sub> capsules (*green*) containing negatively charged DNA (*red*). Reprinted with permission from ACS Nano [61]

materials crosslinked with ethylenediamine. A recent study has shown that, by varying the  $pK_a$  of the acid side chains of these hydrogel capsules, the encapsulation and release of molecules within the capsules can be tuned over a wide pH range (from pH 5 to pH 10) [63]. Cargo can be loaded into these capsules by exploiting these changes in permeability. The cargo may be “locked” in the capsule by the subsequent reversible adsorption of a small cationic component that can be “unlocked” from the capsules under high salt concentrations (0.6 M NaCl) [32].

Similarly, Tong et al. [16] have shown that branched PEI assembled alternately with PAA and crosslinked with GA forms capsules with reversible permeability. In another study, capsules assembled from crosslinked bovine serum albumin (BSA) multilayers have been shown to have a permeability window to 155 kDa dextran below pH 4 and above pH 10 [64].

The use of pH to induce reversible changes in the permeability of capsules has been well documented; however, the film structure can also respond to other stimuli.

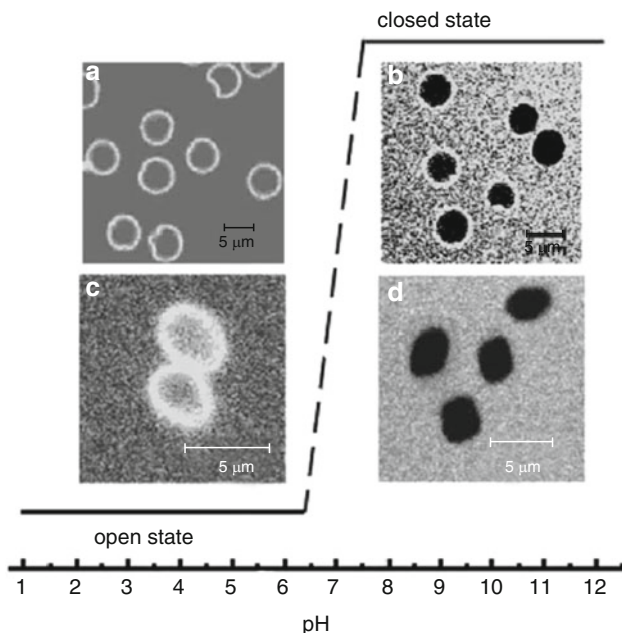


**Fig. 5** Tunable permeability of PSS/PAH capsules in response to changes in pH. At pH 2 the capsules are in an open state, with dextran able to permeate through the capsule wall; however, at pH 8, the capsule wall is impermeable to 75 kDa and 2,000 kDa FITC-labeled dextran. Reprinted with permission from *Colloids and Surfaces A* [50]

Heating the capsules can cause a structural rearrangement of the films that typically leads to shrinkage of the capsule along with a corresponding decrease in the permeability of the capsules. Kohler et al. have shown that for poly(diallyldimethyl ammonium chloride) (PDADMAC)/PSS capsules heated between 40°C and 50°C, the permeability of fluorescein and FITC-Dextran (4 and 10 kDa) decreases by about an order of magnitude (Fig. 6) [49]. Similar work by Bedard et al. has shown that control over the permeability could also be achieved by incorporating gold nanoparticles into the PDADMAC/PSS film [65]. They demonstrated that capsules containing 20 nm gold particles showed a significantly decreased permeability to 4 and 70 kDa FITC-dextran following heating.

The permeability of multilayer films can also be controlled by the extent of crosslinking. Park et al. have shown that, by including a photo-crosslinkable component into the LbL films, the permeability of the capsules can be tuned [66]. In this system, PAH was modified with benzophenone and colayered with PSS. Upon exposure to UV light the benzophenone groups were crosslinked. The release of Rhodamine B from the capsules was measured as a function of time. Capsules exposed to UV light for longer (and thus more highly crosslinked) showed slower release rates than the uncrosslinked capsules.

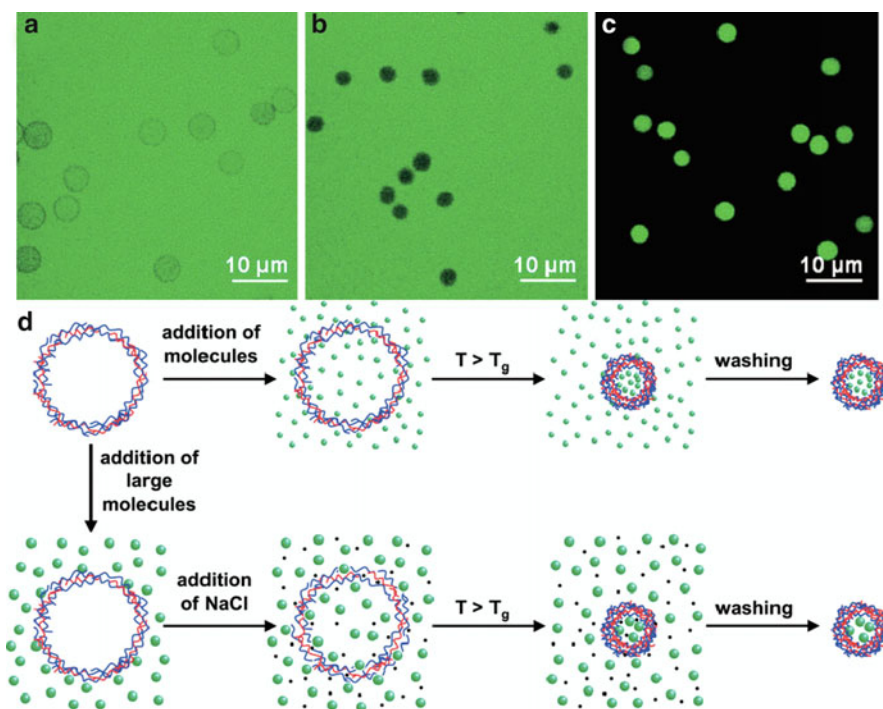


**Fig. 6** Temperature-controlled permeability of PDADMAC/PSS capsules. CLSM images of (a) capsules incubated with 10 kDa FITC-dextran before heat treatment, and (b) after heat treatment. (c) Capsules heat treated in the presence of FITC-dextran and subsequently washed to remove unencapsulated dextran. (d) Schematic showing the encapsulation process for small and large molecules. Reprinted with permission from Advanced Functional Materials [49]

## 4 Microreactors Formed by LbL Assembly

Facile control over polymer capsule construction and the wide range of polymer building blocks available make polymer capsules formed by LbL assembly excellent candidates for encapsulated biocatalysis. The permeability of polymer capsules allows reactions to be self-sustaining, due to the constant supply of reagents from the surrounding media, while affording external control of the reaction by the introduction of a chemical stimulus. The products of the reaction may accumulate or leave the capsule as determined by their interactions with the capsule wall. Typically, small molecules and ions are free to permeate the polymer walls while larger macromolecules are impermeable to the capsule walls. A number of elegant examples of encapsulated biocatalysis have been demonstrated and will be detailed in this section.

## 4.1 *Microreactors by Enzyme Post-Loading*

A fundamental requirement for encapsulated biocatalysis is the localization of the enzyme “machinery” within the microreactor assembly. For LbL microreactors, the enzyme may either be pre-loaded by assembling the capsule around the enzyme or post-loaded by diffusing the enzyme across the polymer walls of the capsule and retaining it within a preassembled capsule [67]. Post-loading is a relatively straightforward paradigm, relying on reversible changes in capsule permeability from changes in solution conditions such as pH (as discussed previously), salt concentration, and solvophobic interactions that cause a reorganization of the polymer chains comprising the capsules. For example, PSS/PAH capsules become permeable to urease by changing the solvent from a purely aqueous to a water/ethanol mixture [68]. Resuspending the capsules into an aqueous solvent, following suspension in water/ethanol with enzyme, traps the urease in the interior of the capsules. These microreactors are capable of catalyzing the hydrolysis of urea, as confirmed by a colorimetric assay. In another instance,  $\alpha$ -chymotrypsin, a proteolytic enzyme, was encapsulated in PSS/PAH capsules aided by pH-induced fluctuations in pore sizes within the capsule [69]. In acidic conditions, the pores in the polymer capsule were enlarged, enabling the enzyme to permeate the capsule. An increase in pH closed the pores, trapping the enzyme within the capsules. The entrapped enzyme remained active with the polymer shell protecting it from external inhibitors.

## 4.2 *Microreactors by Enzyme Pre-Loading*

Some enzymes can form insoluble crystals in aqueous media and such crystals may be used as templates for LbL deposition. A high loading of catalase was encapsulated in PSS/PAH capsules using a catalase crystal template [70]. LbL deposition was performed in high salt conditions to prevent significant dissolution of the enzyme and enhance polymer adsorption. The activity of the enzyme, as measured by the decomposition of hydrogen peroxide, was maintained at 97% that of the uncoated enzyme. The polymer layers protected the enzyme from degradation by proteases, further demonstrating that LbL capsules can inhibit degradation of its contents in a “harsh” environment. However, this method is limited to enzymes that form crystals in aqueous environments. Direct LbL coating of enzymes may also be achieved by the use of protein aggregates in aqueous solutions, as was demonstrated with  $\alpha$ -chymotrypsin [71, 72]. The coated aggregates exhibited controlled release from the capsules, dependent on the solution pH and number of deposited polymer layers. As directly coating enzyme aggregates requires a delicate balance of solution conditions and results in non-uniform assemblies, this technique for enzyme encapsulation has infrequently been pursued.



### 4.2.1 Microreactors from Nanostructured Particle Templates

The use of nanostructured particle templates has become the preferred method whereby enzymes may be preloaded into LbL capsules. Typically, enzymes are infiltrated into the pores of nanostructured colloids prior to their coating with polymer layers [73,74]. A number of microreactor capsules have been developed via the LbL coating of enzyme-containing, nanostructured templates. Subsequent dissolution of the template releases the enzyme in the capsule interior without chemical or physical immobilization to restrict activity. The encapsulated enzymes typically convert small molecules, which permeate the capsules, while the polymer wall protects the enzymes from high molecular weight inhibitors. Mesoporous silica (MS) colloids provide one versatile nanostructured template for enzyme encapsulation. These materials are produced via a sol-gel process that replicates the structure of self-assembled lyotropic phases. MS with a variety of pore sizes and structures have been generated [74]. The mesopores have proven large enough to allow infiltration of a range of enzymes [75]. Non-covalent adsorption of the enzyme allows a high loading to be achieved due to the surface chemistry being easily modified by silane chemistry to achieve an optimal interface for adsorption. For instance, catalase was encapsulated in poly(L-lysine) (PLL)/PGA LbL capsules by layering the polymers onto bimodal silica spheres with adsorbed catalase (Fig. 7) [76]. Dissolution of the silica template with a buffered hydrofluoric acid solution (pH  $\sim 5.5$ ) generated capsules with free-floating enzymes capable of catalyzing the decomposition

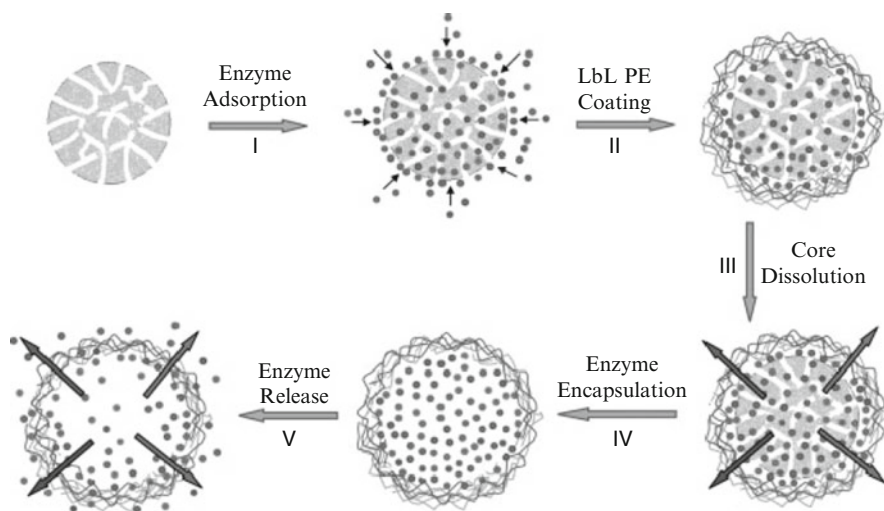


**Fig. 7** Schematic representation of the procedure for encapsulating enzyme in polyelectrolyte microcapsules using MS spheres as templates: (I) enzyme immobilization in MS spheres; (II) LbL assembly of oppositely charged polyelectrolytes (PE); (III) MS sphere template dissolution using buffered hydrofluoric acid; (IV) enzyme encapsulation in a polyelectrolyte microcapsule; and (V) enzyme release via altering the shell permeability by pH or salt changes. Reprinted with permission from Advanced Materials [76]



of hydrogen peroxide. Compared to enzyme immobilized in the silica pores prior to silica dissolution, the capsule microreactors exhibited a greater activity, emphasizing the accessibility of substrates to enzyme active sites on the spatial freedom of the enzyme within its local microenvironment. In a separate example, urease was encapsulated in PLL/PGA capsules with the aid of mesoporous silica templates [77]. Mineralization of calcium carbonate occurred within the peptide capsules by urease-catalyzed hydrolysis of urea in the presence of calcium ions.

Calcium carbonate templates are alternative nanostructured templates for enzyme infiltration and LbL assembly. Their high surface areas ( $8.8 \text{ m}^2 \text{ g}^{-1}$ ) and pore sizes (20–60 nm) allow the infiltration and surface adsorption of relatively high amounts of protein [78]. Capsule microreactors capable of converting hydrogen peroxide by encapsulated horseradish peroxidase (HRP) were assembled with the assistance of calcium carbonate templates [79]. The PSS/PAH capsules were demonstrated to increase the resistance of the HRP to heat denaturation. A similar technique was used for creating LbL microreactors of PLL/PGA capable of reducing dissolved oxygen to hydrogen peroxide in the presence of glucose by encapsulated glucose oxidase (GOx) [80]. An interesting finding of this study is that the addition of polyethylene glycol (PEG) to the solutions of PLL and PGA inhibited desorption of the enzyme during capsule assembly. Protein desorption during capsule assembly is a persistent problem that can be limited by judicious choice of enzyme and polymers. In this instance, the PEG likely creates an environment whereby the enzyme remains preferentially adsorbed to the pore surfaces.

Coprecipitation of calcium carbonate particles in the presence of macromolecular encapsulants may increase their loading into the carbonate templates [53]. Compared to physical adsorption, coprecipitation increased the loading of  $\alpha$ -chymotrypsin in calcium carbonate precipitates nearly fivefold. Following their coating with PSS/PAH layers and dissolution of the carbonate core, the activity of the enzyme was demonstrated. Calcium carbonate templates are easily decomposed in acidic conditions or at neutral pH by the chelating agent ethylenediaminetetraacetic acid (EDTA). Such mild decomposition protects fragile biomolecular encapsulants. However, carbonate templates are often difficult to prepare with reliable shape and size regularity and dissolve in acidic conditions, excluding their use as LbL templates for polymer systems that interact via hydrogen bonding (e.g., PMA and PVPON). Nevertheless, their versatility has been used for creating a number of microreactors.

#### 4.2.2 Microreactors from Self-Assembled and Gel Colloids

In addition to porous templates, fluid-like and gel colloids may be employed as templates for LbL assembly, allowing the enzyme to remain immobilized in a fluid environment without physical adsorption or entrapment. Layering hydrogel microbeads in particular has proven effective in preventing enzymes from leaching out of the inner hydrogel. This is a problem frequently encountered for enzyme immobilization in hydrogels, particularly those with large surface area to volume ratios.

A commonly used alginate hydrogel formed by ionic crosslinking was fabricated into micron-sized spheres containing GOx by an emulsification process [81]. Coating with polymers via LbL assembly effectively reduced enzyme leaching from the hydrogel microspheres while the activity of the enzyme was preserved. A reverse-phase LbL procedure may be used to encapsulate a hydrogel microbead in a polymer thin film, as has been demonstrated with agarose [82]. Following emulsification of the agarose in an organic phase, the hydrogel beads were coated with charged colloids and layered with polymers directly from an organic phase. Fabrication by this method allowed the agarose microbeads to be coated with a polymer thin film with only negligible leaching of water soluble components immobilized in the agarose. For example, the bienzyme system of GOx and HRP immobilized into polymer-coated hydrogel beads assembled by the reverse-phase LbL method retained reaction capability, albeit at significantly reduced rates compared to free enzyme due to diffusion barriers encountered by substrates and reaction intermediates [82]. While hydrogel microbeads coated with polymer thin films by LbL have demonstrated their effectiveness as microreactors by inhibiting the leaching of enzyme encapsulants, the inner hydrogels present significant diffusion barriers, as compared to hollow capsules. Additionally, these colloidal microreactors are limited to larger micron-sized assemblies due to limitations of the emulsification process required for forming the bead templates.

Directly coating liposomes with polymers via LbL, a composite assembly termed the layersome, presents a viable method for obtaining homogeneously sized polymer nanoreactors while maintaining the enzyme in a benign aqueous environment during assembly [83,84]. The liposomes of the assembled system may be left intact, creating a shell-in-shell structure or dissolved, creating the characteristic permeability of LbL thin films. In a demonstration of nanoreactor functionality, the ability of encapsulated acetylcholinesterase to convert acetylthiocholine (liposome impermeable) and *O*-nitrophenyl acetate (liposome permeable) was measured in layersomes with the liposome vesicle solubilized and left intact, respectively [84]. Despite the ability to encapsulate a wide range of water soluble and insoluble cargo in nanometer-sized vessels, layersomes are particularly laborious to fabricate. Time intensive procedures such as dialysis must be used to remove excess polymer following the adsorption of each layer. An alternative liposome/polymer composite capsule, termed capsosomes, incorporates thousands of liposomal subcompartments into a polymer carrier capsule formed by LbL assembly [85]. Like layersomes, the polymer carrier capsule provides a structurally stable scaffold, while the liposomal subcompartments are suitable for efficient entrapment and protection of small and/or fragile (bio)molecules [86]. Advanced capsosome assembly employs cholesterol-modified polymers as a means to anchor non-covalently a controlled amount of liposomes within the polymer film [87]. These subcompartmentalized vessels have proven to preserve the activity of an entrapped model enzyme,  $\beta$ -lactamase, and have a cargo retention time of at least two weeks (Fig. 8). Unlike layersomes, capsosomes may be assembled using standard techniques for LbL assembly of polymers onto colloids, enabling relative ease of fabrication.

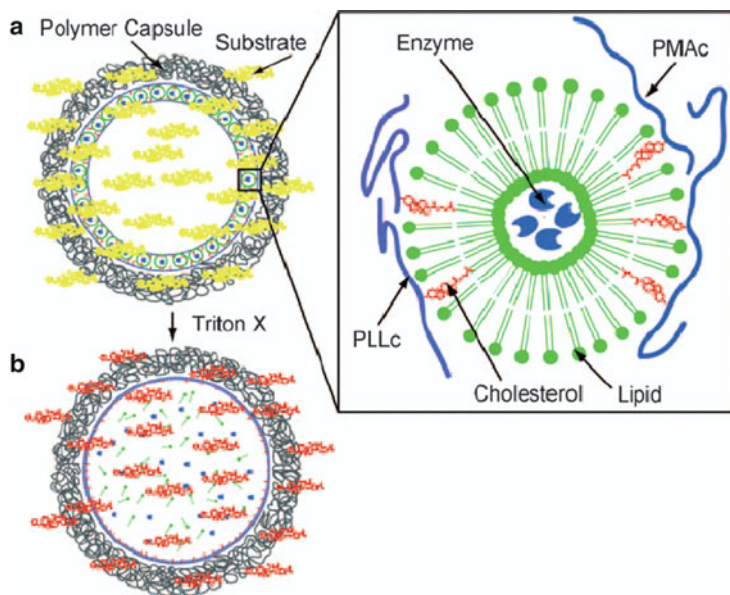


**Fig. 8** Representation of a capsosome. (a) The enzyme  $\beta$ -lactamase is preloaded into liposomes and is sandwiched between two cholesterol-modified polymers, which are then embedded inside a polymer capsule. (b) Upon addition of Triton X, the liposomes are destroyed and the enzyme is released, thus causing the hydrolysis of nitrocefin. Reprinted with permission from *Angewandte Chemie, International Edition* [86]

### 4.3 Bienzymatic Microreactors

The coupled reaction of HRP and GOx is one of the classical bienzymatic systems used for the detection of glucose. GOx catalyzes the oxidation of glucose producing hydrogen peroxide ( $\text{H}_2\text{O}_2$ ) which, in the presence of an electron donor, acts as a substrate for HRP. The reaction by HRP is ideally proportional to the amount of  $\text{H}_2\text{O}_2$  produced in the first reaction. When encapsulated within a single capsule, a coupled catalytic reaction takes place within a limited space. This potentially increases the sensitivity of the reaction to glucose detection while creating a diffusion barrier for the glucose substrate. In one example, these enzymes were coencapsulated within PSS/PAH capsules. The enzymes readily perform the coupling reaction with a glucose substrate, albeit at a significantly reduced level of activity from that observed for free enzyme [88]. The decreased activity was attributed to diffusion limitations of the glucose through the capsule walls, despite a higher concentration of enzyme being localized within the polymer walls. A biomimetic variation of the bienzymatic system is the spatial separation of the two enzymes in a shell-in-shell microcapsule (Fig. 9) [89]. Here, peroxidase (POD) is encapsulated within an inner PSS/PAH capsule surrounded by an outer PSS/PAH capsule containing GOx. Subjecting a PSS/PAH-coated calcium carbonate core-shell particle to a second precipitation forms the shell-in-shell structure following coating the outer shell with

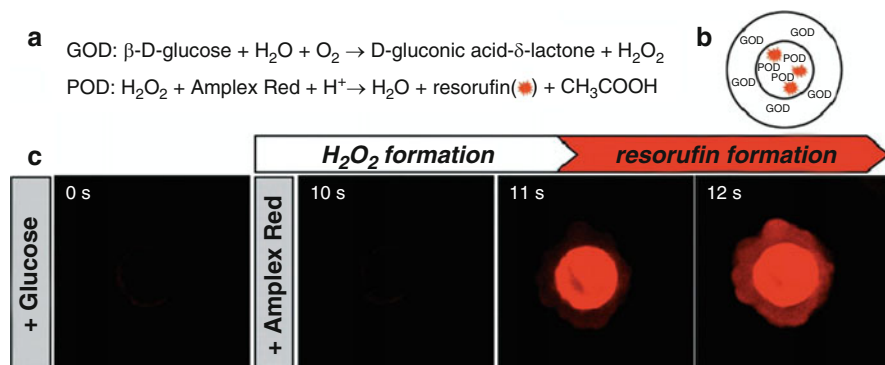


**Fig. 9** Coupled enzymatic test using glucose oxidase (GOx) and peroxidase (POD) in shell-in-shell capsules. **(a)** Reaction schemes. **(b)** Localization of GOx and POD within shell-in-shell capsules. **(c)** CLSM imaging in situ of resorufin formation. Reprinted with permission from *Angewandte Chemie International Edition* [89]

the polymers and dissolution of the carbonate template by EDTA. Glucose readily diffuses into the structure where GOx in the outer shell produces  $\text{H}_2\text{O}_2$ , which may diffuse into the inner shell. The use of the indicator amplex red as the electron donor allows the activity of POD in the inner compartment to be visualized by fluorescence.

#### 4.4 Controlled Release Microreactors

LbL-assembled capsules may function for the controlled release of therapeutics. One approach to release is to encapsulate the enzyme(s), along with the therapeutic, that upon enzyme activation releases the drug. This approach was taken to demonstrate the release of DNA as a model therapeutic within self-degrading capsules [90]. DNA, along with proteolytic enzymes, were encapsulated within a biodegradable, polypeptide capsule assembled by LbL deposition of poly(arginine) and poly(aspartic acid) onto calcium carbonate particles formed by the coprecipitation method. Upon dissolution of the carbonate template, the enzymes began degrading the capsule, thereby releasing the DNA. The rate of DNA release could be tuned by varying the amount of coencapsulated enzyme. Another instance of controlled release was seen by the coencapsulation of DNA and DNase I, a nuclease, within a PMA capsule stabilized by biodegradable disulfide linkages [91]. Intact, the DNA remained trapped; however, the triggered activation of the enzyme by a chemical stimulant caused the digestion of the DNA into smaller pieces that permeated the capsule walls. This function is reminiscent of the cellular lysosome and demonstrates a triggered enzyme-catalyzed modification (and release) of a potential therapeutic from a microreactor assembly.

## 4.5 Encapsulated (Bio)Polymer Synthesis

The permeability of LbL-assembled capsules makes them ideal microreactor candidates for encapsulated synthesis and the entrapment of macromolecules. Small monomers permeate the capsule walls where an entrapped enzyme catalyzes their polymerization. The final macromolecule often remains trapped within the capsule, although this is dependent on the final size, charge, and shape of the polymer and its interactions with the capsule walls. For example, PSS/PAH capsules loaded with HRP readily synthesize a phenolic polymer from phenol monomers [92]. The capsules fill with polymer that remains entrapped, primarily via size exclusion. A natural progression for LbL microreactor technology is the encapsulated synthesis of biomacromolecules such as nucleic acids. Not only does this open up new possibilities for multiplexed biosynthesis and detection, but also creates the possibility of a single reaction vessel being used for the synthesis and delivery of biomolecular therapeutics. The encapsulated synthesis of DNA by polymerase chain reaction (PCR) and RNA by a phage RNA polymerase has been reported. In the former case, PSS/PAH layered agarose beads containing the macromolecular essentials of PCR (a DNA polymerase, DNA template, and primers) are filled with DNA upon thermocycling in the presence of externally introduced nucleotide monomers [93]. Though the large size and nondegradability of the capsules excludes them from biomedical usage, the isolated reaction of each capsule creates a promising platform for carrying out multiplexed PCR. The other demonstration of nucleic acid synthesis within LbL capsules is the encapsulated synthesis of RNA within monodispersed, micron-sized PMA capsules [94]. A DNA template containing a promoter sequence specific to phage RNA polymerase was entrapped within the capsules. The promoter sequence is necessary for binding of the polymerase to the DNA and initiation of RNA synthesis. The capsules comprised of the PMA hydrogel are sufficiently permeable to the enzyme. In the appropriate reaction conditions (presence of nucleotides, cofactors, temperature, etc.) the enzyme binds the promoter sequence and synthesizes RNA. The RNA product accumulated within the capsules with the encapsulated RNA concentration being simply controlled by reaction time (Fig. 10). An advantage to this technology is that the PMA capsules have been specifically designed for drug delivery applications and have been proven nontoxic to various cell lines [37, 58]. The synthesis and subsequent delivery of RNA therapeutics with the same vessel acting as both microreactor and drug delivery vehicle should therefore be possible.

## 5 Outlook

These sections have presented the efforts of numerous researchers toward the realization of microencapsulated biocatalysis within LbL-assembled vessels. While many of the examples demonstrate proof-of-concept enzyme encapsulation and small molecule conversion, we note an increasing trend toward the application

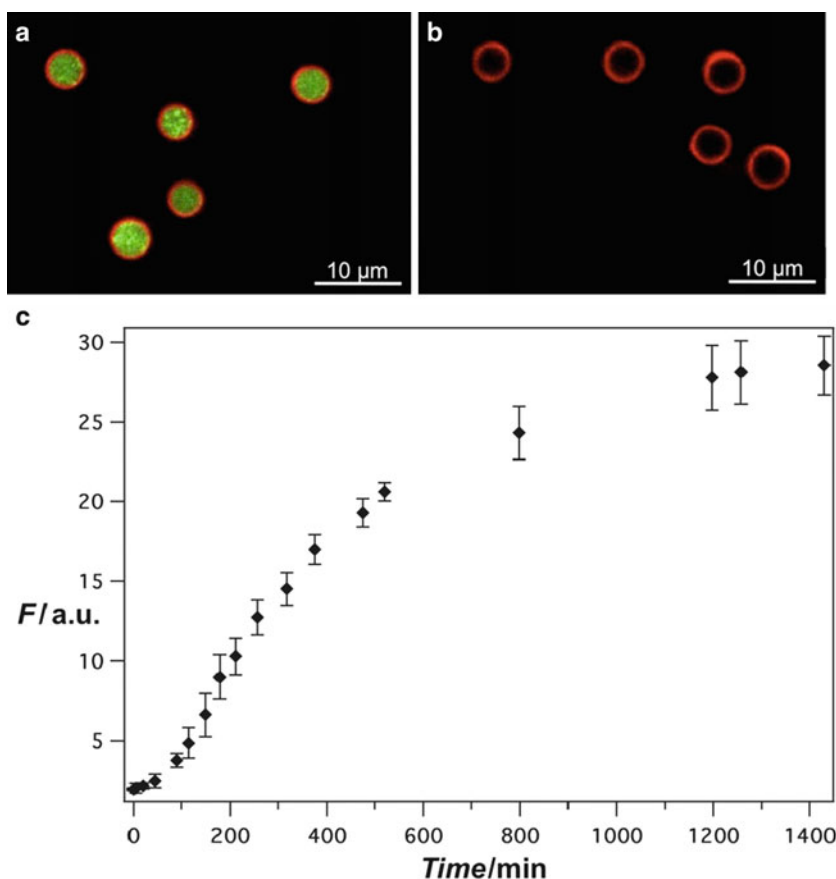


**Fig. 10** The incorporation of fluorescently labeled uridine 5'-triphosphate (*green*) allows the synthesized RNA within the PMA capsules to be measured. CLSM is used to observe RNA accumulation inside 4.35  $\mu\text{m}$  diameter capsules (**a**) containing dsDNA templates with a promoter sequence, while (**b**) capsules containing dsDNA without a promoter sequence show no evidence of transcription. Capsules are fluorescently labeled (*red*). (**c**) Flow cytometry is used to measure the progress of RNA synthesis within unlabeled 1.35  $\mu\text{m}$  diameter PMA capsules. Relative fluorescence,  $F$ , from labeled RNA is expressed as arbitrary units. Reprinted with permission from Advanced Materials [94]

of LbL microreactors for biomedicine with the potential for drug delivery and cellular/organelle mimicry [95]. This will pose enormous challenges and even greater rewards as LbL capsules typically span a size range ( $\sim 300\text{ nm}$ – $5\text{ }\mu\text{m}$ ) often inaccessible to micro/nanoreactors created by emulsification, microfluidic, and self-assembly methods. Moving away from the use of model enzymes (HRP, catalase, etc.) to biologically relevant biocatalysts will most likely prove challenging due primarily to a loss in enzyme activity due to interaction with the capsule constituent polymers. Such studies have already shown that biologically significant enzymes in

PSS/PAH LbL microreactors usually exhibit residual activity that is rather low [96]. However, these findings do not diminish the future potential of LbL-assembled microreactors, as a judicious choice of the enzyme/polymer capsule system will likely mitigate the effect.

## References

1. Kiick K (2007) Polymer therapeutics. *Science* 317:1182–1183
2. Duncan R (2003) The dawning era of polymer therapeutics. *Nat Rev Drug Discov* 2:347–360
3. Lensen D, Vriezema DM, van Hest JCM (2008) Polymeric microcapsules for synthetic applications. *Macromol Biosci* 8:991–1005
4. Decher G, Hong JD (1991) Buildup of ultrathin multilayer films by a self-assembly process. II. Consecutive absorption of anionic and cationic bipolar amphiphiles and polyelectrolytes on charged surfaces. *Ber Bunsen Ges Phys Chem* 95:1430–1434
5. Quinn JF, Johnston APR, Such GK, et al. (2007) Next generation, sequentially assembled ultrathin films: beyond electrostatics. *Chem Soc Rev* 36:707–718
6. Caruso F, Caruso RA, Moehwald H (1998) Nanoengineering of inorganic and hybrid hollow spheres by colloidal templating. *Science* 282:1111–1114
7. Donath E, Sukhorukov GB, Caruso F, et al. (1998) Novel hollow polymer shells by colloid-templated assembly of polyelectrolytes. *Angew Chem Int Ed* 37:2202–2205
8. Kurth DG, Volkmer D, Klitzing RV (2003) Multilayers on solid planar substrates: from structure to function. In: Decher G, Schlenoff JB (eds) *Multilayer thin films*. Wiley-VCH, Weinberg
9. Caruso F, Sukhorukov G (2003) Coated colloids: preparation, characterization, assembly and utilization. In: Decher G, Schlenoff JB (eds) *Multilayer thin films*. Wiley-VCH, Weinberg
10. Shiratori SS, Rubner R (2000) pH-dependent thickness behavior of sequentially absorbed layers of weak polyelectrolytes. *Macromolecules* 33:4213–4219
11. Tong W, Gao C (2008) Multilayer microcapsules with tailored structures for bio-related applications. *J Mater Chem* 18:3799–3812
12. Tong W, Gao C, Möhwald H (2005) Manipulating the properties of polyelectrolyte capsules by glutaraldehyde cross-linking. *Chem Mater* 4610–4616
13. Harris JJ, DeRose PM, Bruenig ML (1999) Synthesis of passivating, nylon-like coatings through cross-linking of ultrathin polyelectrolyte films. *J Am Chem Soc* 121:1978–1980
14. Sun J, Wu T, Sun J, et al. (1998) Fabrication of covalently attached multilayer via photolysis of layer-by-layer self-assembled films containing diazo-resins. *Chem Commun* 17:1853–1855
15. Pastoriza-Santos I, Schöler B, Caruso F (2001) Core-shell colloids and hollow polyelectrolyte capsules based on diazoresins. *Adv Funct Mater* 11:122–128
16. Tong W, Gao C, Möhwald H (2006) Stable weak polyelectrolyte microcapsules with pH-responsive permeability. *Macromolecules* 39:335–340
17. Stockton WB, Rubner MF (1997) Molecular-level processing of conjugated polymers. 4. Layer-by-layer manipulation of polyaniline via hydrogen-bonding interactions. *Macromolecules* 30:2717–2725
18. Wang L, Wang ZQ, Zhang X, et al. (1997) A new approach for the fabrication of an alternating multilayers film of poly(4-vinylpyridine) and poly(acrylic acid) based on hydrogen bonding. *Macromol Rapid Commun* 18:509–514
19. Kharlampiev E, Sukhishvili SA (2006) Hydrogen-bonded layer-by-layer polymer films. *Macromol Sci Part C: Polymer Rev* 46:377–395
20. Kozlovskaya V, Kharlampieva E, Erel I, et al. (2009) Multilayer-derived, ultrathin, stimuli-responsive hydrogels. *Soft Matter* 5:4077–4087
21. Kozlovskaya VA, Shamaev A, Sukhishvili SA (2008) Tuning swelling pH and permeability of hydrogel multilayer capsules. *Soft Matter* 4:1499–1507



22. Wattendorf U, Kreft O, Textor M, et al. (2008) Stable stealth function for hollow polyelectrolyte microcapsules through a poly(ethylene glycol) grafted polyelectrolyte adlayer. *Biomacromolecules* 9:100–108
23. Zelikin AN, Such GK, Postma A, et al. (2007) Poly(vinylpyrrolidone) for bioconjugation and surface ligand immobilization. *Biomacromolecules* 8:2950–2953
24. Quinn JF, Caruso F (2004) Facile tailoring of film morphology. *Langmuir* 20:20–22
25. Huang C-J, Chang F-C (2009) Using click chemistry to fabricate ultrathin thermoresponsive microcapsules through direct covalent layer-by-layer assembly. *Macromolecules* 42:5155–5166
26. Johnston APR, Read ES, Caruso F (2005) DNA multilayer films on planar and colloidal supports: sequential assembly of like-charged polyelectrolytes. *Nano Lett* 5:953–956
27. Johnston APR, Mitomo H, Read ES, et al. (2006) Compositional and structural engineering of DNA multilayer films. *Langmuir* 22:3251–3258
28. Lee L, Johnston APR, Caruso F (2008) Manipulating the salt and thermal stability of DNA multilayer films via oligonucleotide length. *Biomacromolecules* 9:3070–3078
29. Johnston APR, Lee L, Wang Y, et al. (2009) Controlled degradation of DNA capsules with engineered restriction-enzyme cut sites. *Small* 5:1418–1421
30. Yang SY, Rubner MF (2002) Micropatterning of polymer thin films with pH-sensitive cross-linkable hydrogen-bonded polyelectrolyte multilayers. *J Am Chem Soc* 124:2100–2101
31. Yang SY, Lee D, Cohen RE, et al. (2004) Bioinert solution-cross-linked-hydrogen-bonded multilayers on colloidal particles. *Langmuir* 20:5978–5981
32. Kozlovskaya VA, Kharlampieva EP, Mansfield ML, et al. (2006) Poly(methacrylic acid) hydrogel films and capsules: response to pH and ionic strength, and encapsulation of macromolecules. *Chem Mater* 5:328–336
33. Connal LA, Kinnane CR, Zelikin AN, et al. (2009) Stabilization and functionalization of polymer multilayers and capsules via thiol-ene click chemistry. *Chem Mater* 21:27–30
34. Zelikin AN, Quinn JF, Caruso F (2006) Disulfide cross-linked polymer capsules: en route to biodeconstructible systems. *Biomacromolecules* 7:27–30
35. Zelikin AN, Li Q, Caruso F (2006) Degradable polyelectrolyte capsules filled with oligonucleotide sequences. *Angew Chem Int Ed* 45:7743–7745
36. Becker AL, Zelikin AN, Johnston APR, et al. (2009) Tuning the formation and degradation of layer-by-layer assembled polymer hydrogel microcapsules. *Langmuir*. doi:10.1021/la901687a
37. De Rose R, Zelikin AN, Johnston APR, et al. (2008) Binding, internalization, and antigen presentation of vaccine-loaded nanoengineered capsules in blood. *Adv Mater* 20:4698–4703
38. Sivakumar S, Bansal V, Cortez C, et al. (2009) Degradable, surfactant-free, monodisperse polymer-encapsulated emulsions as anticancer drug carriers. *Adv Mater* 21:1820–1824
39. Kinnane CR, Such GK, Antequera-Garcia G, et al. (2009) Low-fouling poly(*N*-vinyl pyrrolidone) capsules with engineered degradable properties. *Biomacromolecules* 10:2839–2846
40. Kohli P, Blanchard GJ (2000) Applying polymer chemistry to interfaces: layer-by-layer and spontaneous growth of covalently bound multilayers. *Langmuir* 16:4655–4661
41. Serizawa T, Nanemeki K, Yamanoto K, et al. (2002) Thermoresponsive ultrathin hydrogels prepared by sequential chemical reactions. *Macromolecules* 35:2184–2189
42. Such GK, Quinn JF, Quinn A, et al. (2006) Assembly of ultrathin polymer multilayer films by click chemistry. *J Am Chem Soc* 128:9318–9319
43. Such GK, Tjijto E, Postma A, et al. (2007) Ultrathin, responsive polymer click capsules. *Nano Lett* 7:1706–1710
44. Ochs CJ, Such GK, Stadler B, et al. (2008) Low-fouling, biofunctionalized and biodegradable click capsules. *Biomacromolecules* 9:3389–3396
45. Kinnane CR, Wark K, Such GK, et al. (2009) Peptide-functionalized, low-biofouling click multilayers for promoting cell adhesion and growth. *Small* 5:444–448
46. Tong W, Gao C, Möhwald H (2006) Single polyelectrolyte microcapsules fabricated by glutaraldehyde-mediated covalent layer-by-layer assembly. *Macromol Rapid Commun* 27:2078–2083
47. Ibarz G, Dahne L, Donath E, et al. (2002) Resealing of polyelectrolyte capsules after core removal. *Macromol Rapid Commun* 23:474–478

48. Ibarz G, Dahne L, Donath E, et al. (2002) Controlled permeability of polyelectrolyte capsules via defined annealing. *Chem Mater* 14:4059–4062
49. Köhler K, Sukhorukov GB (2007) Heat treatment of polyelectrolyte multilayer capsules: a versatile method for encapsulation. *Adv Funct Mater* 17:2053–2061
50. Antipov AA, Sukhorukov GB, Leporatti S, et al. (2002) Polyelectrolyte multilayer capsule permeability control. *Colloids Surf A* 198:535–541
51. Berth G, Voigt A, Dautzenberg H, et al. (2002) Polyelectrolyte complexes and layer-by-layer capsules from chitosan/chitosan sulfate. *Biomacromolecules* 3:517–524
52. White JA, Deen WM (2002) Agarose-dextran gels as synthetic analogs of glomerular basement membrane: water permeability. *Biophys J* 82:2081–2089
53. Petrov AI, Volodkin DV, Sukhorukov GB (2005) Protein-calcium carbonate coprecipitation: a tool for protein encapsulation. *Biotechnol Progr* 21:918–925
54. Angelatos AS, Johnston APR, Wang Y, et al. (2007) Probing the permeability of polyelectrolyte multilayer capsules via a molecular beacon approach. *Langmuir* 23:4554–4562
55. Johnston APR, Caruso F (2005) A molecular beacon approach to measuring the DNA permeability of thin films. *J Am Chem Soc* 127:10014–10015
56. Tyagi S, Kramer FR (1996) Molecular beacons: probes that fluoresce upon hybridization. *Nat Biotechnol* 14:303–308
57. Lee JF, Stovall GM, Ellington AD (2006) Aptamer therapeutics advance. *Curr Opin Chem Biol* 10:282–289
58. Chong SF, Sexton A, De Rose R, et al. (2009) A paradigm for peptide vaccine delivery using viral epitopes encapsulated in degradable polymer hydrogel capsules. *Biomaterials* 30:5178–5186
59. Hagerman PJ (1988) Flexibility of DNA. *Annu Rev Biophys Chem* 17:265–286
60. Levicky RL, Herne TM, Tarlov MJ, et al. (1998) Using self-assembly to control the structure of DNA monolayers on gold: a neutron reflectivity study. *J Am Chem Soc* 120:9787–9792
61. Zelikin AN, Becker AL, Johnston APR, et al. (2007) A general approach for DNA encapsulation in degradable polymer microcapsules. *ACS Nano* 1:63–69
62. De Rose R, Zelikin AN, Johnston APR, et al. (2008) Binding, internalization, and antigen presentation of vaccine-loaded nanoengineered capsules in blood. *Adv Mater* 20:4698–4703
63. Kozlovskaya VA, Kharlampieva EP, Erel-Unal I, et al. (2009) Single-component layer-by-layer weak polyelectrolyte films and capsules: loading and release of functional molecules. *Polym Sci Ser A* 51:719–729
64. Tong W, Gao C, Mohwald H (2008) pH-responsive protein microcapsules fabricated via glutaraldehyde mediated covalent layer-by-layer assembly. *Colloid Polym Sci* 286:1103–1109
65. Bédard MF, Braun D, Sukhorukov GB, et al. (2008) Toward self-assembly of nanoparticles on polymeric microshells: near-IR release and permeability. *ACS Nano* 2:1807–1816
66. Park MK, Deng S, Advincula R (2004) Permeability and permselectivity control in photo-cross-linkable polyelectrolyte ultrathin films containing pH-switchable and benzophenone functional groups. *Polym Mater Sci Eng* 90:133–134
67. Johnston APR, Cortez C, Angelatos AS, et al. (2006) Layer-by-layer engineered capsules and their applications. *Curr Opin Colloid Interface Sci* 11:203–209
68. Lvov Y, Antipov AA, Mamedov A, et al. (2001) Urease encapsulation in nanoorganized microshells. *Nano Lett* 1:125–128
69. Tiourina OP, Antipov AA, Sukhorukov GB, et al. (2001) Entrapment of alpha-chymotrypsin into hollow polyelectrolyte microcapsules. *Macromol Biosci* 1:209–214
70. Caruso F, Trau D, Mohwald H, et al. (2000) Enzyme encapsulation in layer-by-layer engineered polymer multilayer capsules. *Langmuir* 16:1485–1488
71. Balabushevitch NG, Sukhorukov GB, Moroz NA, et al. (2001) Encapsulation of proteins by layer-by-layer adsorption of polyelectrolytes onto protein aggregates: factors regulating the protein release. *Biotechnol Bioeng* 76:207–213
72. Volodkin DV, Balabushevitch NG, Sukhorukov GB, et al. (2003) Inclusion of proteins into polyelectrolyte microparticles by alternative adsorption of polyelectrolytes on protein aggregates. *Biochem-Moscow* 68:236–241

73. Wang Y, Angelatos AS, Caruso F (2008) Template synthesis of nanostructured materials via layer-by-layer assembly. *Chem Mater* 20:848–858
74. Wang Y, Price AD, Caruso F (2009) Nanoporous colloids: building blocks for a new generation of structured materials. *J Mater Chem* 19:6451–6464
75. Wang Y, Caruso F (2005) Mesoporous silica spheres as supports for enzyme immobilization and encapsulation. *Chem Mater* 17:953–961
76. Yu AM, Wang Y, Barlow E, et al. (2005) Mesoporous silica particles as templates for preparing enzyme-loaded biocompatible microcapsules. *Adv Mater* 17:1737–1741
77. Yu AM, Gentle I, Lu GQ, et al. (2006) Nanoassembly of biocompatible microcapsules for urease encapsulation and their use as biomimetic reactors. *Chem Commun* 2150–2152
78. Volodkin DV, Petrov AI, Prevot M, et al. (2004) Matrix polyelectrolyte microcapsules: new system for macromolecule encapsulation. *Langmuir* 20:3398–3406
79. Volodkin DV, Larionova NI, Sukhorukov GB (2004) Protein encapsulation via porous  $\text{CaCO}_3$  microparticles templating. *Biomacromolecules* 5:1962–1972
80. Zhi ZL, Haynie DT (2006) High-capacity functional protein encapsulation in nanoengineered polypeptide microcapsules. *Chem Commun* 147–149
81. Srivastava R, Brown JQ, Zhu HG, et al. (2005) Stable encapsulation of active enzyme by application of multilayer nanofilm coatings to alginate microspheres. *Macromol Biosci* 5:717–727
82. Mak WC, Bai J, Chang XY, et al. (2009) Matrix-assisted colloidosome reverse-phase layer-by-layer encapsulating biomolecules in hydrogel microcapsules with extremely high efficiency and retention stability. *Langmuir* 25:769–775
83. Ciobanu M, Heurtault B, Schultz P, et al. (2007) Layersome: development and optimization of stable liposomes as drug delivery system. *Int J Pharm* 344:154–157
84. Germain M, Grube S, Carriere V, et al. (2006) Composite nanocapsules: lipid vesicles covered with several layers of crosslinked polyelectrolytes. *Adv Mater* 18:2868–2871
85. Stadler B, Chandrawati R, Goldie K, et al. (2009) Capsosomes: subcompartmentalizing polyelectrolyte capsules using liposomes. *Langmuir* 25:6725–6732
86. Stadler B, Chandrawati R, Price AD, et al. (2009) A microreactor with thousands of sub-compartments: enzyme-loaded liposomes within polymer capsules. *Angew Chem Int Ed* 48:4359–4362
87. Chandrawati R, Stadler B, Postma A, et al. (2009) Cholesterol-mediated anchoring of enzyme-loaded liposomes within disulfide-stabilized polymer carrier capsules. *Biomaterials* 30:5988–5998
88. Stein EW, Volodkin DV, McShane MJ, et al. (2006) Real-time assessment of spatial and temporal coupled catalysis within polyelectrolyte microcapsules containing coimmobilized mucose oxiaze and peroxidase. *Biomacromolecules* 7:710–719
89. Kreft O, Prevot M, Mohwald H, et al. (2007) Shell-in-shell microcapsules: a novel tool for integrated, spatially confined enzymatic reactions. *Angew Chem Int Ed* 46:5605–5608
90. Borodina T, Markvicheva E, Kunizhev S, et al. (2007) Controlled release of DNA from self-degrading microcapsules. *Macromol Rapid Commun* 28:1894–1899
91. Price AD, Zelikin AN, Wang Y, et al. (2009) Triggered enzymatic degradation of DNA within selectively permeable polymer capsule microreactors. *Angew Chem Int Ed* 48:329–332
92. Ghan R, Shutava T, Patel A, et al. (2004) Enzyme-catalyzed polymerization of phenols within polyelectrolyte microcapsules. *Macromolecules* 37:4519–4524
93. Mak WC, Cheung KY, Trau D (2008) Diffusion controlled and temperature stable microcapsule reaction compartments for high-throughput microcapsule-PCR. *Adv Funct Mater* 18:2930–2937
94. Price AD, Zelikin AN, Wark KL, et al. (2010) A biomolecular “ship in a bottle”: continuous RNA synthesis within hollow polymer hydrogel assemblies. *Adv Mater* 22:720–723
95. Stadler B, Price AD, Chandrawati R, et al. (2009) Polymer hydrogel capsules: en route toward synthetic cellular systems. *Nanoscale* 1:68–73
96. Wiemann LO, Buthe A, Klein M, et al. (2009) Encapsulation of synthetically valuable biocatalysts into polyelectrolyte multilayer systems. *Langmuir* 25:618–623

# Index

- Acetylcholinesterase 171
- Acrylic acid (AA) 6
- ADMET 4
- Ag/polymer hybrid nanoparticles 20
- Alcohol dehydrogenase (ADH) 63
- Alkylcyanoacrylates (ACA), anionic polymerization 32
- Alumina nanoparticles 20
- Aminoethylmethacrylate (AEMH) 12
- 2-Aminoethylmethacrylate hydrochloride (AEMH) 6
- Anionic polymerization 4, 30, 32
- Anti-cancer drugs 144
- Azo-based dyes 16
  
- Bimodal mesoporous silica (BMS) 79
- Biocompatibility 51
- Biopolymers, encapsulated, synthesis 174
- cis*-1,2-Bis(2,4,5-trimethyl-3-trienyl)ethane (CMTE) 12
- Boron-dipyrromethene (BODIPY)-based dye 12
  
- Cadmium 20
- Calcination 93
- Calcium carbonate 19, 77, 170
- Capsosome 172
- Capsules 91, 155
  - design 161
  - formation, interfacial polymerization 30
  - phase separation 29
- Capsules, tandem assembly 100
- Carbon black 16
- Carbon-based materials 16
- Carbon-coated silver nanoparticles 20
- Carboxymethylation 36
- Catalase-based protective barrier 59
  
- Catalytic polymerization 4
- Cationic polymerization 4
- CdSe/CdS quantum dots 95
- Chromium(III)benzoylacetate 13
- Cl-catechol 1,2-dioxygenase 63
- Cloisite 22
- Closed-shell colloids 99
- Colloidosomes 105
- Controlled release 37
- Cosonication 16, 18
- Cyclodextrins, imidazole-functionalized 54
- Cytochrome c 61
  
- Dendrimers 51, 58, 63, 120, 142
- N*-(2,6-Diisopropylphenyl)perylene-3,4-dicarbonacidimide (PMI) 7
- 1,2-Dimethyl-1-phenyl-butyramide (DMPBA) 28, 30
- DNA, damage detection 60, 61
  - delivery 125
  - encapsulation 32, 146
  - multilayer films 159
  - release 173
  - separation 26
- DNase 79
- Doxorubicin 144, 163
- Dual reporter nanoparticles 9
- DVMAC 20
  
- Electroactive mediators 63
- Electrostatic assembly 92
- Electrostatic interactions 58
- Electrostatic-mediated multilayer assembly 92
- Emulsions 105

- Encapsulation 1, 115
  - amphiphilic molecules 139
  - dyes 6
  - hydrophilic molecules 139
  - hydrophobic molecules 138
  - inorganic materials 19
  - liquids 28
  - metal complexes 13
  - solid materials 16
  - soluble materials 5
- Endocytosis 7
- Enzymatic polymerization 4
- Enzyme films 60
- Enzyme-polyelectrolyte LbL films 56
- Enzymes 51, 58
- Europium- $\beta$ -diketonato complexes 11
  
- Ferromagnetic hybrid nanoparticles 23
- $\alpha$ -1-Fetoprotein antigen (AFP) 62
- Fibronectin 58
- Fluorescein isothiocyanate 163
- Fluorescence recovery after photobleaching (FRAP) 161
- Fluorophores 142
- Foams 105
- Fragrance 28, 37
  
- Glucose biosensors 63, 68
- Glucose oxidase 54
- Guanidinium-bearing molecular clefts 54
  
- HeLa cells 6
- Hexadecane 19
- Hexadecylamine 20
- 12-Hexanoyloxy-9-octadecenoic acid 23
- Hierarchic assemblies 76
- Hollow capsules 51
- Hollow spheres 89, 92
  - metal-NP-shelled 100
  - one-nanoparticle-type 96
  - two-nanoparticle-type 94
- Hyaluronan-*b*-poly( $\gamma$ -benzyl-L-glutamate) 133
- Hybrid particles 1
- Hybridization 76
- 8-Hydroxypyrene-1,3,6-trisulfonate 140
  
- Indium(III)acetylacetonate 13
- Indocyanine green (ICG) 100
- Insulin 69
- Interfacial stabilization 89, 105
  
- Jeffamine M2070/M1000 19
  
- Lanthanide-based nanocrystals, fluorescing 20
- Lanthanide- $\beta$ -diketonato complexes 15
- Laponite RD 22
- Layer-by-layer assemblies (LbL) 51, 89, 155, 157
  - covalent bonding 160
  - electrostatics 157
  - enzyme-embedded 58
  - hydrogen bonding 158
- Lecithin 30
- Lucirin TPO 30
  
- Maghemite nanoparticles 23
- Magnetic resonance imaging (MRI) contrast agents 142
- Magnetite nanoparticles 23
- Medical applications 75
- Membranes 54, 64, 71, 115, 138, 164
  - chitosan 71
  - conformation 117
  - permeability 139, 140
  - polymersomes 117, 127, 139, 140
- Metal-NP-shelled hollow spheres 100
- 2-Methacryloyloxyethyl hexadyltrimethyl ammonium bromide (MA16) 22
- Microreactors, bienzymatic 172
  - controlled release 173
  - enzyme post-loading 168
- Microreactors, enzyme pre-loading 168
  - LbL assembly 167
- Microtubules, self-assembled 66
- Miniemulsion 1
- Molecular beacon 163
- Montmorillonite 22
- MPS-modified silica particles 21
- Multi-enzyme reactors, GOD/glucoamylase (GA) 57
- Multilayer films 155
  
- Nanocapsules, controlled release 37
- Nanocomposites 1
- Nanofabrication, LbL 55
- Nano-onions 15
- Nanoparticle-assembled capsules (NACs) 89, 94
- Nanoparticle-shelled hollow structures, emulsions 105
- Nanoparticle-shelled inorganic capsules 93
- Nanoparticle-polymer tandem assembly 94

- Nanoparticles 1ff, 89
- Nanoprecipitation 37
- Nanoscale imaging agents 142
- Nanostructured particle templates 169
- Near-infrared emissive polymersomes (NIR-polymersomes) 141
- Neobee M5 30
  
- Octadecyl rhodamine B 139
- Octadecyltrimethoxysilane (ODMS) 22
- Oligo(phenylene vinylenes) 4
- Organic pigments 16
- Organic solvent-based methods 136
- OVDAC 20
- Oxidative polymerization 4
  
- P(MMA-*co*-2-EHA) 37
- Paclitaxel 144
- Paraoxon 60
- Particle stabilized emulsion 89
- PBCA 7
- PDADMAC/PSS 167
- PEO-*b*-PCL 142
- PEO-*b*-PMCL 142
- PEO-PEE 139
- Permeability 34, 62, 69, 103, 107, 133, 161
  - control 163
  - polymersome membranes 139, 140
- Phospholipids 71
- Photoresponsive delivery systems 100
- Photoswitches 12
- Phthalocyanines 11, 16
- Platinum(II)acetylacetonate 13
- Poly(acrylic acid) (PAA) 66
- Poly(aminoethylmethacrylate) (PAEMA) 22
- Poly(butylcyanoacrylate) (PBCA) 32
- Poly( $\epsilon$ -caprolactone) 7
- Poly(diallyldimethylammoniumchloride) (PDDA) 62
- Poly(2-(diethylamino)ethyl methacrylate) (PDEAEMA) 12
- Poly(hydroxyethylmethacrylate) (HEMA) 22
- Poly(*N*-isopropylacrylamide) (PNIPAM) 12
- Poly(methylmethacrylate) (PMMA) 7
- Poly(oligo(ethylene glycol) monomethyl ether methacrylate) (POEOMA) 11
- Poly(styrenesulfonic acid) (PSSA) 22
- Poly(vinylalcohol) (PVA) 30
- Poly(*N*-vinyl caprolactam) (PVCL) 159
- Poly(vinyl methyl ether) (PVME) 159
- Poly(*N*-vinyl pyrrolidone) (PVPON) 158
- Polyacrylonitrile 5
- Polyacrylate 5
- Polyaddition 4
- Polyamides 4, 22
- Polyaniline 4
- Polybutylcyanoacrylate (PBCA) 4, 5
- Polybutylene succinimide diethyl triamine (OLOA370) 20
- Polycondensation 4
- Polyepoxides 4, 5
- Polyesters 4, 5
- Polyethylene (PE) 22
- Polyimides 5
- Polyisoprene 5, 7
- Polyketones 4
- Poly lactide (PLLA) 7
- Polymer precipitation, preformed nanodroplets 37
- Polymer-aggregate templating 94
- Polymersomes 115
  - formation kinetics 133
  - formulations 117
  - loading 138
  - near-infrared emissive 141
  - preparation 133
  - responsive 129
  - surface chemistry 131
- Poly-*p*-methoxystyrene 4
- Polynorbonene 4
- Polyolefins 4
- Polystyrene 5
- Polyurea capsules, silver nanoparticles 35
- Polyurethanes 4
- Protein nanotube 67
- PS-*co*-PI 7
- PS-*co*-P4VP/silica hybrid nanoparticles 21
- PVP 66
  
- Quantum dots, semiconducting 20
- Quinacridone pigments 18
  
- Reaction vessels 155
- Rhodamine isothiocyanate (RITC) dextran 11
- Ring opening metathesis polymerization (ROMP) 4
  
- Saponite 22
- Selenium 20
- Self-assembly 54, 76, 91, 94, 98, 155
- Shell-in-shell capsules 173
- Silica nanoparticles 20
- Single wall carbon nanotubes (SWNTs) 19

- Size control 136  
Size-quantization effects 91  
Sodium 1,2-bis(2-ethylhexoxycarbonyl)ethanesulfonate (AOT) 23  
Solvent free methods 135  
Step-growth acyclic diene metathesis (ADMET) polymerization 4  
Styrene/BA 23  
Sudan Black B 11  
Sulforhodamine SR101 39  
Superparamagnetic iron oxide nanoparticles (SPIONs) 144  
  
Tandem assembly 89, 92, 94  
capsules 100  
  
Tellurium 20  
Tetraethylorthosilicate (TEOS) 22  
Thin films 51, 58  
Titania nanoparticles 20  
Toluene-2,4-diisocyanate (TDI) 39  
Trioctylphosphine oxide (TOPO) 20  
  
Vinylmercaptobenzene 20  
  
Wires 63  
Wuestite aggregates 24  
  
Zinc(II)phthalocyanine 13  
Zinc(II)tetramethylheptadionate 13